UNIVERSIDAD COMPLUTENSE DE MADRID
FACULTAD DE CIENCIAS FÍSICAS

TESIS DOCTORAL

Cuerdas bosónicas en AdS3 × S3 con flujo de Neveu-Schwarz-Neveu-Schwarz

Bosonic strings on AdS3 × S3 with Neveu-Schwarz-Neveu-Schwarz flux

MEMORIA PARA OPTAR AL GRADO DE DOCTOR

PRESENTADA POR

Roberto Ruiz Gil

Director

Rafael Hernández Redondo

Madrid

Universidad Complutense de Madrid

Facultad de Ciencias Físicas

Tesis doctoral

Cuerdas bosónicas en AdS_3 x S^3 con flujo de Neveu-Schwarz-Neveu-Schwarz

Bosonic strings on AdS_3 x S^3 with Neveu-Schwarz-Neveu-Schwarz flux

Memoria para optar al grado de doctor

presentada por

Roberto Ruiz Gil

Director

Rafael Hernández Redondo

Cuerdas bosónicas en $AdS_3 \times S^3$ con flujo de Neveu-Schwarz-Neveu-Schwarz

---

Bosonic strings on $AdS_3 \times S^3$ with Neveu-Schwarz-Neveu-Schwarz flux

por

Roberto Ruiz Gil

bajo la supervisión de

Rafael Hernández Redondo

UNIVERSIDAD
COMPLUTENSE
MADRID

Tesis presentada en la

Universidad Complutense de Madrid

para el grado de

Doctor en Física

Departamento de Física Teórica

Facultad de Ciencias Físicas

Febrero 2022

Acknowledgements

I am grateful to Rafael Hernández Redondo for collaboration in [P1, P3–P6] and to Juan Miguel Nieto García for collaboration in [P1–P5]. I acknowledge Rafael Hernández Redondo, Juan Miguel Nieto García, Kostantinos Siampos, and Alessandro Torrielli for comments on the manuscript. The work has been supported through the grant no. PGC2018-095382-B-I00, by Universidad Complutense de Madrid and Banco Santander through the grant no. GR3/14-A 910770, and by Universidad Complutense de Madrid and Banco Santander through the contract no. CT42/18-CT43/18.

Contents

Resumen

La correspondencia $\mathrm{AdS}_3/\mathrm{CFT}_2$ es la dualidad holográfica entre gravitación en AdS_3 y el límite de baja energía de la teoría cuántica de campos bidimensional sobre la frontera de AdS_3. La teoría de supercuerdas de tipo IIB sobre $\mathrm{AdS}_3 \times \mathrm{S}^3 \times \mathrm{T}^4$ con flujos de Ramond-Ramond y Neveu-Schwarz-Neveu-Schwarz (NSNS) concreta la correspondencia $\mathrm{AdS}_3/\mathrm{CFT}_2$. En la tesis titulada *Cuerdas bosónicas en $AdS_3 \times S^3$ con flujo de Neveu-Schwarz-Neveu-Schwarz*, analizamos el sistema por medio de cuerdas bosónicas en $\mathrm{AdS}_3 \times \mathrm{S}^3$ con flujo de NSNS a nivel clásico y semiclásico. El análisis de la tesis se basa en la aplicación de técnicas empleadas en $\mathrm{AdS}_5 \times \mathrm{S}^5$ a cuerdas bosónicas en presencia de flujo de NSNS. El objetivo de la tesis es obtener resultados que permitan precisar la teoría de supercuerdas de tipo IIB sobre $\mathrm{AdS}_3 \times \mathrm{S}^3 \times \mathrm{T}^4$ y su conexión con la correspondencia $\mathrm{AdS}_3/\mathrm{CFT}_2$. El punto de partida de la tesis es el modelo σ no lineal clásico en $\mathrm{AdS}_3 \times \mathrm{S}^3$ junto con su estructura integrable. El modelo σ no lineal es un modelo de Wess-Zumino-Novikov-Witten (WZNW) con múltiples sectores con respecto al flujo espectral en el límite de flujo de NSNS puro. Desde el modelo σ no lineal clásico, procedemos en dos direcciones. En primer lugar, estudiamos dos clases de cuerdas bosónicas: cuerdas pulsantes y superficies mínimas. Las cuerdas pulsantes son cerradas y las superficies mínimas abiertas. Construimos y analizamos las soluciones clásicas. También hallamos las curvas espectrales locales elípticas de ambas clases de cuerdas bosónicas sobre la base de la conexión de Lax, además de una aplicación entre ellas. En el límite de flujo de NSNS puro, las soluciones clásicas de ambas clases se simplifican. Las cuerdas pulsantes se distribuyen en las clases de cuerda corta y cuerda larga de Maldacena y Ooguri. Las superficies mínimas conexas asimismo se distribuyen en dos clases. El límite de flujo de NSNS puro, por otra parte, induce la singularización de la curva elíptica de cuerdas pulsantes y superficies mínimas. En el régimen de flujo mixto, calculamos cantidades que caracterizan cada una de las dos clases de cuerdas bosónicas. Por un lado, escribimos la relación de dispersión de cuerdas pulsantes de forma cerrada mediante la elección apropiada de los módulos. Por otro lado, obtenemos la acción sobre soluciones clásicas regularizada de superficies mínimas. El límite de flujo de NSNS puro de ambas cantidades refleja la distribución de cuerdas bosonícas en dos clases. Tanto la relación de dispersión de cuerdas pulsantes como la acción sobre soluciones clásicas regularizada de superficies mínimas son cantidades a considerar en la correspondencia $\mathrm{AdS}_3/\mathrm{CFT}_2$. En segundo lugar, construimos el modelo σ de cadena de espines de sectores bosónicos del modelo de WZNW a través de la acción efectiva. La acción efectiva es válida en todo sector con respecto al flujo espectral. Calculamos primero la acción efectiva a partir de la acción clásica. El procedimiento consta de la imposición de una condición de fijación de *gauge* en la acción clásica y la subsiguiente expansión en serie de la acción clásica con

respecto al acoplamiento efectivo semiclásico. Recuperamos después la misma acción efectiva desde la cadena de espines de la hoja de mundo. La acción efectiva en este caso resulta de la representación de la amplitud de transición en la cadena de espines en cuanto integral de camino. Para construirla, postulamos estados coherentes en la hoja de mundo y consideramos un límite de Landau-Lifshitz atípico. La conformidad entre los resultados para la acción efectiva sugiere que la aplicabilidad de la cadena de espines en el modelo de WZNW va más allá del problema espectral.

Abstract

The AdS_3/CFT_2 correspondence is the holographic duality between gravity on AdS_3 and the low-energy limit of the two-dimensional quantum field theory on the boundary of AdS_3. Type IIB superstring theory on $AdS_3 \times S^3 \times T^4$ with Ramond-Ramond and Neveu-Schwarz-Neveu-Schwarz (NSNS) fluxes realises the AdS_3/CFT_2 correspondence. In the thesis entitled *Bosonic strings on $AdS_3 \times S^3$ with Neveu-Schwarz-Neveu-Schwarz flux*, we analyse the system by means of bosonic strings on $AdS_3 \times S^3$ with NSNS flux at the classical and semi-classical level. The analysis of the thesis is based on the application of techniques used in $AdS_5 \times S^5$ to bosonic strings in the presence of NSNS flux. The objective of the thesis is to obtain results that permit to specify type IIB superstring theory on $AdS_3 \times S^3 \times T^4$ and its connection with the AdS_3/CFT_2 correspondence. The starting point of the thesis is the classical non-linear σ-model on $AdS_3 \times S^3$ together with its integrable structure. The non-linear σ-model is a Wess-Zumino-Novikov-Witten (WZNW) model with multiple spectrally flowed sectors in the limit of pure NSNS flux. From the classical non-linear σ-model, we follow two directions. First, we study two classes of bosonic strings: pulsating strings and minimal surfaces. Pulsating strings are closed and minimal surfaces are open. We construct and analyse classical solutions. We also find elliptic local spectral curves of both classes of bosonic strings on the basis of the Lax connection, and, in addition, we find a mapping between them. In the limit of pure NSNS flux, classical solutions of both classes simplify. Pulsating strings fall into the short-string and long-string classes of Maldacena and Ooguri. Connected minimal surfaces also fall into two classes. The limit of pure NSNS flux, moreover, singularises the elliptic curve of pulsating strings and minimal surfaces. In the mixed-flux regime, we compute quantities that characterise each of the two classes of bosonic strings. On the one hand, we write the dispersion relation of pulsating strings in a closed form through the proper choice of moduli. On the other hand, we obtain the regularised on-shell action of minimal surfaces. The limit of pure NSNS flux of both quantities reflects the distribution of bosonic strings in two classes. Both the dispersion relation of pulsating strings and the regularised on-shell action of minimal surfaces are quantities to be considered in the AdS_3/CFT_2 correspondence. Second, we construct the spin-chain σ-model of bosonic sectors of the WZNW model by means of the effective action. The effective action is valid in every spectrally flowed sector. We compute first the effective action from the classical action. The procedure consists of the imposition of a gauge-fixing condition to the classical action and the subsequent series expansion of the classical action with respect to the semi-classical effective coupling. We retrieve the same effective action from the world-sheet spin chain afterwards. The effective action in this case follows from the representation of the transition amplitude in the spin chain as a path integral. To construct the path integral, we postulate coherent states on the world-sheet and consider an unconventional Landau-Lifshitz limit. The agreement between the results for the effective action suggests that the applicability of the spin chain in the WZNW model goes beyond the spectral problem.

Publications

[P1] R. Hernández, J. M. Nieto, and R. Ruiz, 'Pulsating strings with mixed three-form flux', *JHEP*, vol. 04, p. 078, 2018. [arXiv:1803.03078]

[P2] J. M. Nieto and R. Ruiz, 'One-loop quantization of rigid spinning strings in $AdS_3 \times S^3 \times T^4$ with mixed flux', *JHEP*, vol. 07, p. 141, 2018. [arXiv:1804.10477]

[P3] R. Hernández, J. M. Nieto, and R. Ruiz, 'Minimal surfaces with mixed three-form flux', *Phys. Rev. D*, vol. 99, no. 8, p. 086003, 2019. [arXiv:1811.08294]

[P4] R. Hernández, J. M. Nieto, and R. Ruiz, 'The SU(2) Wess-Zumino-Witten spin chain sigma model', *JHEP*, vol. 06, p. 080, 2019. [arXiv:1905.05533]

[P5] R. Hernández, J. M. Nieto, and R. Ruiz, 'Quantum corrections to minimal surfaces with mixed three-form flux', *Phys. Rev. D*, vol. 101, no. 2, p. 026019, 2020. [arXiv:1911.01150]

[P6] R. Hernández and R. Ruiz, 'Double Yang-Baxter deformation of spinning strings', *JHEP*, vol. 06, p. 115, 2020. [arXiv:2003.05724]

[P7] R. Ruiz, 'SL$(2,\mathbb{R})$ Wess-Zumino-Novikov-Witten spin-chain σ-model', *Phys. Rev. D*, vol. 103, no. 10, p. 106024, 2021. [arXiv:2101.12119]

Glossary of initialisms

The following list includes the initialisms that appear in the text.

BMN . . . . Berenstein-Maldacena-Nastase

BPS . . . . Bogomol'nyi–Prasad–Sommerfield

GS . . . . Green-Schwarz

LL . . . . Landau-Lifshitz

NG . . . . Nambu-Goto

NR . . . . Neumann-Rosochatius

NSNS . . . . Neveu-Schwarz-Neveu-Schwarz

RNS . . . . Ramond-Neveu-Schwarz

RR . . . . Ramond-Ramond

SYM . . . . supersymmetric Yang-Mills

WZ . . . . Wess-Zumino

WZNW . . . . Wess-Zumino-Novikov-Witten

List of tables

List of figures

Chapter 1

Introduction

The holographic principle states the equivalence between quantum gravity on the bulk of a space and the non-gravitational at the boundary of this space [1, 2]. The prime realisation of the holographic principle is the $\mathrm{AdS}_{d+1}/\mathrm{CFT}_d$ correspondence [3–5]. This duality connects type II superstring theory on a AdS_{d+1}-background and the CFT_d at the conformal boundary thereof. The knowledge of two-point and three-point functions of primary operators in both type II superstring theory and the CFT_d virtually solves each side of the duality. The remaining correlators follow from the operator-product expansion. Primary operators are arranged according to the isometry superalgebra. The quantum numbers of representations supply the mapping between primary operators through the $\mathrm{AdS}_{d+1}/\mathrm{CFT}_d$ correspondence. Thus, the proof of the duality amounts to two steps: first, the computation of two-point and three-point functions of dual primary operators; second, the comparison between them.

In this chapter, we review the overall picture that underlies the body of the text. In section 1.1, we review the spectral problem of the $\mathrm{AdS}_5/\mathrm{CFT}_4$ correspondence. We focus on the semi-classical limit of bosonic strings. In subsection 1.1.1, we present type IIB superstring theory on $\mathrm{AdS}_5 \times \mathrm{S}^5$ with pure Ramond-Ramond (RR) five-form flux and $\mathcal{N} = 4$ supersymmetric Yang-Mills (SYM) theory. We then state the spectral problem. In subsection 1.1.2, we highlight the role of classical solutions and integrability in solving the semi-classical limit of the spectral problem. In section 1.2, we present our focus in the text: $\mathrm{AdS}_3 \times \mathrm{S}^3$ with mixed RR and Neveu-Schwarz-Neveu-Schwarz (NSNS) three-form flux, and with pure NSNS flux. We review advances made within the type IIB superstring theory. In section 1.3, we present the overview of the remaining chapters.

The exhaustive review of the $\mathrm{AdS}_{d+1}/\mathrm{CFT}_d$ correspondence with a complete list of references is beyond the scope of the chapter. Broad and comprehensive reviews already are available. We refer to [6] for a general review on the foundations of the duality. We refer to [7] and, especially, [8] for a review of integrability in the $\mathrm{AdS}_5/\mathrm{CFT}_4$ correspondence. Finally, we refer to [9] for a review of integrability on $\mathrm{AdS}_3 \times \mathrm{S}^3$ with pure RR flux.

1.1 The $\mathrm{AdS}_5/\mathrm{CFT}_4$ correspondence

We devote this section to the spectral problem of the $\mathrm{AdS}_5/\mathrm{CFT}_4$ correspondence between type IIB superstring theory on $\mathrm{AdS}_5 \times \mathrm{S}^5$ with pure RR five-form flux and $\mathcal{N} = 4$ SYM theory.

We focus on the semi-classical limit and integrability. We base the presentation of $\mathrm{AdS}_5 \times \mathrm{S}^5$ on [10], section 1 of [11] and [12]. We base the presentation of closed-superstring vertex operators and $\mathcal{N} = 4$ SYM theory on [13–15] and [16], respectively. The review [16], in particular, includes a complete set of references on $\mathcal{N} = 4$ SYM theory.

1.1.1 The spectral problem

Reference [3] formulated the $\mathrm{AdS}_5/\mathrm{CFT}_4$ correspondence by considering an array of parallel D3-branes in type IIB superstring theory. The $\mathcal{N} = 4$ SYM theory is the system inside the world-volume of D3-branes in the low-energy limit. The near-horizon limit of D3-branes in type IIB supergravity is $\mathrm{AdS}_5 \times \mathrm{S}^5$. The low-energy and near-horizon limits are equivalent.

The $\mathcal{N} = 4$ SYM theory is the planar limit of maximally SYM theory in four-dimensional Minkowski background M_4 whose gauge group is SU(N). The β-function of g_{YM}, where g_{YM} denotes the coupling constant of $\mathcal{N} = 4$ SYM theory, vanishes prior to the planar limit. Therefore, quantum superconformal invariance holds in $\mathcal{N} = 4$ SYM theory. The isometry supergroup of $\mathcal{N} = 4$ SYM theory is $\mathrm{PSU}(2,2|4)$, which has thirty-two supercharges. The supergroup $\mathrm{PSU}(2,2|4)$ is the supersymmetric enhancement of $\mathrm{SO}(2,4) \times \mathrm{SO}(6)$, where $\mathrm{SO}(2,4)$ is the conformal group in four dimensions and $\mathrm{SO}(6)$ is the R-symmetry group of $\mathcal{N} = 4$ SYM theory. The planar limit is $N \to \infty$ with the 't Hooft coupling $\lambda = g_{\mathrm{YM}}^2 N$ fixed. Since the β-function of g_{YM} vanishes, λ is unaffected by the renormalisation-group flow.

The $\mathrm{AdS}_5/\mathrm{CFT}_4$ correspondence also comprises type IIB superstring theory on $\mathrm{AdS}_5 \times \mathrm{S}^5$ with pure RR five-form flux. The isometry groups of AdS_5 and S^5 are $\mathrm{SO}(2,4)$ and $\mathrm{SO}(6)$, respectively. The supersymmetric enhancement of $\mathrm{SO}(2,4) \times \mathrm{SO}(6)$ is $\mathrm{PSU}(2,2|4)$. The isometry supergroup of the Green-Schwarz (GS) action is $\mathrm{PSU}(2,2|4)$. The parameters of $\mathcal{N} = 4$ SYM theory map to the following specifications in $\mathrm{AdS}_5 \times \mathrm{S}^5$. First, N maps to the number of units of RR flux through S^5. Second, the 't Hooft coupling maps to the string tension $\lambda = R^4/\alpha'^2$, where R denotes the common radius of AdS_5 and S^5, and α' denotes the Regge slope. Third, the planar limit $N \to \infty$ with λ fixed corresponds to the vanishing of the string-interaction coupling $g_s = \lambda/4\pi N$.

The isometry supergroup of both $\mathrm{AdS}_5 \times \mathrm{S}^5$ and $\mathcal{N} = 4$ SYM theory is $\mathrm{PSU}(2,2|4)$. Primary operators in the $\mathrm{AdS}_5/\mathrm{CFT}_4$ correspondence (and their descendants) fall into unitary irreducible representations of $\mathrm{PSU}(2,2|4)$ called *multiplets.* [1] The quantum numbers of multiplets identify pairs of dual primary operators. The computation and matching of two-point and three-point functions of dual primary operators comes after the identification.

Correlators are highly constrained by superconformal invariance. Superconformal invariance implies that two-point functions of primary operators vanish unless primary operators have the same quantum numbers (up to signs). Two-point functions are in this way determined up to the conformal dimensions of the primary operators involved. The duality for

[1] We use operator and state interchangeably. The state-operator correspondence ensures the equivalence between primary operators and highest-weight states in both $\mathcal{N} = 4$ SYM theory and the world-sheet CFT_2. Moreover, we often talk about multiplets determined by $\mathrm{PSU}(2,2|4)$ for brevity. Other quantum numbers may be necessary to specify the multiplet. For instance, mode and winding numbers in $\mathrm{AdS}_5 \times \mathrm{S}^5$.

two-point functions is equivalent to the so-called *spectral problem*: the computation of energies in $\mathrm{AdS}_5 \times \mathrm{S}^5$ and conformal dimensions in $\mathcal{N} = 4$ SYM theory of dual primary operators and the matching between them. We state the spectral problem more precisely hereunder.

Primary operators in $\mathcal{N} = 4$ SYM theory are single-trace gauge-invariant composite local operators. By definition, the conformal dimension Δ, that is the eigenvalue with respect to the generator of dilatations D of a primary operator is minimum within its multiplet. Primary operators commute, at the origin of M_4, with the four bosonic generators and the sixteen supercharges that generate special conformal transformations. The trace of primary operators can contain any simple local operators of $\mathcal{N} = 4$ theory. [2] The action of $\mathfrak{psu}(2,2|4)$ on primary operators yield the descendants of each multiplet.

Primary operators are labelled by their eigenvalues with respect to the generators of the Cartan subalgebra of $\mathfrak{so}(2,4) \oplus \mathfrak{so}(6) \subset \mathfrak{psu}(2,2|4)$. The conformal dimension Δ and the Lorentzian spins S_a, with $a = 1, 2$, are the labels with respect to $\mathfrak{so}(2,4)$. The R-charges J_α, with $\alpha = 1, 2, 3$, are the labels with respect to $\mathfrak{so}(6)$.

The conformal dimension Δ depends on λ and the quantum numbers S_a and J_α. The operator D admits a perturbative series if $\lambda \to 0$, whose zeroth-order term is D_0 and whose remainder is δD. Therefore, the conformal dimension of any primary operator admits a perturbative analytic series in λ:

$$\Delta = \sum_{n=0}^{\infty} \lambda^n \Delta_n = \Delta_0 + \gamma \ , \tag{1.1}$$

where Δ_0 and γ are the eigenvalues of D_0 and δD, respectively. The quantity Δ_0 is called *bare dimension*. Each primary operators have the lowest Δ_0 within its multiplet, where Δ_0 equals the sum of S_a and J_α. Any descendant has larger bare dimension, which differs from the bare dimension of primary operators by multiples of one half. The quantity γ is called *anomalous dimension*. The quantity γ depends on λ. Primary operators and their descendants have the same γ. It follows from power counting in Feynman diagrams that the operator D_0 commutes with δD. Thus, primary operators with the same Δ_0, S_a, and J_α form multiplets that are closed sectors under δD (order by order in λ).

Primary operators in $\mathrm{AdS}_5 \times \mathrm{S}^5$ are closed-superstring vertex operators. By definition, primary operators are eigenstates of the generators of the Cartan subalgebra of $\mathfrak{so}(2,4) \oplus \mathfrak{so}(6)$. The expectation value of generators of $\mathfrak{psu}(2,2|4)$ that lie outside the Cartan subalgebra vanishes. The descendants of a primary operator follow from the action of $\mathfrak{psu}(2,2|4)$.

The labels of primary operators with respect to $\mathfrak{so}(2,4)$ are the energy E and the Lorentzian spins S_a, with $a = 1, 2$. (Energies equal conformal dimensions in AdS_{d+1} because the corresponding multiplets in $\mathfrak{so}(2,\mathrm{d})$ are related by global similarity transformations of $\mathrm{SO}(2,\mathrm{d})$; see section 2 of [10].) The labels of primary operators with respect to $\mathfrak{so}(6)$ are the angular momenta J_α, with $\alpha = 1, 2, 3$.

The energy E depends on λ, S_a, and J_α through the dispersion relation of primary operators. The marginality condition of vertex operators with respect to their world-sheet conformal

[2] We refer to section 4 of [16] for an explicit discussion of the representations of simple local operators fields under $\mathfrak{psu}(2,2|4)$. Every simple local operators belongs to the adjoint representation of $\mathrm{SU(N)}$ prior to $N \to \infty$.

dimensions implies dispersion relation. The perturbative series of E in α' demands that $1/\sqrt{\lambda}$ is small, and, hence, $\lambda \to \infty$. The series reads

$$E = \sum_{n=0}^{\infty} \lambda^{(1-n)/2} E_n \ . \tag{1.2}$$

The series (1.2) is non-analytic in λ. In the limit $\lambda \to \infty$, closed sectors correspond to consistent truncations of the GS action.

Quantum numbers of primary operators that are dual under the $\mathrm{AdS}_5/\mathrm{CFT}_4$ correspondence match. Homonymous S_a and J_α of dual primary operators coincide in particular. Therefore, the solution of the spectral problem of the $\mathrm{AdS}_5/\mathrm{CFT}_4$ correspondence amounts to proof that $\Delta = E$ holds for dual primary operators. The perturbative regimes of (1.1) and (1.2) with respect to λ do not overlap nonetheless. The lack of overlap is an instance of the strong/weak duality: the strong-coupling (non-perturbative) regime of $\mathrm{AdS}_5 \times \mathrm{S}^5$ is the weak-coupling (perturbative) regime of $\mathcal{N} = 4$ SYM theory, and vice versa.

The semi-classical limit permits to overcome the strong/weak duality. The semi-classical limit singles out primary operators whose S_a and J_α are comparable to $\sqrt{\lambda}$ when $\lambda \to \infty$. The semi-classical limit eases the comparison between Δ and E partly because it virtually replaces vertex operators by classical solutions at $\lambda \to \infty$. The connection between vertex operators and classical solutions on $\mathrm{AdS}_5 \times \mathrm{S}^5$ is in particular the following.

The spectral problem of primary operators on $\mathrm{AdS}_5 \times \mathrm{S}^5$ is encoded in two-point functions of vertex operators, as we have already mentioned. Vertex operators in the two-point function carry the same Δ and opposite S_a and J_α, otherwise the two-point function would vanish. (The normalisation of two-point functions includes a divergent integral over the Möbius residual symmetry group of the world-sheet and a δ-function evaluated at zero that cancel each other.) Two-point functions can be rephrased as world-sheet path integrals wherein two insertions reflect vertex operators. The world-sheet path integral extends over closed-superstring configurations, that is world-sheet fields that satisfy periodic boundary conditions. The insertions are placed on the Riemann sphere since $g_s = 0$.

If $\lambda \to \infty$, the stationary-phase approximation is applicable to the path integral. The stationary phase approximation gives rise to classical solutions: closed bosonic strings that solve the equations of motion of the classical action. Target-space spinors in the GS action are negligible. Classical solutions are sourced by the vertex operators. The quantum numbers S_a and J_α become the Noether charges of classical solutions. The marginality condition, which implies the dispersion relation, renders into the Virasoro constraints. The world-sheet of classical solutions is cylindrical because insertions are placed on the Riemann sphere.

The actual feasibility of the stationary-phase approximation is limited to simple cases, such as homogeneous classical solutions. If S_a, J_α are semi-classical, that is if $S_a, J_\alpha \sim \sqrt{\lambda} \to \infty$, the problem simplifies. Classical solutions sourced by the vertex operators are then interchangeable with simpler classical solutions ('solitons') with the same Noether charges. (Both classes of solutions may coincide.) The computation of two-point functions then amounts to the construction of classical solutions with semi-classical Noether charges.

We must make some observations before moving forward. Classical solutions solve the equations of motion of the classical action. The classical action is the closed-string Polyakov action on $\mathrm{AdS}_5 \times \mathrm{S}^5$. The Polyakov action is the bosonic truncation of the GS action of type IIB superstring theory on $\mathrm{AdS}_5 \times \mathrm{S}^5$. Reference [17] rephrased the GS action in terms of a non-linear σ-model on $\mathrm{PSU}(2,2|4)/\mathrm{SO}(1,4) \times \mathrm{SO}(5)$. This rephrasing is possible because $g_s = 0$. Classical integrability holds in the non-linear σ-model [18], and it also holds the bosonic truncation of the non-linear σ-model [19]. Classical integrability is indirectly responsible for the availability of classical solutions that we review in the following subsection.

1.1.2 Bosonic strings in $\mathbf{AdS_5 \times S^5}$

The simplest class of primary operators for which the comparison between Δ and E is feasible are Bogomol'nyi–Prasad–Sommerfield (BPS) states. BPS states preserve half of the supersymmetries. In $\mathcal{N} = 4$ SYM theory, BPS states correspond to chiral primary operators. *Chiral* stands for the commutativity of the primary operator at the origin of M_4 with eight out of the sixteen Poincaré supercharges of $\mathfrak{psu}(2,2|4)$. The anomalous dimensions of chiral primary operators vanishes, $\gamma = 0$, and $\Delta = \Delta_0$. Chiral primary operators comprise J copies of a holomorphic scalar made up of two real scalar, say $Z = (\phi_1 + \mathrm{i}\,\phi_4)/\sqrt{2}$. Therefore,

$$\Delta = J \tag{1.3}$$

BPS states correspond to supergravity states on $\mathrm{AdS}_5 \times \mathrm{S}^5$. The energy

$$E = J \ , \tag{1.4}$$

where J is the total angular momentum in S^5, does not depend on λ. It follows from (1.3) and (1.4) that $\Delta = E$. Reference [20] noted that point-like classical solutions realise the semi-classical limit of BPS states, where $J \sim \sqrt{\lambda} \to \infty$. The degenerate world-sheet is a null geodesic along the global time-like direction of AdS_5 that surrounds S^5 along an equator. Both BPS states and their classical solutions are called *Berenstein-Maldacena-Nastase* (BMN) *vacua* in the semi-classical limit. The reasons will be clear later.

Reference [21] considered the so-called *near-BPS states*. Reference [21] realised that Δ and E of near-BPS states match in the so-called *BMN limit*. In $\mathcal{N} = 4$ SYM theory, near-BPS states are primary operators with J copies of Z and a number much less than J of other fields inside the trace. The BMN limit takes J not only much larger than the number of other fields but also $J \to \infty$. The one-loop computation of γ reveals that

$$\gamma = \frac{\lambda}{J^2} a_1 + \frac{\lambda^2}{J^4} a_2 + \frac{\lambda^3}{J^6} a_3 + \mathrm{O}\left(\frac{\lambda^4}{J^8}\right) \ , \tag{1.5}$$

where $\lambda \to 0$. Note that λ appears in the ratio λ/J^2.

Reference [20] presented near-BPS states in $\mathrm{AdS}_5 \times \mathrm{S}^5$, which [22,23] detailed. Near-BPS states correspond to quantum fluctuations around point-like classical solutions of BPS states in the semi-classical limit $J \sim \sqrt{\lambda} \to \infty$. The effective action of quantum fluctuations reduces to the GS action on a pp-wave background. The pp-wave background arises because it is the Penrose limit of $\mathrm{AdS}_5 \times \mathrm{S}^5$ [24]. The spectrum of type IIB superstring theory on the pp-wave background is exactly computable [25]. The energy E of quantum fluctuations reads

$$E - J = \frac{\lambda}{J^2} b_1 + \frac{\lambda^2}{J^4} b_2 + \frac{\lambda^3}{J^6} b_3 + \mathrm{O}\left(\frac{\lambda^4}{J^8}\right) \ . \tag{1.6}$$

The dispersion relation (1.6) just involves λ in the effective coupling λ/J^2.

Both (1.5) and (1.6) are series in λ/J^2. Therefore, (1.1) and (1.2) could overlap. The overlap occurs if the successive application of $\lambda \to 0$ and $J \to \infty$, and $\lambda, J \to \infty$ with λ/J^2 fixed and small yield the same result for Δ and E (at the given order in λ/J^2). The overlap indeed occurs and $a_1 = b_1$ holds [21]. The agreement extends to $a_2 = b_2$ [26].

The next question was whether Δ and E match for semi-classical primary operators that are neither BPS nor near-BPS states (by reason of which they are called *far-from-BPS states*). In the semi-classical limit, far-from-BPS states correspond to classical solutions with extended world-sheets in $\mathrm{AdS}_5 \times \mathrm{S}^5$. A hint of the agreement between (1.1) and (1.2) is that E of far-from-BPS states depends linearly on the sum of the semi-classical S_a and J_α at leading order [27]. Thus, E reproduces Δ_0 in (1.1).

The matching between Δ and E in the semi-classical limit of far-from-BPS states was initiated in [20]. Reference [20] considered twist-two operators with large Lorentzian spin S. In $\mathcal{N} = 4$ SYM theory, twist-two operators are trace of two Z and (for instance) a large number S of covariant derivatives along a given light-cone direction. If $\lambda \to 0$ and $S \to \infty$, the conformal dimension of the operator is

$$\gamma = \Delta - S = F(\lambda) \log S + \mathrm{O}(\log S/S) \ , \quad F(\lambda) = \sum_{n=0}^{\infty} a_n \lambda^n \ , \tag{1.7}$$

where $\lambda \to 0$. The series (1.1) is carried by $F(\lambda)$ at $\mathrm{O}(\log S)$.

Twist-two operators with large S are represented by folded spinning strings on $\mathrm{AdS}_5 \times \mathrm{S}^5$. Folded strings were first considered in [28], and they rigidly rotate in AdS_5 and remain fixed at a point of S^5. The world-sheet is strip-shaped instead of cylindrical. Folded strings just carry E and the Lorenzian spin S. If $E, S \sim \sqrt{\lambda} \to \infty$, the dispersion relation is

$$E - S = F(\lambda) \log S + \mathrm{O}(\log S/S) \ , \quad F(\lambda) = \sum_{n=0}^{\infty} b_n \lambda^{(1-n)/2} \ . \tag{1.8}$$

The series (1.2) is carried by $F(\lambda)$ at $\mathrm{O}(\log S)$.

The patterns of both (1.7) and (1.8) with respect to S agree, which is a non-trivial test of the $\mathrm{AdS}_5/\mathrm{CFT}_4$ correspondence. Nonetheless, the function $F(\lambda)$ precludes the comparison from being quantitative. [3] There exist far-from-BPS states for which the match between Δ and E is quantitatively feasible in the semi-classical limit.

Reference [30] noted that there exist far-from-BPS states whose Δ and E admit overlapping analytic perturbative series, similarly to near-BPS states. In $\mathcal{N} = 4$ SYM theory, the total R-charge of far-from-BPS states must be large: $J = J_1 + J_2 + J_3 \to \infty$. The associated primary operators have a large number of fields inside the trace, by reason of which we call

[3] The function $F(\lambda)$ is called *scaling function of the cusp anomalous dimension* and played a central role in the analysis of the $\mathrm{AdS}_5/\mathrm{CFT}_4$ correspondence. We refer to [29] for a review and a complete set of references.

them *long primary operators*. In $AdS_5 \times S^5$, the total angular momentum of the long primary operator must be semi-classical and large, that is $J = J_1 + J_2 + J_3 \sim \sqrt{\lambda} \to \infty$ with λ/J^2 fixed and small. The comparison between Δ and E is feasible if the successive application of $\lambda \to 0$ and $J \to \infty$, and $\lambda, J \to \infty$ with λ/J^2 fixed and small and are equivalent for Δ and E. The conditions are the same as those of near-BPS states. We are neglecting subleading corrections in $1/J$ unless otherwise stated hereafter.

In $\mathcal{N} = 4$ SYM theory, long primary operators comprise a large number J_1 of Z inside the trace. They may comprise a large number J_2 of $Y = (\phi_2 + \mathrm{i}\,\phi_5)/\sqrt{2}$, a large number J_3 of $X = (\phi_3 + \mathrm{i}\,\phi_6)/\sqrt{2}$, or both. (The pair X and Y are the two holomorphic scalars apart from Z.) Long primary operators may also carry a large number S_1 of covariant derivatives along a light-cone directions, a large number S_2 along the other, or both. BPS states with large J are particular long primary operators. If $\lambda \to 0$ and $J \to \infty$, the analytic perturbative series (1.1) is rearranged as

$$\gamma = \frac{\lambda}{J} a_1 + \frac{\lambda^2}{J^3} a_2 + \frac{\lambda^3}{J^5} a_3 + \mathrm{O}\left(\frac{\lambda^4}{J^7}\right) , \tag{1.9}$$

where $\lambda \to 0$. The bare dimension of (1.9) is $\Delta_0 = J$ (or $\Delta_0 = J + S$). The series (1.5) and (1.9) differ since each term of (1.5) is multiplied by an additional factor of $1/J$ with respect to (1.9). The coefficients a_n depend on the ratios of the large S_a and J_α by J.

The computation of γ based on Feynman diagrams for primary operators that involve a large number of fields is challenging. Reference [31] overcame the problem by mapping δD into the Hamiltonian of an integrable spin chain. More precisely, [31] mapped δD at $\mathrm{O}(\lambda)$ in the SO(6) sector (the sector of primary operators composed of Z, Y and X and their anti-holomorphic partners), to the Hamiltonian of an SO(6) integrable spin chain with nearest-neighbours interactions. The total R-charge J is the number of sites the spin chain. The BPS state with given J maps into the ground state of the spin chain (hence the name *BMN vacuum*). Primary operators other than BPS states map into the remaining states of the spin chain. Since the spin chain is integrable, finding the eigenvalues of the Hamiltonian is equivalent to finding the Bethe roots of a set of algebraic Bethe equations. The Bethe equations are implied by the S-matrix of the spin chain. Solving the Bethe equations is still a non-trivial problem. The anomalous dimension γ of long primary operators at $\mathrm{O}(\lambda)$ follows from the Bethe equations. Bethe equations enable an efficient computation of γ for long primary operators that is prohibitive in terms of Feynman diagrams. The limit $J \to \infty$ with a comparable number of Bethe roots is the continuum limit of the spin chain, also called *thermodynamic limit*. The Bethe equations become a set of integral equations for density functions of Bethe roots in the thermodynamic limit. The integral equations can be solved systematically providing the series (1.9).

The computation of γ through an integrable spin-chain can be extended beyond the SO(6) sector and $\mathrm{O}(\lambda)$. Reference [32] mapped the fields of $\mathcal{N} = 4$ SYM theory into an oscillator algebra. Reference [33] built on [32] to map δD, at $\mathrm{O}(\lambda)$ and for general primary operators, into the Hamiltonian of a $\mathrm{PSU}(2,2|4)$ integrable spin chain. Reference [33] proved that a set of Bethe equations encode the anomalous dimensions of primary operators in $\mathcal{N} = 4$ SYM theory. In parallel, [34] made some considerations on the dilatation operator δD to $\mathrm{O}(\lambda^2)$ and $\mathrm{O}(\lambda^3)$. The analysis of [34] reveals that the range of the spin-chain interaction increases by one with each power of λ, that the length of the spin chain in general varies with the spin-chain state, and that integrability holds beyond $\mathrm{O}(\lambda)$.

Long primary operators correspond to classical solutions on $\mathrm{AdS}_5 \times \mathrm{S}^5$ whose J is semi-classical and large. Hence, at least one J_α is semi-classical and large. Classical solutions may also carry semi-classical and large S_a. If $\lambda, J \to \infty$ with λ/J^2 fixed and small, the non-analytic perturbative series (1.2) is rearranged in an analytic perturbative series:

$$E - J = \frac{\lambda}{J} b_1 + \frac{\lambda^2}{J^3} b_2 + \frac{\lambda^3}{J^5} b_3 + \mathrm{O}\left(\frac{\lambda^5}{J^7}\right) . \tag{1.10}$$

(If $S = S_1 + S_2$ is comparable to J, $E - (J + S)$ replaces $E - J$ in (1.10).) The series (1.6) and (1.10) differ since each term of (1.6) is multiplied by an additional factor of $1/J$ with respect to (1.10).

Classical solutions for which (1.10) holds exist. Reference [30] constructed circular spinning strings with two and three large J_α. Circular strings follow the global time-like direction of AdS_5 and rigidly rotate in S^5. (*Circular* stands for a cylindrical world-sheet, as opposed to folded strings.) Circular strings of [30] prompted the construction, led by [35–38], of multiple spinning strings. A crucial step for the systematisation of spinning strings was connection with effective integrable mechanical systems, in particular the Neumann-Rosochatius (NR) system [37,38]. The coefficients b_m in (1.10) depend on the ratios of semi-classical S_a and J_α by J, and they also on mode and winding numbers. References [39–41] showed on general grounds that (1.10) holds if the world-sheet is a nearly-null surface embedded into $\mathrm{AdS}_5 \times \mathrm{S}^5$. References [42, 43] extended the picture to nearly-null world-sheets embedded into the fully supersymmetric $\mathrm{AdS}_5 \times \mathrm{S}^5$. Reference [44] showed that the primary operators for which (1.10) holds are local BPS operators (in contrast with global BPS operators).

Given the analytic series (1.9) and (1.10) in either side of the $\mathrm{AdS}_5/\mathrm{CFT}_4$ correspondence, the check of $\Delta = E$ for dual long primary operators requires to match a_m and b_m. The first step is the proof at $\mathrm{O}(\lambda/J)$, that is $a_1 = b_1$. References [45,46] explicitly checked that $a_1 = b_1$ holds in the two simplest, closed sector. First, the SU(2) sector. In $\mathcal{N} = 4$ SYM theory, long primary operators have a large number J_1 of Z and J_2 of Y. The integrable spin chain is the $\mathrm{XXX}_{1/2}$ Heisenberg model. The SU(2) sector in $\mathrm{AdS}_5 \times \mathrm{S}^5$ encompasses both folded and circular strings with two large angular momenta J_1 and J_2 in $\mathrm{S}^3 \subset \mathrm{S}^5$. Second, the $\mathrm{SL}(2, \mathrm{R})$ sector. In $\mathcal{N} = 4$ SYM theory, long primary operators have a large number J of Z and S of derivatives along a light-cone direction. The integrable spin chain is the $\mathrm{XXX}_{-1/2}$ model. The $\mathrm{SL}(2, \mathrm{R})$ sector in $\mathrm{AdS}_5 \times \mathrm{S}^5$ contains folded strings with large angular momentum J along an equator of S^5 and large Lorentzian spin S in $\mathrm{AdS}_3 \subset \mathrm{AdS}_5$. Reference [46] in fact demonstrated that the matching holds at $\mathrm{O}(\lambda^2/J^3)$, that is $a_2 = b_2$ in both the SU(2) and $\mathrm{SL}(2, \mathrm{R})$ sectors. References [47] and [48] respectively matched at $\mathrm{O}(\lambda/J)$ and $\mathrm{O}(\lambda^2/J^3)$ the infinite hierarchy of higher conserved charges in the Heisenberg $\mathrm{XXX}_{1/2}$ model and the non-linear σ-model in the SU(2) sector for spinning strings.

Long operator are not only realised by spinning strings but also by pulsating strings. Reference [49] first constructed pulsating strings that correspond to long operators, which [44, 50] elaborated on. They pulsate in S^5 and follow the global time-like direction of AdS_5 [44, 49, 50]. Pulsating strings are realised by the NR system [38]. The dispersion relation resembles (1.10), but a semi-classical and large adiabatic invariant N replaces J. (There also exist pulsating strings on AdS_3 whose dispersion relation is non-analytic [49].) Pulsating strings belong to the SO(6) sector, and they are dual to the spin chain of [31]. The relation and $\Delta = E$ holds at $\mathrm{O}(\lambda/N^2)$ [50].

The results of [45, 46, 50] posed the question of whether the matching between Δ and E is feasible beyond specific examples. Two alternative answers were given. Reference [51] advanced the first answer, which [44, 52] elaborated on. The answer relies on the derivation of an effective action. The effective action corresponds to a spin-chain σ-model and implies the analytic series (1.9) and (1.10) beforehand. In $\mathcal{N} = 4$ SYM theory, the effective action is built on coherent states of the spin chain in the Landau-Lifshitz (LL) limit. In the non-linear σ-model on $\mathrm{AdS}_5 \times \mathrm{S}^5$, the effective action follows from a series with respect to λ/J^2 of the classical action itself. The matching of the results imply the matching between Δ and E at a given order in λ. The effective action justifies the appearance of closed-string configurations in the spin chain through coherent states. The effective action is furthermore applicable to closed-superstring configurations, as proposed in [53]. (Whereas supersymmetric classical solutions demands the assignation of an expectation value to the target-space spinors, the effective action does not; see section 1 of [54].) Reference [51] constructed the SU(2) spin-chain σ-model at $\mathrm{O}(\lambda/J)$ and found agreement; [52] extended the agreement between effective actions to $\mathrm{O}(\lambda^2/J^3)$. Moreover, [55, 56] obtained the $\mathrm{SL}(2,\mathrm{R})$ spin-chain σ-model at $\mathrm{O}(\lambda/J)$. Reference [57] extended the effective action to $\mathrm{O}(\lambda^2/J^3)$ from the non-linear σ-model.

The proposal of [51] does not explicitly resort to integrability. Reference [58] gave a second answer, based on integrability, to the question of whether the general matching between Δ and E for long primary operators. In particular, [58] proposed the use of spectral curves. Being integrable, the non-linear σ-model on $\mathrm{AdS}_5 \times \mathrm{S}^5$ admits a Lax connection [18]. The monodromy matrix of the Lax connection in the closed-superstring world-sheet leads to a spectral curve. Closed-superstring moduli are entirely encoded in the spectral curve, which classifies all the classical solutions. The spectral curve permits to obtain a set of integral finite-gap equations. Finite-gap equations can be matched directly with the thermodynamic limit of the Bethe equations. The agreement between (1.9) and (1.10) follows as a consequence. Spectral curves are the adequate starting point for the quantisation of the non-linear σ-model. Reference [58] in particular applied the approach to the SU(2) sector. Reference [58] found agreement between both sides of the $\mathrm{AdS}_5/\mathrm{CFT}_4$ correspondence at $\mathrm{O}(\lambda/J)$ and $\mathrm{O}(\lambda^2/J^3)$. Reference [59] performed the analogous extension in the $\mathrm{SL}(2,\mathrm{R})$ sector. Reference [60] put forward the spectral curve of the fully supersymmetric $\mathrm{AdS}_5 \times \mathrm{S}^5$, and [61] matched it with the thermodynamic limit of the Bethe equations of the $\mathrm{PSU}(2,2|4)$ spin chain at $\mathrm{O}(\lambda/J)$.

Let us recapitulate the three main approaches used to address the spectral problem of long primary operators in type IIB superstring theory. All of them are ultimately based on the integrable non-linear σ-model on $\mathrm{AdS}_5 \times \mathrm{S}^5$ that was constructed in [17]. First, spinning strings (and pulsating strings), especially through effective integrable mechanical systems. Second, effective actions for spin-chain σ-model, which are linked to coherent states. Third, algebraic curves or, equivalently, finite-gap equations, which encode the closed-string moduli. Each of the three approaches shed light on bosonic strings on $\mathrm{AdS}_5 \times \mathrm{S}^5$ with semi-classical Noether charges from a complementary point of view.

In this text, we apply the first and third points of view to analyse bosonic strings on $\mathrm{AdS}_3 \times \mathrm{S}^3 \subset \mathrm{AdS}_3 \times \mathrm{S}^3 \times \mathrm{T}^4$ with mixed RR and NSNS flux, and pure NSNS flux. [4] We also use coherent states and spin-chain σ-models in the limit of pure NSNS flux. We review $\mathrm{AdS}_3 \times \mathrm{S}^3 \times \mathrm{T}^4$ with mixed RR and NSNS flux, and pure NSNS flux in section 1.2. Before we change the subject, we briefly review the resolution of the spectral problem in the $\mathrm{AdS}_5/\mathrm{CFT}_4$ correspondence, where integrability realised its potential. Integrability in $\mathrm{AdS}_5 \times \mathrm{S}^5$ in turn laid the foundations of large part of the progress made on $\mathrm{AdS}_3 \times \mathrm{S}^3 \times \mathrm{T}^4$.

The matching $a_1 = b_1$ and $a_2 = b_2$ for long operators suggests the coincidence of (1.9) and (1.10). However, [46, 67] encountered the mismatch $a_3 \neq b_3$. The existence of an interpolating, non-perturbative function, called *dressing phase*, is responsible for the mismatch. It also accounts for the mismatch at $\mathrm{O}(\lambda^3/J^6)$ of near-BPS states in the BMN limit [68].

Reference [69] wrote the asymptotic all-loop Bethe equations in the $\mathrm{SU}(2)$ sector of $\mathcal{N} = 4$ SYM theory. The Bethe equations of [69] are called *asymptotic* since they neglect finite-size corrections in the limit $J \to \infty$ (J is the number of sites of the spin chain, and, thus, the size thereof). The Bethe equations of [69] have an analogue in the non-linear σ-model on $\mathrm{AdS}_5 \times \mathrm{S}^5$. Reference [70] proposed a set of algebraic Bethe equations for the $\mathrm{SU}(2)$ sector of $\mathrm{AdS}_5 \times \mathrm{S}^5$, which discretise the finite-gap equations of [58]. The Bethe equations of [70] introduced the dressing phase. The dressing phase accounts for the disagreement between (1.9) and (1.10) in the $\mathrm{SU}(2)$ sector of both sides of the $\mathrm{AdS}_5/\mathrm{CFT}_4$ correspondence at $\mathrm{O}(\lambda^3/J^5)$. In $\mathcal{N} = 4$ SYM theory, (1.9) requires the successive applications of $\lambda \to 0$ and $J \to \infty$, where the dressing phase is exponentially suppressed. In $\mathrm{AdS}_5 \times \mathrm{S}^5$, (1.10) requires the application of $\lambda, J \to \infty$ with λ/J^2 fixed and small, where the dressing phase contributes at $\mathrm{O}(\lambda^3/J^5)$ to the series (1.10). The dressing phase in other sectors, such as the $\mathrm{SL}(2,\mathrm{R})$ sector, was later studied in [71].

Reference [72] put forward the set of asymptotic all-loop Bethe equations of the complete $\mathrm{PSU}(2,2|4)$ spin chain of $\mathcal{N} = 4$ SYM theory. Reference [73] used the symmetries of the asymptotic all-loop S-matrix of [72] to obtain the non-perturbative dispersion relation of magnons. Magnons consist of a linear superposition of creation operators, called *oscillators*, with definite momentum above the BMN vacuum. Reference [74] assembled the creation and annihilation operators in a Zamolodchikov-Faddeev algebra, which is a deformation by the string tension of the canonical harmonic-oscillator algebra that arises in the BMN limit. Magnons are massive excitations. The dispersion of magnons is non-relativistic and periodic with respect to the momentum of the magnon. Reference [75] derived the all-loop Bethe equations of the non-linear σ-model on $\mathrm{AdS}_5 \times \mathrm{S}^5$. The construction of [75] is based on

[4] In this section, we have focused on the duality for primary operators. The $\mathrm{AdS}_5/\mathrm{CFT}_4$ correspondence between Wilson loops in $\mathcal{N} = 4$ SYM theory and partition functions over open-superstrings configurations on (Euclidean) $\mathrm{AdS}_5 \times \mathrm{S}^5$, elaborated in [62, 63], sets the basis of part of the text. Our starting points are nonetheless the minimal surfaces of [64], which are based on the spinning strings of [37, 38], and the algebraic curves of [65, 66], which adapt the proposal of [58] to open-string world-sheets.

the computation of the asymptotic all-loop S-matrix under the imposition of the light-cone gauge-fixing condition on the world-sheet. The dispersion relation of [75] matches the proposal of [73]. Reference [76] used central extensions of the symmetry superalgebra to write a shortening condition that provides the dispersion relation of magnons.

The dressing phase is not given beforehand but must be determined. Reference [72] wrote the structure of the dressing phase. Reference [77] computed the leading quantum corrections to the dressing phase from the non-linear σ-model in the SU(2) and $\mathrm{SL}(2,\mathrm{R})$ sectors. Reference [78] argued that crossing symmetry constrains the dressing phase of the $\mathrm{AdS}_5/\mathrm{CFT}_4$ correspondence. Reference [79] checked that crossing symmetry holds in the first orders available. Reference [80] constructed the solution of the dressing phase in the limit $\lambda \to \infty$; [81] connected the results of [80] with the dressing phase in the limit $\lambda \to 0$.

We close the section with a comment on finite-size corrections. The hitherto ignored subleading corrections in the $J \to \infty$ are not incorporated in the asymptotic all-loop Bethe equations, as we have already mentioned. The asymptotic Bethe equations must be promoted to the thermodynamic Bethe ansatz to include finite-size corrections. Further research eventually yielded the quantum spectral curve of the $\mathrm{AdS}_5/\mathrm{CFT}_4$ correspondence, which constitutes the final answer to the spectral problem of the duality. We refer to [82], [83], and [84] for reviews on the dressing phase, the thermodynamic Bethe equations and the quantum spectral curve, respectively, where complete sets of references can be found.

1.2 $\mathrm{AdS}_3 \times \mathrm{S}^3 \times \mathrm{T}^4$ with Neveu-Schwarz-Neveu-Schwarz flux

The duality between type IIB superstring theory on $\mathrm{AdS}_5 \times \mathrm{S}^5$ with pure RR flux and $\mathcal{N} = 4$ SYM theory triggered the quest for realisations of the $\mathrm{AdS}_{d+1}/\mathrm{CFT}_d$ correspondence where integrability holds. Type IIB superstring theory on $\mathrm{AdS}_3 \times \mathrm{S}^3 \times \mathrm{T}^4$ with pure RR flux, and mixed RR and NSNS flux is integrable. Integrability holds at the point of pure NSNS flux. The $\mathrm{AdS}_3 \times \mathrm{S}^3 \times \mathrm{T}^4$ background realises one side of the $\mathrm{AdS}_3/\mathrm{CFT}_2$ correspondence. In this section, we review advances made in this context. We focus on $\mathrm{AdS}_3 \times \mathrm{S}^3 \times \mathrm{T}^4$ with mixed flux and pure NSNS flux.

Early studies on type IIB superstring theory on $\mathrm{AdS}_3 \times \mathrm{S}^3 \times \mathrm{T}^4$ stemmed from the foundational article [3], where it was proposed to realise the $\mathrm{AdS}_3/\mathrm{CFT}_2$ correspondence. (K3 could replace T^4 without major changes in the remainder of the text.) The near-horizon limit of the combination of the D1/D5 system, which consists of D1-branes and D5-branes, with the F1/NS5 system, which consists of F1-strings and NS5-branes, gives rise to $\mathrm{AdS}_3 \times \mathrm{S}^3 \times \mathrm{T}^4$. The D1/D5 and F1/NS5 systems are responsible for the RR and NSNS three-form fluxes, respectively. The isometry supergroup of the GS action on $\mathrm{AdS}_3 \times \mathrm{S}^3 \subset \mathrm{AdS}_3 \times \mathrm{S}^3 \times \mathrm{T}^4$ is $\mathrm{PSU}(1,1|2)_L \times \mathrm{PSU}(1,1|2)_R$, which has sixteen supercharges, half of the supercharges of $\mathrm{PSU}(2,2|4)$. The dual CFT_2 under the $\mathrm{AdS}_3/\mathrm{CFT}_2$ correspondence is presumably the deformation of the so-called symmetric product orbifold of T^4 [85], which exhibits $\mathcal{N} = (4,4)$ supersymmetry. The $\mathrm{AdS}_3/\mathrm{CFT}_2$ correspondence has been stated with increasing accuracy at the point of pure NSNS flux over the years (see, for instance, [86] and references therein). On the contrary, the formulation of the $\mathrm{AdS}_3/\mathrm{CFT}_2$ correspondence with mixed RR and NSNS flux waits for further clarifications. [5]

Reference [89] started the analysis of $\mathrm{AdS}_3 \times \mathrm{S}^3 \times \mathrm{T}^4$ in the Ramond-Neveu-Schwarz (RNS) formalism. Reference [90] wrote, for the first time, the GS action on $\mathrm{AdS}_3 \times \mathrm{S}^3 \times \mathrm{T}^4$ with mixed flux by imposing a gauge-fixing condition with respect to κ-symmetry transformations. Reference [91] rephrased the classical GS action on $\mathrm{AdS}_3 \times \mathrm{S}^3$ as a non-linear σ-model on $\mathrm{PSU}(1,1|2)_L \times \mathrm{PSU}(1,1|2)_R/\mathrm{SL}(2,\mathrm{R}) \times \mathrm{SU}(2)$ along the lines of [17]. Reference [91] also noticed that the NSNS flux implies a modification of the Wess-Zumino (WZ) term of [17]. Reference [92] addressed the quantisation of type IIB superstring theory on $\mathrm{AdS}_3 \times \mathrm{S}^3$ with mixed flux. To this end, [92] applied the hybrid GS and RNS formalism to the $\mathrm{PSU}(1,1|2)$ Wess-Zumino-Novikov-Witten (WZNW) model, which corresponds to $\mathrm{AdS}_3 \times \mathrm{S}^3$ with pure NSNS flux, with additional RR flux present.

If the RR flux vanishes, the quantum spectrum of energies of the $\mathrm{PSU}(1,1|2)$ WZNW model is exactly computable. The spectrum follows from the analysis of unitary irreducible representations of the Kač-Moody algebra of the world-sheet currents in the RNS formalism. Reference [93] computed the spectrum of the $\mathrm{SL}(2,\mathrm{R})$ WZNW model that realises bosonic-string theory on AdS_3 with pure NSNS flux. The spectrum is distributed among different spectrally flowed sectors characterised by an integer number. The organisation of the spectrum mimics that of the current algebra. The current algebra in each spectrally flowed sector is built on the representations spanned by the zeroth-level generators of the current algebra. The zeroth-level generators realise two possible sequences of representations of $\mathrm{SL}(2,\mathrm{R})$: the principal discrete series and the principal continuous series. The labels of representations in the principal discrete series satisfy a unitarity bound that differs in each spectrally flowed sector. The results of [93] were generalised in [94] to the $\mathrm{PSU}(1,1|2)$ WZNW model, which has analogous properties to the $\mathrm{SL}(2,\mathrm{R})$ WZNW model.

Integrability enabled new advances in type IIB superstring theory on $\mathrm{AdS}_3 \times \mathrm{S}^3 \times \mathrm{T}^4$ with mixed flux. Based on the analysis of [95] of integrability at the point of pure RR flux, [88] proved that the classical non-linear σ-model on $\mathrm{AdS}_3 \times \mathrm{S}^3$ with mixed flux is integrable by constructing the Lax connection. The presence of NSNS flux is reflected in a topologically non-trivial WZ term in the action. The Lax connection degenerates if the RR flux vanishes. The action of the non-linear σ-model on $\mathrm{AdS}_3 \times \mathrm{S}^3$ is equivalent to the GS action on $\mathrm{AdS}_3 \times \mathrm{S}^3 \times \mathrm{T}^4$. Equivalence holds under the imposition of a gauge-fixing condition with respect to κ-symmetry transformations. If the RR flux vanishes, the non-linear σ-model on $\mathrm{AdS}_3 \times \mathrm{S}^3$ with mixed flux reduces to the $\mathrm{PSU}(1,1|2)$ WZNW model.

Following [75], reference [96] computed the tree-level S-matrix for magnons over the BMN vacuum of $\mathrm{AdS}_3 \times \mathrm{S}^3 \times \mathrm{T}^4$, which is a BPS state. As opposed to magnons in $\mathrm{AdS}_5 \times \mathrm{S}^5$, magnons can be massless in $\mathrm{AdS}_3 \times \mathrm{S}^3 \times \mathrm{T}^4$. Massive and massless excitations correspond

[5] Solutions to type IIB supergravity on $\mathrm{AdS}_3 \times \mathrm{S}^3 \times \mathrm{T}^4$ in general involve more parameters than the common radius to both AdS_3 and S^3, and the amount of RR and NSNS fluxes. For instance, [87] formally realised $\mathrm{AdS}_3 \times \mathrm{S}^3 \times \mathrm{T}^4$ as the marginal deformation of the near-horizon limit of a system of F1-strings and NS5-branes with non-trivial dilaton, axion, and RR seven-form which drop in the proper near-horizon limit. In this text, we make the customary assumption that $\mathrm{AdS}_3 \times \mathrm{S}^3 \times \mathrm{T}^4$ realises free type IIB superstring theory in such a way that the non-linear σ-model of [88] realises the truncation to $\mathrm{AdS}_3 \times \mathrm{S}^3$. We refer to [87] and references therein for a discussion of the moduli of type IIB supergravity in general.

to the non-linear σ-model on $\mathrm{AdS}_3 \times \mathrm{S}^3$ and to the flat T^4-directions, respectively. (The flat T^4-directions are in fact also responsible for the existence of BPS states other than the BMN vacuum, associated to massless fermionic states, as [97] first noted; see [98] and references therein.) The construction of [96] led [99] to obtain an asymptotic all-loop S-matrix for massive excitations. Reference [100] checked the proposal of [99] at one-loop and two-loops. Following [76], reference [99] also wrote the dispersion relation of massive magnons by drawing on the shortening condition of the central extension of the isometry superalgebra. While the dispersion relation is in general non-relativistic, the NSNS flux destroys the periodicity of the dispersion relation with respect to the momentum of magnons. The dispersion relation becomes relativistic and chiral at the point of pure NSNS flux. The S-matrix furthermore breaks down at the point of pure NSNS flux due to the contraction of the isometry superalgebra in the light-cone gauge. Reference [101] corroborated the dispersion relation obtained [99] by means of classical solutions with semi-classical Noether charges. Reference [102] used [99] to write a set of asymptotic all-loop Bethe equations. The thermodynamic limit of the Bethe equations of [102] match the finite-gap equations of the non-linear σ-model on $\mathrm{AdS}_3 \times \mathrm{S}^3$ with mixed flux. Reference [102] also computed the dressing phase at leading-order. The dressing phase in the massive sector was also studied at tree and one-loop order in [102–104]. Reference [105] enhanced the asymptotic all-loop S-matrix of [99] to include massive and massless excitations. The associated dressing phase was studied in [106], thus extending the dressing phase of [107, 108] at point of pure RR flux.

Even though the previous advances are not directly valid if the RR flux vanishes, integrability still applies to $\mathrm{AdS}_3 \times \mathrm{S}^3 \times \mathrm{T}^4$ with pure NSNS flux. Reference [109] anticipated and [110] established that the spectrum of the $\mathrm{PSU}(1,1|2)$ WZNW model is retrievable from an integrable spin chain. Supplementary bosonic and fermionic fields in the world-sheet CFT_2 account from the embedding in T^4 [111]. Reference [109] proposed an asymptotic all-loop S-matrix for magnons over the BMN vacuum in the light-cone gauge. The S-matrix is based on $T\bar{T}$-deformations. Reference [110] proved the cancellation of finite-size corrections in the thermodynamic Bethe ansatz. The Bethe equations are then exact. Reference [110] realised that the explicit resolution of the equations is feasible. Thus, the Bethe equations supply the spectrum in representations of the current algebra built on the (highest-weight and lowest-weight) principal discrete series of $\mathrm{PSU}(1,1|2)$ in every spectrally flowed sector. They also admit exceptional solutions that violate the unitarity bound of the principal discrete series. Reference [112] argued that exceptional solutions give the spectrum of the principal continuous series of $\mathrm{PSU}(1,1|2)$ in spectrally flowed sectors.

1.3 Overview

This thesis is devoted to the analysis of bosonic strings on $\mathrm{AdS}_3 \times \mathrm{S}^3$ with mixed RR and NSNS flux, and with pure NSNS flux. Our strategy is based on the use of techniques applied in the semi-classical limit of $\mathrm{AdS}_5 \times \mathrm{S}^5$. Our goal is to provide results on the classical and semi-classical limit of type IIB superstring theory on $\mathrm{AdS}_3 \times \mathrm{S}^3 \times \mathrm{T}^4$ that help to clarify the system itself and the $\mathrm{AdS}_3/\mathrm{CFT}_2$ correspondence. The thesis has the following structure.

- Chapter 2 is a review of classical integrable non-linear σ-models. We discuss coset models based on semi-symmetric spaces and permutation supercosets. We present the bosonic-string action on $\mathrm{AdS}_3 \times \mathrm{S}^3$ with NSNS flux. We review the Lax connection on $\mathrm{AdS}_3 \times \mathrm{S}^3$ with mixed flux. We use the Lax connection to construct local spectral curves for factorised solutions.

- Chapter 3 is based on [P1]. We consider pulsating strings on $\mathrm{AdS}_3 \times \mathrm{S}^3$ with NSNS flux. We present the integrable deformation of the NR system under NSNS flux following [P6]. We construct and analyse classical solutions on $\mathrm{AdS}_3 \times \mathrm{S}^1$ exhaustively. We write their dispersion relation in a closed form by choosing properly closed-string moduli. We retrieve the short-string and long-string classes of pulsating strings of Maldacena and Ooguri in the limit of pure NSNS flux. We construct the local spectral curve of pulsating strings on $\mathrm{AdS}_3 \times \mathrm{S}^1$, which is an elliptic curve, and map it that of minimal surfaces. We prove the singularisation of the elliptic curve in the limit of pure NSNS flux.

- Chapter 4 is based on [P3]. We consider minimal surfaces that subtend an annulus at the boundary of Euclidean AdS_3 with NSNS flux. We construct and analyse connected and disconnected minimal surfaces exhaustively. We present the two classes of connected minimal surfaces in the limit of pure NSNS flux. We compute the regularised on-shell action in the presence of NSNS flux. We construct the local spectral curve of minimal surfaces in Euclidean AdS_3, which is an elliptic curve. We use modular functions to analyse the elliptic curve. We prove the singularisation of the elliptic curve in the limit of pure NSNS flux.

- Chapter 5 is based on [P4, P7]. We compute the effective action of the $\mathrm{SL}(2,\mathrm{R})$ and $\mathrm{SU}(2)$ spin-chain σ-models of the $\mathrm{PSU}(1,1|2)$ WZNW model in every spectrally flowed sector. We compute the effective action by performing a series with respect to the semi-classical effective coupling of the gauge-fixed classical action. We obtain again the effective action from the world-sheet spin chain. We postulate the coherent states in the world-sheet. We prove the that temporal and spatial intervals are discrete and related to each other. We apply an unconventional LL limit to obtain a semi-classical path integral over coherent states, whereby we deduce the effective action. We conclude that the results of both approaches agree.

- Chapter 6 contains conclusions and possible lines of research. We comment briefly on [P2, P5].

- Appendix A summarises our conventions for world-sheet objects.

- Appendix B provides the defining representation of $\mathfrak{su}(1,1|2)$ used in subsection 2.1.2.

- Appendix C presents the coordinate systems of $\mathrm{AdS}_3 \times \mathrm{S}^3$ and related objects.

- Appendix D presents the finite-gap equations of $\mathrm{AdS}_3 \times \mathrm{S}^3$ with mixed flux.

- Appendix E is a review of the background on elliptic curves for sections 3.3 and 4.3.

- Appendix F writes the conventions for the elliptic integrals and Jacobian elliptic functions used in sections 3.2, 4.1, and 4.2 and lists properties and formulae.

Chapter 2

Classical integrable non-linear σ-models

Classical integrability arises in free type II superstring theory realised on semi-symmetric spaces. Classical integrability is explicit in the formulation of the GS action in terms of the non-linear σ-model on the supercoset that underlies the semi-symmetric space.

Reference [113] took the first step towards the uncovering of classical integrability in free type II superstring theory. Reference [113] rephrased the GS action of [114], based on the ten-dimensional Minkowski background M_{10}, as the action of a supercoset model endowed with a three-dimensional WZ term. The WZ term involves both bosonic and fermionic components of the left-invariant current of the supercoset model. The imposition of invariance of the action under κ-symmetry transformations fixes the overall coefficient of the WZ term [114]. Reference [17] applied the approach of [113] to the $\mathrm{AdS}_5/\mathrm{CFT}_4$ correspondence by representing free type IIB superstring theory on $\mathrm{AdS}_5 \times \mathrm{S}^5$ with pure RR five-form flux as a non-linear σ-model on $\mathrm{PSU}(2,2|4)/\mathrm{SO}(1,4) \times \mathrm{SO}(5)$. The supercoset is a semi-symmetric space because $\mathfrak{psu}(2,2|4)$ admits a Z_4-automorphism. Reference [115] noticed the importance of the Z_4-automorphism and used it to prove that the WZ term is topologically trivial. The WZ term admits a two-dimensional formulation that just involves the fermionic components of the left-invariant current which renders the entire action local. Reference [116] wrote an invariant formulation of the action under the Z_4-automorphism.

Reference [19] realised that the bosonic truncation of the supercoset model consists of an integrable coset model on $\mathrm{AdS}_5 \cong \mathrm{SO}(2,4)/\mathrm{SO}(1,4)$ and another on $\mathrm{S}^5 \cong \mathrm{SO}(6)/\mathrm{SO}(5)$. [1] The Virasoro constraints bind together both models, but they do not destroy classical integrability in either of them. The Lax connection of each model remains valid and generates an infinite hierarchy of conserved charges. [2] Reference [18] extended the Lax connection of [19] to the full background by drawing on the Z_4-automorphism of $\mathrm{AdS}_5 \times \mathrm{S}^5$. The Z_4-automorphism permits to write the Lax connection as a linear combination of the components of different grading of

[1] We often identify AdS_{d+1} with a coset. Even thought the identification abridges our discussion, we must emphasise that AdS_{d+1} is actually the universal cover of the coset; AdS_{d+1} would otherwise include closed time-like curves. We make the distinction between the coset and its universal cover explicit when necessary.

[2] Classical integrability defined in terms of the existence of the Lax connection is called *weak integrability*. Hamiltonian classical integrability, or *strong integrability*, requires the conserved charges generated by the Lax connection to be in involution with respect to the symplectic structure. We ignore this property in this text. We refer to subsection 2.3 of [117] for a review of Hamiltonian classical integrability in the $\mathrm{AdS}_5/\mathrm{CFT}_4$ correspondence, which includes a complete set of references on strong integrability.

the left-invariant current. Reference [18] suggested that the existence of the Lax connection in the supercoset model is equivalent to the invariance under κ-symmetry transformations of the action. Reference [118] further hinted towards the equivalence of both properties with quantum world-sheet conformal invariance at one-loop. Reference [119] demonstrated the equivalence between invariance under κ-symmetry transformations of the action and quantum world-sheet conformal invariance at one-loop. Reference [7] proved that the existence of the Lax connection is equivalent to the invariance of the action under κ-symmetry transformations (and to quantum world-sheet conformal invariance at one-loop as a consequence).

The existence of the Lax connection ultimately relies on the structure of $\mathrm{AdS}_5 \times \mathrm{S}^5$ as a semi-symmetric space. This fact poses the question of the classical integrability of other AdS_{d+1}-backgrounds that have a Z_4-automorphism. Reference [120] built on the algebraic classification of semi-symmetric spaces to exhaust AdS_{d+1}-backgrounds on which non-linear σ-models admit a Lax connection. The Lax connection in every semi-symmetric space mimics the decomposition in components of different grading of the Lax connection in $\mathrm{AdS}_5 \times \mathrm{S}^5$. The imposition of both quantum world-sheet conformal invariance at one-loop and invariance under κ-symmetry transformations single out consistent semi-symmetric spaces. The upshot is the existence of two consistent semi-symmetric spaces: $\mathrm{AdS}_5 \times \mathrm{S}^5$ with pure RR five-form flux, which realises type IIB superstring theory, and $\mathrm{AdS}_4 \times \mathrm{CP}^3$ with pure RR four-form flux, which realises type IIA superstring theory. The coupling of supercoset models to a CFT_2 on an external manifold permits to include semi-symmetric spaces of non-critical dimension. Two of them are permutation supercosets with pure RR three-form flux and consistently realise type IIB superstring theory. They are $\mathrm{AdS}_3 \times \mathrm{S}^3 \times \mathrm{S}^3 \times \mathrm{S}^1$, whose permutation supercoset is $\mathrm{D}(2,1;\alpha)_L \times \mathrm{D}(2,1;\alpha)_R/\mathrm{SL}(2,\mathrm{R}) \times \mathrm{SO}(4)$, and $\mathrm{AdS}_3 \times \mathrm{S}^3 \times \mathrm{T}^4$, whose permutation supercoset is $\mathrm{PSU}(1,1|2)_L \times \mathrm{PSU}(1,1|2)_R/\mathrm{SL}(2,\mathrm{R}) \times \mathrm{SU}(2)$. The supercoset models on both permutation supercosets were first constructed in [95] in the light of integrability.

Reference [88] extended the action of these permutation-supercoset models through a topologically non-trivial WZ term. The WZ term accounts for the presence of NSNS flux in the background and preserves the integrability of the supercoset model. The NSNS flux coexists ('mixes') with the RR flux. Topologically non-trivial WZ terms exist in permutation supercosets because their bosonic truncations are group manifolds (as opposed to general semi-symmetric spaces). The action of a principal chiral model, a coset model on a group manifold, admits a topologically non-trivial WZ terms [121–124]. Even though the WZ term is non-local, it respects the locality of the equations of motion. The topologically non-trivial WZ term lifts to a permutation-supercoset model through the addition of non-local terms, which involve both bosonic and fermionic components of the left-invariant current. The lifted WZ term preserves the locality of the equations of motion. The Lax connection exists if a constraint is satisfied. The constraint intertwines the coefficients of the topologically trivial and non-trivial WZ terms, and the RR flux and the NSNS flux. The constraint implies both quantum world-sheet conformal invariance at one-loop and invariance under κ-symmetry transformations. The Lax connection still decomposes under the Z_4-automorphism. Hence, it is the linear combination of components of different grading even under the presence of NSNS flux. References [88, 102] showed that the coefficients of the sum are deformed nonetheless.

Moreover, the permutation-supercoset model reduces to a WZNW model if the RR flux vanishes. The Lax connection of the model degenerates if the RR flux vanishes.

In this chapter, we present the non-linear σ-model on $\mathrm{AdS}_3 \times \mathrm{S}^3$ with NSNS flux, which corresponds to the bosonic truncation of the permutation-supercoset model of type IIB superstring theory on $\mathrm{AdS}_3 \times \mathrm{S}^3 \times \mathrm{T}^4$ with mixed RR and NSNS flux, and pure NSNS flux. The chapter has the following structure. In section 2.1, we construct the action of classical integrable supecoset models. In subsection 2.1.1, we construct the action of supercoset models based on general semi-symmetric spaces. We then discuss the conditions required by type II superstring theory in general semi-symmetric spaces and present consistent backgrounds. In subsection 2.1.2, we specify the procedure of the previous subsection to the class of permutation supercosets within semi-symmetric spaces. We extend the action through a topologically non-trivial WZ term. We finally present the permutation-supercoset of interest. In subsection 2.1.3, we introduce the bosonic truncation of the action on our permutation supercoset to $\mathrm{AdS}_3 \times \mathrm{S}^3$ with NSNS flux, which corresponds to a principal chiral model. We present and comment on the resultant Polyakov action plus a two-dimensional WZ term for the B-field. In section 2.2, we focus on classical integrability in our permutation-supercoset model on $\mathrm{AdS}_3 \times \mathrm{S}^3$ with mixed RR and NSNS flux. In subsection 2.2.1, we construct the Lax connection in a general semi-symmetric space and specify it to our case. In subsection 2.2.2, we present the monodromy matrix. Reference [66] built on the Lax connection and the monodromy matrix to obtain local spectral curves for arbitrary factorisable classical solutions on symmetric spaces. We close subsection 2.2.2 with an extension of the procedure of [66] to $\mathrm{AdS}_3 \times \mathrm{S}^3$ with NSNS flux. Throughout this chapter we use world-sheet differential forms. We list our conventions for world-sheet differential forms and tensor objects in appendix A.

2.1 The action of non-linear σ-models

We devote this section to the action of classical integrable non-linear σ-models on supercosets. In subsection 2.1.1, we present supercoset models on semi-symmetric spaces in the context of type II superstring theory. We follow [95, 120, 125], where we refer the reader for a more exhaustive discussion. In subsection 2.1.2, we specify the construction of the previous section when the semi-symmetric space is a permutation supercoset. We then extend the action with a non-trivial WZ term following [88, 102]. Again, we refer to these references for a more exhaustive discussion. For readability, we have included a brief digression on principal chiral models with non-trivial WZ term along the lines of [122, 123]. We focus on the case of $\mathrm{AdS}_3 \times \mathrm{S}^3 \times \mathrm{T}^4$ with mixed RR and NSNS flux, and NSNS flux at the end of the subsection. In subsection 2.1.2, we introduce the bosonic truncation of $\mathrm{AdS}_3 \times \mathrm{S}^3 \times \mathrm{T}^4$ and present the Polyakov action plus a two-dimensional WZ term for bosonic strings on $\mathrm{AdS}_3 \times \mathrm{S}^3$ with NSNS flux. Considerations on Lie superalgebras of the section can be found in [126].

2.1.1 The action of non-linear σ-models on semi-symmetric spaces

Let G be a Lie supergroup. It has two composition laws: the left and right multiplications. Let H be a Grassmann-even (bosonic) subgroup of G. The supercoset G/H is the set of equivalence classes with respect to the right multiplication of elements of G by elements of H. The supercoset is a manifold whose points are equivalence classes in G/H. The canonical extension of the left multiplication of G to the supercoset G/H is a transitive action (G/H is a left homogeneous space with respect to G).

Let $\mathfrak{g}$ be the Lie superalgebra of G. The supercoset G/H is a semi-symmetric space if $\mathfrak{g}$ has a Z_4-automorphism Ω with respect to the Lie superbracket $[\cdot,\cdot]$. The automorphism Ω satisfies $\Omega^2 = (-)^F$, where $(-)^F$ denotes the Grassmann-parity involution of $\mathfrak{g}$. The automorphism Ω induces the decomposition $\mathfrak{g} = \mathfrak{g}_0 \oplus \mathfrak{g}_1 \oplus \mathfrak{g}_2 \oplus \mathfrak{g}_3$, where $\Omega(\mathfrak{g}_a) = \mathrm{i}^a\, \mathfrak{g}_a$. Subspaces $\mathfrak{g}_0$ and $\mathfrak{g}_2$ are bosonic, whereas $\mathfrak{g}_1$ and $\mathfrak{g}_3$ are Grassmann-odd, that is fermionic. By definition, $\mathfrak{g}_0 \equiv \mathfrak{h}$ is the Lie algebra of H. The subscript a of $\mathfrak{g}_a$ is called *grading*. Subspaces of different grading satisfy $[\mathfrak{g}_a, \mathfrak{g}_b] \subset \mathfrak{g}_{(a+b)\mathrm{mod}4}$.

The decomposition of $\mathfrak{g}$ in terms of $\mathfrak{g}_a$ is orthogonal with respect to the supertrace. The supertrace is not defined in $\mathfrak{g}$ but in a representation of $\mathfrak{g}$, which we assume to be a supermatrix finite-dimensional representation. [3] We do not discriminate between $\mathfrak{g}$ and its representation hereafter as no misunderstanding will arise. Moreover, every $\mathfrak{g}$ that we consider admits a supertrace. The supertrace str is a form in $\mathfrak{g}$ that is bilinear, cyclic, and Ω-invariant. As we have already mentioned, $\mathfrak{g}_a$ are orthogonal with respect to str:

$$\mathrm{str}(M_a M_b) = 0\ , \quad M_a \in \mathfrak{g}_a\ , \quad a + b \neq 0 \mod 4\ . \tag{2.1}$$

To make str explicit, we must know further specifications of $\mathfrak{g}$, for instance the dimension of $\mathfrak{g}$ and the normalisation of its generators.

We introduce the fields involved in a non-linear σ-model on a semi-symmetric space now. The fields are differentiable embedding maps from a two-dimensional smooth manifold Σ, called *world-sheet*, into the supercoset G/H, called both *background* and *target space*. Therefore, the fields map points of Σ onto equivalence classes of G/H. To write the action we must consider differentiable embedding maps $g : \Sigma \to \mathrm{G}$ endowed with a equivalence relation. Two mappings $g, g' : \Sigma \to \mathrm{G}$ are equivalent (they represent the same configuration in the non-linear σ-model) if there exists a third mapping $h : \Sigma \to \mathrm{H}$ such that $g' = gh$ pointwise.

Embedding maps $g : \Sigma \to \mathrm{G}$ allow us to define the Maurer-Cartan form, also known as *left-invariant current*. The left-invariant current is a $\mathfrak{g}$-valued world-sheet one-form defined by $j = g^{-1}\mathrm{d}g$, where d denotes the exterior derivative in the world-sheet. By using Ω, we can decompose j as

$$j = g^{-1}\mathrm{d}g = j_0 + j_1 + j_2 + j_3\ , \quad j_a \in \mathfrak{g}_a\ . \tag{2.2}$$

Under the mapping between equivalent representatives $g \mapsto gh$, the components of different grading transform as

$$j_0 \mapsto h^{-1} j_0 h + h^{-1}\mathrm{d}h\ , \quad j_a \mapsto h^{-1} j_a h\ , \quad a = 1, 2, 3\ . \tag{2.3}$$

[3] If the complexification of $\mathfrak{g}$ is $\mathfrak{psu}\,(N|N)_{\mathrm{C}}$, $\mathfrak{g}$ is not realisable in terms of $(2N \times 2N)$-supermatrices; see, for instance, section 9 of [125]. In this case, one can realise $\mathfrak{g}$ in the defining representation of $\mathfrak{su}\,(N|N)_{\mathrm{C}}$ in terms of $(2N \times 2N)$-supermatrices under the identification of elements that differ by multiples of the identity supermatrix. We adopt this approach to construct $\mathfrak{psu}(1,1|2)$-valued supermatrices in appendix B.

The component j_0 behaves as a connection, whereas the remaining components transform in the adjoint representation of H. Moreover, the left-invariant current is flat by construction:

$$\mathrm{d}j + j \wedge j = 0 \ , \tag{2.4}$$

where $\wedge$ denotes the exterior product in the world-sheet. If we project (2.4) on each subspace $\mathfrak{g}_a$, we obtain

$$\mathrm{d}j_0 + j_0 \wedge j_0 + j_1 \wedge j_3 + j_2 \wedge j_2 + j_3 \wedge j_1 = 0 \ , \tag{2.5}$$
$$\mathrm{d}j_1 + j_0 \wedge j_1 + j_1 \wedge j_0 + j_2 \wedge j_3 + j_3 \wedge j_2 = 0 \ , \tag{2.6}$$
$$\mathrm{d}j_2 + j_0 \wedge j_2 + j_1 \wedge j_1 + j_2 \wedge j_0 + j_3 \wedge j_3 = 0 \ , \tag{2.7}$$
$$\mathrm{d}j_3 + j_0 \wedge j_3 + j_1 \wedge j_2 + j_2 \wedge j_1 + j_3 \wedge j_0 = 0 \ . \tag{2.8}$$

The flatness condition is necessary to both write the equations of motion of the action and demonstrate of exactness of the WZ term thereof.

The action of a supercoset model on a semi-symmetric space G/H follows from two requirements: invariance under the local right action of H and Ω-invariance. The former requirement ensures that G/H is actually the target space; the latter that the structure of semi-symmetric space is preserved. The left and right multiplications of G in G/H are transitive, implying that G is the isometry supergroup. The Noether theorem is applicable to the action and yields the Noether charges of the model. If G/H is not only a semi-symmetric space but also a background of type II superstring theory, G and H realise symmetries of the background. Invariance under the local right action of H equals local Lorentz invariance [7]. This fact together with (2.3) leads to the identification of $h : \Sigma \to \mathrm{H}$ with gauge fields and H with a gauge-symmetry group. In addition, G is the supergroup of background isometries, whose maximal Abelian subgroup yields the energy and the angular momenta.

In fact, we must impose three additional conditions in order for the action to realise type II superstring theory [17]. First, the invariance of the action under world-sheet diffeomorphisms and Weyl transformations of the world-sheet metric, that is classical world-sheet conformal invariance. Second, the invariance of the action under κ-symmetry transformations, which is a fermionic gauge symmetry. This symmetry accounts for the superfluousness of half of components of the target-space spinors in the GS action. If G/H is further a critical ten-dimensional background of either type IIA or IIB superstring theory, κ-symmetry transformations permits to eliminate sixteen out of the thirty-two components of the Majorana or Majorana-Weyl spinors, respectively. The κ-symmetry transformations enlarge gauge-symmetry group of local Lorentz transformations H with supersymmetry transformations [127]. The κ-symmetry transformations on G/H are realisable through the local right action by infinitesimal fermionic elements of G, that is a fermionic element of $\mathfrak{g}$ and a transformation of the world-sheet metric [7, 127]. Third, the action of the supercoset model must reduce to the GS action of type II superstring theory on M_{10} in the limit large radius of the background [17]. This condition ensures that the action has the correct form in the limit of vanishing curvature of the background.

All these conditions determine the action of the supercoset model unambiguously:

$$S = -\frac{\sqrt{\lambda}}{4\pi}\int_{\Sigma} \mathrm{str}(j_2 \wedge *j_2 + \bar{q} j_1 \wedge j_3) \ , \tag{2.9}$$

where $\lambda = R^4/\alpha'^2$ is the string tension, being R the radius of the supercoset and α' the Regge slope, [4] $*$ denotes the Hodge-duality operator in the world-sheet and $\bar{q}$ is a parameter. The parameter $\bar{q}$ must be real in order for the action to be a real (in the sense of Grassmann numbers). The first term in the action involves the world-sheet metric through $*$. Therefore, it yields the Virasoro constraints, that is the equations of motion of the world-sheet metric. The first term reduces to the Polyakov action when G/H is truncated to the maximal bosonic coset thereof. The second term is a two-dimensional WZ term. It does not affect the Virasoro constraints because it does not involve the world-sheet metric. The second term is in fact a rephrasing of a topologically trivial three-dimensional WZ term. The three-dimensional WZ term is the integral over a three-dimensional manifold B whose boundary is Σ of the following exact three-form

$$\Theta = \mathrm{str}(j_1 \wedge j_1 \wedge j_2 - j_3 \wedge j_3 \wedge j_2) = \frac{1}{2}\mathrm{d}\,\mathrm{str}(j_1 \wedge j_3) \ , \tag{2.10}$$

where we have used j_a to denote the extension the components of different grading into B with a slight abuse of notation. The proof of the local exactness of (2.10) draws on (2.1) and (2.5)–(2.8). Exactness holds globally if $\mathfrak{h}$ is the maximal Ω-invariant locus of $\mathfrak{g}$ [115], a property that holds for semi-symmetric spaces by construction.

Note that the action (2.9) enjoys the right symmetries. The absence of j_0 in (2.9) and the cyclicity of str in the integrand implies gauge-invariance. The Ω-invariance of str implies that of the action. The action is explicitly invariant under world-sheet diffeomorphisms. The definition of $*$ implies that is also invariant under Weyl transformations of the world-sheet metric. As opposed to the previous symmetries, the invariance under κ-symmetry transformations is not automatically satisfied by (2.9). The action is only invariant if and only if $\bar{q} = \pm 1$. The condition $\bar{q} = \pm 1$ is equivalent to the existence of a Lax connection [7,18]. The condition is also equivalent to quantum world-sheet conformal invariance at one-loop [18,119]. Moreover, the action (2.9) has the correct flat background limit. The flat GS action is obtained by expanding around $g = 1$ [120].

The equations of motion of (2.9) are obtained through the local right action of G on the embedding maps by an infinitesimal parameter ϵ: $g \mapsto g + \delta g$, where $\delta g = g\epsilon$. Being

[4] In general, λ is the 't Hooft coupling defined in the CFT$_d$ side of the AdS$_{d+1}$/CFT$_d$ correspondence. The dependence of λ on the string tension, and, hence, on both the radius of a maximally symmetric AdS$_{d+1}$-background R and α' is determined by the duality. On $\mathrm{AdS}_5 \times \mathrm{S}^5$, the relationship $\sqrt{\lambda} = R^2/\alpha'$ holds exactly [128]. On $\mathrm{AdS}_4 \times \mathrm{CP}^3$, the relationship $\sqrt{\lambda} \sim R^2/\alpha'$ holds at leading order and breaks down at subleading order when $\alpha' \to 0$; see, for instance, section 14 of [129]. We denote the string tension of (2.9) by $\sqrt{\lambda}$ in other backgrounds by analogy and notational simplicity. In particular, in $\mathrm{AdS}_3 \times \mathrm{S}^3$ with mixed flux the string tension is R^2/α' at leading order and subleading order when $\alpha' \to 0$; see footnote 5 of [102]. If the RR flux vanishes, the string tension exactly equals R^2/α', which in turn equals the WZNW level [92]: $R^2/\alpha' = k$; see (2.41). Moreover, we emphasise that the isolation of R in front of the action implies that the target space of the fields is a maximally symmetric AdS$_{d+1}$-background with $R = 1$.

infinitesimal, ϵ is $\mathfrak{g}$-valued. Therefore, ϵ is decomposable in components of different grading ϵ_a. The equations of motion then follow from the requirement that the variation of (2.9) with respect to each ϵ_a vanishes up to boundary terms. [5] The equations of motion read

$$\mathrm{d} * j_2 + j_0 \wedge *j_2 + *j_2 \wedge j_0 - \bar{q}(j_1 \wedge j_1 - j_3 \wedge j_3) = 0 \ , \tag{2.11}$$

$$*j_1 \wedge j_2 + j_2 \wedge *j_1 + \bar{q}(j_1 \wedge j_2 + j_2 \wedge j_1) = 0 \ , \tag{2.12}$$

$$*j_3 \wedge j_2 + j_2 \wedge *j_3 - \bar{q}(j_3 \wedge j_2 + j_2 \wedge j_3) = 0 \ . \tag{2.13}$$

The flatness condition (2.5)–(2.8) and the properties of $*$ are necessary to obtain (2.12) and (2.13). The $\mathfrak{h}$-valued component ϵ_0 does not provide any equation of motion as it introduces an infinitesimal gauge transformations, under which (2.9) is invariant by construction.

The action (2.9) is invariant under the global (left and right) action of G on the embedding maps. Thus, the Noether theorem can be applied to (2.9). The conservation law of the Noether current turns out to be equivalent to the equations of motion of (2.11)–(2.13). To make the equivalence explicit, we introduce the $\mathfrak{g}$-valued world-sheet one-form

$$k = 2j_2 - \bar{q}(*j_1 - *j_3) \ . \tag{2.14}$$

We can then rephrase (2.11)–(2.13) compactly as

$$\mathrm{d} * k + *k \wedge j + j \wedge *k = 0 \ . \tag{2.15}$$

This form is appropriate to relate the equations of motion with the conservation law of the Noether current:

$$\mathrm{d} * J = 0 \ , \tag{2.16}$$

where the Noether current is $J = gkg^{-1}$.

The symmetries of (2.9) guarantee that the associated supercoset model realises classical type II superstring theory. In order for a semi-symmetric space actually realise quantum type II superstring theory, world-sheet conformal invariance must hold at the quantum level. Quantum world-sheet conformal invariance holds if two conditions hold (under the imposition of the conformal gauge-fixing condition to the world-sheet metric). The conditions are the vanishing of the β-function of λ and the determination of the intrinsic central charge of the world-sheet CFT_2 to $c = 26$ [120]. The background-field expansion renders both conditions into properties of G/H at one-loop [120]. (The first perturbative order is $\mathrm{O}(1/\lambda^{1/4})$ here.) The vanishing of the β-function is satisfied if and only if the Killing form of G degenerates. The Killing form is proportional to the supertrace through $h^\vee$, the dual Coxeter number of $\mathfrak{g}$. Thus, the vanishing of the β-function of λ is equivalent to $h^\vee = 0$ [120]. Moreover, c depends on the dimension of G/H and the rank of κ-symmetry transformations thereof. Fixing $c = 26$, is equivalent to requiring the fulfilment of the Virasoro constraints [120].

[5] Boundary terms can be ignored under the imposition of proper boundary conditions to the embedding maps. However, the choice of boundary conditions is not unique. In this text, we impose periodic boundary conditions in chapters 3 and 5 (corresponding to a closed-string world-sheet) and Dirichet boundary conditions in chapter 4 (corresponding to an open-string world-sheet). We shall specify the boundary conditions there.

There exists two semi-symmetric spaces that satisfy $h^\vee = 0$ and $c = 26$ [120]. First,

$$\frac{\mathrm{PSU}(2,2|4)}{\mathrm{SO}(1,4)\times\mathrm{SO}(5)}\ . \tag{2.17}$$

This supercoset is $\mathrm{AdS}_5\times\mathrm{S}^5$ with pure RR five-form flux, and it is a consistent background of type IIB superstring theory. The action (2.9) is equivalent to the GS action irrespective of the gauge-fixing condition with respect to κ-symmetry transformations [17]. Second,

$$\frac{\mathrm{OSp}(2,2|6)}{\mathrm{SO}(1,3)\times\mathrm{U}(3)}\ . \tag{2.18}$$

This supercoset is $\mathrm{AdS}_4\times\mathrm{CP}^3$ with pure RR four-form flux, and is a consistent background of type IIA superstring theory. The action (2.9) is equivalent to the GS action only under a partial gauge-fixing condition with respect to κ-symmetry transformations [130, 131].

The (2.17) and (2.18) backgrounds are the unique semi-symmetric spaces on which type II superstring theory can be consistently realised. Nonetheless, the action (2.9) is also applicable to another class of backgrounds: the direct product of a non-critical semi-symmetric space G/H and an external manifold [120]. The action (2.9) in this case corresponds to a supercoset model that describes the truncation of type II superstring theory to G/H. The external manifold, for its own part, supports an external CFT_2 coupled to the supercoset model through the Virasoro constraints. The action (2.9) enjoys the right symmetries (local Lorentz invariance, Ω-invariance, invariance under isometry transformations in the background, diffeomorphisms, and Weyl transformations) except for the invariance under κ-symmetry transformations. If the supercoset model is considered on its own, it is invariant under κ-symmetry transformations. The invariance permits to eliminate the redundant components of the target-space spinors of G/H, whose number depends on the dimension of G/H. Nonetheless, the invariance is violated when the model is coupled to the external CFT_2. It is violated because the world-sheet metric is coupled to the external CFT_2 and transforms under κ-symmetry transformations [95]. The violation of the invariance under κ-symmetry transformations permits to retain the sixteen non-redundant components of the target-space spinors in type II superstring theory (which, on the whole, is itself invariant).

Type II superstring theory on the direct product of a non-critical semi-symmetric space and an external manifold must also respect quantum world-sheet conformal invariance. The requirement implies consistency conditions on G/H again [120]. The β-function of λ again vanishes if $h^\vee = 0$ for $\mathfrak{g}$. On the other hand, c must be promoted to a extrinsic central charge c', which is defined as c but with the Virasoro constraints loosened [120]. If $c' < 26$, the deficit of the central charge of the theory can be balanced by imposing that the central charge of CFT_2 on the external manifold is $26 - c'$. The action (2.9) is identified with the GS action (whose target-space is non-critical if $c' < 26$) under the imposition of a gauge-fixing condition with respect to κ-symmetry transformations [95, 120].

There exists two non-critical semi-symmetric spaces that are permutation supercosets [120], that is semi-symmetric spaces for which $\mathrm{G} = \mathrm{G}_L\times\mathrm{G}_R$. First,

$$\frac{\mathrm{D}(2,1;\alpha)_L\times\mathrm{D}(2,1;\alpha)_R}{\mathrm{SL}(2,\mathrm{R})\times\mathrm{SO}(4)}\ . \tag{2.19}$$

The supercoset is $\mathrm{AdS}_3 \times \mathrm{S}^3 \times \mathrm{S}^3$ with pure RR three-form flux; $\mathrm{AdS}_3 \times \mathrm{S}^3 \times \mathrm{S}^3 \times \mathrm{S}^1$, which embeds (2.19), is a consistent background of type IIB superstring theory. The parameter α quantifies the relative radii of the pair of S^3 in (2.19). Second,

$$\frac{\mathrm{PSU}(1,1|2)_L \times \mathrm{PSU}(1,1|2)_R}{\mathrm{SL}(2,\mathrm{R}) \times \mathrm{SU}(2)} \,. \tag{2.20}$$

The supercoset is $\mathrm{AdS}_3 \times \mathrm{S}^3$ with pure RR three-form flux; $\mathrm{AdS}_3 \times \mathrm{S}^3 \times \mathrm{T}^4$, which embeds (2.20), is a consistent background of type IIB superstring theory. The two consistent backgrounds are in fact connected [95]: if we apply the $\alpha \to 0$ (or $\alpha \to 1$) contraction to $\mathrm{AdS}_3 \times \mathrm{S}^3 \times \mathrm{S}^3 \times \mathrm{S}^1$, we obtain $\mathrm{AdS}_3 \times \mathrm{S}^3 \times \mathrm{T}^4$.

Semi-symmetric spaces that we have considered so far are just supported with RR flux. In general, there exists an obstruction in supercoset models that forbids the addition of a topologically non-trivial WZ term [124]. The topological obstruction translates into the impossibility for a semi-symmetric space to support NSNS thee-form flux. Permutation supercosets permit to circumvent the obstruction because their bosonic truncations are group manifolds [121–123]. The action (2.9) can be extended with a topologically non-trivial WZ term in this case [88, 102, 105]. In the case of (2.19) and (2.20), the topologically non-trivial WZ term reflects that a NSNS thee-form flux in the semi-symmetric space mixes with the RR three-form flux. We consider general classical non-linear σ-models on permutation supercosets with NSNS flux in the next subsection.

2.1.2 The action of non-linear σ-models on permutation supercosets

We begin with the specification of the semi-symmetric spaces in subsection 2.1.1 to permutation supercosets. Permutation supercosets are semi-symmetric spaces G/H such that $\mathrm{G} = \mathrm{G}_L \times \mathrm{G}_R$, where $\mathrm{G}_{L,R}$ are two isomorphic Lie supergroups. The subscripts in $\mathrm{G}_{L,R}$ stand for *left* and *right*. (The nomenclature is based on the $\mathrm{AdS}_3/\mathrm{CFT}_2$ correspondence, where $\mathrm{G}_L \times \mathrm{G}_R$ must match the conformal supergroup of the dual CFT_2 with $\mathcal{N} = (4,4)$ supersymmetry.) We denote by G' the Lie supergroup isomorphic to both $\mathrm{G}_{L,R}$. Every group element $g \in \mathrm{G}_L \times \mathrm{G}_R$ is decomposable like $g = (g_L, g_R)$, where $g_{L,R} \in \mathrm{G}_{L,R}$. By definition, H of $\mathrm{G}_L \times \mathrm{G}_R$ is the diagonal embedding of the bosonic subgroup of G' in $\mathrm{G}_L \times \mathrm{G}_R$. Permutation supercosets $\mathrm{G}_L \times \mathrm{G}_R/\mathrm{H}$ (insofar as supercosets) are the set of equivalence classes with respect to the right multiplication $(g_L, g_R) \mapsto (g_L h, g_R h)$, where $(h,h) \in \mathrm{H}$. The bosonic truncation of $\mathrm{G}_L \times \mathrm{G}_R/\mathrm{H}$ is isomorphic to the bosonic truncation of G', which is a Lie group. In addition, the canonical extension of the left multiplication of $\mathrm{G}_L \times \mathrm{G}_R$ to the supercoset $\mathrm{G}_L \times \mathrm{G}_R/\mathrm{H}$ is $(g_L, g_R) \mapsto (g'_L g_L, g'_R g_R)$, with $g'_{L,R} \in \mathrm{G}_{L,R}$.

The Lie superalgebra of $\mathrm{G}_L \times \mathrm{G}_R$ is $\mathfrak{g} = \mathfrak{g}_L \oplus \mathfrak{g}_R$, where $\mathfrak{g}_{L,R}$ are the Lie superalgebras of $\mathrm{G}_{L,R}$, respectively. We denote by $\mathfrak{g}'$ the Lie superalgebra of G' isomorphic to both $\mathfrak{g}_{L,R}$. Permutation supercoset are semi-symmetric spaces because the direct-product structure of $\mathfrak{g}_L \oplus \mathfrak{g}_R$ always permits to define the action of a Z_4-automorphism Ω [88, 95]. To abridge the discussion, we introduce a supermatrix representation of $\mathfrak{g}_L \oplus \mathfrak{g}_R$ [102], which we recall that we identify with $\mathfrak{g}_L \oplus \mathfrak{g}_R$ itself. We can then write $M \in \mathfrak{g}_L \oplus \mathfrak{g}_R$ as the supermatrix

$$M = \begin{bmatrix} M_L & 0 \\ 0 & M_R \end{bmatrix} , \tag{2.21}$$

where $M_{L,R} \in \mathfrak{g}_{L,R}$ are supermatrices themselves. The action of Ω is defined by [102]

$$\Omega(M) = \begin{bmatrix} M_R & 0 \\ 0 & (-)^F M_L \end{bmatrix} , \tag{2.22}$$

where $(-)^F$ is the Grassmann-parity involution in $\mathfrak{g}'$. We note that we write $(-)^F_{L,R} \equiv (-)^F$ with a slight abuse of notation; the involution in $\mathfrak{g}_L \oplus \mathfrak{g}_R$ is $(-)^F \oplus (-)^F$. Moreover, the supertrace in $\mathfrak{g}_L \oplus \mathfrak{g}_R$ is $\mathrm{str} = \mathrm{str}_L + \mathrm{str}_R$, where $\mathrm{str}_{L,R}$ are the supertraces of $\mathfrak{g}_{L,R}$.

The left-invariant current $j = g^{-1}\mathrm{d}g$ is a $\mathfrak{g}_L \oplus \mathfrak{g}_R$-valued world-sheet one-form built on the embedding maps $g : \Sigma \to \mathrm{G}_L \times \mathrm{G}_R$ of the non-linear σ-model on a permutation supercoset. The form $g = (g_L, g_R)$ and (2.21) allows us to express j as

$$j = \begin{bmatrix} j_L & 0 \\ 0 & j_R \end{bmatrix} = \begin{bmatrix} g_L^{-1}\mathrm{d}g_L & 0 \\ 0 & g_R^{-1}\mathrm{d}g_R \end{bmatrix} , \tag{2.23}$$

where $j_L = g_L^{-1}\mathrm{d}g_L$ is called *left current* (not to be confused with *left-invariant current*), and $j_R = g_R^{-1}\mathrm{d}g_R$ is called *right current*. We can further decompose $j_{L,R}$ with respect to $(-)^F$. The bosonic components of $j_{L,R}$ are $j^B_{L,R}$, which satisfy $(-)^F j^B_{L,R} = j^B_{L,R}$. The fermionic component of $j_{L,R}$ are $j^F_{L,R}$, which satisfy $(-)^F j^F_{L,R} = -j^F_{L,R}$. The decomposition of $j_{L,R}$ in terms of $j^B_{L,R}$ and $j^F_{L,R}$ permits to reformulate the decomposition (2.2) of j under Ω. The action (2.22) provides us with

$$j_0 = \frac{1}{2}\begin{bmatrix} j^B_L + j^B_R & 0 \\ 0 & j^B_L + j^B_R \end{bmatrix} , \tag{2.24}$$

$$j_1 = \frac{1}{2}\begin{bmatrix} j^F_L - \mathrm{i}\, j^F_R & 0 \\ 0 & \mathrm{i}\, j^F_L + j^F_R \end{bmatrix} , \tag{2.25}$$

$$j_2 = \frac{1}{2}\begin{bmatrix} j^B_L - j^B_R & 0 \\ 0 & -(j^B_L - j^B_R) \end{bmatrix} , \tag{2.26}$$

$$j_3 = \frac{1}{2}\begin{bmatrix} j^F_L + \mathrm{i}\, j^F_R & 0 \\ 0 & -\mathrm{i}\, j^F_L + j^F_R \end{bmatrix} . \tag{2.27}$$

We can now use (2.24)–(2.27) to rephrase (2.3) and (2.5)–(2.8) for j_a compactly. Consider the pattern of j_a under the local right action of H first. Under the mapping between equivalent representatives $(g_L, g_R) \mapsto (g_L h, g_R h)$, the components $j^B_{L,R}$ and $j^F_{L,R}$ transform as

$$j^B_{L,R} \mapsto h^{-1} j^B_{L,R} h + h^{-1}\mathrm{d}h \ , \quad j^F_{L,R} \mapsto h^{-1} j^F_{L,R} h \ . \tag{2.28}$$

Therefore, $j^B_{L,R}$ behave as a connection and $j^F_{L,R}$ transform in the adjoint representation. Formula (2.3) follows from (2.28). Consider the flatness condition for j_a now. Since j satisfies the flatness condition (2.2), so they do $j_{L,R}$. If we project the flatness condition of $j_{L,R}$ on the eigenspaces of $(-)^F$ in each $\mathfrak{g}_{L,R}$, we obtain

$$\mathrm{d}j^B_{L,R} + j^B_{L,R} \wedge j^B_{L,R} + j^F_{L,R} \wedge j^F_{L,R} = 0 \ , \tag{2.29}$$

$$\mathrm{d}j^F_{L,R} + j^B_{L,R} \wedge j^F_{L,R} + j^F_{L,R} \wedge j^B_{L,R} = 0 \ . \tag{2.30}$$

The equations (2.29)–(2.30) together with (2.24)–(2.27) imply (2.5)–(2.8).

Previous considerations permit us to write to the action (2.9) in terms of $j^B_{L,R}$ and $j^F_{L,R}$ in the class of permutation supercoset. The resultant action enjoys all the properties listed in subsection 2.1.1. We have specified the basics of supercoset models based on permutation supercosets to clarify the introduction of topologically non-trivial WZ terms [88]. This type of WZ terms can be added to (2.9) since the bosonic truncation of $\mathrm{G}_L \times \mathrm{G}_R/\mathrm{H}$ is a Lie group [124]. In terms of the supermatrices (2.21), the existence of the topologically non-trivial WZ term is a consequence of the existence of an outstanding supermatrix within the class of permutation supercosets [102]. The supermatrix is

$$W = \begin{bmatrix} 1 & 0 \\ 0 & -1 \end{bmatrix} \ . \tag{2.31}$$

The grading of W is two because (2.22) implies $\Omega(W) = -W$. The supermatrix W permits to retain Ω-invariance in the action of topologically non-trivial WZ terms.

Topologically non-trivial WZ terms in permutation-supercoset models are largely based on their counterparts in permutation-coset models, called *principal chiral models*. Principal chiral models with topologically non-trivial WZ terms realise bosonic-string theory on backgrounds with NSNS flux. Furthermore, the class of principal chiral models encompasses the non-linear σ-model on $\mathrm{AdS}_3 \times \mathrm{S}^3$ with NSNS flux on which we eventually focus. We then make a brief digression on principal chiral models with WZ terms.

Principal chiral models are a class within coset models based on symmetric spaces. A coset F/H (where F is a Lie group and H is the subgroup thereof) is the set of equivalence classes with respect to the right action of H. A symmetric space is a coset F/H for which $\mathfrak{f}$, the Lie algebra of F, has a Z_2-automorphism Ω. The action of the coset model in a symmetric space is invariant under the local right action of H and Ω-invariant. Principal chiral models are coset models based on symmetric spaces that are permutation cosets. Permutation cosets are defined by the fact that $\mathrm{F} = \mathrm{F}_L \times \mathrm{F}_R$, where $\mathrm{F}_{L,R}$ are two isomorphic Lie groups. Let F' denote the Lie group isomorphic to both $\mathrm{F}_{L,R}$. The subgroup H of $\mathrm{F}_L \times \mathrm{F}_R$ is the diagonal embedding of F' in $\mathrm{F}_L \times \mathrm{F}_R$, which is isomorphic to F' itself. Therefore, we can impose a gauge-fixing condition with respect to the local right action of H in the action of the principal chiral model such that the target space is identifiable with F'. The gauge-fixing condition trivialises the action of Ω, which can be consistently ignored.

Principal chiral models are then coset models whose target space is just a Lie group F'. We assume that F' is compact and simple for the simplicity. The action is constructed along the lines of subsection 2.1.1. We introduce differentiable embedding maps $f : \Sigma \to \mathrm{F}'$; we assume that the world-sheet Σ equals S^2 topologically. We then construct the left-invariant current $j = f^{-1}\mathrm{d}f$, which is a $\mathfrak{f}'$-valued world-sheet one-form ($\mathfrak{f}'$ is the Lie algebra of F'). The action of a principal chiral model parallels the first term of the action (2.9):

$$S_{\mathrm{PCM}} = c_1 \int_\Sigma \mathrm{tr}(j \wedge *j) \ , \tag{2.32}$$

where $\mathrm{tr}(\cdot)$ denotes the matrix trace of $\mathfrak{f}'$. In general, the renormalisation-group flow acts on c_1. The global symmetry group of (2.32) is $\mathrm{F}' \times \mathrm{F}' \cong \mathrm{F}_L \times \mathrm{F}_R$.

To introduce a WZ term, we observe that the second homotopy group of every Lie group is trivial, that is $\pi_2(\mathrm{F}') = 0$. No topological obstruction forbids the extension of $f : \Sigma \to \mathrm{F}'$ to $\bar{f} : \mathrm{B} \to \mathrm{F}'$, where B is a three-dimensional manifold such that $\partial\,\mathrm{B} = \Sigma$. The extension $\bar{f}$ matches f at Σ. A WZ term is defined by the product of three copies of $\bar{j} = \bar{f}^{-1}\mathrm{d}\bar{f}$:

$$S_{\mathrm{WZ}} = c_2 \int_{\mathrm{B}} \mathrm{tr}(\bar{j} \wedge \bar{j} \wedge \bar{j}) \ . \tag{2.33}$$

Despite the fact (2.33) is non-local, the variation the of WZ term by an infinitesimal parameter of $\mathfrak{f}'$ integrates to Σ. Therefore, the equations of motion of $S_{\mathrm{PCM}} + S_{\mathrm{WZ}}$ are local. The central property of (2.33) is its multiple-valuedness. Even though continuous deformations of $\bar{f}$ do not modify the WZ term, different $\bar{f}$ in B may not be continuously connected among them. Since $\pi_3(\mathrm{F}') = \mathrm{Z}$ for every compact and simple Lie group, extensions are arranged into classes labelled by an integer. The path integral associated to (2.33) must be singled-valued, and, thus, the difference between the WZ terms of any pair of extensions must an element of $2\pi\mathrm{Z}$. This requirement fixes $k = 24\pi c_2$, where k is called *level*. Stability demands that the level is a natural number [123]. The quantisation condition prevents k from being affected by the renormalisation-group flow.

The F' WZNW model at level k is a principal chiral model wherein $c_1 = 3c_2 = k/8\pi$. The F' WZNW model is special in that it is a fixed point of the renormalisation-group flow. At the fixed point, the isometry group $\mathrm{F}' \times \mathrm{F}'$ of the principal chiral model lifts to $\mathrm{F}'_+ \times \mathrm{F}'_-$ [132], where the group F'_+ (the group F'_-) denotes the local action by F'-valued functions that just depend on the light-cone world-sheet coordinate σ^+ (respectively, σ^-). The enhancement is reflected in the equations of motion of the action of the F' WZNW model, which reduce to chiral equations of motion. The general solution is $f = f_+ f_-$, where $f_\pm = f_\pm(\sigma^\pm)$, due to the Polyakov-Weigmann identity [124].

Previous considerations on principal chiral models and WZ terms can be transferred to permutation-supercoset models. First, we must remember that the truncation of $\mathrm{G}_L \times \mathrm{G}_R/\mathrm{H}$ to its bosonic component leads to a principal chiral model. The bosonic truncation of the action (2.9) is (2.32) up to the replacement of j by j_2. The use of j_2 reflects that we are taking not only the Lie-group structure but also the symmetric-space structure of the permutation coset. We would like to include in the action a WZ term like (2.33), such that $\bar{j}$ is replaced by the extension of j_2 into a three-dimensional manifold B such that $\mathrm{B} = \partial\Sigma$. The action must be Ω-invariant to respect the symmetric-space structure. The WZ term is not Ω-invariant nonetheless. We can supply (2.33) with Ω-invariance by drawing on W in (2.31). If denote by j_a both the world-sheet one-forms and their extensions into B with a slight abuse of notation, the improved Ω-invariant WZ term (with a convenient normalisation) is

$$S_{\mathrm{WZ}} = q\frac{\sqrt{\lambda}}{6\pi}\int_{\mathrm{B}} \mathrm{tr}(W(j_2 \wedge j_2 \wedge j_2)) \ , \tag{2.34}$$

The use of W in (2.31) is in fact equivalent to the redefinition $\mathrm{str}' = \mathrm{str}_L - \mathrm{str}_R$ in (2.34); see appendix D of [96].

Even though (2.34) suffices in principal chiral models, it is not the topologically non-trivial WZ term in permutation-supercoset models. If (2.34) were added to the action (2.9), the locality of the equations of motion would be lost. The local right action action of $\mathrm{G}_L \times \mathrm{G}_R$ in (2.34) through a $\mathfrak{g}_L \oplus \mathfrak{g}_R$-valued infinitesimal parameter (which provides the equations of motion) would not integrate to a local term. The reason is that (2.5)–(2.8) leave a non-local remnant involving j_1 and j_3 [88]. The non-local remnant can be eliminated if the WZ term is enhanced with additional terms involving j_1 and j_3. Additional terms must have grading two, so that they are Ω-invariant when balanced with W in (2.31) [102]. The topologically non-trivial WZ term is furthermore unique [88].

The extension of the action (2.9) on permutation supercosets through a topologically non-trivial WZ term is [88, 102]

$$\begin{aligned} S = &-\frac{\sqrt{\lambda}}{4\pi}\int_{\Sigma} \mathrm{str}(j_2 \wedge *j_2 + \bar{q} j_1 \wedge j_3) \\ &+ q\frac{\sqrt{\lambda}}{12\pi}\int_{\mathrm{B}} \mathrm{str}(W(2j_2 \wedge j_2 \wedge j_2 + 3j_1 \wedge j_3 \wedge j_2 + 3j_3 \wedge j_1 \wedge j_2)) \ , \end{aligned} \tag{2.35}$$

where $\bar{q}$ and q are real in order for the action to be real (in the sense of Grassmann numbers).

The equations of motion of (2.35) are [88, 102]:

$$\begin{aligned} \mathrm{d} * j_2 + j_0 \wedge *j_2 + *j_2 \wedge j_0 - \bar{q}(j_1 \wedge j_1 - j_3 \wedge j_3) + qW(2j_2 \wedge j_2 + j_1 \wedge j_3 & \\ + j_3 \wedge j_1) = 0 \ , & \qquad (2.36) \\ *j_1 \wedge j_2 + j_2 \wedge *j_1 + \bar{q}(j_1 \wedge j_2 + j_2 \wedge j_1) - qW(j_3 \wedge j_2 + j_2 \wedge j_3) = 0 \ , & \qquad (2.37) \\ *j_3 \wedge j_2 + j_2 \wedge *j_3 - \bar{q}(j_3 \wedge j_2 + j_2 \wedge j_3) - qW(j_1 \wedge j_2 + j_2 \wedge j_1) = 0 \ , & \qquad (2.38) \end{aligned}$$

which extend (2.11)–(2.13).

The equations of motion are equivalent to the conservation law (2.16) of a Noether current $J = gkg^{-1}$, in parallel with (2.11)–(2.13). The presence of the additional WZ term in (2.35) is reflected in an extension of the one-form k in (2.14):

$$k = 2j_2 + \bar{q}(*j_3 - *j_1) - qW(2 * j_2 + *j_1 + *j_3) \ . \tag{2.39}$$

The Noether current follows from the invariance of (2.35) under the global (left and right) action of $\mathrm{G}_L \times \mathrm{G}_R$.

The action (2.35) enjoys the symmetries of any supercoset model based on a semi-symmetric space: invariance under the local right action of H and Ω-invariance. If the supercoset model describes the truncation of type II superstring theory to $\mathrm{G}_L \times \mathrm{G}_R/\mathrm{H}$, the action (2.35) must enjoy other symmetries apart from local Lorentz invariance and Ω-invariance (together with background isometries with respect to $\mathrm{G}_L \times \mathrm{G}_R$). Invariance under world-sheet diffeomorphisms and Weyl transformations is manifest in (2.35). On the contrary, (2.35) is not invariant under κ-symmetry transformations for arbitrary values of $\bar{q}$ and q. (Recall that the violation of the invariance under κ-symmetry transformations in the supercoset model occurs when it is coupled to an external CFT_2.) If we impose the invariance to (2.35), we obtain [88]

$$\bar{q}^2 + q^2 = 1 \ . \tag{2.40}$$

It is worth noting that (2.40) reduces to the constraint $\bar{q} = \pm 1$ of subsection 2.1.1 at the point $q = 0$. The permutation-supercoset model becomes a G' WZNW model at level k at the point $\bar{q} = 0$. The constraint (2.40) at any rate is equivalent to the existence of a Lax connection [88, 102]. If the permutation supercoset of (2.35) corresponds a consistent background, that is to either (2.19) or (2.20), the constraint (2.40) is equivalent to quantum word-sheet conformal invariance at one-loop [88]. [6] We emphasise that each pair $\bar{q}$ and q satisfying (2.40) specify a single consistent background in this case.

We specify the permutation-supercoset model of interest now, namely (2.20). The mode corresponds to the truncation of IIB superstring theory to $\mathrm{AdS}_3 \times \mathrm{S}^3 \subset \mathrm{AdS}_3 \times \mathrm{S}^3 \times \mathrm{T}^4$ with mixed RR and NSNS flux. The target space is $\mathrm{PSU}(1,1|2)_L \times \mathrm{PSU}(1,1|2)_R/\mathrm{SL}(2,\mathrm{R}) \times \mathrm{SU}(2)$. The model is supplemented with a CFT_2 on $\mathrm{T}^4 \subset \mathrm{AdS}_3 \times \mathrm{S}^3 \times \mathrm{T}^4$. We need supermatrices of $\mathfrak{psu}(1,1|2)_L \oplus \mathfrak{psu}(1,1|2)_R$ to write (2.35) explicitly . We choose the defining representation of $\mathfrak{su}(1,1|2)_L \oplus \mathfrak{su}(1,1|2)_R$, wherein the supermatrices of $\mathfrak{psu}(1,1|2)_L \oplus \mathfrak{psu}(1,1|2)_R$ are defined (consult footnote 3 of this chapter). We present our conventions in appendix B. The supermatrices permit to express the action (2.35) in the coordinates of the embedding of Σ into $\mathrm{PSU}(1,1|2)_L \times \mathrm{PSU}(1,1|2)_R$. The expression is involved and unenlightening due to the presence of target-space spinors, which are brought into play by through (B.4). One must furthermore impose a gauge-fixing condition to the world-sheet metric and with respect κ-symmetry transformations to match the GS action of type IIB superstring theory [95]. The GS action of type II superstring theory is however just known explicitly at second order [133] and fourth order [134] in the target-space spinors. Moreover, we are interested in the bosonic truncation of the action, which we present in the next subsection. In the light of the situation, we just present to various statements based on the introduction of the $\mathfrak{psu}(1,1|2)_L \oplus \mathfrak{psu}(1,1|2)_R$-valued supermatrices.

First and foremost, both the RR and NSNS three-form fluxes are proportional to the sum of volume forms of AdS_3 and S^3 [96, 105]. The proportionality coefficients of the RR and the NSNS fluxes are $\bar{q}$ and q, respectively; see (C.5). The constraint (2.40) then intertwines both fluxes. We shall assume $0 \leq q \leq 1$ and $\bar{q} = \sqrt{1-q^2}$. We make the assumption for conciseness. We could introduce other ranges for $\bar{q}$ and q that are compatible with (2.40)

[6] The statement holds if $\bar{q}$ does not vanish. If $\bar{q} = 0$, other permutation supercosets are consistent with type II superstring theory. The emergence of new consistent permutation supercosets is a consequence of the vanishing of the one-loop β-function of λ irrespective of the Killing form of the supergroup $\mathrm{G}_L \times \mathrm{G}_R$ [88]. (The total central charge must be $c = 26$ however [120].) The vanishing of the β-function of λ is in turn connected with the fact that a G' WZNW model is a fixed point of the renormalisation-group flow. Nonetheless, $h^\vee = 0$ holds for permutation supercosets that interpolate between the limits of pure RR flux and pure NSNS flux.

with minor modifications. The point $q = 0$ is called *limit of pure RR flux* as the NSNS flux vanishes. The point $q = 1$ is called *limit of pure NSNS flux* as the RR vanishes. Finally, the range $0 < q < 1$ is called *mixed-flux regime*.

The topologically non-trivial WZ term in the permutation-supercoset model on $\mathrm{AdS}_3 \times \mathrm{S}^3$ quantises $\sqrt{\lambda}$. The quantisation of $\sqrt{\lambda}$ is a consequence of the single-valuedness of the path integral and also of the topology of $\mathrm{PSU}(1,1|2)$ [92]. According to the normalisation of the action (2.35), the quantisation condition is

$$k = q\sqrt{\lambda} \;, \tag{2.41}$$

where $k \in \mathrm{N}$ is the level. Note that (2.41) holds if the NSNS flux does not vanish in $\mathrm{AdS}_3 \times \mathrm{S}^3$.

The permutation-supercoset model becomes the $\mathrm{PSU}(1,1|2)$ WZNW model at the level k in the limit of pure NSNS flux [92,94]. The level is given by the quantisation condition (2.41), which reduces to $k = \sqrt{\lambda}$. The action of the supersymmetric $\mathrm{PSU}(1,1|2)$ WZNW model can be rephrased as the sum of three terms [94]. The first term is the action of the bosonic $\mathrm{SL}(2,\mathrm{R})$ WZNW model at the level $k+2$ [93], whose target space is AdS_3 with NSNS flux. The second term is the action of the bosonic $\mathrm{SU}(2)$ WZNW model at the level $k-2$ [123], whose target space is S^3 with NSNS flux. The shift of the level of the bosonic WZNW models follows from considerations on the path integral of the model [94]. The third term couples the bosonic fields of the two previous models between them, and it couples bosonic fields with fermionic fields. This term modifies the chiral equations of motion of the bosonic $\mathrm{SL}(2,\mathrm{R})$ and $\mathrm{SU}(2)$ WZNW models.

The truncation of the permutation-supercoset model that we have discussed so far is the principal chiral model on $\mathrm{AdS}_3 \times \mathrm{S}^3$ plus a WZ term for the NSNS flux, which realises bosonic-string theory in a non-critical background. The central element of the model is the classical action, which is a Polyakov action plus a two-dimensional WZ term that accounts for the NSNS flux. We devote the following subsection to this action and its properties.

2.1.3 The action on $\mathrm{AdS}_3 \times \mathrm{S}^3$ with Neveu-Schwarz-Neveu-Schwarz flux

We want to construct the principal chiral model on $\mathrm{AdS}_3 \times \mathrm{S}^3$ plus a WZ term for the NSNS flux from the permutation-supercoset model that embeds it. We must first truncate $\mathrm{PSU}(1,1|2)_L \times \mathrm{PSU}(1,1|2)_R/\mathrm{SL}(2,\mathrm{R}) \times \mathrm{SU}(2)$ to its bosonic component. The bosonic component is the permutation coset

$$\mathrm{AdS}_3 \times \mathrm{S}^3 \cong \frac{\mathrm{SL}(2,\mathrm{R})_L \times \mathrm{SU}(2)_L \times \mathrm{SL}(2,\mathrm{R})_R \times \mathrm{SU}(2)_R}{\mathrm{SL}(2,\mathrm{R}) \times \mathrm{SU}(2)} \;. \tag{2.42}$$

Since we have truncated the target space to (2.42), we must truncate the left-invariant current $j = g^{-1}\mathrm{d}g$ to its bosonic component. Recall that the left-invariant current decomposes in the left current j_L and the right current j_R according to (2.23). Being $\mathfrak{psu}(1,1|2)$-valued, both $j_{L,R}$ are supertraceless supermatrices of the form (B.1) (and supplemented with the constraints (B.5), (B.6), and (B.7) on their constitutive matrices). The currents $j_{L,R}$ split into $j^B_{L,R}$ and $j^F_{L,R}$. The components $j^B_{L,R}$ are block-diagonal supermatrices whose blocks are bosonic and given by (B.5) and (B.6); the components $j^F_{L,R}$ are block-anti-diagonal supermatrices whose blocks are fermionic and given by (B.4). The bosonic truncation of $\mathfrak{psu}(1,1|2)$ to $\mathfrak{sl}(2,\mathrm{R})\oplus\mathfrak{su}(2)$ amounts to the imposition of $j^F_{L,R}=0$. It is clear that $j^F_{L,R}=0$ is consistent with the equations of motion (2.36)–(2.38). We use $j_{L,R}$ for the bosonic component to keep the notation simple. According to (2.25) and (2.27), $j^F_{L,R}=0$ imply $j_1=j_3=0$. Therefore, we just need to consider the bosonic component j_0 in (2.24) and j_2 in (2.26). We could introduce (2.26) in the action (2.35) to obtain an expression in terms of $j_{L,R}$. The resultant action corresponds to a principal chiral model on (2.42) plus a WZ term for the NSNS flux.

We can obtain a simpler expression for the action following our discussion on principal chiral models in subsection 2.1.2. We have emphasised there that a permutation coset $\mathrm{F}_L\times\mathrm{F}_R/\mathrm{H}$ is isomorphic to the Lie group $\mathrm{F}'\cong\mathrm{F}_{L,R}$. The observation applies to (2.42). Therefore, we need to identify $\mathrm{AdS}_3\times\mathrm{S}^3$ with $\mathrm{SL}(2,\mathrm{R})\times\mathrm{SU}(2)$. We perform the identification through the imposition of a gauge-fixing condition with respect to local Lorentz transformations of $\mathrm{SL}(2,\mathrm{R})\times\mathrm{SU}(2)$ in (2.42). (Recall that a generic embedding map $g=(g_L,g_R)$ into $\mathrm{SL}(2,\mathrm{R})_L\times\mathrm{SU}(2)_L\times\mathrm{SL}(2,\mathrm{R})_R\times\mathrm{SU}(2)_R$ transforms like $(g_L,g_R)\mapsto(g_Lh,g_Rh)$ under the local right action of $\mathrm{SL}(2,\mathrm{R})\times\mathrm{SU}(2)$ by h.) We set $g_R=1$. The principal chiral model then involves embedding maps of the form $g=(g_L,1)$. This form makes manifest that the principal chiral model is based on $\mathrm{AdS}_3\times\mathrm{S}^3\cong\mathrm{SL}(2,\mathrm{R})\times\mathrm{SU}(2)$.

Since $j_R=g_R^{-1}\mathrm{d}g_R=0$, just $j_L=g_L^{-1}\mathrm{d}g_L$ remains, which is a $\mathfrak{sl}(2,\mathrm{R})\oplus\mathfrak{su}(2)$-valued world-sheet one-form. The block-diagonal (8×8)-supermatrices (2.24) and (2.26) simplify to

$$j_0=\frac{1}{2}\begin{bmatrix} j_L & 0\\ 0 & j_L\end{bmatrix}\ , \tag{2.43}$$

$$j_2=\frac{1}{2}\begin{bmatrix} j_L & 0\\ 0 & -j_L\end{bmatrix}\ . \tag{2.44}$$

The left current is the block-diagonal (4×4)-supermatrix

$$j_L=\begin{bmatrix} l_1 & 0\\ 0 & l_2\end{bmatrix}\ . \tag{2.45}$$

The (2×2)-matrices l_1 and l_2 are $\mathfrak{sl}(2,\mathrm{R})$-valued and $\mathfrak{su}(2)$-valued world-sheet one-forms, respectively; see (B.5), (B.6), and (B.7). In the remainder of the text, we also denote both l_1 and l_2 by j with a slight abuse of notation. We denote the corresponding embedding maps by g. Whether j corresponds j_L, l_1, or l_2 will be clear from the context.

If we use (2.44), the action (2.35) reduces to

$$S=-\frac{\sqrt{\lambda}}{8\pi}\int_\Sigma \mathrm{str}'(j\wedge *j)+q\frac{\sqrt{\lambda}}{24\pi}\int_{\mathrm{B}}\mathrm{str}'(j\wedge j\wedge j)\ , \tag{2.46}$$

were we have used that $\mathrm{str}=\mathrm{str}_L+\mathrm{str}_R$ and denoted by str' the supertrace (B.2). Note that the traces over $\mathfrak{sl}(2,\mathrm{R})$ and $\mathfrak{su}(2)$ occur with opposite signs in (B.2). The action (2.46) corresponds to a principal chiral model on $\mathrm{SL}(2,\mathrm{R})\times\mathrm{SU}(2)$, see (2.32) and (2.33).

Our analyses in chapters 3–5 are based on specific coordinate systems of $\mathrm{AdS}_3\times\mathrm{S}^3$. Coordinate systems parameterise of g_L and j_L through the coordinates of the target space Z^A.

Coordinate systems allow us to advance a explicit form for the target-space metric G_{AB} of $\mathrm{AdS}_3 \times \mathrm{S}^3$. Coordinate systems also allow us to write, locally, the NSNS three-form flux as the exterior derivative of the Kalb-Ramond two-form B called *B-field*. The B-field is uniquely determined modulo the addition of an exact two-form. The appropriate coordinate system in each case depends on the traits of the problem being considered. We list in appendix C the coordinate systems of $\mathrm{AdS}_3 \times \mathrm{S}^3$ that we use in chapters 3–5. Appendix C also contains the parameterisation of g_L and j_L that correspond to each coordinate system, the target-space metric, and the B-field.

Whatever the coordinate system is, the action (2.46) always presents the following form:

$$S = -\frac{\sqrt{\lambda}}{4\pi} \int \mathrm{d}\tau \int \mathrm{d}\sigma \left(\sqrt{-h} h^{\alpha\beta} G_{AB}(Z) + \epsilon^{\alpha\beta} B_{AB}(Z) \right) \partial_\alpha Z^A \partial_\beta Z^B \ , \tag{2.47}$$

where we have assumed the Einstein summation convention on lower-case Greek indices, which run over world-sheet indices, and upper-case Latin indices, which run over background indices. We have assumed that the world-sheet is Lorentzian, where τ and σ parameterise the time-like and space-like world-sheet directions, respectively, $h_{\alpha\beta}$ is the world-sheet metric, $\epsilon^{\alpha\beta}$ is the skew-symmetric symbol. We refer to appendix A for conventions. The action (2.47) is the Brink-di Vecchia-Deser-Howe-Zumino-Polyakov action plus a WZ term, called *Polyakov action* for short. We shall also need the counterpart of (2.47) in an Euclidean world-sheet. We refer to appendix A again for our conventions on the Wick rotation of the world-sheet.

The ranges of the world-sheet coordinates in (2.47) depend on the boundary conditions of Z^A. Chapters 3 and 5 are based closed-string Lorentzian world-sheets. Therefore, Z^A satisfy periodic boundary conditions with respect to σ and do not satisfy any particular boundary condition with respect to τ. The ranges are $\tau \in (-\infty, \infty)$ and $\sigma \in [0, 2\pi)$. Chapter 4 is based on action associated to open-string Euclidean world-sheets. Target-space coordinates Z^A are supplied with Dirichlet boundary conditions at the conformal boundary of Euclidean AdS_3. To write the ranges of the σ and τ we need to specify open-string world-sheet. For further details, we refer to chapter 4.

The equations of motion of $h_{\alpha\beta}$ in (2.47) provide the Virasoro constraints:

$$G_{AB}(Z) \left(\partial_\alpha Z^A \partial_\beta Z^B - \frac{1}{2} h_{\alpha\beta} h^{\gamma\delta} \partial_\gamma Z^A \partial_\delta Z^B \right) = 0 \ . \tag{2.48}$$

The Virasoro constraints ensure that Weyl invariance, which implies that classical world-sheet conformal invariance is respected by the solution to the equations of motion. There exist two main gauge-fixing conditions of $h_{\alpha\beta}$ that simplify the Virasoro constraints. First, the conformal gauge-fixing condition: $h_{\alpha\beta} = \eta_{\alpha\beta}$ if the signature is $(-,+)$ and $h_{\alpha\beta} = \delta_{\alpha\beta}$ if the signature is $(+,+)$. It fixes two local symmetries of the action: world-sheet diffeomorphisms and Weyl transformations. The Virasoro constraints read

$$G_{AB}(Z)(\dot{Z}^A \dot{Z}^B + Z^{A\prime} Z^{B\prime}) = 0 \ , \quad G_{AB}(Z) \dot{Z}^A Z^{B\prime} = 0 \ , \quad \text{if} \quad h_{\alpha\beta} = \eta_{\alpha\beta} \ , \tag{2.49}$$

$$G_{AB}(Z)(\dot{Z}^A \dot{Z}^B - Z^{A\prime} Z^{B\prime}) = 0 \ , \quad G_{AB}(Z) \dot{Z}^A Z^{B\prime} = 0 \ , \quad \text{if} \quad h_{\alpha\beta} = \delta_{\alpha\beta} \ , \tag{2.50}$$

where $\dot{}$ denotes the derivative with respect to τ and the prime $'$ with respect to σ. We use (2.49) and (2.50) in chapters 3 and 4, respectively. Second, the static gauge-fixing condition, which solves (2.48) directly. [7] The Virasoro constraints are solved by identifying the independent world-sheet metric with the induced metric on the world-sheet:

$$h_{\alpha\beta} = G_{AB}\left(Z\right)\partial_\alpha Z^A \partial_\beta Z^B \ . \tag{2.51}$$

The action (2.47) is accordingly rephrased as the Nambu-Goto (NG) action (plus the WZ term). The condition (2.51) fixes $h_{\alpha\beta}$ under Weyl transformations, but not under world-sheet diffeomorphisms. The static gauge-fixing condition is complete when two target-space space coordinates are properly identified with τ and σ. We use the static gauge-fixing condition in section 5. The conformal and static gauge-fixing conditions provide equivalent classical actions. The corresponding generating functionals (or partition functions) are equivalent in the semi-classical limit $\lambda \to \infty$. It is worth emphasising that the equivalence extends to the quantum level at one-loop at least [135, 136].

2.2 The classical integrable structure

We devote this section to the classical integrable structure of the permutation-supercoset model on $\mathrm{AdS}_3 \times \mathrm{S}^3$ in the mixed-flux regime. In subsection 2.2.1, we present the Lax connection on a semi-symmetric space following [95, 137]. We then extend the Lax connection under NSNS flux following [102] and write its bosonic truncation. We refer to these references for a more thorough discussion. In subsection 2.2.2, we present the monodromy matrix on a closed-superstring world-sheet along the lines of [95, 137]. We refer to these references for a more throughout discussion. We close subsection 2.2.2 with an extension of the proposal of [66] to $\mathrm{AdS}_3 \times \mathrm{S}^3$ with NSNS flux. (See subsection 2.4 of [138] for a summary of the proposal of [66].) The method permits to construct a spectral curve for factorised classical solutions irrespective of their boundary conditions.

2.2.1 The Lax connection

We start from the Lax connection in a supercoset model on a general semi-symmetric space G/H. The Lax connection is a flat $\mathfrak{g}_\mathrm{C}$-valued world-sheet one-form L, where $\mathfrak{g}_\mathrm{C}$ be the complexification of $\mathfrak{g}$. The Lax connection L is defined by the fact its flatness condition

$$\mathrm{d}L + L \wedge L = 0 \ , \tag{2.52}$$

implies both the flatness condition (2.5)–(2.8) and the equations of motion (2.11)–(2.13) of j_a. The Lax connection depends on the world-sheet coordinates σ^α and the complex parameter x, which is called *spectral parameter*; in general, L is a multi-valued functions of x. Both (2.5) and (2.11)–(2.13) follow from the imposition that (2.52) holds almost everywhere in x. The series of L around every x generate an infinite hierarchy of conserved charges via the quasi-momenta, which are related to L through the monodromy matrix (see subsection 2.2.2).

[7] The Virasoro constraints (2.49) and (2.50) can be solved in symmetric spaces by drawing on the Pohlmeyer reduction. The change of variables in the Pohlmeyer reduction is non-local however, which hinders computing expressions in the initial Z^A. See subsection 4.4 of [12] for a summary and references of the Pohlmeyer reduction in the context of classical solutions on $\mathrm{AdS}_5 \times \mathrm{S}^5$.

The Lax connection is obtained by means of an educated guess, which relies on Ω to write L as a linear combination of j_a. The imposition of (2.52) and the use of (2.5)–(2.8) and (2.11)–(2.13) yields an overdetermined system of non-linear algebraic equations for the coefficients. A one-parameter family of solutions exists if and only if $\bar{q} = 1$ is satisfied in the equations of motion. Recall that $\bar{q} = 1$ is implied by the invariance under κ-symmetry transformations of the action [7]. (We have excluded $\bar{q} = -1$ for conciseness and later clarity.) The family of solutions is parameterised by a coefficient, which is an arbitrary function of x. The coefficient is fixed by using the analytic structure of the quasi-momenta [60].

In the end [18], the result is

$$L = j_0 + \frac{x^2+1}{x^2-1} j_2 - \frac{2x}{x^2-1} * j_2 + \sqrt{\frac{x+1}{x-1}} j_1 + \sqrt{\frac{x-1}{x+1}} j_3 \ . \tag{2.53}$$

The Lax connection displays some remarkable properties. First, Ω acts on (2.53) as

$$\Omega(L\,(\sigma^\alpha, x)) = L(\sigma^\alpha, 1/x) \ . \tag{2.54}$$

Second, the Lax connection is related to the symmetry algebra. In particular, (2.53) has a simple pole at $x = \infty$, whose residue is related to the Noether current:

$$\operatorname*{res}_{x=\infty} L = k \ , \tag{2.55}$$

where k is (2.14) and $J = gkg^{-1}$ is the Noether current. Note that L then has a simple pole at $x = 0$ because of (2.54). Third, (2.53) has simple poles at $x = \pm 1$, whose residues are

$$\operatorname*{res}_{x=\pm 1} L = \pm(j_2 \mp * j_2) \ . \tag{2.56}$$

Fourth, the coefficients of the bosonic components j_0 and j_2 are rational functions of x. In $\mathrm{AdS}_5 \times \mathrm{S}^5$, (2.53) furthermore leads to a set of finite-gap equations that match the thermodynamic limit of the Bethe equations of $\mathcal{N} = 4$ SYM theory [61].

The attainment of the Lax connection in the permutation-supercoset model on $\mathrm{AdS}_3 \times \mathrm{S}^3$ in the mixed-flux regime parallels the general case [88, 102]. The starting point is again a flat world-sheet $\mathfrak{psu}(2|2)_{\mathrm{C},L} \oplus \mathfrak{psu}(2|2)_{\mathrm{C},R}$-valued one-form L, where $\mathfrak{psu}(2|2)_{\mathrm{C}}$ is the complexification of $\mathfrak{psu}(1,1|2)$. Being $\mathfrak{psu}(2|2)_{\mathrm{C},L} \oplus \mathfrak{psu}_{\mathrm{C}}(2|2)_{\mathrm{C},R}$-valued, L admits the decomposition (2.21) in left and right components $L_{L,R} \in \mathfrak{psu}(1,1|2)_{L,R}$. By definition, the flatness condition (2.52) of L implies the flatness condition (2.5)–(2.8) and the equations of motion (2.36)–(2.38). The ansatz for L is again a general linear combination of j_a. The imposition of (2.52) and the use of (2.5)–(2.8) and (2.36)–(2.38) provides an overdetermined system of non-linear algebraic equations for the coefficients. A one-parameter family of solutions exists provided that the constraint (2.40) holds for $\bar{q}$ and q. Thus, the existence of a Lax connection is equivalent to quantum world-sheet conformal invariance at one-loop and invariance under κ-symmetry transformations of the action [88]. The family of solutions is parameterised by a coefficient, which is an arbitrary function of both x and q. The free coefficient is determined by the following requirements [102]: L matches (2.53) in the limit of pure RR flux , the action of Ω on L is given by (2.54), the residue of L at $x = \infty$ provides the Noether current similarly to (2.55), and the coefficients of j_0 and j_2 in (2.53) remain rational functions of x. In addition, L must be compatible with the thermodynamic limit of the Bethe equations of the permutation-supercoset model, which were written in [102] by using the S-matrix of [99].

The Lax connection that fulfils these conditions is the following [102]:

$$\begin{aligned} L_L &= j_{0,L} + \frac{x^2+1}{(x-s)(x+1/s)} j_{2,L} - \frac{2x}{\bar{q}(x-s)(x+1/s)} * j_{2,L} \\ &\quad + \frac{x+1}{\sqrt{(x-s)(x+1/s)}} j_{1,L} + \frac{x-1}{\sqrt{(x-s)(x+1/s)}} j_{3,L} \ , \end{aligned} \tag{2.57}$$

$$\begin{aligned} L_R &= j_{0,R} + \frac{x^2+1}{(x+s)(x-1/s)} j_{2,R} - \frac{2x}{\bar{q}(x+s)(x-1/s)} * j_{2,R} \\ &\quad + \frac{x+1}{\sqrt{(x+s)(x-1/s)}} j_{1,R} + \frac{x-1}{\sqrt{(x+s)(x-1/s)}} j_{3,R} \ , \end{aligned} \tag{2.58}$$

where, recall, $\bar{q} = \sqrt{1-q^2}$ and

$$s = \sqrt{\frac{1-q}{1+q}} \ . \tag{2.59}$$

The Lax connection has some new properties that are worth mentioning. First, the residue of (2.57) and(2.58) at $x = \infty$ is corrected by $1/\bar{q}$ with respect to (2.55):

$$\operatorname*{res}_{x=\infty} L = \frac{1}{\bar{q}} k \ , \tag{2.60}$$

where k is (2.39). The residue at $x = \infty$ is not defined in the limit of pure NSNS flux. Second, the simple poles of the Lax connection (2.57) are shifted from $x = \pm 1$ in the limit of pure RR flux to $x = \pm s$ and $x = \pm 1/s$ in the mixed-flux regime. The pairs $x = s, -1/s$ and $x = -s, 1/s$ are the simple poles of (2.57) and (2.58), respectively, whose residues read

$$\operatorname*{res}_{x=s} L_L = s(j_{2,L} - *j_{2,L}) \ , \qquad \operatorname*{res}_{x=-1/s} L_L = -\frac{1}{s}(j_{2,L} + *j_{2,L}) \ , \tag{2.61}$$

$$\operatorname*{res}_{x=-s} L_R = -s(j_{2,R} + *j_{2,R}) \ , \qquad \operatorname*{res}_{x=1/s} L_R = \frac{1}{s}(j_{2,R} - *j_{2,R}) \ . \tag{2.62}$$

Finally, the coefficients of (2.57) and (2.58) in map to each other under $q \mapsto -q$.

The Lax connection degenerates in the limit of pure NSNS flux. The limit of pure NSNS flux merges the simple poles $x = \pm s$ at $x = 0$ and $x = \pm 1/s$ at $x = \infty$, where (2.57) and (2.58) reduce to

$$L_L = j_{0,L} + *j_{2,L} \ , \tag{2.63}$$

$$L_R = j_{0,R} - *j_{2,R} \ . \tag{2.64}$$

Therefore, the dependence of L on both x and the fermionic components of j is lost. [8] We stress that not only the Lax connection but also the Zhukovsky variables that underpin the Bethe equations of [102] are not defined in the limit of pure NSNS flux.

[8] Reference [88] considers that the degeneration reflects the simplification of the equations of j_a into the equations of motion of the PSU(1, 1|2) WZNW model. On the other hand, [102] noted that the degeneration is not bound to occur if other coefficients for L are chosen, but in this case all the assumptions that lead to (2.57) and (2.58) cannot hold. For instance, footnote 3 of [102] writes an alternative L that is regular the limit of pure NSNS flux at the expense of the degeneration of (2.54) in this limit.

We conclude by writing the bosonic truncation of the Lax connection in (2.57) and (2.58), which we use in the next subsection. We follow subsection 2.1.3 and impose a gauge-fixing condition with respect to local Lorentz transformations of $\mathrm{SL}(2,\mathrm{R}) \times \mathrm{SU}(2)$. We then write embedding maps of the principal chiral model on $\mathrm{AdS}_3 \times \mathrm{S}^3$ as in terms of the $\mathrm{SL}(2,\mathrm{R}) \times \mathrm{SU}(2)$-valued mapping g. We eventually draw on (2.43) and (2.44) to obtain the following gauge-fixed bosonic truncation of L:

$$L_L = \frac{(\bar{q}x + q)x}{\bar{q}(x-s)(x+1/s)} j - \frac{x}{\bar{q}(x-s)(x+1/s)} * j \ , \tag{2.65}$$

$$L_R = -\frac{qx + \bar{q}}{\bar{q}(x+s)(x-1/s)} j + \frac{x}{\bar{q}(x+s)(x-1/s)} * j \ , \tag{2.66}$$

whose limit of pure NSNS flux is

$$L_L = \frac{1}{2}(j + *j) \ , \tag{2.67}$$

$$L_R = \frac{1}{2}(j + *j) \ . \tag{2.68}$$

2.2.2 The local spectral curve

We begin with the monodromy matrix of a supercoset model on a general semi-symmetric space G/H. In order for the monodromy matrix to be definable, a non-contractible loop must exist in Σ. Therefore, we assume that Σ is a closed-superstring world-sheet. Since the closed-superstring world-sheet is cylindrical, it just has one non-contractible loop. (We focus on free type II superstring theory, where the string-interaction coupling vanishes; closed-superstring world-sheets have minimal genus, that is they are cylindrical.) The non-contractible loop is the mapping $\gamma : [0, 2\pi] \to \Sigma$, where $\gamma_0 = \gamma(0) = \gamma(2\pi) \in \Sigma$ is the base point. *Non-contractible* means that γ is not homotopic to the trivial mapping onto γ_0.

We consider the auxiliary problem $\mathrm{d}\Psi = -L\Psi$ now, where Ψ depends on both σ^α and x. Being nilpotent, d implies the flatness condition (2.52). The monodromy matrix is defined as the G_C-valued function of x that encodes the monodromy of Ψ under its parallel transport by L along γ, where G_C is the complexification of G.

Therefore, the monodromy matrix is the path-ordered exponential of the Lax connection:

$$M = \overleftarrow{\exp}\left(-\oint_\gamma L\right) \ . \tag{2.69}$$

The monodromy matrix display a definite pattern under various transformations [95,137]. The monodromy matrix transforms in the adjoint representation of H under gauge transformations, that is $M \mapsto h^{-1}Mh$. Since L is flat, M defined by any non-contractible loop homotopic to γ equals (2.69). The monodromy matrix transforms as $M \mapsto P^{-1}MP$ under the change of γ_0, where P denotes the path-ordered exponential of L along the simple curve that connects γ_0 and the new base point. Thus, the conjugacy class of M is gauge-invariant and independent of the shape of γ and so they are their eigenvalues. The eigenvalues are isochronous if γ is specified to a space-like section of constant τ. Moreover, the pattern of M under Ω follows from (2.54).

The diagonalisation of (2.69) yield the quasi-momenta, whose number equals the rank of $\mathfrak{g}$. The quasi-momenta are single-valued meromorphic functions of the spectral parameter over a Riemann surface, which is called *spectral curve*. The spectral curve comprises multiple cycles and sheets on account of the branch-cuts of the quasi-momenta. The integration of the meromorphic differential built on the quasi-momenta yield the set of closed-superstring moduli, which are the action variables of the associated classical solutions. The determination of the quasi-momenta is a Riemann-Hilbert problem, which is equivalent to the so-called *finite-gap equations*: a set of linear integral equations for the density functions of the quasi-momenta. In appendix D, we review the finite-gap equations of [102] of the permutation-supercoset model on $\mathrm{AdS}_3 \times \mathrm{S}^3$ in the mixed-flux regime. In this subsection, we present an extension of the proposal of [66] to the principal chiral model on $\mathrm{AdS}_3 \times \mathrm{S}^3$ with NSNS flux. The extension allows us to obtain the local spectral curve in sections 3.3 and 4.3.

Reference [66] relied on [65] to advance a systematic procedure to construct a local spectral curve for factorisable classical solutions. The procedure just draws on the Lax connection, which is local. The procedure permits to obtain a spectral curve in an open-string world-sheet, where non-contractible loops may not exist. Locality also circumvents the computation of the path-ordered exponential in (2.69). Moreover, the proposal of [66] leaves out the integration of an Abelian differential over the spectral curve and the moduli of the solution. In order for the moduli to be defined, the analytic structure of the quasi-momenta, which is affected by the boundary conditions, would be required. In spite of their limitations, local spectral curves can be used to classify classical solutions to some extent.

Our starting point is the principal chiral model on AdS_3 supported with NSNS flux and the $\mathrm{SL}(2,\mathrm{R})$-valued embedding map g. We have truncated the background to AdS_3 as we shall be concerned with this case in sections 3.3 and 4.3; we could have focused on S^3 analogously. (Since $\mathrm{AdS}_3 \times \mathrm{S}^3$ is a direct product, the local spectral curve comprises the local spectral curve of each space such that they are intertwined by the Virasoro constraints.) Let j be the AdS_3-component of (2.45). A string configuration is factorisable if its j fulfils two conditions. First, either

$$j(\tau,\sigma) = S(\sigma) j(\tau,0) S^{-1}(\sigma) \ , \tag{2.70}$$

or

$$j(\tau,\sigma) = S(\tau) j(0,\sigma) S^{-1}(\tau) \ , \tag{2.71}$$

where S is a $\mathrm{SL}(2,\mathrm{R})$-valued function of τ in (2.70) and a $\mathrm{SL}(2,\mathrm{R})$-valued function of σ in (2.71). Second, $S^{-1}\mathrm{d}S$ is a constant $\mathrm{SL}(2,\mathrm{R})$-valued world-sheet one-form. We further assume that σ in (2.70) or τ in (2.71) are defined over $[0,2\pi)$ since we shall encounter this range in sections 3.3 and 4.3, and we also make the assumption because the discussion is simplified. We specify the procedure to (2.70) for definiteness; being the steps of the specification to (2.71) are almost identical.

The truncation to AdS_3 implies that L is a $\mathfrak{sl}(2,\mathrm{C})_L \oplus \mathfrak{sl}(2,\mathrm{C})_R$-valued world-sheet one-form and M is a $\mathrm{SL}(2,\mathrm{C})_L \times \mathrm{SL}(2,\mathrm{C})_R$-valued matrix. Due to (2.21), both L and M are decomposed into $L_{L,R} \in \mathfrak{sl}(2,\mathrm{C})_{L,R}$ and $M_{L,R} \in \mathrm{SL}(2,\mathrm{C})_{L,R}$, respectively. In the representation of $\mathfrak{psu}(1,1|2)$ that we consider (see appendix B), the components $L_{L,R}$ and $M_{L,R}$ are (2×2)-matrix-valued. Formulae (2.65) and (2.66) relate L_L and L_R to j, respectively.

We focus on M_L for definiteness. If we choose γ to be a section of constant τ, we have

$$M_L = \overleftarrow{\exp}\left(\int_0^{2\pi} \mathrm{d}\sigma L_{L\sigma}(\tau,\sigma)\right) \ , \tag{2.72}$$

where we have kept implicit the dependence on x. Since j factorises, so it does L_L by virtue of (2.65). By using the properties of M under gauge transformations, we obtain

$$\begin{aligned} M_L &= \overleftarrow{\exp}\left(\int_0^{2\pi} \mathrm{d}\sigma S(\sigma) L_{L\sigma}(\tau,0) S^{-1}(\sigma)\right) \\ &= S(0)\exp(2\pi A) S^{-1}(2\pi) \ , \end{aligned} \tag{2.73}$$

where A is the following $\mathfrak{sl}(2,\mathrm{C})$-valued function of x:

$$A = L_{L\sigma} + S^{-1}S' \ . \tag{2.74}$$

Following [66] (see (2.7), (3.1) and (3.2) thereof), we postulate the local spectral curve to be defined by the polynomial

$$\det(y - 2\bar{q}(x-s)(x+1/s)A) = y^2 - 4\bar{q}^2(x-s)^2(x+1/s)^2 \det A = y^2 - \sum_{n=0}^{4} a_n x^n \ , \tag{2.75}$$

where a_n are coefficients. If we had started from M_R, we would have obtained (2.75) up to the replacement of $L_{L\sigma}$ by $L_{R\sigma}$ in (2.74) and the replacement of s and $-1/s$ by $-s$ and $1/s$ in (2.75), respectively.

Our definition deserves some comments. We have removed the poles of L_L at $x = s, -1/s$ (the poles of L_R at $x = -s, 1/s$) to render the local spectral curve algebraic. We have used the (2×2)-matrix form of $L_{L,R}$ together with (2.65) and (2.66) to write the right-hand side of (2.75) as a quartic polynomial. Moreover, we have removed the factor $\bar{q}^2 = 1 - q^2$. This choice allows us to obtain finite a_n in the limit of pure NSNS flux. [9]

The definition (2.75) also allows us to advance some observations. First, A just depends on L_L (or L_R) via (2.74). Therefore, (2.75) is always definable provided that factorisability holds. This fact permits the definition of a local spectral curve irrespective of the existence of non-contractible loops on Σ. Second, the dependence on σ^α in (2.75) must be ultimately deleted because $M_{L,R}$ are (pseudo-)isochronous. This property can be used as a cross-check to validate explicit expressions. Third, the local spectral curve defined by (2.75) is an elliptic curve, that is a compact algebraic variety of complex-dimension one whose genus is one. Finally, locality implies that the correspondence between factorisable classical solutions and local algebraic curves via (2.75) is neither one-to-one nor onto [65]. The reason is that the closed-superstring moduli that discriminate between solutions are not available in a local

[9] Subsection 3.2.1 of reference [66] also presents a method to determine whether the Virasoro constraints are fulfilled by looking at a_n. Formulae (3.81) and (4.43) imply that the method must be rectified under the presence of NSNS flux. We do not inquiry this problem as the Virasoro constraints are always satisfied by construction in the local spectral curves which we obtain. Moreover, one could in principle use the local spectral curve to reconstruct Ψ in the auxiliar problem, and g afterwards, along the lines of section 6 of [65].

spectral curve. Despite the impediment, local spectral curves can still be used to analyse factorisable classical solutions. We classify in particular factorisable classical solutions by means of the modular functions of the associated elliptic curve. We review the necessary background on elliptic curves for sections 3.3 and 4.3 in appendix E.

Chapter 3

Pulsating strings with Neveu-Schwarz-Neveu-Schwarz flux

The central role of spinning strings in the $\mathrm{AdS}_5/\mathrm{CFT}_4$ correspondence prompted several lines of research. The connection between closed-string ansatze and effective integrable mechanical systems in $\mathrm{AdS}_5 \times \mathrm{S}^5$ stands out among them [37, 38]. The connection is based on the Pohlmeyer reduction of the coset model on $\mathrm{AdS}_5 \times \mathrm{S}^5$: since the Pohlmeyer-reduced model is integrable, integrability should be indirectly reflected in the initial coset model. Mechanical systems enable the systematic construction of classical solutions and their semi-classical Noether charges in terms of hyperelliptic functions and hyperelliptic integrals, respectively.

Reference [37] first systematised the construction of mechanical systems by means of the spinning-string ansatz on $\mathrm{AdS}_5 \times \mathrm{S}^5$. The ansatz reduces the equations of motion of the coset model on $\mathrm{AdS}_5 \times \mathrm{S}^5$ to those of a mechanical system. It collapses the infinite hierarchy of higher conserved charges of the non-linear σ-model into the finite set of fist integrals of the mechanical system [47, 48]. The spinning-string ansatz is specified in the global coordinate system of $\mathrm{AdS}_5 \times \mathrm{S}^5$. Coordinates of the maximal Abelian subgroup of $\mathrm{AdS}_5 \times \mathrm{S}^5$, the Cartan coordinates, are proportional to τ. Non-Cartan coordinates are periodic trial functions of σ. The ansatz leads to the sum of the actions of two mechanical systems: the three-dimensional Neumann systems on AdS_5 and S^5. The $(d+1)$-dimensional Neumann system consists of $d+1$ one-dimensional simple harmonic oscillators in a d-dimensional sphere. (The ansatz in S^{2d-1} provides the $(d+1)$-dimensional Neumann system; the ansatz in AdS_{2d-1} rather provides an analytic continuation of the Neumann system whose oscillators are placed in a d-dimensional hyperboloid.) The existence of d independent first integrals in involution, called *Uhlenbeck constants*, implies the Liouville integrability of the Neumann system.

Reference [38] generalised the spinning-string ansatz of [37] by allowing winding numbers in $\mathrm{AdS}_5 \times \mathrm{S}^5$. The addition of quasi-periodic trial functions of σ to the Cartan coordinates accounts for the winding numbers. These trial functions are cyclic coordinates in the mechanical system and eventually generalise the Neumann system to the NR system. The NR system involves an additional centrifugal potential for each oscillator of the Neumann system. The coefficients of centrifugal potential are the canonically conjugate momenta of the cyclic coordinates. The Uhlenbeck constants of the Neumann system lift to first integrals of the NR system, and, thus, Liouville integrability holds. The NR system interpolates between the Neumann and Rosochatius systems. The Neumann system corresponds to vanishing centrifugal potential. The Rosochatius system corresponds to vanishing harmonic potential.

The Rosochatius system is the model of geodesic motion on a d-dimensional ellipsoid (or its non-compact counterpart); see, for example, appendix A.1 of [139].

Neither the Neumann system nor the NR system incorporate the Virasoro constraints, which must be imposed to the classical trajectories of the mechanical system. In particular, the Virasoro constraints impose that the total mechanical energy vanishes and lead to the dispersion relation of spinning strings. The energy E admits a series in λ and the semi-classical Noether charges. If the total Lorentzian spin S is semi-classical and large, and the total angular momentum J is negligible in S^5, the series of E is non-analytic in λ and S. If J is semi-classical and large, the series of E is analytic in λ and J. The coefficients of the series involve, apart from the semi-classical Noether charges, the winding numbers and the mode numbers that follow from the periodicity of the non-Cartan coordinates.

Reference [38] noted that the interchange of τ and σ in the spinning-string ansatz leads to the NR system that follows the pulsating-string ansatz. Harmonic frequencies map to winding numbers. The Noether charges are just proportional to the momenta of the cyclic coordinates and determine the centrifugal potential. This advantage over the spinning-string ansatz is counterbalanced by the automatic fulfilment of periodicity in σ. No mode numbers can be defined. The impediment renders the Bohr-Sommerfeld quantisation necessary [49]. The energy E of pulsating strings admits series in λ and the semi-classical and large adiabatic invariant N. If classical solutions do not pulsate in S^5, the series of E is non-analytic in λ and N [49]. Otherwise, the series of E is analytic in λ and N otherwise [44, 49, 50]. [1]

The relationship between closed-string ansatze in $\mathrm{AdS}_5 \times \mathrm{S}^5$ and mechanical systems raises the question of its realisation on other AdS_{d+1}-backgrounds, $\mathrm{AdS}_3 \times \mathrm{S}^3 \subset \mathrm{AdS}_3 \times \mathrm{S}^3 \times \mathrm{T}^4$ with NSNS flux in particular. The deformation is expected to be integrable on the basis of [96], which presented the Pohlmeyer reduction of the permutation-supercoset model on $\mathrm{AdS}_3 \times \mathrm{S}^3$ with mixed flux. (The analysis of [96] is an extension of the results of [142] in the limit of pure RR flux.) The spinning-string ansatz of [38] enabled [143, 144] to obtain the integrable deformation of the NR system by NSNS flux. The system of [143, 144] comprises the spinning strings considered earlier, see subsection 2.3 of [101] and section 7 of [102]. The NSNS flux does not break Liouville integrability. If the mode number vanishes, E admits a series in the semi-classical and large Noether charges [143]. The coefficients of the series involve the parameter of the NSNS flux apart from the semi-classical Noether charges and the winding numbers. The series simplifies in the limit of pure NSNS flux, where the dispersion relation is exactly computable. The limit of pure NSNS flux permits to compute the dispersion relation exactly even for non-vanishing mode numbers [144].

The results of [143,144] raise the question of whether other classical solutions on $\mathrm{AdS}_3 \times \mathrm{S}^3$ with mixed flux that are analysable by similar techniques but whose dispersion relation is more tractable exist. In this chapter, we analyse pulsating strings on $\mathrm{AdS}_3 \times \mathrm{S}^3$ in the mixed-flux regime and in the limit of pure NSNS flux. The chapter has the following structure. In section 3.1, we rederive the integrable deformation of the NR system of [143,144] by using the

[1] Reference [140] proved that the supercoset model on $\mathrm{AdS}_5 \times \mathrm{S}^5$ admits a Pohlmeyer reduction. Therefore, mechanical systems can be argued to exist beyond the bosonic truncation of $\mathrm{AdS}_5 \times \mathrm{S}^5$. As a matter of fact, [141] constructed the integrable system of the SU(1|1) sector of $\mathrm{AdS}_5 \times \mathrm{S}^5$.

pulsating-string ansatz. In section 3.2, we analyse pulsating strings on $\mathrm{AdS}_3 \times \mathrm{S}^1 \subset \mathrm{AdS}_3 \times \mathrm{S}^3$ with NSNS flux. In subsection 3.2.1, we construct classical solutions in the mixed-flux regime. We write a closed formula for the dispersion relation of pulsating strings on the basis of considerations on the $\mathrm{SL}(2,\mathrm{R})$ WZNW model. In subsection 3.2.2, we retrieve the pulsating strings of the $\mathrm{SL}(2,\mathrm{R})$ WZNW model of [93] by Maldacena and Ooguri. We recover the short-string and long-string classes of [93] in the limit of pure NSNS flux of subsection 3.2.1. In section 3.3, we follow subsection 2.2.2 to construct the local spectral curve of pulsating strings of section 3.2, which is an elliptic curve. We write the mapping to the local spectral curve of minimal surfaces of section 4.3. In the limit of pure NSNS flux, we prove the singularisation of the elliptic curve and classify classical solutions.

This chapter is based on [P1]. [2] For background material on the connection between closed-string ansatze and mechanical systems, we refer to [10,12]. We refer to [101,146–148] for the deformation by NSNS flux of giant magnons. We refer to [146,149–153] for deformed generalised folded strings. We refer to [154–160] for the deformed (m,n)-strings .

3.1 The deformation of the Neumann-Rosochatius system

In this section, we construct the integrable deformation of the NR system by NSNS flux. We use the pulsating-string ansatz and formally obtain the same mechanical system as the one of [143,144] for spinning strings. We illustrate illustrate the method of [P6] by rederiving the Uhlenbeck constant. We also comment on the scope of the method.

Our starting point is the global coordinate system (C.6) and (C.10) of $\mathrm{AdS}_3 \times \mathrm{S}^3$ with NSNS flux. The metric and the B-field read (C.9) and (C.13), and (C.19) and (C.20), respectively. The pulsating-string ansatz consists of the trial functions

$$\cosh\rho = z_0(\tau)\ , \quad \sinh\rho = z_1(\tau)\ , \quad t = \beta_0(\tau)\ , \quad \psi = \beta_1(\tau) + k_1\sigma\ , \tag{3.1}$$

$$\cos\theta = r_1(\tau)\ , \quad \sin\theta = r_2(\tau)\ , \quad \varphi_1 = \alpha_1(\tau) + m_1\sigma\ , \quad \varphi_2 = \alpha_2(\tau) + m_2\sigma\ , \tag{3.2}$$

where $k_1, m_a \in \mathrm{Z}$ are winding number, and z_a and r_a are constrained by

$$-z_0^2 + z_1^2 = -1\ , \tag{3.3}$$

$$r_1^2 + r_2^2 = 1\ . \tag{3.4}$$

Periodic boundary conditions on σ hold because $k_1, m_a \in \mathrm{Z}$. Note that t has no winding number on account for the definition of AdS_3 as the universal cover of $\mathrm{SL}(2,\mathrm{R})$.

If we impose the conformal gauge-fixing condition $h_{\alpha\beta} = \eta_{\alpha\beta}$, (3.1) and (3.2) consistently truncate the equations of motion of the Polyakov action (2.47). The truncation follows from the action of an effective mechanical system whose coordinate along the temporal direction

[2] Reference [P1] and sections 3.1 and 3.2 build on the seminal content of subsection 3.5 of [145]. We correct and clarify [P1] in this chapter. We also use the chapter to address some issues. We use section 3.1 to illustrate the method to compute Uhlenbeck constant proposed in [P6] in the trivial case of [143,144]. We use section 3.2 to complement our analysis of local spectral curves of section 3.3 with explicit solutions. In subsection 3.2.2, we make more precise the analogy of pulsating strings and minimal surfaces of subsection 4.1.2, and we introduce the class of solutions of constant radius that reappear in subsection 5.1.1.

is τ. The Lagrangian of the truncation of the equations of motion follows from the introduction of (3.1) and (3.2) into (2.47). It reads

$$L = \frac{1}{2}\left[\sum_{a=0}^{1}\eta^{aa}(\dot{z}_a^2 + z_a^2\dot{\beta}_a^2) - k_1^2 z_1^2 - 2qk_1 z_1^2\dot{\beta}_0 - \Lambda_1(-z_0^2 + z_1^2 + 1)\right.$$
$$\left. + \sum_{a=1}^{2}(\dot{r}_a^2 + r_a^2\dot{\alpha}_a^2 - m_a^2 r_a^2) + 2qr_2^2(m_2\dot{\alpha}_1 - m_1\dot{\alpha}_2) - \Lambda_2(r_1^2 + r_2^2 - 1)\right] , \tag{3.5}$$

where $\eta^{00} = -\eta^{11} = -1$, and the Lagrange multipliers Λ_1 and Λ_2 impose (3.3) and (3.4), respectively. (In the Hamiltonian formalism, (3.3) and (3.4) are second-class constraints [37].) The Lagrangian realises the integrable deformation of the NR system of [143, 144]. If we introduce (3.1) and (3.2) in (2.49), the Virasoro constraints reduce to

$$\sum_{a=0}^{1}\eta^{aa}(\dot{z}_a^2 + z_a^2\dot{\beta}_a^2) + k_1^2 z_1^2 + \sum_{a=1}^{2}[\dot{r}_a^2 + (\dot{\alpha}_a^2 + m_a^2)r_a^2] = 0 , \tag{3.6}$$

$$k_1 z_1^2\dot{\beta}_1 + \sum_{a=1}^{2} m_a r_a^2\dot{\alpha}_a = 0 . \tag{3.7}$$

We do not write the equations of motion of r_a and z_a (see equations (8)–(11) of [P1]). We just note that they are independent. The sets z_a and β_a, and r_a and α_a are just intertwined through the Virasoro constraints (3.6) and (3.7). Moreover, the generalised coordinates β_a and α_a are cyclic in (3.5). Therefore, their associated canonically conjugate momenta

$$u_0 = -z_0^2\dot{\beta}_0 - qz_1^2 k_1 , \tag{3.8}$$
$$u_1 = z_1^2\dot{\beta}_1 , \tag{3.9}$$
$$v_1 = r_1^2\dot{\alpha}_1 + qr_2^2 m_2 , \tag{3.10}$$
$$v_2 = r_2^2\dot{\alpha}_2 - qr_2^2 m_1 . \tag{3.11}$$

are conserved. If we invert (3.8)–(3.11), we obtain

$$\dot{\beta}_0 = -\frac{u_0 + qk_1 z_1^2}{z_0^2} , \tag{3.12}$$
$$\dot{\beta}_1 = \frac{u_1}{z_1^2} , \tag{3.13}$$
$$\dot{\alpha}_1 = \frac{v_1 - qr_2^2 m_2}{r_1^2} , \tag{3.14}$$
$$\dot{\alpha}_2 = \frac{v_2 + qr_2^2 m_1}{r_2^2} . \tag{3.15}$$

The momenta (3.8)–(3.11) are proportional to the energy E, the Lorentzian spin S_1 and the angular momenta J_a, respectively:

$$E = \int_0^{2\pi} \mathrm{d}\sigma \frac{\delta S}{\delta \dot{t}} = -\sqrt{\lambda} u_0, \tag{3.16}$$

$$S_1 = \int_0^{2\pi} \mathrm{d}\sigma \frac{\delta S}{\delta \dot{\psi}} = \sqrt{\lambda} u_1 \ , \tag{3.17}$$

$$J_1 = \int_0^{2\pi} \mathrm{d}\sigma \frac{\delta S}{\delta \dot{\varphi}_1} = \sqrt{\lambda} v_1 \ , \tag{3.18}$$

$$J_2 = \int_0^{2\pi} \mathrm{d}\sigma \frac{\delta S}{\delta \dot{\varphi}_2} = \sqrt{\lambda} v_2 \ . \tag{3.19}$$

The Noether charges are, in principle, semi-classical, that is $\mathrm{O}(\sqrt{\lambda})$. We also introduce the total angular momentum $J = J_1 + J_2$ for later convenience.

The Hamiltonian H associated to (3.5) is $H = H_1 + H_2$, where

$$H_1 = \frac{1}{2}\left[-\dot{z}_0^2 + \dot{z}_1^2 + z_1^2 k_1^2 - \frac{(u_0 + q k_1 z_1^2)^2}{z_0^2} + \frac{u_1^2}{z_1^2} + \Lambda_1(-z_0^2 + z_1^2 + 1)\right] \ , \tag{3.20}$$

$$H_2 = \frac{1}{2}\left[\sum_{a=1}^{2}(\dot{r}_a^2 + r_a^2 m_a^2) + \frac{(v_1 - q m_2 r_2^2)^2}{r_1^2} + \frac{(v_2 + q m_1 r_2^2)^2}{r_2^2} + \Lambda_2(r_1^2 + r_2^2 - 1)\right] \ . \tag{3.21}$$

We have not introduced the momenta of z_a and r_a because they are just $\dot{z}_a$ and $\dot{r}_a$, respectively. Both H_a are conserved on their own due to the independence of their Hamilton equations. The functions H_1 and H_2 are the Hamiltonians of an integrable deformation of the two-dimensional NR system over a circumference and a branch of a hyperbola, respectively. Both mechanical systems have three first integrals, (the Hamiltonian (3.20) or (3.21), the pair of momenta (3.8) and (3.9), or (3.10) and (3.11)) for four generalised coordinates with one constraint. We deduce that each mechanical system is separately integrable. The Virasoro constraints force the classical trajectories of (3.20) and (3.21) to represent pulsating strings, as they guarantee classical world-sheet conformal invariance.

Integrability of the $(d+1)$-dimensional undeformed Neumann system (recall that $d+1$ denotes the number of non-cyclic coordinates subject to one constraint) follows from the conservation of d independent first integrals: the Uhlenbeck constants [37]. The integrability of the $(d+1)$-dimensional NR system follows from the $d+1$ conjugate momenta of the cyclic coordinates and d enhanced independent Uhlenbeck constants [38]. The Uhlenbeck constants of the NR system are in fact a degenerate limit of the Uhlenbeck constants of the $2(d+1)$-dimensional Neumann system [38]. Given a deformation of the $(d+1)$-dimensional NR system that preserves the cyclicity of $d+1$ generalised coordinates, integrability can be proved by obtaining a deformation of the Uhlenbeck constants. This goal can be achieved, for instance, by using an ansatz for the deformation [144, 161] or by drawing on the deformed Lax connection [139, 162]. The mechanical system of (3.20) and (3.21) is two-dimensional, and, hence, the Uhlenbeck must be proportional to the Hamiltonian. We can compute them using the procedure proposed in [P6] in this rather trivial example.

First, we must solve the constraints (3.3) and (3.4) in the limit of pure RR flux. The step is equivalent to the restriction of the coordinates of the phase space to the constraint submanifold, and it is accomplished by using the initial coordinates θ and ρ in (3.1). The step removes Λ_1 and Λ_2 from (3.20) and (3.21), respectively.

Second, we must consider the Uhlenbeck constants. We denote the pairs of Uhlenbeck constants of the NR systems of H_1 and H_2 by F_0 and F_1, and I_1 and I_2, respectively. The Uhlenbeck constants satisfy the constraints [38, 144], which read

$$H_1 = \frac{1}{2}(k_1^2 F_1 - u_0^2 - u_1^2)\ , \quad -F_0 + F_1 = -1\ , \tag{3.22}$$

$$H_2 = \frac{1}{2}(m_1^2 I_1 + m_2^2 I_2 + v_1^2 + v_2^2)\ , \quad I_1 + I_2 = 1\ . \tag{3.23}$$

Note that the vanishing winding number of t implies the absence of F_0 in H_1. We assume that k_1^2 does not vanish, which implies that the world-sheet has extension in AdS_3. We also assume that m_1^2 differs from m_2^2, which implies that the world-sheet has extension in AdS_3. If these conditions were not satisfied, we would confront a degenerate point-like case of the NR system connected to the Rosochatius system; see (2.12) of [162]. If we invert (3.22) and (3.23), we obtain

$$F_0 = \frac{2H_1 + u_0^2 + u_1^2 - k_1^2}{k_1^2}\ , \tag{3.24}$$

$$F_1 = \frac{2H_1 + u_0^2 + u_1^2}{k_1^2}\ , \tag{3.25}$$

$$I_1 = \frac{2H_2 - m_2^2 - v_1^2 - v_2^2}{m_1^2 - m_2^2}\ , \tag{3.26}$$

$$I_2 = \frac{2H_2 - m_1^2 - v_1^2 - v_2^2}{m_2^2 - m_1^2}\ . \tag{3.27}$$

Since each H_a is conserved, so they are the associated Uhlenbeck constants.

Given a deformation of the two-dimensional NR system that preserves both the cyclicity of two coordinates and the conservation of the Hamiltonian, we can derive the Uhlenbeck constants if we assume that (3.24)–(3.27) still holds. In the case of (3.20) and (3.21), formulae (3.24)–(3.27) provide

$$F_0 = (1-q^2)z_0^2 + \frac{1}{k_1^2}\left[(z_0\dot{z}_1 - z_1\dot{z}_0)^2 + (u_0 - qk_1)^2\frac{z_1^2}{z_0^2} + u_1^2\frac{z_0^2}{z_1^2} + q^2k_1^2\right], \tag{3.28}$$

$$F_1 = (1-q^2)z_1^2 + \frac{1}{k_1^2}\left[(z_0\dot{z}_1 - z_1\dot{z}_0)^2 + (u_0 - qk_1)^2\frac{z_1^2}{z_0^2} + u_1^2\frac{z_0^2}{z_1^2}\right], \tag{3.29}$$

$$\begin{aligned} I_1 = (1-q^2)r_1^2 - \frac{1}{m_2^2 - m_1^2}\Bigg[&(r_1\dot{r}_2 - r_2\dot{r}_1)^2 + (v_1 - qm_2)^2\frac{r_2^2}{r_1^2} + (v_2 + qm_1)^2\frac{r_1^2}{r_2^2} \\ &+2qm_1v_2 - q^2(m_1^2 - m_2^2)\Bigg], \end{aligned} \tag{3.30}$$

$$\begin{aligned} I_2 = (1-q^2)r_2^2 + \frac{1}{m_2^2 - m_1^2}\Bigg[&(r_1\dot{r}_2 - r_2\dot{r}_1)^2 + (v_1 - qm_2)^2\frac{r_2^2}{r_1^2} + (v_2 + qm_1)^2\frac{r_1^2}{r_2^2} \\ &+2qm_1v_2\Bigg]. \end{aligned} \tag{3.31}$$

which match, up to the sign of q and some constants, (2.24) and (4.14) of [144].

We emphasise that the application of the method of [P6] is merely justified by completeness. We could have used the Hamiltonian. However, we note the the scope of the method of [P6] is not limited to deformations of the two-dimensional NR system. The method is in principle applicable to integrable deformations of the $(d+1)$-dimensional NR system that preserve the ciclicity of $d+1$ coordinates. The procedure there would start from all the possible consistent truncations of the deformed NR system to one dimension, where the previous steps are applicable. Next, the pairs of Uhlenbeck constants of each mechanical system would be uplifted to the $(d+1)$-dimensional NR system by demanding the compatibility among different truncations. The method, which is entirely algebraic, should permit to avoid the cumbersome steps that arise in the alternative approaches of [139,144,161,162]. We emphasise that this approach does not guarantee that the deformation of the Uhlenbeck constants of the deformed $(d+1)$-dimensional NR system are in involution, and this property must be studied separately. However, the problem is superfluous in the deformation of the two-dimensional NR system, where just one independent first integral exists.

Formulae (3.28)–(3.31) allow us to reduce of the equations of motion of the model to a couple of independent first-order ordinary differential equations. These equations can be conveniently parameterised by coordinates that solve (3.3) and (3.4). These are the ellipsoidal coordinate ζ if the oscillators are confined to a circumference and the hyperboloidal coordinate μ if they are confined to the branch of a hyperbola. Formulae (3.28)–(3.31) are rational functions of ζ and μ. In the end, (3.28)–(3.31) provide simple equations of motion that involve a cubic polynomial ζ and μ. Even though the polynomial roots are intricate, the solution is formally available; see (23)–(27) of [P1]. We can write tractable expressions if the mechanical system is truncated consistently. We adopt this approach in the next section.

3.2 Pulsating strings on $\mathbf{AdS_3 \times S^1}$

In this section, we analyse and construct pulsating strings on $\mathrm{AdS}_3 \times \mathrm{S}^1 \subset \mathrm{AdS}_3 \times \mathrm{S}^3$ with NSNS flux, where S^1 is an equator S^3. In subsection 3.2.1, we write the solutions together with their dispersion relation in the mixed-flux regime. Our results generalise under RR flux the pulsating strings of the $\mathrm{SL}(2,\mathrm{R})$ WZNW model constructed in section 2 of [93] by Maldacena and Ooguri. To write the dispersion relation we draw on considerations on the $\mathrm{SL}(2,\mathrm{R})$ WZNW model. In subsection 3.2.2, we connect subsection 3.2.1 with [93]. We retrieve the short-string and long-string classes and the threshold between them. We use elliptic integrals and Jacobian elliptic functions in this section. Our conventions, together with properties and formulae, are collected in appendix F.

3.2.1 Pulsating strings in the mixed-flux regime

First, we must truncate (3.2) consistently. Since the equations of motion of (3.20) are divided into two independent sets, we can truncate the ansatz (3.2) to $\mathrm{AdS}_3 \times \mathrm{S}^1$ by finding a solution to the equations of motion along $\mathrm{S}^1 \subset \mathrm{S}^3$. The solution is $r_1 = 1$, $r_2 = 0$, $\alpha_1 = \omega\tau$, and $\alpha_2 = 0$, for instance. The total angular momentum J is proportional to ω through $J = \sqrt{\lambda}\omega$, see (3.18) and (3.19). The truncation of the pulsating-string ansatz represents the degeneration of the world-sheet inside S^3, where it is a geodesic that surrounds S^3 along a great ring. We thus obtain the geodesic motion of the Rosochatius system in S^3, whose Hamiltonian is H_2 in (3.20) with $m_1 = m_2 = 0$.

The Virasoro constraints (3.6) and (3.7) simplify to

$$\dot{z}_0^2 + \frac{(u_0 + qk_1 z_1^2)^2}{z_0^2} = \dot{z}_1^2 + \frac{u_1^2}{z_1^2} + k_1^2 z_1^2 + \omega^2 \ , \tag{3.32}$$

$$u_1 k_1 = 0 \ . \tag{3.33}$$

Equation (3.32) provides the dispersion relation. Equation (3.33) implies either $u_1 = 0$ or $k_1 = 0$. If $k_1 = 0$, we would have a degenerate world-sheet which is a geodesic in AdS_3. Therefore, we must set $u_1 = 0$. In subsection 3.2.2, we shall connect the geodesic motion in AdS_3 of $k_1 = 0$ with solutions with $k_1 \neq 0$ via the spectral flow of the $SL(2,R)$ WZNW model.

We follow [144] now and define the hyperboloidal coordinate μ by

$$-\frac{z_0^2}{\mu} + \frac{z_1^2}{\mu - k_1^2} = 0 \ , \tag{3.34}$$

or, equivalently, by

$$z_0^2 = \frac{\mu}{k_1^2} \ , \quad z_1^2 = \frac{\mu - k_1^2}{k_1^2} \ . \tag{3.35}$$

The positivity of the hyperbolic radius $\rho \geq 0$ in (3.1) implies $\mu \geq k_1^2$. The hyperboloidal coordinate satisfies

$$\frac{\dot{\mu}^2}{4\mu(\mu - k_1^2)} = (z_0 \dot{z}_1 - z_1 \dot{z}_0)^2 \ . \tag{3.36}$$

If we use (3.35) and (3.36) in, for instance, the expression of F_1 in (3.29), we obtain [3]

$$\begin{aligned} \dot{\mu}^2 &= -4(\mu - k_1^2)(\bar{q}^2\mu^2 + [(u_0 - qk_1)^2 - (F_1 + \bar{q}^2)k_1^2]\mu - (u_0 - qk_1)^2 k_1^2) \\ &= 4\bar{q}^2(\mu_3 - \mu)(\mu - \mu_2)(\mu - \mu_1) \ , \end{aligned} \tag{3.37}$$

where we have used $\bar{q} = \sqrt{1 - q^2}$ for compactness. The roots μ_a of the cubic polynomial read

$$\begin{aligned} \mu_1 &= \frac{(F_1 + \bar{q}^2)k_1^2 - (u_0 - qk_1)^2 - \sqrt{[(F_1 + \bar{q}^2)k_1^2 - (u_0 - qk_1)^2]^2 + 4\bar{q}^2(u_0 - qk_1)^2 k_1^2}}{2\bar{q}^2} \ , \\ \mu_2 &= k_1^2 \ , \\ \mu_3 &= \frac{(F_1 + \bar{q}^2)k_1^2 - (u_0 - qk_1)^2 + \sqrt{[(F_1 + \bar{q}^2)k_1^2 - (u_0 - qk_1)^2]^2 + 4\bar{q}^2(u_0 - qk_1)^2 k_1^2}}{2\bar{q}^2} \ . \end{aligned} \tag{3.38}$$

[3] Equation (3.37) defines an elliptic curve. It would be then possible to analyse the solutions to (3.37) by using the quantities of appendix E. In this section, we solve directly (3.37) instead. We defer the construction of an elliptic curve for pulsating strings until section 3.3, where we rely on subsection 2.2.2. We prefer the curve of section 3.3 over the one defined by (3.37) because of two reasons. First, in section 3.3, we just need a coordinate system wherein pulsating strings are factorisable, not a privileged coordinate system. Second, the curve of elliptic section 3.3 relies on the spectral parameter, which is independent of the coordinate system, whereas the curve of (3.37) is defined by μ itself. The same argument applies to (4.8) in subsection 4.1.1.

We consider the limit of pure RR flux and the mixed-flux regime first, where $0 \leq q < 1$. The roots μ_a are finite. Equation (3.29) implies that $F_1 > 0$. The roots (3.38) are arrayed in the hierarchy $\mu_1 < \mu_2 < \mu_3$. Furthermore, they satisfy $\mu_1 < 0$ and $0 < \mu_2 < \mu_3$. Since μ is real and subject to $\mu \geq k_1^2 = \mu_2$, (3.37) implies that μ belongs to $\mu_2 \leq \mu \leq \mu_3$. This bound implies that μ can be either constant or non-constant.

We assume that μ is non-constant first. We can solve (3.37) by an integration and a subsequent inversion. If we use (F.26), we obtain [4]

$$\mu = \mu_2 + \frac{(\mu_3 - \mu_2)(\mu_2 - \mu_1)}{\mu_3 - \mu_1} \operatorname{sd}^2(\sqrt{(1-q^2)(\mu_3 - \mu_1)}\tau, \kappa) \ , \tag{3.39}$$

where $\operatorname{sd}(x, m)$ is defined in (F.35), the elliptic modulus is

$$\kappa = \sqrt{\frac{\mu_3 - \mu_1}{\mu_3 - \mu_2}} \ , \tag{3.40}$$

and we have set the integration constant to zero. Note that the $\mu_1 < \mu_2 < \mu_3$ implies that κ belongs to the fundamental domain: $0 < \kappa < 1$. Solution (3.39) periodic on τ due to (F.43). The period is

$$L = \frac{2\,\mathrm{K}(\kappa)}{\sqrt{(1-q^2)(\mu_3 - \mu_1)}} \ , \tag{3.41}$$

where $\mathrm{K}(m)$ is defined in (F.2). The bound $\mu_2 \leq \mu \leq \mu_3$ is respected because of (F.51).

The behaviour of the pulsating string is the following. The world-sheet of the solution is confined within a finite region of AdS_3 because the hyperbolic radius ρ is bounded. Inside this region, the pulsation occurs. Consider one pulsation. The solution (3.39) collapses to the centre of AdS_3 at $\rho = 0$ when $\tau = 2nL$, with $n \in \mathrm{Z}$. The more τ increases, the more the radius of the solution (3.39) increases. The maximum radius $\rho_0 = \operatorname{arcsinh}(\sqrt{\mu_3 - k_1^2}/|k_1|)$ is reached at $\tau = (2n+1)L$. The radius of the solution (3.39) then decreases until it collapses again at $\rho = 0$ when $\tau = (2n+2)L$. Each pulsation corresponds to a lobe in the world-sheet. The world-sheet consists of a concatenation of the lobes linked at the end points.

Equation (3.37) also permits to write $t = \beta_0$ in (3.12) through a direct integration. Formula (F.27) leads us to

$$\begin{aligned} t = &- \frac{(u_0 - qk_1)k_1^2 + qk_1\mu_1}{\mu_1}\tau \\ &- \frac{(u_0 - qk_1)(k_1^2 - \mu_1)}{\mu_1\sqrt{(1-q^2)(\mu_3 - \mu_1)}}\Pi\left(\operatorname{am}(\sqrt{(1-q^2)(\mu_3 - \mu_1)}\tau, \kappa), \nu, \kappa\right) \ , \end{aligned} \tag{3.42}$$

where $\Pi(x, n, m)$ and $\operatorname{am}(x, m)$ are defined in (F.6) and (F.32), respectively, and the elliptic characteristic reads

$$\nu = \frac{(\mu_3 - \mu_2)\mu_1}{(\mu_3 - \mu_1)\mu_2} \ . \tag{3.43}$$

[4] Pulsating strings in the mixed-flux regime were also constructed in [163]. The difference between [163] and this section is the treatment of the dispersion relation and limit of pure NSNS flux of pulsating strings. If we identify $R_+ = \mu_3/k_1^2 - 1$, $R_- = \mu_1/k_1^2 - 1$ and $m = k_1$ in [163], we retrieve our expressions, in particular (3.39).

Note that $\nu < 0$. The pulsations are isochronous with respect to t. The target-space period T elapsed in one pulsation is

$$T = -\frac{2\left|(u_0 - qk_1)(k_1^2 - \mu_1)\Pi(\nu,\kappa) + \left[(u_0 - qk_1)k_1^2 + qk_1\mu_1\right]\mathrm{K}(\kappa)\right|}{\mu_1\sqrt{(1-q^2)(\mu_3 - \mu_1)}} , \tag{3.44}$$

where $\Pi(n,m)$ is defined in (F.6).

Consider the case where μ is constant. The right-hand side of (3.37) must vanish identically. Since $q < 1$, either $\mu = k_1^2$ or $\mu = \mu_3$ must hold. If $\mu = k_1^2$, the world-sheet collapses at $\rho = 0$. There is a polar coordinate singularity at $\rho = 0$ in the global coordinate system, where ψ is not defined. If we set $\rho = 0$ and $k_1 = 0$ in (3.12), we obtain $t = -u_0\tau$. The pulsating string collapses to the BMN vacuum: a point-like solution whose world-sheet is a null geodesics along direction of t at the centre of AdS_3 that surrounds S^3 along an equator.

If $\mu = \mu_3$, the hyperbolic radius is non-vanishing and constant: $\rho_0 = \operatorname{arcsinh}(\sqrt{\mu_3 - k_1^2}/|k_1|)$. It follows from (3.12) t depends linearly on τ. The solution does not pulsate; the world-sheet is a cylinder of constant ρ_0. We emphasise for later convenience that, given the parameters that determine μ_a in (3.38), the value of $\rho_0 > 0$ is unique.

We can write the dispersion relation of pulsating strings on $\mathrm{AdS}_3 \times \mathrm{S}^1$ with NSNS flux in a closed form. The closed form extends the results of [93] beyond the limit of pure NSNS flux. We begin with solutions of non-constant μ. The mechanical system has three first integrals, H_1 and u_a, for four generalised coordinates with one constraint. Formulae (3.16) and (3.17) states the proportionality between u_a and the Noether charges: $E = -\sqrt{\lambda}u_0$ and $S_1 = \sqrt{\lambda}u_1$. The Virasoro constraints (3.32) and (3.33) are alien to the mechanical system and must be imposed to classical trajectories. Equations (3.17) and (3.33) imply $S_1 = 0$. Equation (3.32) implies $H_1 = J^2/\lambda$, and, therefore, it implies the dispersion relation.

The mechanical model has three independent first integrals, but we have just identified two closed-string moduli, namely E and S_1. To write a sensible dispersion relation, we must identify an additional modulus. As opposed to spinning strings, periodicity on σ does not supply the mode number of pulsating strings. One convenient choice of modulus is the adiabatic invariant N that follows from the quantisation of the action variables of the mechanical system [49, 50]. This approach was adopted, with $J = 0$, in section 3 of [163] and subsection 4.4 of [164] near the limits of pure RR flux and NSNS flux, respectively. The resultant dispersion relation is not closed however.

We adopt an alternative approach. First, we make some preliminary observations on the $\mathrm{SL}(2,\mathrm{R})$ WZNW model [93]. The world-sheet CFT_2 has different spectrally flowed sectors that organise the unitary irreducible representations of the current algebra and the spectrum of energies. These representations are built on representations of $\mathrm{SL}(2,\mathrm{R})$ spanned by zeroth-level generators; see subsection 4.1 of [93]. The zeroth-level generators realise the unitary irreducible representations of the principal discrete series, called *short-string representations*, and the principal continuous series, called *long-string representations*. Short-string representations are labelled by the Casimir invariant $c_2 = -l(l-1)$, where $l \in \mathrm{R}$. Unitarity holds if $1/2 < l < (k+1)/2$; see appendix C of [165]. Long-string representations are labelled by $c_2 = -l(l-1)$, where $l = 1/2 + \mathrm{i}\, s$. Unitarity holds if $s \in \mathrm{R}$.

If $k \to \infty$, the Casimir invariant appears at the semi-classical level: $c_2 \sim k^2 \to \infty$. The Casimir invariant turns out to appear in the ratio $\alpha^2 = \pm 4c_2/k^2$, where $+$ and $-$ correspond to short-string and long-string representations, respectively. The quantity $\mp k\alpha^2/4$ is the on-shell energy-momentum tensor of the point-like strings of short-string representations (corresponding to $-$) and long-string representations (corresponding to $+$). Point-like strings give rise to pulsating strings under spectral flow. The spectral flow maps α to the frequency of pulsating strings. The frequency is the analogue of the mode number of spinning strings.

We argue that we can use α beyond the limit of pure NSNS flux by the following argument. The RNS formalism (specifically, in closed-superstring field theory; see [164] and references therein) corresponds to a non-local deformation of the world-sheet CFT_2 that is treated perturbatively. The Hilbert space does not contain long-string representations since the RR flux spoils their unitary [165]. The Hilbert space however contains short-string representations, at least from the perturbative point of view. Then α is a meaningful closed-string modulus in the mixed-flux regime for short-string representations when $\lambda \to \infty$.

In sum, we use α, the frequency of the pulsating string, to derive the dispersion relation. If we look at (3.39), we deduce that

$$\alpha^4 = \bar{q}^2(\mu_3 - \mu_1)^2 = [k_1^2(F_1 + \bar{q}^2) - (u_0 - qk_1)^2]^2 + 4\bar{q}^2(u_0 - qk_1)^2 k_1^2 \ . \tag{3.45}$$

If we use the expression of F_1 in (3.29) and (3.32), we end up with

$$4(u_0 - qk_1)^2 k_1^2 + 4qk_1(k_1^2 - \omega^2)(u_0 - qk_1) + (k_1^2 - \omega^2)^2 - \alpha^4 = 0 \ . \tag{3.46}$$

This equation is a quadratic algebraic equation for u_0. If we solve the equation for u_0 and use (3.12), we obtain

$$E = -\frac{\sqrt{\lambda}}{2k_1}\left[q\left(k_1^2 + \frac{J^2}{\lambda}\right) \mp \sqrt{\alpha^4 - \bar{q}^2\left(k_1^2 - \frac{J^2}{\lambda}\right)}\right] \ . \tag{3.47}$$

The dispersion relation corresponds to pulsating strings of (3.39) and (3.42).

If the solution has constant μ, α is not definable. We need to obtain the dispersion relation separately. If $\mu = k_1^2$, we have $z_0 = 1$ and $z_1 = 0$. If we use (3.32), we obtain

$$E = |J| \ , \tag{3.48}$$

which is the dispersion relation of BPS states in $\mathrm{AdS}_5 \times \mathrm{S}^5$, see (1.4).

If $\mu = \mu_3$, we have instead $z_0 = \cosh\rho_0$ and $z_1 = \sinh\rho_0$. We decide to express the dispersion relation in terms of ρ_0 (even though is not a sensible closed-string moduli). If we use (3.32), we obtain

$$E = \sqrt{\lambda}\left(qk_1 \sinh^2\rho_0 \mp \sqrt{k_1^2 \sinh^2\rho_0 + \frac{J^2}{\lambda}}\cosh\rho_0\right) \ . \tag{3.49}$$

The dispersion relation, as written in (3.49), will allow us to clarify the limit of pure NSNS flux. In particular, it will allows us to justify the enhancement of the class of solutions with constant ρ_0.

Some observations are in order. First and foremost, (3.47) (and (3.49) as well) involves two branches if the radicand does not vanish. We keep both branches as the limit of pure NSNS flux gives rise to two classes of pulsating strings. Each class corresponds to one sign of (3.47). The threshold between them corresponds to the case of vanishing radicand. Since the RR flux destroys the unitarity of long-string representation [92, 165], the positive branches of (3.47) and (3.49) are nonetheless likely to be forbidden. (The exclusion is qualitatively supported by the behaviour of pulsating strings in the mixed-flux regime: classical solutions of short-string representations display bounded pulsations in AdS_3 as opposed to classical solutions of long-string representations.) Second, the dispersion relation (3.47) does not automatically correspond to pulsating string sourced to vertex operators that are primary operators. The property is satisfied if the Noether charges of the generators of $SL(2, R)$ that lie outside the Cartan algebra vanish [30]. If we wrote the action (2.47) in terms of (C.6), applied the Noether theorem and used the pulsating-string ansatz (3.1), we would obtain that the condition holds. Third, neither (3.47) nor (3.49) display the BMN scaling in the semi-classical limit $J \sim \sqrt{\lambda} \to \infty$ with λ/J^2 fixed and small; see (1.10). The violation BMN scaling is a consequence of the introduction of α in (3.47) and ρ_0 in (3.49). If a semi-classical adiabatic invariant N were introduced [49], the appropriate BMN scaling could be recovered if N and J scale properly. Finally, the dispersion relation (3.47) should hold in $\lambda \to \infty$, where it could receive corrections under quantisation. Corrections indeed arise in the limit of pure NSNS limit; see (75) and (80) in subsection 4.4 of [93].

3.2.2 Maldacena-Ooguri pulsating strings

We focus on the limit of pure NSNS flux now, where $q = 1$. We can apply the limit from the outset in (3.37). We can also apply the limit to (3.39), (3.42), and the dispersion relation (3.47). We choose the last point of view because it makes clear the connection with the mixed-flux regime. The results are the same irrespective of the starting point. We focus on solutions with non-constant μ and analyse the solutions with constant μ in the end.

Pulsating strings in the limit of pure NSNS flux fall into two classes separated by a threshold. The classes are called *short-string class* and *long-string class* and are associated to short-string and long-string representations, respectively. The limit of pure NSNS flux reduces (3.37) to a quadratic polynomial. Since μ_a must respect $\mu_1 < \mu_2 < \mu_3$, either μ_1 or μ_3 must diverge. The sign of $(u_0 - k_1)^2 - k_1^2 F_1$ dictates which root diverges. The short-string class corresponds to $(u_0 - k_1)^2 > k_1^2 F_1$, where μ_1 diverges; the long-string class corresponds to $(u_0 - k_1)^2 < k_1^2 F_1$, where μ_3 diverges. The point $(u_0 - k_1)^2 = k_1^2 F_1$ corresponds to the threshold, where both μ_1 and μ_3 diverge. The limit of pure NSNS flux reduces (3.37) to a linear polynomial in the threshold.

The classical solution reflects the degeneration of (3.37) as the reduction of (3.39) and (3.42) to trigonometric and hyperbolic functions in the short-string and long-string classes, respectively. In the threshold,(3.39) and (3.42) reduce to polynomials. We note that $(u_0 - k_1)^2 - k_1^2 F_1$ for pulsating string is analogous to $k^2 - 2kp$ for connected minimal surfaces in subsection 4.1.2: the sign of $k^2 - 2kp$ discriminates between two different classes in limit of pure NSNS flux. In section 3.3, we bear the analogy out by writing the map between the local algebraic curves of pulsating strings and minimal surfaces.

Let $(u_0 - k_1)^2 > k_1^2 F_1$, which corresponds to the short-string class. If we apply the limit of pure NSNS flux to (3.38), we obtain

$$\mu_1 = -\infty \ , \quad \mu_2 = k_1^2 \ , \quad \mu_3 = \frac{(u_0 - k_1)^2 k_1^2}{(u_0 - k_1)^2 - k_1^2 F_1} \ . \tag{3.50}$$

The elliptic modulus (3.40) vanishes: $\kappa = 0$. If we use (F.55), we obtain that (3.39) is

$$\mu = k_1^2 + \frac{k_1^4 F_1}{(u_0 - k_1)^2 - k_1^2 F_1} \sin^2\left(\sqrt{(u_0 - k_1)^2 - k_1^2 F_1} \tau\right) \ . \tag{3.51}$$

The frequency is

$$\alpha = \sqrt{(u_0 - k_1)^2 - k_1^2 F_1} \ , \tag{3.52}$$

consistently with (3.45). Formula (3.51) implies that the period L simplifies to

$$L = \frac{\pi}{\sqrt{(u_0 - k_1)^2 - k_1^2 F_1}} \ . \tag{3.53}$$

This formula also follows from the introduction of (F.16) in (3.41).

The behaviour of the pulsating string in the short-string class is analogous to that in the mixed-flux regime. The world-sheet consists of a chain of lobes confined within a finite region of AdS_3. Each lobe corresponds to a pulsation. The hyperbolic radius ρ is bounded, and the maximum radius of the solution is

$$\rho_0 = \operatorname{arcsinh}\left(\sqrt{\frac{k_1^2 F_1}{(u_0 - k_1^2)^2 - k_1^2 F_1}}\right) \ . \tag{3.54}$$

Moreover, (3.42) simplifies to

$$t = -k_1 \tau - \arctan\left(\frac{u_0 - k_1}{\sqrt{(u_0 - k_1)^2 - k_1^2 F_1}} \tan\left(\sqrt{(u_0 - k_1)^2 - k_1^2 F_1} \tau\right)\right) \ , \tag{3.55}$$

where we have used that the elliptic characteristic (3.43) reduces to

$$\nu = -\sinh\rho_0 = -\frac{k_1^2 F_1}{(u_0 - k_1)^2 - k_1^2 F_1} \ , \tag{3.56}$$

and also (F.15) and (F.52). Each pulsation is isochronous with respect to t and the target-space period is

$$T = \frac{k_1 \pi}{\sqrt{(u_0 - k_1)^2 - k_1^2 F_1}} + \pi, \tag{3.57}$$

which follows from (3.42) once we use (F.16) and (F.18).

We rephrase (3.51) as $\sinh\rho = \sinh\rho_0 |\sin(\alpha\tau)|$ now, where ρ_0 is (3.54) and (3.55) is

$$\tan t = \frac{\tan(-k_1\tau) + \cosh\rho_0 \tan(\alpha\tau)}{1 - \cosh\rho_0 \tan(-k_1\tau)\tan(\alpha\tau)} \ . \tag{3.58}$$

We have introduced the redefinition $\alpha \mapsto -\mathrm{sign}(u_0-k_1)\alpha$, irrelevant to the dispersion relation. If we identify $\psi = -\phi + \pi/2$ and $k_1 = -w$, where w is the spectral-flow parameter, [5] we reproduce (34) of [93] (up to the replacement $1/\cosh\rho_0 \mapsto \cosh\rho_0$). The upshot of the identification is that pulsating strings in the short-string class are generated by the time-like geodesic at centre of AdS_3, that is the BMN vacuum under spectral flow.

If we apply the limit of pure NSNS flux to the negative branch of (3.47), we obtain

$$E = -\frac{k}{2}\left[k_1 + \frac{1}{k_1}\left(\frac{J^2}{k^2} - \alpha^2\right)\right] \ , \tag{3.59}$$

where we have used (2.41) to write $\sqrt{\lambda} = k$. If we identify $k_1 = -w$ and $J = \sqrt{4hk}$, this expression agrees with (33) of [93] (up to the replacement of $\alpha^2 \mapsto (1/2)\alpha^2$). Formula (3.59) is the dispersion relation of pulsating strings in the short-string class.

Let $k_1^2 F_1 < (u_0 - k_1)^2$, which corresponds to the long-string class. The application of the limit of pure NSNS flux to (3.38) provides

$$\mu_1 = -\frac{(u_0-k_1)^2 k_1^2}{k_1^2 F_1 - (u_0-k_1)^2} \ , \quad \mu_2 = k_1^2 \ , \quad \mu_3 = \infty \ . \tag{3.60}$$

As opposed to the short-string class, the elliptic modulus (3.40) becomes one: $\kappa = 1$. According to (F.59), the expression (3.39) reduces to

$$\mu = k_1^2 + \frac{k_1^4 F_1}{k_1^2 F_1 - (u_0-k_1)^2}\sinh^2\left(\sqrt{k_1^2 F_1 - (u_0-k_1)^2}\,\tau\right) \ . \tag{3.61}$$

The solution (3.61) is unbounded, consistently with the divergence of μ_3, and aperiodic. To define the frequency α, we apply the limit of pure NSNS flux to (3.45). We obtain

$$\alpha = \sqrt{k_1^2 F_1 - (u_0-k_1)^2} \ . \tag{3.62}$$

Moreover, aperiodicity is reflected in the divergence of (3.41). If we use (F.22), we are led to

$$L = \infty \ . \tag{3.63}$$

The behaviour of the pulsating string is the following. The world-sheet of the solution is unbounded in AdS_3 because the hyperbolic radius ρ is unbounded. Just one pulsation occurs. The solution (3.61) collapses at the centre of AdS_3 at $\rho = 0$ when $\tau = 0$. Since the growth of ρ is not bounded, (3.61) increases indefinitely until it reaches the conformal boundary of AdS_3 at $\rho = \infty$ when $\tau = \infty$. The reverse situation holds between $\tau = -\infty$ and $\tau = 0$: (3.61) starts from $\rho = \infty$ and collapses at $\rho = 0$. Therefore, the world-sheet consists of two half-lobes connected at the centre of AdS_3.

To write (3.61), we have relied tacitly on the choice of the integration constant in (3.39). We could have shifted $\tau \mapsto \tau + \mathrm{K}(\kappa)/\sqrt{(1-q^2)(\mu_3-\mu_1)}$ in (3.39) without further consequences. However, if we had applied the limit of pure NSNS flux to (3.39), we would have

[5] The equality w between k_1 is rather accidental and just concerns pulsating strings. The spectral-flow parameter w in general just labels spectrally flowed sectors in the world-sheet CFT_2; see section 3 of [93].

obtained $\mu = \infty$ instead of (3.61). The seeming inconsistency is a consequence of the localisation of μ in the region where (3.61) reaches the boundary of AdS_3, instead of in the region where (3.61) traverses the bulk of AdS_3. We encounter an analogous situation in subsection 4.1.2, where we need to fix properly the integration range to construct connected minimal surfaces with $k^2 - 2kp > 0$ in the limit of pure NSNS flux.

Moreover, (3.42) reduces to

$$t = -k_1\tau - \arctan\left(\frac{u_0 - k_1}{\sqrt{k_1^2 F_1 - (u_0 - k_1)^2}} \tanh\left(\sqrt{k_1^2 F_1 - (u_0 - k_1)^2}\tau\right)\right) , \tag{3.64}$$

where we have used that elliptic characteristic (3.43) simplifies to

$$\nu = -\frac{(u_0 - k_1)^2}{k_1^2 F_1 - (u_0 - k_1)^2} , \tag{3.65}$$

together with (F.21) and (F.56). The motion is no longer isochronous, but involves one everlasting pulsation. Therefore, the target-space period diverges:

$$T = \infty , \tag{3.66}$$

as also follows from the application of (F.22) and (F.24) to (3.44).

To match [93], we must reword (3.61) and (3.64). Let $\sinh\rho = \cosh\rho_0 |\sinh^2(\alpha\tau)|$, with

$$\rho_0 = \operatorname{arcsinh}\left(\frac{|u_0 - k_1|}{\sqrt{k_1^2 F_1 - (u_0 - k_1)^2}}\right) , \tag{3.67}$$

and (3.64) as

$$\tan t = \frac{\tan(-k_1\tau) + \sinh\rho_0 \tanh\left(-\mathrm{sign}(u_0 - k_1)\sqrt{k_1^2 F_1 - (u_0 - k_1)^2}\tau\right)}{1 - \sinh\rho_0 \tan(-k_1\tau) \tanh\left(-\mathrm{sign}\,(u_0 - k_1)\sqrt{k_1^2 F_1 - (u_0 - k_1)^2}\tau\right)} , \tag{3.68}$$

where we have introduced the redefinition $\alpha \mapsto -\mathrm{sign}(u_0 - k_1)\alpha$ again. Note that ρ_0 in (3.67) is not the maximum radius since (3.61) is unbounded. If we identify $\psi = -\phi$ and $k_1 = -w$, we match (44) of [93]. The upshot is that pulsating strings in the long-string class are generated by space-like geodesics in AdS_3 under spectral flow.

If we apply the limit of pure NSNS flux to (3.47), we are led to

$$E = -\frac{k}{2}\left[k_1 + \frac{1}{k_1}\left(\frac{J^2}{k^2} + \alpha^2\right)\right] , \tag{3.69}$$

where we have replaced $\sqrt{\lambda}$ by k by virtue of (2.41). If we identify $k_1 = -w$ and $J = \sqrt{4hk}$, we recover equation (40) of [93]. The dispersion relation (3.69) is the dispersion relation of pulsating strings in the long-string class.

Let $(u_0 - k_1)^2 = k_1^2 F_1$, which corresponds to the threshold between the short-string and long-string classes. If apply the limit of pure NSNS flux in (3.38), we obtain

$$\mu_1 = -\infty \ , \quad \mu_2 = k_1^2 \ , \quad \mu_3 = \infty \ . \tag{3.70}$$

The coordinate μ in (3.39) now reads

$$\mu = k_1^2 + k_1^2 (u_0 - k_1)^2 \tau^2 \ , \tag{3.71}$$

which is retrievable from both (3.51) and (3.61). The expression (3.71) is bounded and aperiodic. The limit of pure NSNS flux of (3.45) vanishes:

$$\alpha = 0 \ . \tag{3.72}$$

Aperiodicity is reflected in the divergence of the period:

$$L = \infty \ . \tag{3.73}$$

The behaviour of the pulsating string is similar to that present in the long-string class. The world-sheet reaches the boundary of AdS_3 at $\rho = \infty$ when $\tau = \pm\infty$. Moreover, (3.42) simplifies to

$$t = -k_1 \tau \ . \tag{3.74}$$

Hence, the target-space period is infinite:

$$T = \infty. \tag{3.75}$$

Solution (3.71) and (3.74) are generated by a null geodesic in AdS_3 under spectral flow. Finally, if we apply the limit of pure NSNS flux to (3.47), we obtain

$$E = -\frac{1}{2}\left(k k_1 + \frac{J^2}{k_1 k}\right) \ , \tag{3.76}$$

where we have used (2.41).

Until this point, we have considered the limit of pure NSNS flux of solutions to (3.37) whose μ is non-constant. We focus on solutions with constant μ now.

Being point-like, $\mu = k_1^2$ does not couple to the B-field. Therefore, the limit of pure NSNS flux is superfluous.

Consider $\mu = \mu_3$. In the short-string class, the situation of $\mu = \mu_3$ is parallel to that of the mixed-flux regime. The solution does not pulsate, but instead remains at the constant value $\rho_0 = \operatorname{arcsinh}(\sqrt{\mu_3 - k_1^2}/|k_1|)$. The world-sheet is a cylinder. The coordinate t depends linearly on τ via (3.12). The dispersion relation in terms of ρ_0 is, by analogy with (3.47), the negative branch of (3.49) with $q = 1$ and $\sqrt{\lambda} = k$.

In the long-string class, where $\mu_3 = \infty$, the hyperbolic radius diverges: $\rho_0 = \infty$. If we choose the positive branch of (3.49), we encounter that the energy also diverges $E = \infty$. Hence, we must exclude $\mu = \mu_3 = \infty$.

In the threshold between the short-string and long-string classes, the class of solutions with constant μ, that is constant hyperbolic radius ρ_0 is enhanced. If we set both $q=1$ and $(u_0-k_1)^2=k_1^2F_1$ in (3.37), we deduce that the quadratic polynomial vanishes identically for $u_0=k_1$ irrespective of μ. We then obtain a continuous class of solutions parameterised by ρ_0. The class corresponds to $J=k|k_1|$ and $E=kk_1$ in (3.49), where the dispersion relation becomes independent of ρ_0. (The choice of branch of (3.49) depends on the sign of k_1; recall that there is no reason to prefer either sign in the threshold.) Note that $\mu=k_1^2$ is the particular case with $\rho_0=0$ in this class. If we identify $k_1=-w$, we retrieve (38) of [93]. The point $J=k|w|$ saturates the unitarity bound of the w-th spectrally flowed sector in the world-sheet CFT_2 of the $\mathrm{SL}(2,\mathrm{R})$ WZNW model of [93] when $k\to\infty$; see (5.37) of subsection 5.1.2. We encounter this class of solutions insofar as solutions to the effective action (5.17) in subsection 5.1.1. Moreover, we refer to section 3 of [93] for an analysis of this class of solution in the semi-classical limit of the world-sheet CFT_2.

3.3 The local spectral curve of pulsating strings

In this section, we construct the local spectral curve of the pulsating strings with NSNS flux of section 3.2. We follow the procedure of subsection 2.2.2. We map the local spectral curve of pulsating strings to that of minimal surfaces on section 2.2.2. We write local spectral curve, which is an elliptic curve, in the Weierstrass form. We prove that the limit of pure NSNS flux renders the elliptic curve singular E. We discuss the emergence of the short-string and the long-string classes of subsection 3.2.2. We refer to appendix E for the basics of elliptic curves that we use in this section.

According to subsection 2.2.2, the first step is writing the left current j in AdS_3 which renders the pulsating-string ansatz (3.1) on $\mathrm{AdS}_3\times\mathrm{S}^1$ factorisable. Formula (C.8) leads to the factorisability as defined in (2.70). If we introduce (3.1) in (C.8) with $\beta_1=0$, the world-sheet components of j are

$$j_\tau=S\begin{bmatrix}\mathrm{i}\,z_0^2\dot\beta_0 & \mathrm{e}^{-\mathrm{i}\,\beta_0}(z_0\dot z_1-z_1\dot z_0+\mathrm{i}\,z_0z_1\dot\beta_0)\\ \mathrm{e}^{\mathrm{i}\,\beta_0}(z_0\dot z_1-z_1\dot z_0-\mathrm{i}\,z_0z_1\dot\beta_0) & -\mathrm{i}\,z_0^2\dot\beta_0\end{bmatrix}S^{-1}\ , \tag{3.77}$$

$$j_\sigma=\mathrm{i}\,k_1S\begin{bmatrix}z_1^2 & \mathrm{e}^{-\mathrm{i}\,\beta_0}\,z_0z_1\\ \mathrm{e}^{\mathrm{i}\,\beta_0}\,z_0z_1 & -z_1^2\end{bmatrix}S^{-1}\ , \tag{3.78}$$

where

$$S=\begin{bmatrix}\exp(\mathrm{i}\,k_1\sigma/2) & 0\\ 0 & \exp(-\mathrm{i}\,k_1\sigma/2)\end{bmatrix} \tag{3.79}$$

Note that $S^{-1}\mathrm{d}S$ does not depend on σ.

The next step is the computation of the determinant of A, defined in (2.74). The matrix A involves the truncation of L_L to AdS_3 in (2.65). If we introduce (3.77) and (3.78) in (2.65), we obtain

$$\begin{aligned}\det A=\frac{1}{\bar q^2(s-x)^2(1/s+x)^2}\Bigg(&\frac{k_1^2}{4}(x^4+1)-\frac{k_1}{\bar q}z_0^2(\dot\beta_0-qk_1)(x^3-x)\\ &-\frac{1}{2\bar q^2}[2(z_0\dot z_1-z_1\dot z_0)^2-2z_0^2\dot\beta_0(\dot\beta_0-2qk_1)-k_1^2(4q^2z_0^2-2z_0^2-q^2+1)]x^2\Bigg)\ .\end{aligned} \tag{3.80}$$

By using (3.12) and (3.32), we can rephrase (3.80) as

$$\det A = \frac{k_1^2\bar{q}^2(x^4+1) + 4k_1\bar{q}(qk_1 - u_0)(x^3 - x) + 2(3q^2k_1^2 - 4qu_0k_1 - k_1^2 + 2\omega^2)x^2}{4\bar{q}^2(s-x)^2(1/s+x)^2} \ . \tag{3.81}$$

The local spectral curve is defined by (2.75) through (3.81).

We note that (3.81) does not depend on τ, in agreement with the isochrony of the monodromy matrix. We also emphasise that the total angular momentum $J = \sqrt{\lambda}\omega$ of the pulsating string enters in (3.81) through (3.32). Moreover, if we had used L_R, given in (2.66) instead, we would have obtained (3.81) up to $x \mapsto -x$ and the replacement of s and $-1/s$ by $-s$ and $1/s$, respectively. Therefore, L_R defines the same local spectral curve.

If $\omega = 0$, there exists a mapping between (3.81) and the determinant of A in (4.43) for minimal surfaces in Euclidean AdS_3. Hence, there exists a mapping between the local spectral curves of pulsating strings and minimal surfaces. (Recall, as [65] remarked, that the correspondence between local spectral curves and factorisable classical solutions is neither one-to-one nor onto.) The mapping is $k_1 \mapsto k$ and $u_0 \mapsto p$. The condition $\omega = 0$ is necessary because minimal surfaces of section 4.1 have vanishing total angular momentum. The mapping is partly justified by the fact that both pulsating strings of section 3.2 and minimal surfaces of section 4.1 follow from the NR system in the limit of pure RR flux [64] and the fact that the NR system manifests an integrable deformation by NSNS flux in each case. We note however that neither the NR systems nor the integrable deformations are derivable from a common ansatz. The ansatze (3.1) of pulsating strings and (4.1) of minimal surfaces are not compatible in general. The claim follows from (C.18), which relates the global coordinate system (C.6) and the Poincaré patch (C.14) of AdS_3. [6]

The local spectral curve of pulsating strings is defined by the quartic polynomial of (2.75) via (3.81). Hence, it is an elliptic curve. We can write the local spectral curve in the Weierstrass form (E.1) by a birational transformation. The modular forms in (E.1) are

$$g_2 = \frac{64}{3}[k_1^4 - 4qu_0k_1^3 + (q^2+3)u_0^2k_1^2 + (3q^2-1)\omega^2k_1^2 - 4qu_0\omega^2k_1 + \omega^4] \ , \tag{3.82}$$

$$\begin{aligned} g_3 = -\frac{256}{27}\Big(&2k_1^6 - 12qu_0k_1^5 + 3[(5q^2+3)u_0^2 + (3q^2-1)\omega^2](k_1^2+\omega^2)k_1^2 \\ &+2[(q^2-9)u_0^2 - 3(3q^2+1)\omega^2]qu_0k_1^3 - 12qu_0\omega^4k_1 + 2\omega^6\Big) \ . \end{aligned} \tag{3.83}$$

The roots e_a in (E.2) can be computed through (E.3) and (E.4); the modular discriminant Δ and the j-invariant can be computed through (E.5) and (E.7), respectively. The resultant expressions are intricate and do not offer any significant insight.

We can overcome this impediment by focusing on two special cases that simplify the modular functions of the elliptic curve. The first case is $\omega = 0$, which corresponds to vanishing total angular momentum. The value $\omega = 0$ does not simplify the solution (3.39) and (3.42)

[6] We could draw on (3.81) to advance the local spectral curve of minimal surfaces in Euclidean $\mathrm{AdS}_3 \times \mathrm{S}^1$ with NSNS flux, whose limit of pure RR flux was written in [138]. The mapping is $k_1 \mapsto k$, $u_0 \mapsto p$ and $\omega^2 \mapsto a$, where a is a non-vanishing real number [138]. Nonetheless, the inclusion of a would obscure modular functions; compare (3.82) and (3.83) with (4.45) and (4.46). The impediment would prevent an analysis parallel to section 4.3 in the mixed-flux regime (but not in the limit of pure NSNS flux).

but rather the dispersion relation (3.47). The analysis of this case $\omega = 0$ would mimic the one of section 4.3 due to the mapping $k_1 \mapsto k$ and $u_0 \mapsto p$. Unlike minimal surfaces, pulsating strings with $\omega = 0$ however do not display any property that encourages us to consider this case from the elliptic curve. We then refer the reader to the parallel analysis of section 4.3.

The second case is $q = 1$, which corresponds to the limit of pure NSNS flux. If we set $q = 1$ in (3.82) and (3.83), the modular forms simplify to

$$g_2 = \frac{64}{3}(k_1^2 - 2k_1 u_0 + \omega^2)^2 \ , \tag{3.84}$$

$$g_3 = -\frac{512}{27}(k_1^2 - 2u_0 k + \omega^2)^3 \ . \tag{3.85}$$

The roots in (E.2) reduce to

$$e_1 = \frac{4}{3}(k_1^2 - 2k_1 u_0 + \omega^2) \ , \tag{3.86}$$

$$e_2 = \frac{2}{3}[-(k_1^2 - 2k_1 u_0 + \omega^2) + 3|k_1^2 - 2k_1 u_0 + \omega^2|] \ , \tag{3.87}$$

$$e_3 = \frac{2}{3}[-(k_1^2 - 2k_1 u_0 + \omega^2) - 3|k_1^2 - 2k_1 u_0 + \omega^2|] \ . \tag{3.88}$$

At least two of the three roots coincide. The sign of $k_1^2 - 2k_1 u_0 + \omega^2$ determines which roots do so. If we look at (3.29) and (3.32), we conclude $k_1^2 - 2k_1 u_0 + \omega^2 = (u_0 - k_1)^2 - k_1^2 F_1$, which is the quantity that discriminates between the short-string and long-string classes in subsection 3.2.2. If $k_1^2 - 2k_1 u_0 + \omega^2 > 0$, we have $e_1 = e_2$ and the elliptic curve is associated to the short-string class. If $k_1^2 - 2k_1 u_0 + \omega^2 < 0$, we have $e_1 = e_3$ and the elliptic curve is associated to the long-string class. If $k_1^2 - 2k_1 u_0 + \omega^2 = 0$, we have $e_1 = e_2 = e_3$ and the elliptic curve is associated to the threshold between the short-string and long-string classes. In section 4.3, we encounter that the sign of $k^2 - 2kp$, the counterpart of $k_1^2 - 2k_1 u_0$, governs the limit of pure NSNS flux of the elliptic curve. This fact strengths the parallels between pulsating strings and minimal surfaces that we have commented in subsection 3.2.2.

The coincidence of two or three e_a implies that the limit of pure NSNS flux singularises the elliptic curve. From either the use of (3.84) and (3.85) in (E.5) or the coincidence of among roots, we indeed deduce

$$\Delta = 0 \ . \tag{3.89}$$

The type of singularity depends on whether $g_2 = 0$ or $g_2 \neq 0$. In both the short-string ans long-string classes, where $g_2 \neq 0$, the elliptic curve presents a node singularity. In the threshold, where $g_2 = 0$, the elliptic curve presents a cusp singularity.

Chapter 4

Minimal surfaces with Neveu-Schwarz-Neveu-Schwarz flux

The $\mathrm{AdS}_5/\mathrm{CFT}_4$ correspondence establishes a connection between supersymmetric Wilson loops in $\mathcal{N}=4$ SYM theory and open-superstring partition functions in Euclidean $\mathrm{AdS}_5 \times \mathrm{S}^5$. References [62,63] proposed the duality, which states that the correlator of Wilson loops with support on a curve equals the partition function over open-superstring configurations with boundary conditions along the same curve at the conformal boundary of Euclidean $\mathrm{AdS}_5 \times \mathrm{S}^5$.

In the strong-coupling limit of $\mathcal{N}=4$ SYM theory, the steepest-descent approximation is applicable to the open-superstring partition function. The correlator of Wilson loops along the curve is encoded in the regularised on-shell action of the classical solution with Dirichlet boundary conditions along the curve at the conformal boundary of Euclidean $\mathrm{AdS}_5 \times \mathrm{S}^5$. (Ten Dirichlet boundary conditions are equivalent to four Dirichlet and six Neumann boundary conditions if the curve smooth; see subsection 3.1 of [166].) The classical solution is called *minimal surface* because it solves the Plateau problem in Euclidean $\mathrm{AdS}_5 \times \mathrm{S}^5$. The on-shell action of minimal surfaces is the area of the world-sheet and diverges. The divergence is a consequence from the imposition of boundary conditions at an infinite distance.

Since the on-shell action diverges, it must be regularised. References [62,63] proposed a regularisation to perform the computation. The regularisation is based on the introduction of a cut-off ϵ in the Poincaré parch. The cut-off ϵ restricts the integration of the action to a finite region inside the bulk of Euclidean AdS_5. The series of the on-shell action around $\epsilon = 0$ isolates the divergent term. Reference [166] showed that the divergence is induced by the simple pole of the action at $\epsilon = 0$ if the parameterisation of the curve is smooth: the minimal surface is governed by the conformal factor of the Poincaré patch near the boundary. The residue of the on-shell action at $\epsilon = 0$ is the perimeter of the curve with respect to the flat Euclidean metric. The zeroth-order term, the finite remnant, is the regularised on-shell action. Reference [166] proved that it equals the on-shell Legendre-transformed NG action.

To cancel divergences, [62,63] introduced with boundary counterterms. Reference [167] reproduced these counterterms by means of a reference open-string configuration with the same Dirichlet boundary conditions as the actual minimal surface. If this configuration solves the equations of motion and the Virasoro constraints, the configuration is related to a partition function itself. Both approaches yields equivalent results.

References [62,63] realised the duality between Wilson loops and minimal surfaces in two cases. First, the duality between BPS Wilson loops and minimal surfaces ending at an infinite line. Second, the duality for the $Q\bar{Q}$-potential and semi-cylindrical minimal surfaces in Euclidean AdS_5 that end at a pair of parallel infinite lines [62, 63]. The world-sheet of both classes of minimal surfaces extends over Euclidean AdS_5 and is fixed at a point of S^5. References [166, 168] later analysed circular Wilson loops, and [166] also considered Wilson loops over curves with non-smooth cusps. References [169–171] then constructed minimal surfaces ending at coaxial circles, and [172–174] constructed minimal surfaces that extended over S^5. These results raised the question of the systematisation of minimal surfaces that delineate generic curves at the boundary of Euclidean $\mathrm{AdS}_5 \times \mathrm{S}^5$.

Progress towards the answer was initiated in [64]. Reference [64] used the spinning-string ansatz of [38] to construct minimal surfaces with Dirichlet boundary conditions at smooth curves. The ansatz reduces the equations of motion of minimal surfaces to those of an effective integrable mechanical system. The mechanical system comprises classes of minimal surfaces that end at one infinite line or circle, two parallel infinite lines and an annulus.

Minimal surfaces nonetheless have properties with no analogue in spinning strings. First, minimal surfaces are characterised by the parameters of the curves at the boundary; for instance, the distance between two lines and the ratio of the radii of an annulus. The expression of the first integrals of the mechanical system in terms of the parameters of the curves in a closed form is often not available. Second, the solution to the equations of motion with Dirichlet boundary conditions at the boundary of Euclidean $\mathrm{AdS}_5 \times \mathrm{S}^5$ is in general non-unique: more than one minimal surface can end at a given curve. Both connected and disconnected minimal surfaces can end at a pair of parallel lines. Connected minimal surfaces ending at an annulus cease to exist if the ratio of the radii is greater than a threshold [170, 171], while disconnected minimal surfaces always exist. Two different connected minimal surfaces can furthermore end at the same annulus [138].

The construction of minimal surfaces through mechanical systems is not the only connection of Wilson loops with integrability via the $\mathrm{AdS}_5/\mathrm{CFT}_4$ correspondence. Reference [65] used spectral curves to analyse minimal surfaces. Spectral curves rely on the existence of non-contractible cycles on the world-sheet. To overcome the problem of the existence of non-trivial cycles on open-string world-sheets, [65] used that a spectral curve can be defined by using the logarithmic derivative of the monodromy matrix, which is a flat connection. Reference [65] then used local functions with appropriate features to construct local spectral curves for open-string world-sheets. Factorisability, defined for spinning strings in [38], hold in the cases analysed in [65]. Reference [66] postulated a procedure to obtain the local spectral curve of factorisable classical solutions (see subsection 2.2.2). References [175, 176] alternatively defined spectral curves in the Pohlmeyer-reduced non-linear σ-model, where classical solutions are expressed through Riemann θ-functions. The equivalence between the approaches of [175, 176] and [65, 66] was proved in [177] by means of the Pohlmeyer-reduced Lax connection. The approach of [65, 66] presents downsides: locality obstructs the computation of string moduli from the quasi-momenta.

The duality between Wilson loops and minimal surfaces poses the problem of the construction of minimal surfaces in other Euclideanised AdS_{d+1}-backgrounds where the $\mathrm{AdS}_{d+1}/\mathrm{CFT}_d$ is less understood. In this chapter, we analyse annular minimal surfaces in Euclidean AdS_3

in the mixed-flux regime and in the limit of pure NSNS flux. The chapter has the following structure. In section 4.1, we construct minimal surfaces with Dirichlet boundary conditions along an annulus of Euclidean AdS_3. In subsection 4.1.1, we construct connected and disconnected minimal surfaces in the mixed-flux regime. In subsection 4.1.2, we analyse the limit of pure NSNS flux of the minimal surfaces of subsection 4.1.1 and prove the appearance of two classes of minimal surfaces separated by a threshold. In section 4.2, we compute the regularised on-shell action of the minimal surfaces of section 4.1. We regularise the on-shell action by introducing a cut-off and cancel divergences by using a reference minimal surface. n section 4.3, we follow subsection 2.2.2 to construct the local spectral of minimal surfaces of 4.1, which is an elliptic curve. We analyse connected minimal surfaces in terms of elliptic invariants. We prove that the limit of pure NSNS flux singularises the elliptic curve and identify the two classes of subsection 4.1.2.

This chapter is based on [P3]. [1] We refer to [178] for an early review on the application of the AdS_5/CFT_4 correspondence to Wilson loops; we refer to [179] for a review of the topic from the point of view of localisation. Reference [150] constructed minimal surfaces on $AdS_3 \subset AdS_3 \times S^3 \times T^4$ with NSNS flux that end at a light-like cusp. Reference [180] constructed minimal surfaces on $AdS_3 \times S^3 \times S^3 \times S^1$ with NSNS flux.

4.1 Minimal surfaces on Euclidean AdS_3

In this section, we construct minimal surfaces that subtend an annulus at the boundary of Euclidean AdS_3 with NSNS flux. Our results generalise under NSNS flux the annular minimal surfaces of [64] and section 2 of [138] on the basis of the ansatz of [64]. In subsection 4.1.1, we construct minimal surfaces in the mixed-flux regime. We differentiate connected and disconnected minimal surfaces, and construct classical solutions. We analyse the effect of the NSNS flux on the ratio of the radii of the annulus of connected minimal surfaces and extend the analysis of [170, 171] under NSNS flux. In subsection 4.1.2, we consider the limit of pure NSNS flux of minimal surfaces of subsection 4.1.1. We prove the appearance of two classes separated by a threshold for connected minimal surfaces. We use elliptic integrals and Jacobian elliptic functions in this section. We refer to appendix F for our conventions, properties and formulae. We refer to appendix F for our conventions, properties and formulae.

4.1.1 Minimal surfaces in the mixed-flux regime

Our starting point is the annular ansatz of [64]. The ansatz is written in the Poincaré patch of Euclidean AdS_3 (C.14), where the metric and the B-field read (C.17) and (C.21), respectively. We must adjust the coordinate system (C.14) to describe an annulus at the boundary of Euclidean AdS_3. We introduce the polar coordinates $r \in [0, \infty)$ and $\theta \in [0, 2\pi)$,

[1] We expand and clarify minimal surfaces and local spectral curves of sections 2 and 3 of [P3] in sections 4.1 and 4.3, respectively. We add the discussion on the regularised on-shell action in section 2.1.3. We make some changes with respect to [P3] and correct a few errors. We refer to section 2 of [P3] for the application of the $SL(2, Z)$ symmetry of type IIB superstring theory to minimal surfaces that we do not consider here.

defined by $x^0 = r\sin\theta$ and $x^1 = r\cos\theta$. The ansatz consists of the trial functions [2]

$$r = r(\sigma)\ , \quad \theta = k\tau\ , \quad z = z(\sigma)\ , \tag{4.1}$$

where τ and σ are the coordinates along the temporal and spatial directions of the Euclidean world-sheet (see appendix A), and $k \in \mathrm{Z}\backslash\{0\}$ is a non-vanishing integer winding number. [3] (It is clear that k differs from the level of the WZNW model.) We set the target-space coordinates of S^3 to fixed values, which provides a consistent truncation. Since (4.1) must describe an annulus at the boundary of Euclidean AdS_3, (4.1) satifies with Dirichlet boundary conditions with respect to σ:

$$r(-L/2) = R_1\ , \quad r(L/2) = R_2\ , \quad z(-L/2) = z(L/2) = 0\ , \tag{4.2}$$

where R_i are the two radii of the annulus at the boundary.

The world-sheet described by (4.1) and (4.2) subtends an annulus centred at the origin of the boundary of Euclidean AdS_3 in the Poincaré patch (C.14). The world-sheet of minimal surfaces can be either connected or disconnected. Given R_i, (4.1) can in fact correspond to both connected and disconnected minimal surfaces. The existence of a connected solution is dictated by the value of R, whereas disconnected solutions always exist. Whether R_1 or R_2 corresponds to the outer or the inner radius depends on the value of $R = R_2/R_1$.

The coordinate τ parameterises the rim of the annulus, and, thus, $\tau \in [0, 2\pi)$. The integer k accounts for the winding along the inner and outer circumferences of the annulus. The coordinate σ parameterises the penetration of the world-sheet into the bulk of Euclidean AdS_3. The range of σ is finite for connected minimal surfaces with non-vanishing dilatation charge in the mixed-flux regime, hence our choice $\sigma \in [-L/2, L/2]$. The boundary conditions (4.2) then state that the world-sheet reaches the boundary of Euclidean AdS_3 at $\sigma = \pm L/2$. Being centred at the origin, $\sigma \in [-L/2, L/2]$ also facilitates the application of the limit of pure NSNS flux, where $\sigma \in (-\infty, \infty)$. On the contrary, both connected solutions with vanishing dilatation charge and disconnected solutions (in both the mixed-flux regime and limit of pure NSNS flux) will demand us to change the interval to $\sigma \in [0, \infty)$.

[2] We note that (4.1) matches the conventions of [64], that is the customary conventions where τ parameterises the boundaries of the open-string world-sheet. The ansatz (4.1) differs from ansatze used in the bibliography, where τ and σ are interchanged. These other ansatze were used to compute the correlators of two circular Wilson loops alone [138, 170, 171] and circular Wilson loops with a local operator [181, 182]. Other conventions are justified by the knowledge of the $\mathrm{AdS}_5/\mathrm{CFT}_4$ correspondence between Wilson loops and minimal surfaces. If the annulus degenerates to a punctured circle (and the total angular momentum in S^5 is large), the minimal surface encodes the correlator of a circular Wilson loop and the BMN vacuum when [64, 168, 174]. In Lorentzian signature, the BMN vacuum is dual to a null geodesic in $\mathrm{AdS}_5 \times \mathrm{S}^5$ [20]; the Wick-rotated counterpart is a complexified geodesic in S^5 parameterised by τ [174]. (We refer to [173] and especially footnote 3 of [181] for a discussion of this point.) If we interchanged τ and σ and inverted the sign of the q, we would in any case obtain classical solutions that the alternative ansatz to (4.1) would provide.

[3] In Euclidean $\mathrm{AdS}_5 \times \mathrm{S}^5$, k must be negligible compared to the number of units of RR flux N in the planar limit $N \to \infty$. The $\mathrm{AdS}_5/\mathrm{CFT}_4$ correspondence must be otherwise analysed with D3-branes or even in terms of the back-reaction of Euclidean $\mathrm{AdS}_5 \times \mathrm{S}^5$; see section 1 of [183] ad references therein. From the point of view of the $\mathrm{AdS}_3/\mathrm{CFT}_2$ correspondence, analogous considerations could be needed in (4.1). However, a better understanding of the duality is necessary to clarify this point.

If we impose the conformal gauge-fixing condition $h^{\alpha\beta} = \delta^{\alpha\beta}$, (4.1) consistently truncates the equations of motion of the Wick rotation of (2.47). The truncation follows from the action of a mechanical system whose coordinate along the temporal direction is σ. The associated Lagrangian is [4]

$$L = \frac{1}{2z^2}(r'^2 + z'^2 - 2qkrr' + k^2r^2) \ . \tag{4.3}$$

The mechanical system of (4.3) is integrable due to the existence of two first integrals: the dilatation charge p and the Hamiltonian. The dilatation charge follows from the invariance of (4.3) under $z \mapsto \Lambda z$ and $r \mapsto \Lambda r$, with Λ a constant. The Noether theorem provides

$$\Delta = \int_0^{2\pi} \mathrm{d}\tau \left(r' \frac{\delta S}{\delta r'} + z' \frac{\delta S}{\delta z'} \right) = \sqrt{\lambda} p = \frac{\sqrt{\lambda}}{z^2}(rr' + zz' - qkr^2) \ . \tag{4.4}$$

The Hamiltonian is not only conserved, but vanishes,

$$r'^2 + z'^2 - k^2r^2 = 0 \ , \tag{4.5}$$

due to the unique non-trivial Virasoro constraint in (2.50).

We can solve (4.4) and (4.5) by a change of variables from z and r to u and v:

$$z = \frac{u}{\sqrt{1+u^2}}\,\mathrm{e}^v \ , \quad r = \frac{1}{\sqrt{1+u^2}}\,\mathrm{e}^v \ . \tag{4.6}$$

The inversion of (4.6) leads us to

$$u = \frac{z}{r} \ , \quad v = \log\sqrt{z^2+r^2} \ . \tag{4.7}$$

The coordinate u is non-negative, and $u = 0$ corresponds to the boundary of Euclidean AdS_3. In the coordinate system of [64], u is related to a hyperbolic radial coordinate and v is the Wick-rotated coordinate along the temporal direction of Euclidean AdS_3. The coordinates (4.7) allow us to rephrase (4.4) and (4.5) as

$$u'^2 = -p^2u^4 + (k^2 - 2qkp)u^2 + (1-q^2)k^2 \ , \tag{4.8}$$

$$v' = p - \frac{p - qk}{1+u^2} \ , \tag{4.9}$$

These equations satisfy the boundary conditions (4.2), which become

$$u(-L/2) = u(L/2) = 0 \ , \quad v(-L/2) = \log R_1 \ , \quad v(L/2) = \log R_2 \ . \tag{4.10}$$

We can construct minimal surfaces and compute R if we solve (4.8) and then integrate (4.9) taking into account (4.10). In this subsection, we restrict ourselves to the limit of pure RR flux and the mixed-flux regime. We apply the limit of pure NSNS flux in subsection 4.1.2.

To solve (4.8), we discriminate between $|p| > 0$ and $p = 0$. If $|p| > 0$, the right-hand side of (4.8) is a biquadratic polynomial in u, and minimal surfaces are always connected. In

[4]In the limit of pure RR flux, (4.3) is connected with the NR system [64]. Following section 3.1, one could consider (4.3) in light of an integrable deformation of the NR system, expressed in unconventional although appropriate generalised coordinates.

this case, R_i indirectly determine p. On the contrary, if $p = 0$, the quartic term of the right-hand side (4.8) vanishes. Thus, the polynomial is quadratic. Minimal surfaces can be either connected or disconnected in this case. We can construct connected solutions either directly or by applying a limit to classical solutions with $|p| > 0$. Disconnected minimal surfaces follow from the considerations on connected ones. The radii R_i of disconnected minimal surfaces is arbitrary. We assume $|p| > 0$ first, and we focus on $p = 0$ at the end of the subsection.

If $|p| > 0$, we can write (4.8) as

$$u'^2 = p^2(u_-^2 + u^2)(u_+^2 - u^2) \ , \tag{4.11}$$

where

$$u_\pm^2 = \frac{\pm(k^2 - 2qkp) + \sqrt{(k^2 - 2qkp)^2 + 4(1-q^2)k^2p^2}}{2p^2} \ . \tag{4.12}$$

By definition, $u_\pm$ are non-negative. The inequality $u_\pm^2 > 0$ holds because $0 \leq q < 1$. Since u is real and subject to $u \geq 0$, equation (4.11) implies $0 \leq u \leq u_+$.

We can solve (4.11) by a direct integration and a subsequent inversion. If we consider the two branches of u' separately and use (F.29), we eventually obtain

$$u^2 = u_+^2 \operatorname{cn}^2\left(p\sqrt{u_+^2 + u_-^2}\sigma, \kappa\right) \ , \tag{4.13}$$

where $\operatorname{cn}(z, m)$ is defined in (F.34) and the elliptic modulus is

$$\kappa = \frac{u_+}{\sqrt{u_+^2 + u_-^2}} \ . \tag{4.14}$$

We recall that (4.13) is just valid in the interval $\sigma \in [-L/2, L/2]$. Formula (4.13) together with (F.42) implies that the length L of the range of σ is

$$L = \frac{2\,\mathrm{K}(\kappa)}{|p|\sqrt{u_+^2 + u_-^2}} \ . \tag{4.15}$$

where $\mathrm{K}(m)$ is defined in (F.2). The elliptic modulus (4.14) belongs to the fundamental domain: $0 \leq \kappa \leq 1$.

We discuss the behaviour of connected minimal surfaces now. The world-sheet delineates a circumferences of radius R_1 at $u(-L/2) = 0$, which corresponds to the boundary of Euclidean AdS_3. Formula (4.13) states that u increases from $u(-L/2) = 0$ until $u(0) = u_+$, which corresponds to the positive branch $u' > 0$. The coordinate u reaches the maximum value $u(0) = u_+$ at the midpoint $\sigma = 0$ since u is invariant under $\sigma \mapsto -\sigma$. In this first interval, the world-sheet gradually enters into the bulk of Euclidean AdS_3. Beyond the turning point $u'(0) = 0$, the negative branch $u' < 0$ starts. The negative branch extends from $u(0) = u_+$ to $u(L/2) = 0$. In the second interval, the world-sheet gradually returns to the boundary. The world-sheet reaches the boundary and describes a circumference of radius R_2, when $u(L/2) = 0$. The world-sheet has the shape of a half-torus. We conclude that the minimal surface that solves (4.11) has a connected world-sheet.

We could integrate (4.9) directly, but the resultant expression is not particularly enlightening. We refer to (2.20) of [P3] for an expression for v. It is more instructive for the analysis of connected minimal surfaces to integrate (4.9) between $\sigma = -L/2$ and $\sigma = L/2$. This step permits us to express the ratio of the radii of the annulus $R = R_2/R_1$ in terms of the parameters of the connected minimal surface. If we use (F.29) and (F.30), we obtain

$$R = \exp\left(\frac{2p(1+u_+^2)\,\mathrm{K}(\kappa) - 2(p-qk)\Pi(\nu,\kappa)}{|p|(1+u_+^2)\sqrt{u_+^2+u_-^2}}\right) , \tag{4.16}$$

where $\Pi(m,n)$ is defined in (F.6) and the elliptic characteristic is

$$\nu = \frac{u_+^2}{1+u_+^2} . \tag{4.17}$$

The expression (4.16) cannot be explicitly inverted to write p in terms of R, k and q.

Formula (4.9) provides R, rather than each R_i separately. The reason is that the ratio of the radii is the scale-invariant, meaningful quantity that we can be assemble from R_i [64, 138]. Therefore, we can fix one radius without loss of generality. We set $R_1 = 1$ until the end of the section to simplify the discussion. (We must restore R_1 in section 4.2 since our regularisation will not respect conformal invariance [178].) Conformal invariance also implies the equivalence of minimal surfaces under the inversion $R \mapsto 1/R$. The mapping $R \mapsto 1/R$ is equivalent to $p \mapsto -p$ and $k \mapsto -k$. We shall see in section 4.2 that the regularised on-shell action is indeed invariant under $p \mapsto -p$ and $k \mapsto -k$. Therefore, we assume $p > 0$ in the following discussion. (We shall restore a generic p in the discussion around (4.16) of subsection 4.1.2.) We note that disconnected minimal surfaces are invariant under $R \mapsto 1/R$ because the independent R_i can be paired in two different ways.

We plot (4.16) with $k > 0$ and $k < 0$ in figure 4.1. We have written R in terms of p/k because (4.16) is a function of of p/k up to the sign of k. Figure 4.1 shows that R in (4.16) is in general a bounded function of p for fixed k and q. Therefore, (4.16) determines the values of R for which connected minimal surfaces exist. We can analyse the effect of the NSNS flux in (4.16) by considering R a function of p for fixed $0 \leq q < 1$. To perform the analysis, it is convenient to use some relevant quantities. We introduce them in the following discussion and list some numerical values of these relevant quantities in table 4.1. The situation, which extends the results of [170, 171] under NSNS flux, is the following.

$k > 0$				$k < 0$			
q	p_+/k	R_+	R_0	q	p_+/k	R_+	R_0
0.000	0.581	2.72	1.00	0.000	0.581	2.72	1.00
0.250	0.462	4.55	1.83	0.250	0.857	1.75	0.618
0.500	0.402	8.89	3.35	0.500	2.04	1.18	0.299
0.750	0.379	27.2	6.12	0.750	-	1.00	0.164

Table 4.1: Relevant quantities of connected minimal surfaces for $0 \leq q < 1$.

In the limit of pure RR flux, where $q = 0$, R reaches a global maximum $R_+ > 1$ at $p_+ > 0$. The value p_+ cannot be written in a closed form [138]. The correspondence between p and R is

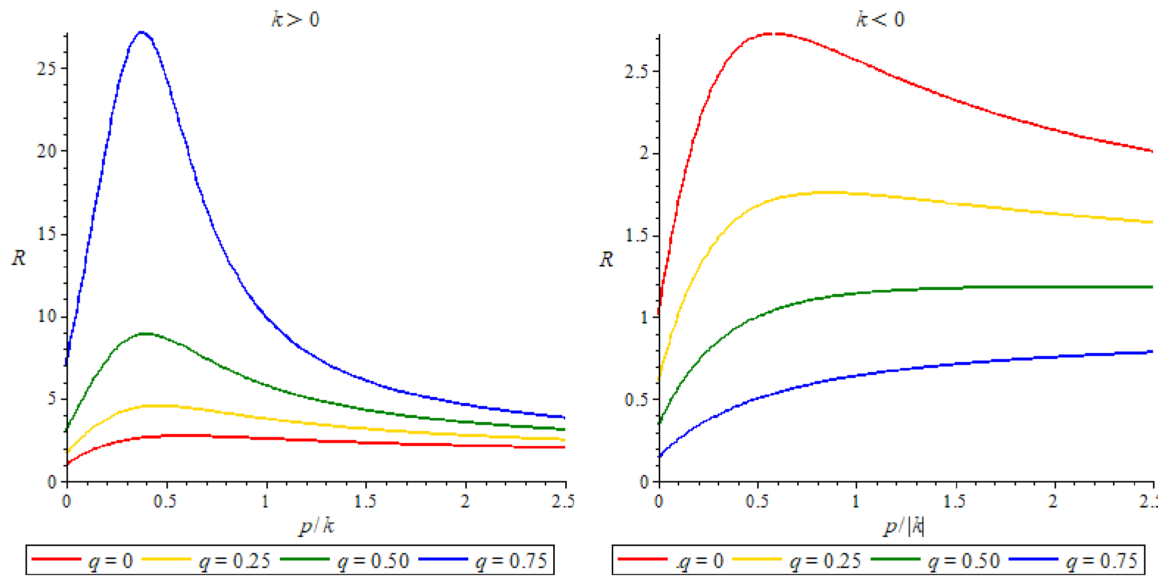

Figure 4.1: The quantity R of connected minimal surfaces against p/k for $0 \leq q < 1$.

in general two-to-one. Thus, two different connected minimal surfaces with the same boundary conditions exist. The correspondence between p and R is just one-to-one at $p = p_+$, where a unique connected solution exists. Moreover, $R = 1$ bounds (4.16) from below and corresponds to $p = 0$ and $p = \infty$. (The value $p = \infty$ corresponds the semi-cylindrical minimal surface, associated to the $Q\bar{Q}$-potential in the $\mathrm{AdS}_5/\mathrm{CFT}_4$ correspondence; see appendix H of [138].)

In the mixed-flux regime, where $0 < q < 1$, the behaviour of R with respect to p depends on the sign of k. If $k > 0$, the value R_+ increases as q increases. The value p_+ oscillates around $p = k/2$ as q increases. The value $R = 1$, which corresponds to $p = \infty$, bounds R from below. The value of R at $p = 0$ shifts to $R_0 > 1$. The correspondence between p and R is one-to-one for $1 \leq R < R_0$ and two-to-one for $R_0 \leq R < R_+$.

If $k < 0$, the situation is complementary. The more q increases, the more R_+ decreases. The value p_+ tends to $p = \infty$ as q increases. The value $R_0 < 1$, which corresponds to $p = 0$, bounds R from below. The value $R = 1$ holds at $p = \infty$. The correspondence between p and R is one-to-one for $R_0 \leq R < 1$, and two-to-one for $1 \leq R < R_+$. The value $p_+ = \infty$ is reached at $q \approx 0.652$. From there on, $R = 1$ starts to bound R from above, while $R_0 < 1$ still bounds R from below. The correspondence between p and R is one-to-one.

The effect of the NSNS flux on the coexistence of the classes of connected and disconnected minimal surfaces is the following. First, we recall that disconnected minimal surfaces have arbitrary R. If $k > 0$, the NSNS flux enlarges the range $1 \leq R \leq R_+$ for which both classes coexist, because it increases the maximum $R_+ > 1$. If $k < 0$, the NSNS flux introduces the new range $R_0 < R < 1$ for which both classes coexist, which becomes gradually wider.

We turn our attention to $p = 0$ now. Both connected and disconnected minimal surfaces exist. We consider connected minimal surfaces first. The limit $p \to 0$ of the ratio of the radii (4.16) is R_0. The value R_0 exists and is finite. The equality $R_0 = 1$ holds in the limit of pure RR flux, which implies that the boundaries of the annulus merge and the annulus collapses into a single circumference. This is not longer the case in the mixed-flux regime, where R_0 follows our discussion on (4.16).

From the point of view of the quartic polynomial (4.11), $p \to 0$ realises the divergence of two out of four roots, which renders (4.8) quadratic. If we apply $p \to 0$ to (4.12), we obtain

$$u_+^2 = \infty \ , \quad u_-^2 = 1 - q^2 \ . \tag{4.18}$$

Therefore, $0 \leq u < \infty$ as a consequence. We conclude that u is unbounded. To compute u, we can either solve directly (4.11) with $p = 0$ or apply $p \to \infty$ to (4.13).

If we apply $p \to 0$ to (4.14), we obtain $\kappa = 1$, which implies $L = \infty$ via (F.22). The length for the interval of σ diverges, but R is finite. If we applied $p \to 0$ to (4.13), we would obtain $u = \infty$. The result is a consequence the localisation of (4.13) around the upper bound u_+ at the midpoint of the interval $\sigma \in [-L/2, L/2]$, which $p = 0$ translates into the localisation of (4.13) around the divergent upper bound $u_+ = \infty$ at the midpoint of the infinite interval $\sigma \in (-\infty, \infty)$. To write u, we must replace the range of σ.

We then consider the interval $\sigma \in [0, L]$, whose midpoint is $\sigma = L/2$. The boundary conditions (4.10) are the same up to the replacement $\sigma \mapsto \sigma + L/2$. If we solve (4.8) consistently with the shifted boundary conditions and use (F.60), we are led to

$$u^2 = \frac{u_+^2 u_-^2}{u_+^2 + u_-^2} \, \mathrm{sd}^2 \left(p\sqrt{u_+^2 + u_-^2}\sigma, \kappa \right) \ , \tag{4.19}$$

where $\mathrm{sd}(z, m)$ is defined in (F.35). If we apply $p \to 0$ to (4.19) and take into account (4.12) and (4.14), we obtain

$$u^2 = (1 - q^2) \sinh^2(k\sigma) \ , \tag{4.20}$$

where we have used (F.56). Formula (4.20) implies that u' does not reach any finite turning point, consistently with our expectations. The positive branch of u' ranges from $u(0) = 0$ to $u(\infty) = \infty$. The negative branch of u' ranges from $u(\infty) = \infty$ to $u(0) = 0$. Formula (4.20) also follows from (4.8) with $p = 0$. To obtain (4.20), we must fix the boundary condition at the leftmost point $u(0) = 0$ and duplicate (4.20) to reproduce each branch of u'.

To elucidate the behaviour of the minimal surface (4.20), we come back to the coordinates r and z through (4.6). We have a different expression for each of the two branches of u' (the coordinate v would have accounted for the difference if the corresponding solution had been written). The connected minimal surface with $p = 0$ is

$$z = R_i \sqrt{\frac{1 + q\tanh(k\sigma)}{1 - q\tanh(k\sigma)}} \frac{\bar{q}\sinh(|k|\sigma)}{\sqrt{1 + \bar{q}^2 \sinh^2(k\sigma)}} \ , \tag{4.21}$$

$$r = R_i \sqrt{\frac{1 + q\tanh(k\sigma)}{1 - q\tanh(k\sigma)}} \frac{1}{\sqrt{1 + \bar{q}^2 \sinh^2(k\sigma)}} \ , \tag{4.22}$$

where $i = 1$ corresponds the positive branch of u', $i = 2$ corresponds the negative branch of u', and we have introduced $\bar{q} = \sqrt{1 - q^2}$ to compact the expressions. According to (4.21) and (4.22), the situation is the following.

If $\sigma = 0$, the world-sheet delineates a circumference of radius $r = R_1 = 1$ at the boundary of Euclidean AdS_3, which corresponds $z = 0$. The coordinate σ then increases; the world-sheet separates from the boundary and enters into the bulk. The world-sheet penetrates until $\sigma = \infty$, where $z = \sqrt{(1+q)/(1-q)}$ and $r = 0$. The value $r = 0$ means that the radius of the world-sheet vanishes. As opposed to connected minimal surfaces with $|p| > 0$, the world-sheet closes. The first component of the world-sheet has the shape of a dome that subtends a circle of radius $R_1 = 1$. Once the minimal surface reaches $\sigma = \infty$, it turns around and returns to the boundary. The second component of the world-sheet has the shape of a dome again, but it subtends a circle of radius $R_2 = R$. The full world-sheet, which consists of two components, is connected because the apexes of the domes come into contact.

Each component subtends a circle of radius R_i that is wrapped $|k|$ times. Hence, $|k| = 1$, each dome provides the deformation under NSNS flux of the circular minimal surface in the Euclidean $\mathrm{AdS}_5 \times \mathrm{S}^5$ dual to the circular Wilson loop [166, 168]. (If $|k| > 1$, each dome is equivalent to the superposition of $|k|$ equally-oriented hemispherical world-sheets with $|k| = 1$ and has a counterpart Euclidean $\mathrm{AdS}_5 \times \mathrm{S}^5$ [64].) We bear this identification out in section 4.3 from the point of view of the local spectral curve.

The analogy with connected minimal surfaces in Euclidean $\mathrm{AdS}_5 \times \mathrm{S}^5$ suggests us that disconnected minimal surfaces are (4.21) and (4.22), but with R being arbitrary instead of given by (4.16). We can confirm our guess by solving (4.4) and (4.5) with $p = 0$. Classical solutions with $p = 0$. are consistent with any R_i in (4.2). The disconnected world-sheet consists of two separate domes that subtend a circle of radius $R_1 = 1$ and $R_2 = R$, respectively. (Recall that conformal invariance at the boundary of Euclidean AdS_3 still permits us to set $R_1 = 1$.) If R coincides with (4.16) when $p \to 0$, the disconnected world-sheet becomes connected due to the union of the domes at their apexes.

4.1.2 Minimal surfaces with pure Neveu-Schwarz-Neveu-Schwarz flux

We focus on the limit of pure NSNS flux, where $q = 1$. Following subsection 4.1.1, we discriminate between $|p| > 0$ and $p = 0$. We focus on connected minimal surfaces with $|p| > 0$ first. We begin with the pure NSNS flux limit of R in (4.16). We drop the assumption of positivity on p that we held in subsection 4.1.1 for clarity.

In the limit of pure NSNS flux, where $q = 1$, the behaviour of R with respect to p depends on the sign of k. If $k > 0$, the maximum at $p_+ = k/2$: $R_+ = \infty$. If $k^2 - 2kp \leq 0$, R is finite and reads

$$R = \exp\left(\frac{k\pi}{\sqrt{|k^2 - 2kp|}}\right) . \tag{4.23}$$

The correspondence between $k/2 \leq p \leq \infty$ and $1 \leq R < \infty$ is one-to-one. The value $R = 1$ corresponds at $p = \infty$. If $k^2 - 2kp \geq 0$, that is if $-\infty \leq p \leq k/2$, we have $R = \infty$. In particular, $R_0 = \infty$ at $p = 0$. We encounter two regimes separated by a threshold.

If $k < 0$, the situation is complementary. If $k^2 - 2kp \leq 0$, R is finite and given by (4.23). The value $R = 1$ corresponds to $p = -\infty$. The correspondence between $-\infty \leq p \leq k/2$ and $0 < R \leq 1$ is one-to-one. If $k^2 - 2kp \geq 0$, that is if $k/2 \leq p \leq \infty$, we have $R = 0$. In particular, $R_0 = 0$ at $p = 0$. We find again two regimes separated by a threshold.

The enlargement of the range of R that we have remarked in subsection 4.1.1 culminates in the limit of pure NSNS flux. Connected minimal surfaces exist for every $1 \leq R \leq \infty$ if $k > 0$ and every $0 \leq R \leq 1$ if $k < 0$.

Conformal invariance states the equivalence between $R \mapsto 1/R$ for minimal surfaces, as we have already mentioned in section 4.1.1. It is clear that $R \mapsto 1/R$ is equivalent to $p \mapsto -p$ and $k \mapsto -k$ in the limit of pure NSNS flux. We then assume $k > 0$ until the end of the subsection without loss of generality. The analysis of $k < 0$ is analogous.

The sign of $k^2 - 2kp$ dictates which alternative for connected minimal surfaces in the limit of pure NSNS flux is realised. This fact hints at a classification into two classes that depends on the sign of $k^2 - 2kp$. The situation is analogous to that of pulsating strings of subsection 3.2.2, which fall into the short-string or the long-string classes depending on the sign of $(u_0 - k_1)^2 - k_1^2 F_1$. We shall confirm the parallelism in subsection 4.3.

From the point of view of the quartic polynomial (4.8), the limit of pure NSNS flux implies the vanishing of two out of four roots. If $k^2 - 2kp \leq 0$, $u_+^2 = 0$ holds. If $k^2 - 2kp \geq 0$, $u_-^2 = 0$ holds. If $k^2 - 2kp = 0$, both pairs of roots vanish: $u_+^2 = u_-^2 = 0$.

Let $k^2 - 2kp < 0$. It follows that (4.12) reduces to

$$u_+^2 = 0 \ , \quad u_-^2 = -\frac{k^2 - 2kp}{p^2} \ . \tag{4.24}$$

The elliptic modulus (4.14) vanishes: $\kappa = 0$. If we set $q = 1$ in (4.13), we obtain

$$u = 0 \ . \tag{4.25}$$

Therefore, the world-sheet is adhered to the boundary of Euclidean AdS_3. The length of the interval (4.15) simplifies to

$$L = \frac{\pi}{\sqrt{|k^2 - 2kp|}} \ , \tag{4.26}$$

where we have used (F.13). We finally conclude

$$R = \exp(kL) \ , \tag{4.27}$$

which follows from (4.23).

If $k^2 - 2kp < 0$, the response of connected minimal surfaces to the NSNS flux is the following. The world-sheet departs from the circumference of radius $R_1 = 1$ at the boundary of Euclidean AdS_3, enters into the bulk until $u = u_+$, turns around and arrives to the boundary at a circumference of radius $R_2 = R$. The more q increases, the more u_+ decreases, and the world-sheet penetrates less distance into the bulk. In the limit of pure NSNS flux, $u_+ = 0$, and the world-sheet does not detach from the boundary. The world-sheet just ranges between the inner and outer circumferences of the annulus, with which coincides.

Let $k^2 - 2kp > 0$. It follows from that (4.12) read

$$u_+^2 = \frac{k^2 - 2kp}{p^2} \ , \quad u_-^2 = 0 \ . \tag{4.28}$$

The elliptic modulus (4.14) equals one: $\kappa = 1$. The solution (4.13) reduces to

$$u^2 = u_+^2 \operatorname{sech}^2\left(\sqrt{k^2 - 2kp}\,\sigma\right) \ , \tag{4.29}$$

where we have used (F.58). The length of the interval (4.15) diverges:

$$L = \infty \ , \tag{4.30}$$

where we have used (F.22). We have stated before that $R = \infty$. If we however express (4.15) and (4.16) as asymptotic series around $q = 1$, we can relate R and L at leading order:

$$R \sim \exp(kL) \ , \quad q \to 1 \ . \tag{4.31}$$

If $k^2 - 2kp > 0$, the response of minimal surfaces to the NSNS flux is the following. The increasing of q does not prevent the world-sheet from penetrating into the bulk of Euclidean AdS_3, but dilates the outer boundary of the annulus. In the limit of pure NSNS flux, the outer circumference collapses at the point of infinity. Hence, the annulus degenerates. The world-sheet has the shape of half of a horn torus.

We note that (4.29) relies on the choice of the interval $\sigma \in [-L/2, L/2]$ in the mixed-flux regime. If we had chosen $\sigma \in [0, L]$, we would have (4.19), and the application of the limit of pure NSNS flux would have provided $u = 0$. The situation is analogous to that of connected minimal surfaces with $p = 0$ in the mixed-flux regime. As opposed to (4.19), the expression (4.13) is localised around u_+ at the midpoint of $\sigma \in [-L/2, L/2]$. If $L \to \infty$, (4.13) can reach u_+, but (4.19) cannot. The shift of the interval of σ is tantamount to keeping the integration constant in solving the equation of motion; to compute (4.29) we then need to fix the integration constant in the mixed-flux regime properly. The situation is analogous to that of pulsating strings in the long-string class of subsection 3.2.2.

Let $k^2 - 2kp = 0$, which the threshold between the previous classes of connected minimal surfaces. We have that (4.12) read $u_+^2 = u_-^2 = 0$. The solution is $u = 0$. The length of the interval is $L = \infty$. It follows from (4.23) that $R = \infty$. The world-sheet of the connected minimal surface $k^2 - 2kp = 0$ adheres to the boundary of Euclidean AdS_3 and ranges between the boundaries of a degenerate annulus. The threshold shares features with both classes.

Consider $p = 0$. First, we focus on the limit of pure NSNS flux of the connected minimal surface. We have $R = \infty$. To obtain the minimal surface, we apply the limit of pure NSNS flux to (4.21) and (4.22). We must consider just the part of the classical solution associated to $R_1 = 1$; the other, associated to $R_2 = \infty$, degenerates. The result is

$$z = 0 \ , \tag{4.32}$$

$$r = \exp(k\sigma) \ , \tag{4.33}$$

Formula (4.32) holds, in principle, everywhere but at $z = \sqrt{(1+q)/(1-q)}$, where the limit of pure NSNS flux provides $z = \infty$. The point $z = \infty$ however belongs to the conformal boundary of Euclidean AdS_3. We can compute the r associated to $z = \infty$. If we set $\sigma = \infty$ in (4.33), we obtain $r = \infty$, which is $R = \infty$. We conclude that the world-sheet adheres to the boundary and that it ranges between the boundaries of a degenerate annulus. One might have expected the adhesion of the world-sheet when $k^2 - 2kp < 0$, but not when $k^2 - 2kp > 0$.

We clarify the limit of pure NSNS flux of connected minimal surfaces by considering their behaviour with respect to the variation of p. We begin with $p = 0$. The world-sheet does not abandon the boundary. Once p increases, the world-sheet detaches from the boundary of Euclidean AdS_3 at $z = \infty$, while $R = \infty$. The more p increases, the less distance the world-sheet gradually penetrates into the bulk. Once p reaches $p = k/2$, the minimal surface adheres to the boundary. From then on, he world-sheet remains at the boundary and R is finite and given by (4.23).

Connected minimal surfaces with $p = 0$ and $k^2 - 2kp = 0$ are indistinguishable in the limit of pure NSNS flux. Analogously, every connected minimal surface with $k^2 - 2kp < 0$ with given R is paired with the the limit of pure NSNS flux of a disconnected minimal surface with the same $R \leq 1$. To prove the statement, we must express the connected minimal surface (4.25) in terms of z and r through (4.6) (and introduce an unimportant shift in the range of σ). We are then led to (4.32) and (4.33). The expression holds between $\sigma \in [0, L]$, where L is related to R via (4.27).

If we apply the limit of pure NSNS flux to each component of a disconnected minimal surface, we obtain (4.32) and (4.33), with $R_2 = R$ arbitrary. The world-sheet consists of two concentric circles at the boundary. Since the two pieces overlap, the disconnected world-sheet becomes connected. Each pair $R_1 = 1$ and $R_2 = R$ of disconnected minimal surface corresponds to one R in (4.23).

4.2 The regularised on-shell action

In this section, we compute the regularised on-shell action of the minimal surfaces of section 4.1. We apply the regularisation of [62, 63]. We find the proper counterterms by means of a reference minimal surface, following [167] and subsection 2.3 of [138]. The regularised on-shell action extends that of subsection 2.3 of [138] in the limit of pure RR flux.

We begin with a brief review of the regularisation of [62, 63] for minimal surfaces with Dirichlet boundary conditions along smooth curves. The regularisation comprises three steps: the introduction of a cut-off at $z = \epsilon$ in the action, the isolation and cancellation of the simple pole at $\epsilon = 0$, and the computation of the finite remnant, that is the regularised on-shell action. The result drives the partition function associated to the minimal surface when $\lambda \to \infty$. The counterterms that cancel the simple pole can be obtained by subtracting the on-shell action of an open-string configuration [167]. If the open-string configuration is a minimal surface, the finite remnant is the ratio of two partition functions when $\lambda \to \infty$.

The direct application of the regularisation of [62, 63] to the minimal surfaces of section 4.1 raises some objections. First, we ignore the dual objects to the minimal surfaces of section 4.1 through the $\mathrm{AdS}_3/\mathrm{CFT}_2$ correspondence (if any). The lack not only implies that we cannot ensure that the result corresponds to the limit $\lambda \to \infty$ of actual dual objects, but also that we cannot confirm that the regularisation is correct from the point of view of the $\mathrm{AdS}_3/\mathrm{CFT}_2$ correspondence. Second, we must modify the regularisation of [62, 63] to embrace the topologically non-trivial WZ term of the NSNS three-form flux. We have expressed the NSNS flux as the exterior derivative of the B-field, which is defined modulo a gauge ambiguity, that is modulo the addition of an exact world-sheet two-form. We have then written the local WZ term in (2.47). The gauge ambiguity affects neither the equations of motion nor the Virasoro constraints. The gauge ambiguity however matters in the computation of the regularised on-shell action: exact world-sheet two-forms can contribute in the form of boundary terms.

Our answer to the objections is the following. First, the computation of the regularised on-shell action is meaningful by itself (as the result of the steepest-descent approximation in path integral of the partition function) irrespective of the $\mathrm{AdS}_3/\mathrm{CFT}_2$ correspondence. The finite remnant of minimal surfaces could encode the limit $\lambda \to \infty$ of a dual object, but the duality is not necessary for the computation to be consistent. Second, we exclude boundary terms introduced by the gauge ambiguity of the B-field by an additional condition. We just admit exact world-sheet two-forms that are the exterior derivative of one-forms that vanish at the boundary of Euclidean AdS_3, and, hence, one-forms that vanish at the boundary of the open-string world-sheet. (Therefore, p in (4.4) is not corrected by boundary terms either.) This condition is the gauge invariance of the action with respect to the B-field in an open-string world-sheet.[5]

We compute the regularised on-shell action now. Following section 4.1, we discriminate between $0 \leq q < 1$ and $q = 1$, and we discriminate between minimal surfaces with $|p| > 0$ and $p = 0$. We begin with connected minimal surfaces with $|p| > 0$ in the mixed-flux regime.

First, we introduce the cut-off $z = \epsilon$, which circumscribes the integration of the action to the bulk of Euclidean AdS_3. It is convenient to use the coordinate u in (4.7) instead of z, as the use of (4.11) simplifies the computation. We must then incorporate the cut-off at each branch of u'. Let $u_1 = u(-L/2 + \sigma_1)$ and $u_2 = u(L/2 - \sigma_2)$ be the cut-offs in the branches $u' > 0$ and $u' < 0$, respectively. They are related to $z = \epsilon$ as $u_1 = \epsilon/R_1$ and $u_2 = \epsilon/R_2$ (up to higher-order corrections in ϵ that vanish at $\epsilon = 0$). Note that we restored R_1 in (4.2) since the regularisation does not respect conformal invariance.

The on-shell action is

$$S = \sqrt{\lambda}\left(\int_{u_1}^{u_+} - \int_{u_+}^{u_2}\right) \mathrm{d}u \frac{1}{|p|\sqrt{(u_-^2 + u^2)(u_+^2 - u^2)}}\left[\frac{\bar{q}^2 k^2}{u^2} - \frac{qk(p - qk)}{u^2 + 1}\right] . \tag{4.34}$$

$$= \left(\frac{\bar{q}^2 k^2 \sqrt{\lambda}}{|p|}\left[\frac{\sqrt{(u_-^2 + u_0^2)(u_+^2 - u_0^2)}}{u_+^2 u_-^2 u_0} + \frac{1}{u_+^2\sqrt{u_+^2 + u_-^2}}\,\mathrm{F}(\beta, \kappa) - \frac{\sqrt{u_+^2 + u_-^2}}{u_+^2 u_-^2}\,\mathrm{E}(\beta, \kappa)\right]\right.$$
$$\left. - \frac{qk(p - qk)\sqrt{\lambda}}{|p|(1 + u_+^2)\sqrt{u_+^2 + u_-^2}}\Pi(\beta, \nu, \kappa)\right)\left(\bigg|_{u=u_1} + \bigg|_{u=u_2}\right) , \tag{4.35}$$

where we have introduced (4.7) in (4.3) in the first step, we have used (4.9) and (4.11) in the second step, and we have used (F.30) and (F.31) in the third step. The functions $\mathrm{F}(z, m)$, $\mathrm{E}(z, m)$, and $\Pi(z, n, m)$ are defined in (F.1), (F.3), and (F.5), respectively, β reads

$$\beta = \arccos \frac{u}{u_+} , \tag{4.36}$$

[5]To write the on-shell action (4.34), we shall ignore a total derivative, which arises from the WZ term via (4.7). The resultant boundary term diverges at $u = 0$. We have cancelled the contribution by adding an exact world-sheet two-form that does not satisfy our assumptions. The introduction is correct for two reasons. First, the conformal boundary of Euclidean AdS_3 changes under coordinate transformations [184]. Second, the B-field that satisfies the assumptions of appendix C in terms of u and v would have led us directly to (4.34).

and κ and ν are (4.14) and (4.17), respectively. Formula (4.34) follows from both the NG action and the conformally gauge-fixed Polyakov action.

The next step is the introduction of the series around $\epsilon = 0$ of (4.34), which provides both the divergence and the finite remnant. If we use $u_i = R_i/\epsilon$, we obtain

$$\begin{aligned} S = & \frac{\sqrt{\lambda}}{2\pi}\frac{\bar{q}2\pi|k|(R_1+R_2)}{\epsilon} - 2\sqrt{\lambda}\left[\frac{\bar{q}^2k^2\sqrt{u_+^2+u_-^2}}{|p|u_+^2u_-^2}\mathrm{E}(\kappa) - \frac{\bar{q}^2k^2}{|p|u_+^2\sqrt{u_+^2+u_-^2}}\mathrm{K}(\kappa)\right. \\ & \left. + \frac{qk(p-qk)}{|p|(1+u_+^2)\sqrt{u_+^2+u_-^2}}\Pi(\nu,\kappa)\right] + \mathrm{O}(\epsilon)\ , \end{aligned} \tag{4.37}$$

where $\mathrm{E}(m)$ is defined in (F.4).

The series (4.37) has a simple pole. Simple poles account for the divergence of the action of minimal surfaces that subtend smooth curves [170]. The reason for simple poles is that the conformal factor of the metric in the Poincaré patch drives the integrand in the vicinity of the boundary. The conformal factor is also responsible for the proportionality between the residue of on-shell action at $\epsilon = 0$ and the perimeter of the curve with respect to the flat metric at the boundary [170]. In formula (4.37), the conformal factor is responsible for the proportionality between the residue and the sum of the lengths of the two circumferences of radii R_1 and R_2 ranged $|k|$ times at the boundary. We note that the residue is not conformally invariant due to the violation of conformal invariance by the regularisation. [6]

We must find the counterterms that cancel the divergence of (4.37) at $\epsilon = 0$. We then look for the appropriate reference minimal surface. Unlike minimal surfaces in Euclidean AdS_5, the residue of (4.37) is dressed by $\bar{q} = \sqrt{1-q^2}$ due to the NSNS flux. The reference minimal surface must then couple to the B-field. The adequate candidate is the deformation under NSNS flux of the circular minimal surface of subsection 4.1.2, see (4.21) and (4.22). Since we must duplicate the circular minimal surface to cancel the pole of (4.37), the reference minimal surface is indistinguishable from the disconnected minimal surface with radii R_i subsection 4.1.1 (or from the connected solution if R_2/R_1 satisfies (4.16) with $p = 0$).

We set $p = 0$ in the mixed-flux regime now. We restrict ourselves to one component of (4.21) and (4.22), and we duplicate the result later. Let R be the radius of the circumference. The cut-off is then $u_0 = u(\sigma_0) = R/\epsilon$. (Recall that $\sigma \in [0,\infty)$ before the regularisation.) The on-shell action is

$$\begin{aligned} S &= \sqrt{\lambda}\int_{u_0}^{\infty}\mathrm{d}u\frac{|k|}{\sqrt{u^2+1-q^2}}\left(\frac{\bar{q}^2}{u^2}+\frac{q^2}{1+u^2}\right) \\ &= \frac{\sqrt{\lambda}}{2\pi}\frac{\bar{q}2\pi|k|R}{\epsilon} - \sqrt{\lambda}|k|(1-q\,\mathrm{arctanh}\,q) + \mathrm{O}(\epsilon)\ . \end{aligned} \tag{4.38}$$

Formula (4.38) displays the proper simple pole. We can then us e (4.38) to cancel the divergence of (E.5). Moreover, the finite remnant of (4.38) follows from the application of $p \to 0$ to (4.37) up to a factor of two. Note that the finite remnant of (4.38) does not depend on R.

[6] In the $\mathrm{AdS}_5/\mathrm{CFT}_4$ correspondence, the violation of conformal invariance persists after the removal of the regularisation, which implies a conformal anomaly for Wilson loops; see, for instance, subsection 2.1 of [178]. The conformal anomaly concerns extended objects of $\mathcal{N} = 4$ SYM theory, not local operators.

The regularised on-shell action S' is (4.37) minus twice (4.38) and reads

$$\begin{aligned} S' = -2\sqrt{\lambda}\Bigg[& \frac{\bar{q}^2 k^2 \sqrt{u_+^2 + u_-^2}}{|p| u_+^2 u_-^2}\,\mathrm{E}(\kappa) - \frac{\bar{q}^2 k^2}{|p| u_+^2 \sqrt{u_+^2 + u_-^2}}\,\mathrm{K}(\kappa) \\ & + \frac{qk(p-qk)}{|p|(1+u_+^2)\sqrt{u_+^2+u_-^2}}\Pi(\nu,\kappa) - |k|(1 - q\,\mathrm{arctanh}\,q)\Bigg] \, . \end{aligned} \tag{4.39}$$

The quantity (4.39) drives the limit $\lambda \to \infty$ of the ratio between of the partition function of a connected annular minimal surface in the mixed-flux regime and the partition functions of two reference circular minimal surfaces.

Formula (4.39) deserves some observations. First, $S' = 0$ holds for connected minimal surfaces with $p = 0$ and disconnected minimal surfaces in the mixed-flux regime. Second, S' is invariant under $k \mapsto -k$ and $p \mapsto -p$. Invariance is consistent with our discussion on R in (4.16), where we have argued $R \mapsto 1/R$ represent equivalent situations. Third, S' in (4.39) cannot be directly written in terms the quantity R in (4.16), which characterises connected minimal surfaces. Pairs of connected minimal surfaces whose R is the same and whose S' differs furthermore exist for each k and $0 \leq q < 1$. Therefore, a numerical analysis study is mandatory to study the relationship between R and S'.

We close the section with a discussion of the limit of pure NSNS flux, where $q = 1$. We have encountered in subsection 4.1.2 that connected minimal surfaces fall into two classes. The sign of $k^2 - 2kp$ states which class is realised. Following subsection 4.1.2, we assume $p \geq 0$ and $k > 0$ for brevity. The analysis of the alternatives is analogous.

If $k^2 - 2kp \leq 0$, connected minimal surfaces adhere to the boundary of Euclidean AdS_3. We cannot introduce a cut-off at $z = \epsilon$, and the steps that have led us to (4.39) are not valid. The on-shell action is evaluated directly at the boundary. Connected minimal surfaces however coincide with reference minimal surfaces in the limit of pure NSNS flux. We can then argue that the regularised on-shell action is $S' = 0$. The same argument holds for $p = 0$ and disconnected minimal surfaces.

If $k^2 - 2kp > 0$, connected minimal surfaces penetrate into the bulk of Euclidean AdS_3. We can apply the limit of pure NSNS flux to (4.39). The result is $S' = \infty$. If we applied the regularisation from the outset, we would encounter $S \sim \log(R_1/\epsilon) + \log(R_2/\epsilon)$ when $\epsilon \to 0$. (Recall that we restore R_1 and R_2 in the regularisation.) This class of divergences are typical of curves with non-smooth points [166]. The annulus has a non-smooth point because $R = \infty$, which corresponds to either $R_1 = 0$ or $R_2 = \infty$, and one boundary of the annulus always collapses into a point. The regularisation does not remove divergences [166]. Since $S' = \infty$, connected minimal surfaces with $k^2 - 2kp > 0$ are in fact are not realisable. A limiting procedure on both R_i is ϵ may overcome the problem, but this is an open question.

4.3 The local spectral curve of minimal surfaces

In this section, we construct the local spectral curve of minimal surfaces with NSNS flux of section 4.1. We follow the procedure of subsection 2.2.2. We write local spectral curve, which is an elliptic curve, in the Weierstrass form. We connect special values of the j-invariant with distinguished minimal surfaces. We eventually focus on the limit of pure NSNS flux, where the elliptic curve singularises. We identify the two classes of subsection 4.1.2. We collect the necessary background material on elliptic curves for this section in appendix E. Moreover, we refer to section 2.4 of [138] for a brief analysis of the local spectral curve of annular minimal surfaces in the limit of pure RR flux.

The starting point of the procedure of section 2.2.2 is writing the left current j in Euclidean AdS_3 with render the ansatz (4.1) is factorisable. Formula (C.16) implies factorisability as defined in (2.71). If we introduce (4.1) in (C.16), the world-sheet components of j read

$$j_\tau = S\frac{\mathrm{i}\,k}{z^2}\begin{bmatrix} r^2 & r \\ (r^2+z^2)r & -r^2\end{bmatrix}S^{-1} , \tag{4.40}$$

$$j_\sigma = S\frac{1}{z^2}\begin{bmatrix} rr'+zz' & r' \\ (z^2-r^2)r'-2rzz' & -(rr'+zz')\end{bmatrix}S^{-1} , \tag{4.41}$$

where

$$S = \begin{bmatrix} \exp(\mathrm{i}\,k\tau/2) & 0 \\ 0 & \exp(-\mathrm{i}\,k\tau/2)\end{bmatrix} . \tag{4.42}$$

Note that $S^{-1}\mathrm{d}S$ does not depend on τ.

Next, we must compute the determinant of A, which is the matrix (2.74) under the replacement of τ by σ. The matrix A involves the truncation of L_L to Euclidean AdS_3 in (2.65). (We emphasise that $* \mapsto \mathrm{i}\,*$ in (2.65) because of the Wick rotation $\tau \mapsto -\mathrm{i}\,\tau$; see appendix A.) If we introduce (4.40) and (4.41) in (2.65), we obtain

$$\begin{aligned}\det A = \frac{1}{(s-x)^2(1/s+x)^2}\Bigg(&\frac{k^2}{4}(x^4+1)+\frac{k}{\bar{q}}\left[kq\left(1+\frac{r^2}{z^2}\right)-\frac{zz'+rr'}{z^2}\right](x^3-x)\\ &+\frac{1}{\bar{q}^2}\left[\frac{z'^2+r'^2}{z^2}-\frac{2qk(zz'+rr')}{z^2}+\frac{k^2(2q^2-1)r^2}{z^2}+\frac{k^2(3q^2-1)}{2}\right]x^2\Bigg) .\end{aligned} \tag{4.43}$$

If we use (4.4) and (4.5), (4.43) simplifies to

$$\det A = \frac{k^2\bar{q}^2(x^4+1)+4k\bar{q}(qk-p)(x^3-x)+2(3q^2k^2-4qpk-k^2)x^2}{4\bar{q}^2(s-x)^2(1/s+x)^2} . \tag{4.44}$$

The local spectral curve follows from (2.75) through (4.44).

The expression (4.44) does not depend on σ. Independence on σ is in agreement with the isotropy of the monodromy matrix. Moreover, if we had started from L_R, given in (2.66), we would have obtained (3.81) up to $x \mapsto -x$ and the substitution of s and $-1/s$ by $-s$ and $1/s$, respectively. Therefore, the local spectral curve that L_R would provide is identical to that of (4.44). Finally, we note that (4.44) equals the determinant (3.81) through the mapping $k \mapsto k_1$ and $p \mapsto u_0$. We have commented on the mapping in subsection 3.3.

The local spectral curve of minimal surfaces defined by (4.44) via (2.75) involves a quartic polynomial. Thus, it is an elliptic curve. We can obtain the Weierstrass form of the elliptic curve (E.1) by a birational transformation. The modular forms of (E.1) read

$$g_2 = \frac{64}{3}k^2[k^2 - 4qpk + (q^2+3)p^2] \ , \tag{4.45}$$

$$g_3 = -\frac{256}{27}k^3[2k^3 - 12qpk^2 + (15q^2+9)p^2k + 2(q^2-9)qp^3] \ . \tag{4.46}$$

The roots of (E.2) read

$$e_1 = \frac{4}{3}(k^2 - 2qkp) \ , \tag{4.47}$$

$$e_2 = \frac{2}{3}[-(k^2 - 2qkp) + 3\sqrt{k^2 - 4qpk + 4p^2}k] \ , \tag{4.48}$$

$$e_3 = \frac{2}{3}[-(k^2 - 2qkp) - 3\sqrt{k^2 - 4qpk + 4p^2}k] \ . \tag{4.49}$$

If we introduce (4.45) and (4.46) in (E.5), we obtain that the modular discriminant is

$$\Delta = 65536p^4(1-q^2)^2(k^2 - 4qpk + 4p^2)k^6 \ . \tag{4.50}$$

Formulae (4.45) and (4.46) also permit us to obtain the j-invariant through (E.7), which reads

$$j = 256\frac{(k^2 - 4kpq + (q^2+3)p^2)^3}{p^4(1-q^2)^2(k^2 - 4qpk + 4p^2)} \ , \tag{4.51}$$

We focus on the mixed-flux regime first. Then, we analyse the limit of pure NSNS flux.

We note first that $p = 0$ holds for disconnected minimal surfaces of section 4.1 throughout the mixed-flux regime. The elliptic quantities (4.45)–(4.51) are then blind to differences among disconnected minimal surfaces. We do not expect the elliptic curve to reflect connectedness because it is local. Disconnected minimal surfaces share the elliptic curve with connected minimal surfaces with $p = 0$. We restrict ourselves to connected minimal surfaces hereafter.

The j-invariant classifies non-singular elliptic curves. We recall that the j-invariant admits three distinguished values, $j = 0$, $j = 1728$, and $j = \infty$. These values single out special elliptic curves. The values $j = 0$ and $j = 1728$ reflect the enhancement of the Z_2-automorphism of the elliptic curve to a Z_6-automorphism and a Z_4-automorphism, respectively. The value $j = \infty$ corresponds to the singularisation of the elliptic curve. The modular form g_2 dictates the type of singularity.

We propose to associate special values of the j-invariant with distinguished connected minimal surfaces. We compute the real values of p associated to a given j-invariant in the limit of pure RR flux. We then assume that the relationship holds under the NSNS flux and use the j-invariant to identify the deformation of connected minimal surfaces. We argue that we can relate $j = 1728$ and $j = \infty$ to distinguished solutions. More precisely, we argue that we can identify $j = \infty$ and $j = 1728$ with the hemispherical and semi-cylindrical minimal surfaces, respectively. On the other hand, no real p lead us to $j = 0$ in the mixed-flux regime.

We begin with $j = \infty$. By solving $1/j = 0$ with $q = 0$, we obtain $p = 0$. We have shown in subsection 3.2.1 that $p = 0$ uniquely corresponds the connected minimal surface that consists of two domes [166, 168], see (4.21) and (4.22). Since the presence of two components is nonetheless irrelevant for local spectral curve, we identify $j = \infty$ with the hemispherical minimal surface. The value $j = \infty$ does not classify the singular elliptic curve completely. We must compute g_2. If we set $p = q = 0$ in (4.45) and (4.46), we obtain

$$g_2 = \frac{64}{3}k^4 \ , \tag{4.52}$$

$$g_3 = -\frac{512}{27}k^6 \ . \tag{4.53}$$

We identify the deformation of the hemispherical minimal surface by NSNS flux with the singular elliptic curve with a node singularity.

If we solve $1/j = 0$ for p with $0 \leq q < 1$, we obtain $p = 0$. The local spectral curve of the solution is unaffected by the NSNS flux. The result is consistent with our considerations in subsection 4.1.1. We have associated $p = 0$ to the hemispherical minimal surface throughout the mixed-flux regime.

If we set $p = 0$ in the roots (4.47)–(4.49), we obtain

$$e_1 = e_2 = \frac{4}{3}k^2 \ , \tag{4.54}$$

$$e_3 = -\frac{8}{3}k^2 \ . \tag{4.55}$$

Since e_1 and e_2 coincide, we conclude that

$$\Delta = 0 \ , \tag{4.56}$$

which also follows from (E.5) when $p = q = 0$.

We consider $j = 1728$ now. If we solve $j = 1728$ for p with $q = 0$, we obtain $p = \infty$. The value $p = \infty$ corresponds to the semi-cylindrical minimal surface, which subtends two parallel infinite lines at the boundary of Euclidean AdS_3 [62, 63]. To obtain the semi-cylindrical minimal surface from the ansatz (4.1), we must rescale τ and σ, and apply $R_i \to \infty$ in (4.2) with $R_2 - R_1$ fixed; see appendix H of [138]. Note that $|k| = 1$ would be needed since winding along the infinite lines is forbidden. The elliptic curve, which is blind to global issues, does not account for this condition. We keep k general to clarify the discussion. We identify the semi-cylindrical surface with the elliptic curve endowed with a Z_4-automorphism.

If we solve $j = 1728$ for p with $0 \leq q < 1$, we obtain $p = k/2q$. (If $k < 0$, the limit of pure RR flux of $p = k/2q$ becomes $p = -\infty$ instead of $p = \infty$, but both $p = \pm\infty$ correspond to the point at infinity.) The result hints at the identification of the connected minimal surface with $p = k/2q$ with the semi-cylindrical minimal surface with NSNS flux. Even though the connection is not manifest from classical solutions of subsection 4.1.1, we recall that curves at the conformal boundary of Euclidean AdS_3 are determined up to conformal transformations. [7]

[7] The correspondence between minimal surfaces and local spectral curves is neither one-to-one nor onto [65, 66]; the elliptic curve may simply correspond to the annular minimal surface with $p = k/2q$. However, our identification is somewhat supported by the semi-cylindrical minimal surface deformed by NSNS flux of section 10 of [185]. This minimal surface adheres to the boundary in the pure limit of NSNS flux and connects infinitely distant lines. This properties parallel those of the connected minimal surface with $k^2 - 2kp = 0$.

If we set $p = k/2q$ in (4.45) and (4.46), we obtain

$$g_2 = 16\frac{1-q^2}{q^2} \ , \tag{4.57}$$

$$g_3 = 0 \ . \tag{4.58}$$

We identify the deformation of the semi-cylindrical minimal surface by NSNS flux with elliptic curve associated to $j = 1728$.

If we set $p = k/2q$ in the roots (4.47)–(4.49), we obtain

$$e_1 = 0 \ , \tag{4.59}$$

$$e_2 = 2\sqrt{\frac{1-q^2}{q^2}}|k|k \ , \tag{4.60}$$

$$e_3 = -2\sqrt{\frac{1-q^2}{q^2}}|k|k \ . \tag{4.61}$$

If we set $p = k/2q$ in (4.50), we obtain that the modular discriminant is

$$\Delta = 4096\frac{(1-q^2)^3}{q^6} \ . \tag{4.62}$$

In the limit of pure NSNS flux, we have $p = k/2$, which corresponds to the threshold between the two classes of connected minimal surfaces of subsection 3.2.2.

The elliptic curve associated to $j = 1728$ and the discussion on R in (4.16) of subsection 4.1.1 suggests us the following situation. The situation involves different minimal surfaces with the same boundary conditions along the parallel infinite lines. Recall first that we have stated that $p = \infty$ corresponds to $R = 1$ and to the semi-cylindrical minimal surface in the limit of pure RR flux. We have also stated that $p = \infty$ corresponds to $R = 1$ in the mixed-flux regime. We have argued at the same time that p for the semi-cylindrical minimal surface is $p = k/2q$ in the mixed-flux regime. We propose to attribute the duplicity to the non-uniqueness of the problem. Dirichlet boundary conditions at two parallel lines at the boundary of Euclidean AdS_3 are compatible with both connected and disconnected minimal surfaces. In the limit of pure RR flux, $p = \infty$ corresponds to both classes. Connected minimal surfaces couple to the B-field (C.21) and correspond to the elliptic curve with $p = k/2q$. On the contrary, $p = \infty$ continues to correspond to disconnected minimal surfaces, whose ansatz does not couple to the B-field, see formula (21) of [173]. Connected and disconnected minimal surfaces would be indistinguishable in the limit of pure RR flux, and the NSNS flux would differentiate them.

We turn to the limit of pure NSNS flux, where $q = 1$. We perform first the series of the j-invariant in (4.51) around $q = 1$. We obtain

$$\begin{aligned} j = &\frac{64(k-2p)^4}{p^4}(1-q)^{-2} - \frac{64(k-2p)^2(k^2+4kp-2p^2)}{p^4}(1-q)^{-1} \\ &+ \frac{16(3k^3+8k^3p-4k^2p^2-16kp^3+48p^4)}{p^3} + \mathrm{O}(1-q) \ . \end{aligned} \tag{4.63}$$

It follows that $j = \infty$ always holds in the limit of pure NSNS flux unless $k^2 - 2kp = 0$.

If we set $q = 1$ in the roots (4.47)–(4.49), we obtain

$$e_1 = \frac{4}{3}(k^2 - 2kp) \ , \tag{4.64}$$

$$e_2 = \frac{2}{3}[-(k^2 - 2kp) + 3|k^2 - 2kp|] \ , \tag{4.65}$$

$$e_3 = \frac{2}{3}[-(k^2 - 2kp) - 3|k^2 - 2kp|] \ . \tag{4.66}$$

Two out of three roots coincide at least. The sign of $k^2 - 2kp$, the quantity that discriminates between the two classes of the minimal surfaces of subsection 4.1.2, dictates which roots coincide. If $k^2 - 2kp < 0$, $e_1 = e_3$ holds. The elliptic curve corresponds to class of minimal surfaces that adhere to boundary of Euclidean AdS_3. If $k^2 - 2kp > 0$, $e_1 = e_2$ holds. The elliptic curve corresponds to the class of minimal surfaces that subtend a degenerate annulus at the boundary Euclidean AdS_3. If $k^2 - 2kp = 0$, we conclude that $e_1 = e_2 = e_3 = 0$. The elliptic curve corresponds to the threshold between the previous classes of minimal surfaces. We have argued on the basis of the elliptic curve that the threshold corresponds to the limit of pure NSNS flux of the semi-cylindrical minimal surface. It is worth noting that this situation is analogous to the one that we encounter for the long-string and short-string classes of pulsating strings. The quantity that controls the local spectral curve of pulsating strings is indeed $k_1^2 - 2k_1 u_0 + \omega^2$, the counterpart of $k^2 - 2kp$ under the mapping of section 3.3.

Since at least two out of the three roots (4.64)–(4.66) coincide, the modular discriminant vanishes:

$$\Delta = 0 \ , \tag{4.67}$$

which also follows from setting $q = 1$ in (4.50). Therefore, the elliptic curve is singular (even for $p = k/2$). The type of singularity is dictated by g_2. If we apply the limit of pure NSNS flux to (4.45) and (4.46), we obtain

$$g_2 = \frac{64}{3}(k^2 - 2kp)^2 \ , \tag{4.68}$$

$$g_3 = -\frac{512}{27}(k^2 - 2kp)^3 \ . \tag{4.69}$$

The elliptic curve has a node singularity if $k^2 - 2kp \neq 0$, in which case $g_2 \neq 0$. On the contrary, it has a cusp singularity if $k^2 - 2kp \neq 0$, where $g_2 = 0$. The cusp singularity corresponds to the threshold $k^2 - 2kp = 0$, in parallel to the situation of the elliptic curve of pulsating strings in section 3.3.

Chapter 5

Wess-Zumino-Novikov-Witten spin-chain σ-models

The semi-classical limit of the $\mathrm{AdS}_5/\mathrm{CFT}_4$ correspondence allowed the matching between the energies of classical solutions on $\mathrm{AdS}_5 \times \mathrm{S}^5$ and the conformal dimensions of their dual long primary operators in $\mathcal{N} = 4$ SYM theory. The agreement posed two questions. First, the availability of the matching of spectra irrespective of specific solutions in the semi-classical limit. Second, the realisation of classical solutions themselves from the spin chain of $\mathcal{N} = 4$ SYM theory. Reference [51] proposed a simultaneous answer to both questions.

The answer of [51] relies on the construction of an effective action in the semi-classical limit $J \sim \sqrt{\lambda} \to \infty$, and it was advanced in the SU(2) sector of the $\mathrm{AdS}_5/\mathrm{CFT}_4$ correspondence. The effective action corresponds to an SU(2) spin-chain σ-model. It is retrievable from both sides of the duality. The effective action admits the series in the effective coupling λ/J^2 by construction. The series implies the matching of the spectra at leading order in λ/J^2 and also of the infinite hierarchy of conserved charges of the non-linear σ-model and the spin chain. From the point of view of $\mathcal{N} = 4$ SYM theory, the effective action builds on coherent states. Coherent states precisely realise closed-string configurations in the semi-classical limit.

In the SU(2) sector of $\mathrm{AdS}_5 \times \mathrm{S}^5$, the starting point of [51] was the Polyakov action on $\mathrm{R} \times \mathrm{S}^3$. References [44, 52] clarified that the derivation of [51] consist of three steps. First, the identification of fast and slow coordinates among target-space coordinates. They are defined by the fact their generalised velocities are respectively large and small with respect to the effective coupling λ/J^2 when it is fixed and small. Second, the imposition of a gauge-fixing condition to the fast coordinates in the Hamiltonian formalism, which [44] rephrased as a static gauge-fixing condition under a formal T-duality. Third, the series of the gauge-fixed action with respect to λ/J^2, which leads to the effective action. Being small compared to λ/J^2, the generalised velocities of the slow coordinates are consistent with the series. The effective action is linear in the generalised velocities of the slow coordinates and quadratic in the derivatives of the slow coordinates with respect to σ, the spatial derivatives.

In the SU(2) sector of the $\mathcal{N} = 4$ SYM theory, the starting point of [51] was the $\mathrm{XXX}_{1/2}$ Heisenberg model. The $\mathrm{XXX}_{1/2}$ Heisenberg model is the spin chain that encodes the spectral problem at one-loop under the mapping of [31]. Reference [51] in particular began with a transition amplitude in the spin chain. The derivation of the effective action involves two steps. First, the representation of the transition amplitude as an exact path integral over coherent states. The construction of the path integral is standard [186]: the temporal interval of the spin chain is first discretised, the spectral decomposition of the identity over coherent states is used next, and coherent-state configurations are finally written in an analytic series with respect to the coordinate along the temporal interval. (The path integral has the problem [186]; for instance, the existence of non-analytic coherent-state configurations, the definition of the path-integral measure and the convergence of the path integral.) The second step is the LL limit of the action inside the exact path integral. The LL limit is the continuum limit on the spatial interval of the spin chain. It is semi-classical by construction. The LL limit provides the effective action. The coordinates that parameterise continuously the spin chain match the world-sheet coordinates. Coherent-state coordinates in the effective action match the slow coordinates.

The proposal of [51] was extended in a number of directions. References [44, 52] analysed higher orders in λ/J^2. Spin-chain σ-models in other bosonic sectors were also constructed. References [55–57] constructed the $\mathrm{SL}(2,\mathrm{R})$ spin-chain σ-model in the $\mathrm{SL}(2,\mathrm{R})$ sector; [55,187] and [44] analysed the SU(3) sector in the SO(6) sectors, respectively.

Reference [101] applied the proposal of [51] to the SU(2) sector of $\mathrm{AdS}_3 \times \mathrm{S}^3 \times \mathrm{T}^4$ in the mixed-flux regime. Reference [101] started from the Polyakov action on $\mathrm{R} \times \mathrm{S}^3$, which has a WZ term that incorporates the NSNS flux. Reference [101] followed the steps of [51] to obtain the effective action of the SU(2) spin-chain σ-model. Due to the NSNS flux, the generalised velocities of the slow coordinates are not suppressed by the effective coupling but in a combination with the spatial derivatives. The effective action of [101] consists of a term that is linear in both the generalised velocities and the spatial derivatives, and a quadratic term in the spatial derivatives. The quadratic term vanishes in the limit of pure NSNS flux.

Type IIB superstring theory on $\mathrm{AdS}_3 \times \mathrm{S}^3 \times \mathrm{T}^4$ with pure NSNS flux admits a spin chain whose finite-size corrections cancel. Reference [110] built on [109] to construct the integrable spin chain that encodes the spectrum of the $\mathrm{PSU}(1,1|2)$ WZNW model exactly (see section 1.2 for a summary). This situation raises the question of whether the effective action of a given sector of $\mathrm{AdS}_3 \times \mathrm{S}^3$ with pure NSNS flux is retrievable from the spin chain of [110]. In this chapter, we construct the $\mathrm{SL}(2,\mathrm{R})$ and SU(2) spin-chain σ-models in the $\mathrm{PSU}(1,1|2)$ WZNW model. We obtain the effective action from both the Polyakov action and from the spin chain of [110] in the semi-classical limit.

Our derivation of the effective action starting from the spin chain of [110] is atypical. We summarise it for clarity. First, we postulate the coherent states in a given sector. We keep the relationship between coherent states and states in the world-sheet CFT_2 of the $\mathrm{PSU}(1,1|2)$ WZNW model implicit. Our guess for coherent states is somewhat justified by the fact they eventually yields the correct effective action in both the $\mathrm{SL}(2,\mathrm{R})$ and the SU(2) sectors. We then consider a transition amplitude in the spin chain. We argue that the temporal interval is discretised in terms of the spatial interval of the spin chain. We apply a LL limit to the transition amplitude. The LL involves the synchronised continuum limit of both the temporal and spatial intervals of the spin chain. The LL limit provides us with a path integral which is already semi-classical, as opposed to exact. The LL limit also provides us with the bound that discriminates among spectrally flowed sectors.

The chapter has the following structure. In section 5.1, we construct the $\mathrm{SL}(2,\mathrm{R})$ WZNW spin-chain σ-model. In subsection 5.1.1, we obtain the effective action from the Polyakov action on $\mathrm{AdS}_3 \times \mathrm{S}^1$ with pure NSNS flux. We follow the steps of [44,57]. We briefly consider the emergence of the solutions of subsection 3.2.2. In subsection 5.1.2, we obtain the effective action from the SL(2, R) sector of the spin chain of [110]. We follow the procedure that we have summarised in the previous paragraph. In section 5.2, we construct the SU(2) WZNW spin-chain σ-model along the lines of section 5.1. In subsection 5.2.1, we obtain the effective action from the Polyakov action on $\mathrm{R} \times \mathrm{S}^3$ with pure NSNS flux. We follow the steps of subsection 5.1.1. In subsection 5.2.2, we compute the effective action from the SU(2) sector of the spin chain of [110]. We follow again the procedure that we have summarised in the previous paragraph.

The chapter is based on [P4,P7]. [1] We refer to [11] for a review of spin-chain σ-models in the $\mathrm{AdS}_5/\mathrm{CFT}_4$ correspondence. We refer to [188] and [189] for the construction of coherent states in unitary irreducible representations of on SL(2, R) and SU(2), respectively. We refer to appendix A of [55] for a summary of the construction of coherent states on general groups.

5.1 The SL(2, R) Wess-Zumino-Novikov-Witten spin-chain σ-model

In this section, we construct the SL(2, R) WZNW spin-chain σ-model by obtaining the effective action in the semi-classical limit. In subsection 5.1, we derive the effective action from the classical SL(2, R) WZNW model, which corresponds to the SL(2, R) sector of $\mathrm{AdS}_3 \times \mathrm{S}^3$ with pure NSNS flux. Our starting point is the Polyakov action on $\mathrm{AdS}_3 \times \mathrm{S}^1$ with pure NSNS flux, where S^1 is an equator of S^3. Our approach builds on [44], which focused on the SU(2) sector of $\mathrm{AdS}_5 \times \mathrm{S}^5$, and [57], which applied the method of [44] to the SL(2, R) sector thereof. We also consider the emergence of the solutions of subsection 3.2.2 briefly. In subsection 5.1.2, we derive the effective action from the SL(2, R) sector the spin chain of [110]. We postulate the coherent states of the SL(2, R) sector on the basis of [188]. We then the steps that provides to the effective action, in particular the LL limit.

5.1.1 The effective action from the classical action on $\mathrm{AdS}_3 \times \mathrm{S}^1$

We begin with the division of target-space coordinates into two sets, called *fast coordinates* and *slow coordinates*. Fast coordinates parameterise time-like and space-like directions in the target space. Their generalised velocities are large in the limit $k \to \infty$. We must impose the static gauge-fixing condition to fast coordinates under a formal T-duality of the coordinate along the space-like direction. Fast coordinates parameterise the temporal and spatial directions in the continuum limit of the spin chain. Slow coordinates are the remaining coordinates. The generalised velocities of slow coordinates are not suppressed when $k \to \infty$.

[1] In subsection 5.2.1, we rederive for completeness the results section 4 of [101] in the limit of pure NSNS flux. In subsection 5.2.2, we improve the derivation of [P4] following [P7]. The point of view of [P7] is advantageous because it avoids unnecessary assumptions on the transition amplitude of [P4] and clarifies some features of the associated path integral. The effective action obtained from either the steps of subsection 5.2.2 or [P4] is nonetheless the same. We do not discuss of subleading corrections advanced [P4] it is unclear if it is correct in the light of [P7].

Instead, linear combinations of generalised velocities and spatial derivatives of slow coordinates are suppressed when $k \to \infty$. Slow coordinates parameterise coherent states in the continuum limit of the spin chain.

We need an adequate coordinate system in $\mathrm{AdS}_3 \times \mathrm{S}^1$ to get a split into fast and slow coordinates. We use the Hopf fibration of both AdS_3 and S^3 [55, 57]. Consider AdS_3. The Hopf fibration reveals the local resemblance between $\mathrm{H}_2 \times \mathrm{S}^1$ and $\mathrm{PSL}(2, \mathrm{R})$, of which AdS_3 is the universal cover. The Hopf fibration specifically accounts for the fibre-bundle structure of $\mathrm{PSL}(2, \mathrm{R})$, whereby H_2 is the base space and S^1 is the fibre. The gauge group of the fibre bundle is $\mathrm{U}(1)$. The Hopf fibration is conveniently expressed in the embedding coordinates (C.1) of AdS_3:

$$Y^0 + \mathrm{i}\, Y^3 = \mathrm{e}^{\mathrm{i}\,\alpha}\, Z_0 \ , \qquad Y^1 + \mathrm{i}\, Y^2 = \mathrm{e}^{\mathrm{i}\,\alpha}\, Z_1 \ , \tag{5.1}$$

The coordinate α is real and parameterises the fibre S^1 and Z_a are complex coordinates subject to the constraint $-\overline{Z_0} Z_0 + \overline{Z_1} Z_1 = -1$. The action of $\mathrm{U}(1)$ on α and Z_a respectively reads $\alpha \mapsto \alpha + \beta$ and $Z_a \mapsto \exp(-\mathrm{i}\,\beta) Z_a$, and, thus, it preserves the constraint of Z_a. Therefore, Z_a parameterise the base space H_2. By construction, the coordinate α is fast, whereas Z_a are slow.

The effective action that we obtain in subsection 5.1.2 is not expressed in (5.1); it is written instead in the global coordinate system (C.6). The comparison with subsection 5.1.2 requires us to identify α and Z_a in (C.6). The relationship between (5.1) and (C.6) is not straightforward due to the action of $\mathrm{U}(1)$ group of the fibre bundle on α and Z_a.

To resolve the ambiguity, we draw on the the gauge-fixing condition for the fast coordinates with respect to the world-sheet coordinates. According to [44], we must impose the static gauge-fixing condition to the fast coordinates, which fixes α proportionally to τ. Each admissible identification of α in (C.6) leads to a gauge-fixing condition. However, we need a proper choice α for the comparison with subsection 5.1.2. Reference [110] constructed the spin chain on the basis of the light-cone gauge-fixing condition, where t is proportional to τ. Since we must ensure that the static and light-cone gauge-fixing conditions are compatible, we conclude [2]

$$\alpha = t \ , \quad Z_0 = \cosh\rho \ , \quad Z_1 = \mathrm{e}^{\mathrm{i}\,\varphi} \sinh\rho \ , \tag{5.2}$$

where $\varphi = \psi - t$. We identify t with the fast coordinate and ρ and φ with slow coordinates. We shall consistently implement this identification by means of the static gauge-fixing condition. Analogous identifications were introduced in [55–57].

We must identify the fast coordinate along the space-like direction, which is singled out by the Hopf fibration of S^3 [44, 52]. The Hopf fibration manifests the fibre-bundle structure of S^3, whereby S^2 is the base space and S^1 is the fibre. In (5.43), we express the Hopf fibration through the embedding coordinates (C.2) and the global coordinate system (C.10) of S^3. We perform the truncation to $\mathrm{AdS}_3 \times \mathrm{S}^1$ by setting set $\theta = 0$ in (C.10). Hence, the base space S^2 collapses to a point. The fast coordinate is the coordinate ϕ along the equator $\mathrm{S}^1 \subset \mathrm{S}^3$.

Having identified the fast and slow coordinates, we can start the derivation of the effective action. We begin with the Polyakov action (2.47) on $\mathrm{AdS}_3 \times \mathrm{S}^1$ with pure NSNS flux. The

[2] We introduce $t \mapsto \pi/2 - t$ in (C.6) to match the conventions of [P7] in this subsection.

metric in the global coordinate system is (C.9); the B-field is (C.19) with $q = 1$. If we introduce $\varphi = \psi - t$ in (C.9) and (C.19), we obtain the Lagrangian

$$\begin{aligned} L = -\frac{k}{4\pi}\Big[\,&\gamma^{\alpha\beta}(-\partial_\alpha t\partial_\beta t + 2\sinh^2\rho\partial_\alpha t\partial_\beta\varphi + \sinh^2\rho\partial_\alpha\varphi\partial_\beta\varphi + \partial_\alpha\rho\partial_\beta\rho + \partial_\alpha\phi\partial_\beta\phi) \\ &- 2\epsilon^{\alpha\beta}\sinh^2\rho\partial_\alpha t\partial_\beta\varphi\,\Big] \ . \end{aligned} \tag{5.3}$$

To write (5.3) from (2.47), we have used (2.41) with $q = 1$, and we have replaced $h_{\alpha\beta}$ by the unimodular world-sheet metric $\gamma_{\alpha\beta} = h_{\alpha\beta}/\sqrt{-h}$ for later convenience. We have not imposed any gauge-fixing condition to $\gamma_{\alpha\beta}$. The coordinates of the target space in (5.3) are supplied with periodic boundary conditions:

$$t(\tau, \sigma + 2\pi) = t(\tau, \sigma) \ , \quad \phi(\tau, \sigma + 2\pi) = \phi(\tau, \sigma) + 2\pi n \ , \tag{5.4}$$

$$\rho(\tau, \sigma + 2\pi) = \rho(\tau, \sigma) \ , \quad \varphi(\tau, \sigma + 2\pi) = \varphi(\tau, \sigma) + 2\pi m \ , \tag{5.5}$$

where $m, n \in \mathrm{Z}$ are winding numbers. The number n determines the level-matching condition [110].

We must impose the gauge-fixing condition to the fast coordinates now. We look for a static gauge-fixing condition compatible with the light-cone gauge-fixing condition of [110]. We focus on ϕ first. The light-cone gauge-fixing condition for ϕ in [110] is $p_\phi = J/2\pi$, where p_ϕ denotes the canonically conjugate momentum of ϕ and J denotes the total angular momentum:

$$J = -\frac{k}{2\pi}\int_0^{2\pi} \mathrm{d}\sigma\gamma^{\tau\alpha}\partial_\alpha\phi \ . \tag{5.6}$$

Fixing ϕ proportionally to σ is not consistent with (5.6). The direct use of $p_\phi = J/2\pi$ would require us the Hamiltonian formalism [44,52]. We can both find a static gauge-fixing condition and avoid the Hamiltonian formalism by the formal T-duality of ϕ into $\widehat{\phi}$ [44, 57].

We T-dualise ϕ into $\widehat{\phi}$ on the basis of the Buscher procedure (see, for instance, [190]). We replace $\mathrm{d}\phi$ by a one-form A in (5.3), and we add a term to the Lagrangian:

$$L \mapsto L - \frac{k}{2\pi}\widehat{\phi}\epsilon^{\alpha\beta}\partial_\alpha A_\beta \ . \tag{5.7}$$

The Lagrange multiplier $\widehat{\phi}$ ensures that A is closed, that is $\mathrm{d}A = 0$. Being closed, A is locally exact, which means that $A = \mathrm{d}\phi$ locally. If exactness held globally, we could integrate out $\widehat{\phi}$ in (5.7) and $A = \mathrm{d}\phi$ would provide (5.3) again. Nonetheless, the world-sheet is cylindrical, its first Betti number equals one, and A may not be globally exact. We overcome this obstruction by arguing that T-duality is formal (*two-dimensional* in the nomenclature of [44]), which means that T-duality is a computational device and that global issues can be ignored. Formal T-duality allows us to derive the correct action of the SL(2, R) spin-chain σ-model without need for the Hamiltonian formalism. Thus, we ignore topological issues concerning the global exactness of A. We also pass over the dual quantisation of (5.6) and the dilatonic contribution from the path-integral measure (which would vanish in any case).

Bearing in mind the previous caveat, we can eliminate A from (5.7) by solving its equations of motion. We obtain

$$A_\alpha = -\epsilon_{\alpha\beta}\gamma^{\beta\delta}\partial_\delta\widehat{\phi} \ . \tag{5.8}$$

If we introduce (5.8) in (5.7), we arrive to the Lagrangian (5.3) up to the replacement of ϕ by $\widehat{\phi}$ (once we omit the contribution of a total derivative). The central advantage of formal T-duality concerns (5.6). If we use (5.8) in this formula, we conclude

$$J = \frac{k}{2\pi}(\widehat{\phi}(\tau, 2\pi) - \widehat{\phi}(\tau, 0)) \ . \tag{5.9}$$

Therefore, $p_\phi = J/2\pi$ translates into the static gauge-fixing condition $\widehat{\phi} = (J/k)\sigma$. The coordinate $\widehat{\phi}$ parameterises the spatial direction of the spin chain in the continuum limit.

We are interested in the semi-classical limit, where $J \sim k \to \infty$. The coordinate ϕ is fast by assumption. By definition, its generalised velocity $v^\phi = \gamma^{\tau\alpha}\partial_\alpha\phi$ is large when $k \to \infty$. The condition $p_\phi = -(k/2\pi)v^\phi = J/2\pi$ then implies that J is not semi-classical, but also large large. The ratio J/k is non-vanishing and large, and, thus, k/J is small. Therefore, we have that k/J is a sensible effective coupling, just as λ/J^2 in $\mathrm{AdS}_5 \times \mathrm{S}^5$ [30].[3]

In addition, we must impose the static gauge-fixing condition to t. As we have discussed before, the light-cone gauge-fixing condition of [110] demands $t = a\tau$. The choice reflects the coincidence of the time-like directions on the target-space and the world-sheet, as well as the temporal direction of the spin chain in the continuum limit. No obstruction forbids $t = a\tau$ as the fields in the Lagrangian do not satisfy any explicit boundary conditions with respect to τ. We determine the proportionality coefficient a by arguing that t is fast if a is large when $k \to \infty$ [51, 56]. If we further insist on the BMN scaling of the energy that follows from the effective action E (see (1.10)), we conclude that $a = J/k$. [4]

In sum, the static gauge-fixing condition is

$$t = \frac{J}{k}\tau \ , \quad \widehat{\phi} = \frac{J}{k}\sigma \ . \tag{5.10}$$

We can use (5.10) in the equations of motion that follow from (5.3) (once ϕ is replaced by $\widehat{\phi}$). This step is convenient because the equations of motion supplies us with a cross-check to validate the equations of motion from the effective action. If we use (5.10), the equations of motion of (5.3) read

$$\frac{J}{k}\partial_\alpha\gamma^{\alpha\tau} - \partial_\alpha[(\gamma^{\alpha\beta} - \epsilon^{\alpha\beta})\sinh^2\rho\partial_\beta\varphi] = 0 \ , \tag{5.11}$$

$$\frac{J}{k}[\sinh^2\rho\partial_\alpha\gamma^{\alpha\tau} + \sinh(2\rho)(v^\rho - \rho')] + \partial_\alpha(\gamma^{\alpha\beta}\sinh^2\rho\partial_\beta\varphi) = 0 \ , \tag{5.12}$$

$$\frac{J}{k}\sinh(2\rho)(v^\varphi - \varphi') - \partial_\alpha(\gamma^{\alpha\beta}\partial_\beta\rho) + \frac{1}{2}\sinh(2\rho)\gamma^{\alpha\beta}\partial_\alpha\varphi\partial_\beta\varphi = 0 \ , \tag{5.13}$$

$$\frac{J}{k}\partial_\alpha\gamma^{\alpha\sigma} = 0 \ , \tag{5.14}$$

where $v^\rho = \gamma^{\tau\alpha}\partial_\alpha\rho$ and $v^\varphi = \gamma^{\tau\alpha}\partial_\alpha\varphi$ are the generalised velocities of ρ and φ, respectively. The equations of motion are split in terms that are multiplied by J/k and terms that are

[3] It may seem that series in k/J are not analytic as k is not quantised in the $\mathrm{SL}(2,\mathrm{R})$ WZNW model [93]. However, this is not the case: k is indeed quantised in the $\mathrm{PSU}(1,1|2)$ WZNW model [92].

[4] Alternatively, we could have followed [44, 57]. We would have fixed $t = \tau$, and we would have rescaled τ afterwards in a NG action with a WZ term akin to (5.15). The same observation applies to t in subsection 5.2.1.

not. Both sets of equations must be satisfied separately for the consistency of series in the effective coupling k/J. At leading order in k/J, equations (5.11) and (5.14) imply that $\gamma^{\alpha\beta}$ is divergenceless. Since the unimodular world-sheet metric $\gamma_{\alpha\beta}$ is covariantly constant with respect to the torsionless connection, we deduce $\gamma^{\alpha\beta} = \eta^{\alpha\beta} + \mathrm{O}(k/J)$. This result simplifies (5.12) and (5.13), which respectively reduce to $\dot{\rho} + \rho' = \mathrm{O}(k/J)$ and $\dot{\varphi} + \varphi' = \mathrm{O}(k/J)$ (as long as ρ does not vanish). The generalised velocities v^ρ and v^φ are not suppressed by k/J. They are suppressed in the combination with ρ' and φ'. The appearance of ρ' and φ' is due to the NSNS flux in $\mathrm{AdS}_3 \times \mathrm{S}^1$.

The next step we need to take is the reduction of the gauge-fixed action to a NG form with a WZ term. We then restore $h_{\alpha\beta}$ in the Lagrangian and solve the Virasoro constraints by identifying $h_{\alpha\beta}$ with the induced metric on the world-sheet as in (2.51). We obtain

$$S = -\frac{k}{2\pi}\int_{-\infty}^{\infty} \mathrm{d}\tau \int_0^{2\pi} \mathrm{d}\sigma \left(\sqrt{-h} - \frac{J}{k}\sinh^2\rho\varphi'\right) . \tag{5.15}$$

The expression of h is arranged in powers of the inverse effective coupling J/k; explicitly,

$$\begin{aligned} h = &-\frac{J^4}{k^4} + 2\frac{J^3}{k^3}\sinh^2\rho\dot{\varphi} - \frac{J^2}{k^2}[-\dot{\rho}^2 + \rho'^2 + \sinh^2\rho(-\dot{\varphi}^2 + \cosh^2\rho\varphi'^2)] \\ &- 2\frac{J}{k}\sinh^2\rho\rho'(\dot{\rho}\varphi' - \rho'\dot{\varphi}) + \sinh^2\rho(\dot{\rho}\varphi' - \rho'\dot{\varphi})^2 . \end{aligned} \tag{5.16}$$

We deduce that we can perform an analytic series of (5.15) (or rather $(k^2/J^2)S/k$) with respect to k/J. Note also that $\sqrt{-h}h^{\alpha\beta} = \eta^{\alpha\beta} + \mathrm{O}(k/J)$, consistently with (5.11) and (5.14).

We perform the series of (5.15) with respect to k/J. If we neglect terms at $\mathrm{O}(k/J)$ and omit the divergent constant contribution of the fast coordinates, we obtain

$$S = \frac{J}{2\pi}\int_{-\infty}^{\infty} \mathrm{d}\tau \int_0^{2\pi} \mathrm{d}\sigma \sinh^2\rho(\dot{\varphi} + \varphi') . \tag{5.17}$$

The effective action corresponds to a SL(2, R) spin-chain σ-model and is linear in both $\dot{\varphi}$ and φ'. Formula (5.17) is in exact agreement with the expression for the effective action (5.41) that we derive in subsection 5.1.2 from the spin chain. The equations of motion of (5.17) are anti-chiral:

$$\sinh(2\rho)(\dot{\rho} + \rho') = 0 , \tag{5.18}$$

$$\sinh(2\rho)(\dot{\varphi} + \varphi') = 0 . \tag{5.19}$$

The equations of motion (5.18) and (5.19) are consistent with (5.12) and (5.13), respectively. The general solution to (5.19) and (5.18) are 'right-moving waves':

$$\rho(\tau, \sigma) = \rho(\tau - \sigma) , \tag{5.20}$$

$$\varphi(\tau, \sigma) = \varphi(\tau - \sigma) . \tag{5.21}$$

Classical solutions (5.20) and (5.21) are endowed with the periodic boundary conditions (5.5). Equation (5.4) supplies the boundary conditions of t and ϕ. The periodicity of t trivially holds due to (5.10). The quasi-periodicity of ϕ imposes an additional constraint on (5.20). If we use (5.19), the constraint reads

$$2\pi n = -2\int_0^{2\pi} \mathrm{d}\sigma \sinh^2\rho\varphi' \ , \tag{5.22}$$

where we have ignored $\mathrm{O}(k/J)$ terms.

Formulae (5.21) and (5.20) encompass the semi-classical limit of classical solutions that are reproducible from the spin chain, in particular pulsating strings of subsection 3.2.2. We begin with $\rho = 0$. There is a polar coordinate singularity at $\rho = 0$ in the global coordinate system, where neither ψ nor $\varphi = \psi - t$ are defined. Therefore, we set $\psi = 0$. This point-like classical solution is the BMN vacuum, which is the ground state of the spin chain of [110]. It corresponds to $\mu = k_1^2$ of subsection 3.2.2.

The pulsating-string ansatz (3.1) demands $\rho = \rho(\tau)$, $t = t(\tau)$, and $\psi = k_1\sigma$, where (5.4) implies $k_1 = m$. The static gauge-fixing condition (5.10) and (5.21) and (5.20) imply $\rho = \rho_0$ and $t = (J/k)\tau$, and also $m = J/k$. Thus, the semi-classical limit of pulsating strings belongs to the continuous class of constant radius ρ_0 that we have discussed at the end of subsection 3.2.2. The solutions with $\rho = \rho_0$ raise in the threshold between pulsating string in the short-string and the long-string classes. The spectral-flow parameter w equals m up to the sign. As we have commented in subsection 3.2.2, the continuous class of solutions arises when J saturates the unitarity bound of the w-th spectrally flowed sector in the world-sheet CFT_2. Moreover, the world-sheet never collapses to a geodesic as the winding number $m = J/k$ is always large.

Our solutions are compatible with the unitarity bound of [93] on the principal discrete series of $\mathrm{SL}(2,\mathrm{R})$ discussed in [109, 110]. We prove in subsection 5.1.2 that J/k is indeed bounded from below by w if $k \to \infty$, see (5.37). Solutions with $\rho = \rho_0$ are also compatible with the claim made in [112] on the violation of the unitarity bound in the principal continuous series. The reason is that $k \to \infty$ permits the saturation of the end points of the unitarity bound by exceptional solutions to the Bethe equations.

5.1.2 The effective action from the spin chain in the $\mathrm{SL}(2,\mathrm{R})$ sector

We rederive the effective action (5.17) from the $\mathrm{SL}(2,\mathrm{R})$ sector of the spin chain proposed in [110]. We begin with a review of the aspects of the spin chain of [110] that we need. We refer to [110] for details that we skip.

The spin chain of [110] encodes the spectrum of the $\mathrm{PSU}(1,1|2)$ WZNW model in a system of all-loop Bethe equations. The Bethe equations are built on the transition amplitudes of the all-loop S-matrix. The Bethe equations are not only asymptotic but also exact due to the cancellation of wrapping corrections. The Bethe equations determine the set of admissible momenta for magnons above the BMN vacuum. Magnons are eigenstates of the Hamiltonian of the spin chain that consist of a linear superposition of oscillators, that is creation operators with definite momentum above the BMN vacuum. Single magnons, in particular, are expressed as a linear superposition each of whose terms involves just one oscillator.

The dispersion relation of single magnons follows from the imposition of a shortening condition to the Hamiltonian of the spin chain. The condition reads

$$H^2 = \left(\frac{k}{2\pi}P + M\right)^2 , \tag{5.23}$$

where H denotes the Hamiltonian of the spin chain, P denotes the momentum operator, and M is a linear operator that shifts the dispersion relation according to the excitations on which it acts. The Hamiltonian is semi-definite positive due to a BPS bound. Therefore, the dispersion relation involves the positive branch of the absolute value following from (5.23). Magnons are called *chiral* and *anti-chiral* if the expression inside the absolute value of the dispersion relation is positive and negative, respectively.

We focus on the $\mathrm{SL}(2,\mathrm{R})$ sector of the spin chain. *Sector* denotes a choice of the type of oscillator that acts on the BMN vacuum. The type of oscillator is determined by its representation labels under the superisometry algebra of $\mathrm{AdS}_3 \times \mathrm{S}^3 \times \mathrm{T}^4$. The various types of oscillators in the general mixed-flux regime of $\mathrm{AdS}_3 \times \mathrm{S}^3 \times \mathrm{T}^4$ are listed in [105]. [5] The matrix elements of the S-matrix between states with different kinds of oscillator are in general non-trivial. Thus, the determination of whether a sector is closed or not is elaborate. The limit $k \to \infty$ allows us to circumvent this problem because it maps sectors to truncations of the classical $\mathrm{PSU}(1,1|2)$ WZNW model. A sector is closed if the corresponding truncation is consistent, which is a property that immediately holds for the $\mathrm{SL}(2,\mathrm{R})$ sector.

In fact, there are not one but two $\mathrm{SL}(2,\mathrm{R})$ sectors in the spin chain: the left-handed sector $\mathrm{SL}(2,\mathrm{R})_\mathrm{L}$ and right-handed sector $\mathrm{SL}(2,\mathrm{R})_\mathrm{R}$. Both sectors are present because AdS_3 is $\mathrm{SL}(2,\mathrm{R}) \cong \mathrm{SL}(2,\mathrm{R})_\mathrm{L} \times \mathrm{SL}(2,\mathrm{R})_\mathrm{R}/\mathrm{SL}(2,\mathrm{R})$ as a permutation coset (see (2.42)). The duplicity is reflected in the eigenvalue m of M in (5.23). The BMN vacuum has $m = 0$. Single magnons that transform under $\mathrm{SL}(2,\mathrm{R})_\mathrm{L}$ have $m = 1$; single magnons that transform under $\mathrm{SL}(2,\mathrm{R})_\mathrm{R}$ have $m = -1$. The dispersion relation of composite magnons follows from these considerations. The important point is that the restriction of m reflects the restriction of the spin chain to a sector of given handedness. For definiteness, we focus on the $\mathrm{SL}(2,\mathrm{R})_\mathrm{L}$ sector of the spin chain.

The last element of the spin chain of [110] that we need to begin is the number of sites J of the spin chain, which is bounded. [6] The number of sites J equals the total angular momentum of the BMN vacuum in the spin-chain frame where the spin chain is defined. The value J is constrained by a unitarity bound [93, 110], which differs among spectrally flowed sectors. In

[5] Reference [105] listed the canonical harmonic-oscillator creation and annihilation operators in the BMN limit. We denote by *oscillator* the deformation by the string tension of the creation operators of [105] along the lines of [74]. Both the oscillators and the creation operators of [105] carry the same representation labels. Oscillators have not explicitly appeared in the bibliography to the best of our knowledge.

[6] Reference [110] identifies J with the length of the spin chain. The choice clarifies the decompactification limit where the S-matrix is definable. The convention is shared by [51] in the SU(2) sector of $\mathcal{N} = 4$ SYM theory. We follow [44, 52] in the SU(2) sector of $\mathcal{N} = 4$ SYM theory and [55, 56] follow in the $\mathrm{SL}(2,\mathrm{R})$ sector thereof, where J denotes the number of sites of the spin chain. Our identification clarifies the LL limit. Both choices are related by a rescaling of σ in the effective action. The same observation holds in subsection 5.2.2.

particular, the unitary bound of the w-th spectrally flowed sectors reads

$$kw + 1 \leq J \leq k(w+1) - 1 \ , \tag{5.24}$$

where w denotes the integer spectral-flow parameter and $k \in \mathrm{N}$ denotes the level. In writing (5.24), we have further assumed that $k > 1$ and $w \geq 0$. The exclusion of $k = 1$ is unimportant because we are interesting in $k \to \infty$. We have made the assumption $w \geq 0$ for simplicity. One may consider $w < 0$ by inverting the sign of J in (5.24) without major modifications in the subsequent derivation.

In general, the action of a spin-chain σ-model is built on coherent states. Coherent states in the spin chain are constructed from the tensor product of J copies of one-site coherent states. The construction of one-site coherent states is prescribed by the Perelomov procedure. The procedure requires three elements: a group, a representation thereof, and a reference state. The reference state must be invariant under the action of the maximal Abelian subgroup of the group up to a phase.

The group is $\mathrm{SL}(2,\mathrm{R})$. The unitary irreducible representations of $\mathrm{SL}(2,\mathrm{R})$ that are non-trivial are infinite-dimensional; see, for instance, subsection 4.1 of [93]. We choose the representation by postulating an ansatz for one-site coherent state. Specifically, we postulate that one-site coherent states belong to the $j = 1/2$ lowest-weight representation in the principal discrete series of $\mathrm{SL}(2,\mathrm{R})$, which is realised in each one-site Hilbert space $\mathcal{H}_a$, with $a = 0, ..., J-1$. Our ansatz is supported by the effective action we obtain in (5.41), which matches (5.17) of subsection 5.1.1. We must emphasise that the representation of coherent states under $\mathrm{SL}(2,\mathrm{R})$ does not coincide with the representation of zeroth-level generators of the current algebra. We assume instead the existence of the mapping between our coherent states and states in the world-sheet CFT_2 of the $\mathrm{PSU}(1,1|2)$ WZNW model. Moreover, we choose the reference state in each $\mathcal{H}_a$ as the state whose isotropy group is maximal.

One-site coherent states are in this way unambiguously determined. They read

$$|\vec{n}_a\rangle = \operatorname{sech}\rho_a \sum_{m=0}^{\infty} \mathrm{e}^{-\,\mathrm{i}\,m\varphi_a} \tanh^m \rho_a \, |m\rangle \ , \tag{5.25}$$

where $|m\rangle$ is an orthonormal basis of $\mathcal{H}_a$. One-site coherent states would present a global phase in general, but (5.25) suffices to recover (5.17). (On the contrary, we keep the global phase coherent states of subsection 5.2.2.) The pair ρ_a and φ_a is the discrete counterpart of ρ and φ in the coordinate system (5.2). The range of both ρ_a and φ_a, and ρ and φ is the same; ρ_a and φ_a will in fact match ρ and φ under the application of the LL limit. We have defined short-hand notation $\vec{n}_a$ as

$$\vec{n}_a = [\cosh(2\rho_a), -\sinh(2\rho_a)\sin\varphi_a, \sinh(2\rho_a)\cos\varphi_a] \ , \tag{5.26}$$

which labels the one-site coherent state. The vector (5.26) is assembled from the expectation value of the generators of $\mathfrak{sl}(2,\mathrm{R})$ in (5.25).

A general coherent state in the Hilbert space of the spin chain $\mathcal{H} = \mathcal{H}_0 \otimes ... \otimes \mathcal{H}_{J-1}$ is

$$|\vec{n}\rangle = \bigotimes_{a=0}^{J-1} |\vec{n}_a\rangle \ . \tag{5.27}$$

Since the spin chain is closed, we must furthermore identify $\vec{n}_0$ with $\vec{n}_J$. This identification permits to realise the periodic boundary conditions of closed-string configurations in the continuum limit of the spin chain. We furthermore identify the particular state with every $\rho_a = 0$, which consists of J copies of $|0\rangle$, with the BMN vacuum. Coherent states (5.27) are an overcomplete basis of $\mathcal{H}$. This fact implies two correlative properties which we use later. The first is the resolution of the identity operator in $\mathcal{H}$ in the coherent-state basis:

$$1 = \int \mathrm{d}\mu[\vec{n}]\, |\vec{n}\rangle\langle\vec{n}| \ , \tag{5.28}$$

where $\mathrm{d}\mu[\vec{n}]$ is the measure which comprises the product of one-site measures $\mathrm{d}\mu[\vec{n}_a]$. [7] The second property is that coherent states are not orthonormal, but rather satisfy

$$\langle\vec{n}|\vec{n}'\rangle = \prod_{a=0}^{J-1} \left[\cosh\rho_a \cosh\rho_a' - \mathrm{e}^{\mathrm{i}(\varphi_a - \varphi_a')} \sinh\rho_a \sinh\rho_a'\right]^{-1} \ . \tag{5.29}$$

Once we have presented the spin chain and our coherent states, we can start considering the LL limit of the spin chain. The starting point is the transition amplitude between an initial state $|\Psi_1\rangle$ at $t = -T/2$ and a final state $|\Psi_2\rangle$ at $t = T/2$. The parameter t is the coordinate along the temporal direction of the spin chain. The limit $T \to \infty$ must be applied as the time-like direction in the world-sheet is non-compact. The transition amplitude is

$$Z = \lim_{T\to\infty} \langle\Psi_2| \exp(-\,\mathrm{i}\, HT)\, |\Psi_1\rangle \ . \tag{5.30}$$

This transition amplitude involves the Hamiltonian H. The action of the Hamiltonian in the spin chain is not directly available, but encoded in the quadratic constraint (5.23). The form of H is not achievable in general because it depends on the specific state in which it acts. To proceed, we assume that $|\Psi_1\rangle$ (or the final state $|\Psi_2\rangle$) to is a magnon, that is an eigenstate of H, P and M with eigenvalues E, p and m, respectively. (Note that $E \geq 0$ due to the fact H is semi-definite positive, p is quantised since the spin chain is closed, and $m \geq 0$ because $|\Psi_1\rangle$ belongs to the $\mathrm{SL}(2,\mathrm{R})_{\mathrm{L}}$ sector; these properties are secondary for the LL limit.) The magnon is expressed as a linear superposition of coherent states since they form a basis of $\mathcal{H}$. (The decomposition is non-unique because the basis is overcomplete.) Let the dispersion relation of $|\Psi_1\rangle$ be

$$E = -\left(\frac{k}{2\pi}p + m\right) \ . \tag{5.31}$$

We have assumed that $|\Psi_1\rangle$ is anti-chiral in view of the equations of motion (5.18) and (5.19). We can replace the Hamiltonian H by E in (5.30). We can then replace E with (5.31). If we

[7] We write neither $\mathrm{d}\mu[\vec{n}]$ nor $\mathrm{d}\mu[\vec{n}_a]$ explicitly for two reasons. First, AdS_3 is the universal cover of SL(2, R). Therefore, φ is not compact, and the use of the measure of SL(2, R) in (2.14) of [56] is not applicable, see thereof. (Reference [56] introduced the compact counterpart of φ in SL(2, R), and decompactified φ in the effective action.) Second, the measure at $j = 1/2$ is defined through an analytic continuation of the measure of arbitrary j [56]. These impediments are not directly relevant for us as $\mathrm{d}\mu[\vec{n}_a]$ eventually becomes a formal path-integral measure $[\mathrm{d}\mu]$ in the path integral (5.39). We finally note that we do not need $\mathrm{d}\mu[\vec{n}_a]$ in subsection 5.2.2 either. In this case, however, $\mathrm{d}\mu[\vec{n}_a]$ is quite straightforward; see, for instance formula (9) of [P4]

lift p to an operator level, (5.30) reads

$$Z = \lim_{T\to\infty} \mathrm{e}^{\mathrm{i}\,Tm} \langle\Psi_2|\exp(\mathrm{i}\,T(k/2\pi)P)|\Psi_1\rangle \ . \tag{5.32}$$

This form is suited to the path-integral representation of the transition amplitude.

To construct a path integral, we have to introduce a partition of $[-T/2, T/2]$. We slice $[-T/2, T/2]$ in N subintervals $[t_{\alpha+1}, t_\alpha]$ of equal step length $\Delta t = T/N$. The end points of the subintervals are $t_\alpha = (2\alpha - N)T/2N$, with $\alpha = 0, ..., N$. If we introduce the resolution of the identity (5.28) between the end points of every pair of consecutive subintervals, (5.32) is rephrased as

$$Z = \lim_{T\to\infty} \int \mathrm{d}\mu[\vec{n}_N] ... \int \mathrm{d}\mu[\vec{n}_0] \overline{\Psi_2(\vec{n}_N)} \left(\prod_{\alpha=0}^{N-1} \mathrm{e}^{\mathrm{i}\,\Delta t m} \langle\vec{n}_{\alpha+1}|\exp(\mathrm{i}\,\Delta t(k/2\pi)P)|\vec{n}_\alpha\rangle \right) \Psi_1(\vec{n}_0) \ . \tag{5.33}$$

Here, $|\vec{n}_\alpha\rangle = |\vec{n}_{\alpha,0}\rangle \otimes ... \otimes |\vec{n}_{\alpha,J-1}\rangle$, $\Psi_1(\vec{n}_0) = \langle\vec{n}_0|\Psi_1\rangle$ and $\overline{\Psi_2(\vec{n}_N)} = \langle\Psi_2|\vec{n}_N\rangle$. Note that $\Psi_1(\vec{n}_0)$ and $\overline{\Psi_2(\vec{n}_N)}$ are wave functions in the basis of coherent states.

Formula (5.33) involves the matrix elements of $U = \exp(\mathrm{i}\,\epsilon P)$, the anticlockwise shift operator, raised to the power $(k/2\pi)\Delta t/\epsilon$, where ϵ is the spatial step length. Any shift in the spin chain must correspond to an integer multiple of times ϵ. In order for U to be defined on $\mathcal{H}$, the step length must then satisfy

$$\Delta t = \frac{2\pi}{k}\epsilon \ . \tag{5.34}$$

Therefore, the temporal interval of the closed spin chain is discretised. In general, one may write Δt as a positive integer multiple of (5.34), but $\Delta t = (2\pi/k)\epsilon$ is always obtained when $[-T/2, T/2]$ is divided into the maximum amount of subintervals.

The condition (5.34) allows us to reformulate (5.33) as

$$\begin{aligned} Z = \lim_{T\to\infty} \int \mathrm{d}\mu_N ... \int \mathrm{d}\mu_0 \overline{\Psi_2(\vec{n}_N)} \Bigg(\prod_{\alpha=0}^{N-1} \mathrm{e}^{\mathrm{i}\,\Delta t m} \prod_{a=0}^{J-1} \Big[&\cosh\rho_{\alpha+1,a}\cosh\rho_{\alpha,a-1} \\ - \mathrm{e}^{\mathrm{i}(\varphi_{\alpha+1,a}-\varphi_{\alpha,a-1})} &\sinh\rho_{\alpha+1,a}\sinh\rho_{\alpha,a-1}\Big]^{-1} \Bigg) \Psi_1(\vec{n}_0) \ , \end{aligned} \tag{5.35}$$

where we have used

$$U|\vec{n}_\alpha\rangle = \bigotimes_{a=0}^{J-1} |\vec{n}_{\alpha,a-1}\rangle \ , \tag{5.36}$$

and the scalar product (5.29). Formula (5.35) is susceptible to the application to the LL limit.

For customary spin chains in quantum mechanics, such as the Heisenberg $\mathrm{XXX}_{1/2}$ model, the LL limit yields an effective action in the form of a non-linear σ-model [186]. The LL limit is a spatial continuum limit applied to the classical action inside an exact path integral over coherent states. The LL limit is defined by $\epsilon \to 0$ and $J \to \infty$ with the spin-chain length $R = J\epsilon$ fixed. Under the assumption that coherent states depend analytically on their site labels, the leading term in the LL limit of the action provides the non-linear σ-model. The exact path integral over coherent states follows from a continuum limit that precedes the LL limit. This continuum limit is applied to a transition amplitude with respect to the temporal interval parameterised by t. This continuum limit is standard in path integrals, and it involves $\Delta t \to 0$ and $N \to \infty$ with $T = N\Delta t$ fixed under the assumption that coherent states depend analytically on t.

The application of an analogous steps to (5.35) is forbidden. First and foremost, the step lengths Δt and ϵ are intertwined as stated by (5.34), which implies that $T = 2\pi NR/kJ$. If the continuum limits with respect to α and a in (5.35) keep T and R respectively finite, the condition $N/kJ \sim \mathrm{O}(1)$ must hold. The limits $N \to \infty$ and $J \to \infty$ must be synchronised: the LL limit in (5.35) involves the simultaneous application of the limit $\Delta t \to 0$ and $N \to \infty$ with $T = N\Delta t$ fixed and $\epsilon \to 0$ and $J \to \infty$ with $R = J\epsilon$ fixed. Furthermore, the LL limit is a semi-classical limit, that is the LL limit presupposes $J \sim k \to \infty$. The inequality (5.24) bounds J in terms of k and w. Since the spectral-flow parameter remains finite, $J \to \infty$ already implies $k \to \infty$ (which in turn implies that $\Delta t \to 0$). The counterpart of (5.24) if $J \sim k \to \infty$ is

$$w \leq J/k \leq w + 1 \ . \tag{5.37}$$

The inequality (5.37) indicates that the spin chain belongs to the w-th spectrally flowed sector in the semi-classical limit, see formula (59) of [93]. We emphasise that the effective coupling of subsection 5.1.1 is k/J. Therefore, (5.37) states that the LL limit is accurate in highly spectrally flowed sectors.

We apply the LL limit to (5.35) following the previous discussion. If we assume that $\rho_{\alpha,a}$ and $\varphi_{\alpha,a}$ depend analitically on α and a, and we assume that ϵ and $\Delta t = (2\pi/k)\epsilon$ are small, we can write (5.35) as

$$Z = \lim_{T\to\infty} \int \mathrm{d}\mu_N ... \int \mathrm{d}\mu_0 \overline{\Psi_2(\vec{n}_N)} \prod_{\alpha=0}^{N-1} \Bigg(\mathrm{e}^{\mathrm{i}\,\Delta t m} \prod_{a=0}^{J-1} \Big[1 + \mathrm{i} \sinh^2 \rho_{\alpha,a} (\Delta t \dot{\varphi}_{\alpha,a} + \epsilon \varphi'_{\alpha,a}) \\ + \mathrm{O}(\epsilon^2) \Big] \Bigg) \Psi_1(\vec{n}_0) \ , \tag{5.38}$$

where $\dot{}$ and $'$ denote derivatives with respect to t_α and $x_a = a\epsilon$, respectively. If we introduce the short-distance cut-off ϵ (or, equivalently, Δt), we can consider the expression between round brackets the formal product of two continuous products. We can then reword (5.38) as the path integral

$$Z = \int [\mathrm{d}\mu] \overline{\Psi_2(\vec{n}_\infty)}\, \mathrm{e}^{\mathrm{i}\,S}\, \Psi_1(\vec{n}_{-\infty}) \ . \tag{5.39}$$

The path integral involves various elements. First, the classical action. At leading order in ϵ, the classical action reads

$$S = \frac{1}{\epsilon} \int_{-\infty}^{\infty} \mathrm{d}t \int_0^R \mathrm{d}x \left[\frac{\epsilon}{R} m + \sinh^2 \rho \left(\dot{\varphi} + \frac{k}{2\pi} \varphi' \right) \right] \ , \tag{5.40}$$

where $\rho = \rho(t, x)$ and $\varphi = \varphi(t, x)$ are the continuous counterparts of $\rho_{\alpha,a}$ and $\varphi_{\alpha,a}$. Note we have applied the limit $T \to \infty$ with respect to the interval over t. The expression (5.39) also involves the path-integral measure $[\mathrm{d}\mu]$, which is the formal measure that arises from the product of measures $\mathrm{d}\mu[\vec{n}_\alpha]$. The path integral extends over continuous coherent-state configurations $\vec{n} = \vec{n}(t, x)$ with respect to $[\mathrm{d}\mu]$. As we have anticipated, these coherent-state configurations satisfy periodic boundary conditions: $\vec{n}(t, x + R) = \vec{n}(t, x)$. They are also subject to the asymptotic boundary conditions $\vec{n}(\pm\infty, x) = \vec{n}_{\pm\infty}(x)$, where $\vec{n}_\infty$ and $\vec{n}_{-\infty}$ are the continuous counterparts of $\vec{n}_N$ and $\vec{n}_0$, respectively. [8] Finally, the path integral involves $\Psi_1(\vec{n}_{-\infty})$ and $\overline{\Psi_2(\vec{n}_\infty)}$. They are the counterparts of the wave functions $\Psi_1(\vec{n}_0)$ and $\overline{\Psi_2(\vec{n}_N)}$ in the LL limit. [9]

We have to introduce a change of variables to retrieve the effective action (5.17) of subsection 5.1.1. The change of variables is based on the form (5.15), which is a NG action with a WZ term. To obtain the effective action in subsection 5.1.1, we performed a series of the NG action with respect to k/J. Apart from an overall factor of J, the N-th derivative in both τ and σ appears at order $\mathrm{O}((k/J)^N)$. We must find the same pattern here to obtain the series in the effective coupling k/J. To put (5.40) in the proper form, we set $\tau = kt$. We also set $R = 1$, that is $\epsilon = 1/J$ and $\sigma = 2\pi x$ to match the conventions of section 5.1.1. In this way, we conclude

$$S = \frac{J}{2\pi} \int_{-\infty}^{\infty} \mathrm{d}\tau \int_0^{2\pi} \mathrm{d}\sigma \sinh^2 \rho(\dot{\varphi} + \varphi') \ , \tag{5.41}$$

which matches the action of the $\mathrm{SL}(2,\mathrm{R})$ spin-chain σ-model (5.17) under the identification of homonymous world-sheet and target-space coordinates.

We emphasise that we have omitted the constant contribution of m in (5.40). Our assumption is that m (the eigenvalue of the magnon under M) is finite in the limit $k \to \infty$. Thus, its integral is $\mathrm{O}(1/k)$, which is subleading in the large J/k expansion. In addition, we have assumed that $|\Psi_1\rangle$ is an anti-chiral magnon, see (5.31). If $|\Psi_1\rangle$ had been a chiral magnon, we would have obtained (5.41) up to the replacement $\varphi' \mapsto -\varphi'$. This change trades (5.20) and (5.21) by 'left-moving waves'. The chirality of the magnon then maps to the chirality of classical solutions in the $\mathrm{SL}(2,\mathrm{R})$ spin-chain σ-model.

5.2 The SU(2) Wess-Zumino-Novikov-Witten spin-chain σ-model

In this section, we derive the action of the SU(2) WZNW spin-chain σ-model by obtaining the effective action. In subsection 5.2.1, we derive the effective action from the classical SU(2) WZNW model, which corresponds to the SU(2) sector of $\mathrm{AdS}_3 \times \mathrm{S}^3$ with pure NSNS flux. We begin with the Polyakov action on $\mathrm{R} \times \mathrm{S}^3$ with pure NSNS flux, where R is the time-like direction of AdS_3 at the centre of the global coordinate system. Our approach builds on [44, 57], just as subsection 5.1.1. In subsection 5.2.2, we derive the effective action from

[8] Path integrals alike (5.39) have been constructed for the partition function spin chains in the bibliography; see, for instance, the textbook reference [186]. The partition function, defined under a Wick rotation, reads $Z = \lim_{T\to\infty} \operatorname{tr} \exp(-TH)$. The path integral of Z extends over $\vec{n}$ that are periodic not only in x but also in t. Periodicity quantises the coefficient of the WZ term. Our approach differs because the starting point is transition amplitude between two states rather the partition function.

[9] In a sense, the wave functions act as sources at $t = \pm\infty$ of the semi-classical solutions to (5.39), since Ψ_1 determines the energy of the system. This point of view makes hints at an analogy with closed-superstring vertex operators $\mathrm{AdS}_5/\mathrm{CFT}_4$ correspondence [13–15];see subsection 1.1.1).

the SU(2) sector the spin chain of [110] along the lines of subsection 5.1.2, but we keep the global phase of coherent states. We omit the steps that parallel closely those of section 5.1.

5.2.1 The effective action from the classical action on $\mathbf{R} \times \mathbf{S}^3$

The first step is the identification of fast and slow target-space coordinates. We use the Hopf fibration of AdS_3 and S^3 as in subsection 5.1.1. We have argued in subsection 5.1.1 the fast coordinate of AdS_3 is t in (C.6). The coordinate t parameterises time-like direction $\mathrm{R} \subset \mathrm{AdS}_3$ along the centre of the global coordinate system (C.6). We perform the truncation to $\mathrm{R} \times \mathrm{S}^3$ by setting $\rho = 0$ in (C.6) and (5.2). The base space H_2 collapses into a point.

We must identify the fast coordinate along the space-like direction of S^3. As we have already anticipated in subsection 5.1.1, the Hopf fibration makes manifest the fibre-bundle structure of S^3, whereby S^2 is the base space and S^1 the fibre. The gauge group of the bundle is U(1). If we use the embedding coordinates (C.2) of S^3, the Hopf fibration corresponds to

$$X^1 + \mathrm{i}\, X^2 = \mathrm{e}^{\mathrm{i}\,\phi}\, R_1 \ , \quad X^3 + \mathrm{i}\, X^4 = \mathrm{e}^{\mathrm{i}\,\phi}\, R_2 \ . \tag{5.42}$$

The coordinate ϕ is the fast coordinate that we have used in subsection 5.1.1; ϕ parameterises the fibre S^1. On the other hand, R_a are complex coordinates subject to $\overline{R_1}R_1 + \overline{R_2}R_2 = 1$. The action of U(1) on ϕ and R_a is $\phi \mapsto \phi + \chi$ and $R_a \mapsto \exp(-\mathrm{i}\,\chi)R_a$. Since the action of U(1) preserves the constraint of R_a, they parameterise S^2. By definition, R_a are slow.

The effective action that we obtain in subsection 5.2.2 is written in the global coordinate chart (C.10) of S^3. We need to identify ϕ and R_a in (C.10). The action of U(1) nonetheless obstructs a direct identification. We overcome the ambiguity by imposing the compatibility between the static gauge-fixing condition and the light-cone gauge-fixing condition of [110]. We have already stated in subsection 5.1.1 that the light-cone gauge-fixing condition for ϕ reads $p_\phi = J/2\pi$. (Recall that p_ϕ denotes the canonically conjugate momentum of ϕ and J denotes the total angular momentum.) Invariance under shifts of ϕ of the Polyakov action must be provide to J via the Noether theorem. We conclude

$$\phi = \frac{\varphi_1 + \varphi_2}{2} \ , \quad R_1 = \mathrm{e}^{\mathrm{i}\,\zeta} \cos\theta \ , \quad R_2 = \mathrm{e}^{-\,\mathrm{i}\,\zeta} \cos\theta \ , \tag{5.43}$$

where $\zeta = (\varphi_1 - \varphi_2)/2$. The coordinates θ and ζ are slow. The identification (5.43) was also introduced in [44, 52, 101]. We note that ϕ in subsection 5.1.1 parameterises an equator S^1 in S^3. This case corresponds to $\theta = 0$, where φ_2 in not defined and ϕ equals φ_1.

We begin with the derivation of the effective action. The starting point is the Polyakov action on $\mathrm{R} \times \mathrm{S}^3$ with pure NSNS flux. The metric in the global coordinate system is (C.13); the B-field is (C.20) with $q = 1$. If we introduce (5.43) in (C.13) and (C.20), we are led to the Lagrangian

$$\begin{aligned} L = -\,\frac{k}{4\pi} \Big[\, & \gamma^{\alpha\beta}(-\partial_\alpha t \partial_\beta t + \partial_\alpha\phi\partial_\beta\phi + 2\cos{(2\theta)}\,\partial_\alpha\phi\partial_\beta\zeta + \partial_\alpha\zeta\partial_\beta\zeta + \partial_\alpha\theta\partial_\beta\theta) \\ & - 4\epsilon^{\alpha\beta}\sin^2\theta\partial_\alpha\phi\partial_\beta\zeta \,\Big] \ , \end{aligned} \tag{5.44}$$

where we have used (2.41) with $q = 1$, and we have replaced $h_{\alpha\beta}$ by the unimodular world-sheet metric $\gamma_{\alpha\beta} = h_{\alpha\beta}/\sqrt{-h}$. The coordinates t and ϕ in (5.44) satisfy the periodic boundary conditions (5.4). The coordinates θ and ζ in (5.44) also satisfy the periodic boundary conditions:

$$\theta(\tau,\sigma+2\pi)=\theta(\tau,\sigma)\ ,\quad \zeta(\tau,\sigma+2\pi)=\zeta(\tau,\sigma)+2\pi l\ , \tag{5.45}$$

where $l \in \mathrm{Z}$ is a winding number.

We must impose the static gauge-fixing condition to the fast coordinates. The steps parallel subsection 5.1.1. First, we look for an static gauge-fixing condition for ϕ equivalent to $p_\phi = J/2\pi$, where the total angular momentum reads

$$J=-\frac{k}{2\pi}\int_0^{2\pi}\mathrm{d}\sigma[\gamma^{\tau\alpha}(\partial_\alpha\phi+\cos(2\theta)\partial_\alpha\zeta)-2\sin^2\theta\partial_\sigma\zeta]\ . \tag{5.46}$$

We perform a formal T-duality to convert ϕ into $\widehat{\phi}$. We follow the Buscher procedure, which prescribes the introduction of the world-sheet one-form A via (5.7). The equations of motion for A are solved by

$$A_\alpha=-\epsilon_{\alpha\beta}\gamma^{\beta\gamma}(\partial_\gamma\widehat{\phi}-2\sin^2\theta\partial_\gamma\zeta)-\cos{(2\theta)}\,\partial_\alpha\zeta\ . \tag{5.47}$$

Note that (5.47) is always invertible because the Killing vector along the direction of ϕ has not fixed points. Equation (5.47) leads us to the Lagrangian

$$\begin{aligned}L=-\frac{k}{4\pi}\Big[\,&\gamma^{\alpha\beta}(-\partial_\alpha t\partial_\beta t+\partial_\alpha\widehat{\phi}\partial_\beta\widehat{\phi}-4\sin^2\theta\partial_\alpha\widehat{\phi}\partial_\beta\zeta+4\sin^2\theta\partial_\alpha\zeta\partial_\beta\zeta+\partial_\alpha\theta\partial_\beta\theta)\\&+2\epsilon^{\alpha\beta}\cos{(2\theta)}\,\partial_\alpha\widehat{\phi}\partial_\beta\zeta\,\Big]\ .\end{aligned} \tag{5.48}$$

The B-field in (5.44) does not affect the WZ term in (5.48), which is introduced by the formal T-duality [44,51]. If we use (5.47) in (5.46), we obtain (5.9). We conclude that $p_\phi = J/2\pi$ is equivalent to $\widehat{\phi} = (J/k)\sigma$. Our discussion of subsection 5.1.1 also allows us to state that k/J is a sensible effective coupling in the semi-classical limit, and that we must set $t = (J/k)\tau$. The static gauge-fixing condition is then (5.10). The pair t and $\widehat{\phi}$ parameterise the temporal and spatial directions of the spin chain in the continuum limit, respectively.

We write the equations of motion of (5.48) under the static gauge-fixing condition (5.10) now. These equations of motion, analogously to (5.11)–(5.14), provide us with means to validate the equations of motion of the effective action. They read

$$\frac{J}{k}\partial_\alpha\gamma^{\alpha\tau}=0\ , \tag{5.49}$$

$$\frac{J}{k}\partial_\alpha\gamma^{\alpha\sigma}-\partial_\alpha(2\sin^2\theta\gamma^{\alpha\beta}\partial_\beta\zeta+\cos(2\theta)\epsilon^{\alpha\beta}\partial_\beta\zeta)=0\ , \tag{5.50}$$

$$\frac{J}{k}[-\partial_\alpha\gamma^{\alpha\sigma}+\sin(2\theta)(\dot{\theta}-\gamma^{\sigma\alpha}\partial_\alpha\theta)]+2\partial_\alpha(\sin^2\theta\gamma^{\alpha\beta}\partial_\beta\zeta)=0\ , \tag{5.51}$$

$$\frac{J}{k}\sin(2\theta)(\dot{\zeta}-\gamma^{\sigma\alpha}\partial_\alpha\zeta)-\frac{1}{2}\partial_\alpha(\gamma^{\alpha\beta}\partial_\beta\theta)+\sin(2\theta)\gamma^{\alpha\beta}\partial_\alpha\zeta\partial_\beta\zeta=0\ \ , \tag{5.52}$$

where $v^\theta = \gamma^{\tau\alpha}\partial_\alpha\theta$ and $v^\zeta = \gamma^{\tau\alpha}\partial_\alpha\zeta$ are the generalised velocities of θ and ζ, respectively. Equations (5.49)–(5.52) involve terms that are multiplied by J/k and terms that are not. The consistency with the series in the effective coupling k/J demands both sets of equations to be satisfied separately. Equation (5.49) and (5.50) imply $\gamma^{\alpha\beta} = \eta^{\alpha\beta} + \mathrm{O}(k/J)$. Equations (5.51) and (5.52) imply $\dot{\theta} - \theta' = \mathrm{O}(k/J)$ and $\dot{\zeta} - \zeta' = \mathrm{O}(k/J)$, respectively (unless either $\theta = 0$ or $\theta = \pi/2$). The generalised velocities v^θ and v^ζ are not suppressed by k/J. They are suppressed in the combination with θ' and ζ'. The appearance of θ' and ζ' is due to the NSNS flux in $\mathrm{R} \times \mathrm{S}^3$.

The next step is to reduce the action of (5.48) to a NG form with a WZ term. If we replace $\gamma^{\alpha\beta}$ by $\sqrt{-h}h^{\alpha\beta}$ in (5.48), and we use (2.51) and (5.10), we obtain

$$S = \frac{k}{2\pi}\int_{-\infty}^{\infty} \mathrm{d}\tau \int_0^{2\pi} \mathrm{d}\sigma \left(\frac{J}{k}\cos(2\theta)\,\dot{\zeta} - \sqrt{-h}\right) , \tag{5.53}$$

where

$$\begin{aligned} h = &-\frac{J^4}{k^2} + 4\frac{J^3}{k^3}\sin^2\theta\zeta' - \frac{J^2}{k^2}[-\dot{\theta}^2 + \theta'^2 + 4\sin^2\theta(-\cos^2\theta\dot{\zeta}^2 + \zeta'^2)] \\ &- 4\frac{J}{k}\sin^2\theta\zeta'(\dot{\theta}\zeta' - \theta'\dot{\zeta}) + 4\sin^2\theta(\dot{\theta}\zeta' - \theta'\dot{\zeta})^2 . \end{aligned} \tag{5.54}$$

The expression (5.54) is arranged with respect to J/k. Moreover, $\sqrt{-h}h^{\alpha\beta} = \eta^{\alpha\beta} + \mathrm{O}(k/J)$, consistently with (5.49) and (5.50).

If we perform a series in (5.53) with respect to k/J, we obtain

$$S = \frac{J}{2\pi}\int_{-\infty}^{\infty} \mathrm{d}\tau \int_0^{2\pi} \mathrm{d}\sigma (\cos(2\theta)\,\dot{\zeta} + 2\sin^2\theta\zeta') , \tag{5.55}$$

where we have omitted a divergent constant contribution of the fast coordinate and terms at $\mathrm{O}(k/J)$. The effective action (5.55) corresponds to a SU(2) spin-chain σ-model and matches (5.65) of subsection 5.2.2. The effective action (5.55) matches the limit of pure NSNS flux of (4.9) in [101] under the identification of θ and ζ in (5.55) with $\pi/2 - \theta$ and β in (4.9) of [101], respectively, and the replacement of τ and σ by $t = (J/k)\tau$ and $\widehat{\phi} = (J/k)\sigma$ as local world-sheet coordinates in (5.55). The equations of motion of (5.55) are chiral:

$$\sin(2\theta)(\dot{\theta} - \theta') = 0 , \tag{5.56}$$

$$\sin(2\theta)(\dot{\zeta} - \zeta') = 0 , \tag{5.57}$$

consistently with (5.50) and (5.51). The general solution to (5.56) and (5.57) are 'left-moving waves':

$$\theta(\tau,\sigma) = \theta(\tau+\sigma) , \tag{5.58}$$

$$\zeta(\tau,\sigma) = \zeta(\tau+\sigma) . \tag{5.59}$$

The classical solution (5.56) and (5.57) are endowed with the boundary conditions (5.45). The boundary conditions of ϕ in equation (5.4) imposes the additional constraint

$$2\pi n = -\int_0^{2\pi} \mathrm{d}\sigma\cos(2\theta)\zeta' . \tag{5.60}$$

Formulae (5.58) and (5.59) encompass the semi-classical limit of classical solutions that are reproducible from the spin chain. We refer to section 4 of [101] for examples, namely spinning strings and dyonic giant magnons.

5.2.2 The effective action from the spin chain in the SU(2) sector

We derive the effective action from the SU(2) sector of the spin chain proposed in [110] now. Except for the ansatz of coherent states, the derivation of the effective action from the transition amplitude is identical to that of subsection 5.1.2. Therefore, we omit some steps.

We recall that the exact Bethe equations of [110] encode the admissible momenta of magnons in the spin chain. Magnons are created by oscillators above the BMN vacuum, the ground state of the spin chain. The dispersion relation of the magnons is given by the shortening condition (5.23). We truncate the spin chain to the SU(2) sector; the truncation is consistent in the strong-coupling limit $k \to \infty$. Two SU(2) sectors are present in the spin chain: the left-handed sector $\mathrm{SU}(2)_L$ and the right-handed sector $\mathrm{SU}(2)_R$. Single magnons that transform under $\mathrm{SU}(2)_L$ correspond the eigenvalue $m = 1$ of M in (5.23). Single magnons that transform under $\mathrm{SU}(2)_R$ correspond to $m = -1$ of M in (5.23). The BMN vacuum satisfies $m = 0$. We restrict ourselves to the $\mathrm{SU}(2)_L$ sector for definiteness. Finally, the number sites is J. In the w-th spectrally flowed sector, J satisfies the unitarity bound (5.24).

We present the coherent states that permit to construct the spin-chain σ-model now. Coherent states of the spin chain equal the tensor product of J copies one-site coherent states. We construct one-site coherent states following the Perelomov procedure, as in subsection 5.1.2. We need a group, a representation and a reference state.

The group is SU(2). The unitary irreducible representations of SU(2) are finite-dimensional. We postulate that one-site coherent states belong to the $s = 1/2$ fundamental representation of SU(2), which is realised in each one-site Hilbert space $\mathcal{H}_a$, with $a = 1, ..., J-1$. Our ansatz is supported by the agreement between (5.55) and the effective action (5.65). We assume the existence of a mapping between coherent states and states in the world-sheet CFT_2 of the $\mathrm{PSU}(1,1|2)$ WZNW model in parallel to subsection 5.1.1. Moreover, the isotropy group of each of the two states in the basis of $\mathcal{H}_a$ is the same. Hence, either state can be the reference state. Let $|1\rangle$ and $|2\rangle$ constitute a basis of $\mathcal{H}_a$. We assign the role of reference state to $|1\rangle$.

One-site coherent states are unambiguously determined and read

$$|\vec{n}_a\rangle = \mathrm{e}^{-\mathrm{i}\,\chi_a}(\mathrm{e}^{-\mathrm{i}\,\zeta_a}\cos\theta_a\,|1\rangle + \mathrm{e}^{\mathrm{i}\,\zeta_a}\sin\theta_a\,|2\rangle)\ . \tag{5.61}$$

As opposed to the one-site coherent states of subsection 5.1.1 (see (5.25)), the state (5.61) keeps the global phase χ_a. The range of the global phase is $\chi_a \in [0, 2\pi)$. The global phase maps to the U(1)-valued gauge field in the final effective action under the LL limit. We use χ_a to retrieve (5.55). On the other hand, θ_a and ζ_a are the discrete counterparts of θ and ζ in (5.43), whose range share. The pair θ_a and ζ_a matches the pair θ and ζ under the application of the LL limit. Finally, we have introduced the short-hand notation $\vec{n}_a$ to label one-site coherent states. The vector $\vec{n}_a$ is defined by

$$\vec{n}_a = \exp(\mathrm{i}\,\chi_a)[\sin(2\theta_a)\cos(2\varphi_a), \sin(2\theta_a)\sin(\varphi_a), \cos(2\theta_a)]\ , \tag{5.62}$$

which labels the one-site coherent state. The components between square brackets, which form a real vector, are build on the expectation value of the generators of $\mathfrak{su}(2)$ in (5.61). The additional global phase to (5.62) in order to account for χ_a in (5.61).

General coherent states in the Hilbert space of the spin chain $\mathcal{H} = \mathcal{H}_0 \otimes ... \otimes \mathcal{H}_{J-1}$ have the form (5.27), where $\vec{n}_0$ is identified with $\vec{n}_J$ to provide closed-string boundary conditions in the continuum limit. We identify the BMN vacuum with the tensor product of J copies of $|1\rangle$. Coherent states form an overcomplete basis of $\mathcal{H}$. Thus, it provide the resolution of the identity in $\mathcal{H}$ alike (5.28). Coherent states are not orthonormal, but satisfy

$$\langle \vec{n} | \vec{n}' \rangle = \prod_{a=0}^{J-1} \mathrm{e}^{\mathrm{i}(\chi_a - \chi'_a)} \left(\mathrm{e}^{\mathrm{i}(\zeta_a - \zeta'_a)} \cos\theta_a \cos\theta'_a - \mathrm{e}^{-\mathrm{i}(\zeta_a - \zeta'_a)} \sin\theta_a \sin\theta'_a \right) . \tag{5.63}$$

The coherent states that we have postulated permit to obtain the effective action under the application of the LL limit. The steps are the formally same to those in subsection 5.2.2, and the only difference is introduced by (5.63). For this reason, we do not detail the derivation, but offer a summary instead.

The starting point is the transition amplitude Z in (5.30) between the initial state $|\Psi_1\rangle$ and the final state $\langle\Psi_2|$. We assume that $|\Psi_1\rangle$ is a magnon. We assume that $|\Psi_1\rangle$ is chiral. Hence, the dispersion relation is $E = ((k/2\pi)p + m)$. We then restore the momentum operator in Z, we slice the interval of the time coordinate, and we insert the resolution of the identity over coherent state between consecutive time subintervals. The resultant expression involves the clockwise shift operator, which implies that the temporal and spatial step length are proportional through (5.34). The next step is the application of the LL limit that we have discussed in subsection 5.1.2. The LL limit is a synchronised continuum limit in the temporal and spatial intervals of the spin chain. The LL limit is furthermore semi-classical because it implies $J \sim k \to \infty$. The unitarity bound in the w-th spectrally flowed sector is rephrased as (5.37). The LL limit leads us to the path-integral representation of Z, which is of the form (5.39). Finally, if we perform the change of variables that we have introduced in (5.40), we obtain the effective action.

The effective action reads

$$S = \frac{J}{2\pi} \int_{-\infty}^{\infty} \mathrm{d}\tau \int_0^{2\pi} \mathrm{d}\sigma [\dot{\chi} + \cos(2\theta)\dot{\zeta} - (\chi' + \cos(2\theta)\zeta')] . \tag{5.64}$$

The pair τ and σ, which parameterise the temporal and spatial intervals of the continuous spin chain, match the homonymous world-sheet coordinates in (5.55). The fields $\chi = \chi(\tau, \sigma)$, $\zeta = \zeta(\tau, \sigma)$, and $\theta = \theta(\tau, \sigma)$ are the continuous counterpart of the coordinates of coherent states that follow from (5.61). The pair ζ and θ matches the pair of homonymous target-space coordinates in (5.55). On the contrary, χ lacks a parallel in (5.55).

The field χ is a U(1)-valued gauge field. The field χ accounts for redundancy in the global phase of one-site coherent states (5.61). We can identify χ with the gauge field associated to the WZ term in the action (5.53). If we integrate $\dot{\chi}$, we obtain $\chi(\pm\infty, \sigma)$. If assume that the fields decay fast enough at $\tau = \pm\infty$, we can set $\chi(\pm\infty, \sigma) = 0$. On the contrary, we cannot ignore χ', whose integration leads to $\chi(\tau, 2\pi) - \chi(\tau, 0)$. The term $\chi(\tau, 2\pi) - \chi(\tau, 0)$ contributes to the angular momenta of dyonic giant magnons, which follow from the aperiodic limit of periodic classical solutions [191–193]. Since dyonic giant magnons are solitons over the BMN vacuum, we must fix χ' in such a way that the angular momenta of dyonic giant magnons are finite. Reference [101] proved that finiteness holds if and only if $\chi' = -\zeta'$.

If we impose $\chi' = -\zeta'$, we obtain

$$S = \frac{J}{2\pi}\int_{-\infty}^{\infty} \mathrm{d}\tau \int_0^{2\pi} \mathrm{d}\sigma (\cos(2\theta)\dot{\zeta} + 2\sin^2\theta\zeta') \ , \tag{5.65}$$

which matches the action of the SU(2) spin-chain σ-model (5.55). We note that (5.65) is based on the assumption that $|\Psi_1\rangle$ is a chiral magnon. If $|\Psi_1\rangle$ had been anti-chiral, we would have obtained (5.65) up to the replacement $\zeta' \mapsto -\zeta'$. This change trades (5.58) and (5.59) by 'right-moving waves'. The chirality of the magnon then maps to the chirality of classical solutions in the SU(2) spin-chain σ-model.

Chapter 6

Conclusions and outlook

In this thesis, we have analysed bosonic strings on $\mathrm{AdS}_3 \times \mathrm{S}^3$ with NSNS flux. We have adapted different approaches that were applied to the $\mathrm{AdS}_5/\mathrm{CFT}_4$ correspondence in the semi-classical limit of $\mathrm{AdS}_5 \times \mathrm{S}^5$. We have obtain results on the semi-classical limit of type IIB superstring theory on $\mathrm{AdS}_3 \times \mathrm{S}^3 \times \mathrm{T}^4$ with mixed RR and NSNS flux, and with pure NSNS flux. Our results should shed light on the $\mathrm{AdS}_3 \times \mathrm{S}^3 \times \mathrm{T}^4$ background and the $\mathrm{AdS}_3/\mathrm{CFT}_2$ correspondence, and they open various research lines that comment on hereunder.

In chapter 3, we have analysed pulsating strings on $\mathrm{AdS}_3 \times \mathrm{S}^1$ with NSNS flux. We have constructed classical solutions. In the limit of pure NSNS flux, we have recovered the short-string and long-string classes of [93]. We have computed (3.47), the dispersion relation of pulsating strings in the mixed-flux regime in a closed form, which extends to the mixed-flux regime the dispersion relation of [93]. To write (3.47), we have used the frequency of pulsating strings α instead of the conventional semi-classical adiabatic invariant N. We have argued that α is a sensible closed-string modulus. If α is a sensible closed-string modulus when $\lambda \to \infty$, then (3.47) provides data to determine dressing phase of $\mathrm{AdS}_3 \times \mathrm{S}^3 \times \mathrm{T}^4$ with mixed RR and NSNS flux [102–104,106], in particular at tree level [70]. Moreover, it may be possible to use (3.47) to make precise statement in the $\mathrm{AdS}_3/\mathrm{CFT}_2$ correspondence, in parallel with the duality between $\mathcal{N} = 4$ SYM theory and type IIB superstring theory on $\mathrm{AdS}_5 \times \mathrm{S}^5$.

Based on advances made on the $\mathrm{AdS}_5/\mathrm{CFT}_4$ correspondence, [1] [P2] analysed quantum fluctuations around classical solutions in $\mathrm{AdS}_3 \times \mathrm{S}^3 \times \mathrm{T}^4$ in the mixed-flux regime, in particular around the spinning strings of [143]. Reference [P2] proved that the one-loop energy in the mixed-flux regime is finite in the semi-classical limit ($J \sim \sqrt{\lambda} \to \infty$ with λ/J^2 large), but did not manage to obtain an analytical expression. Reference [P2] also proved that one-loop energy vanishes in the limit of pure NSNS flux and argued that the vanishing also holds for the more general spinning strings of [144]. The reason for the computation of the one-loop energy of classical solutions is that it provides data to determine the dressing phase at one-loop [77]. The results of [P2] raise the question of whether quantum corrections around the pulsating strings with NSNS flux of chapter 3 are more manageable. To compute the one-loop energy, one could follow the parallel computation of [195] for pulsating strings in $\mathrm{AdS}_5 \times \mathrm{S}^5$.

[1] The analysis of quantum fluctuations around classical solutions on $\mathrm{AdS}_5 \times \mathrm{S}^5$ was pioneered in [22, 30, 35, 136]. We refer to [194] for a review of the topic and a complete set of references. Moreover, we refer to [143] for the computation of the one-loop energy of the BMN vacuum in the mixed-flux regime.

Pulsating strings of chapter 3 nonetheless have features that demand the adaptation of the steps of [195], namely the use α instead of N, the mixture of RR and NSNS fluxes, and quantum fluctuations along the T^4-directions, which give rise to massless excitations.

In chapter 4.1, we have analysed annular minimal surfaces on Euclidean AdS_3 with NSNS flux. We have constructed connected and disconnected classes of minimal surfaces in the mixed-flux regime. We have proved that the ratio of the radii R in (4.16) determines whether connected minimal surfaces exist, and that disconnected minimal surfaces exist for every R. We have also computed the regularised on-shell action S' in (4.3). Formula (4.3) vanishes for disconnected minimal surfaces due to our choice of regularisation. By analogy with Wilson loops in $\mathcal{N} = 4$ SYM theory, one could expect that (4.3) specifies the strong-coupling limit through the $\mathrm{AdS}_3/\mathrm{CFT}_2$ correspondence. There are different lines of research that could help to clarify both the status of minimal surfaces themselves and their duals.

First, the analysis of phase transitions. If more than one classical solution exists for given Dirichlet boundary conditions, the application of the steepest-descent approximation to the open-superstring partition function selects the minimal surface whose S' is lower. The situation in the limit of pure RR flux is the following [64, 138, 169]. Recall first that there exist two connected minimal surfaces for each R in (4.16). Given R, one of the two connected minimal surfaces always have the greatest S'. Therefore, it is not preferential. Whether the alternative connected minimal surface or the disconnected minimal surface predominates depends on R. If R is small, $S' < 0$, and connected minimal surface prevail. If R is large enough (but lower than the maximum R_+), $S' > 0$, and disconnected minimal surface prevail instead. The change of connectedness of the predominant minimal surface is the Gross-Ooguri first-order phase transition [169]. The extension of the phase transition under NSNS flux should be more involved. The reasons are that either one or two connected minimal surfaces exist for each R and that the NSNS flux widens the range of R where connected minimal surfaces exist.

Second, the analysis of quantum fluctuations around minimal surfaces. In the $\mathrm{AdS}_5/\mathrm{CFT}_4$ correspondence, minimal surfaces in Euclidean $\mathrm{AdS}_5 \times \mathrm{S}^5$ drive the expectation value of dual Wilson loops at leading order when $\lambda \to \infty$. Quantum fluctuations around classical solutions provide the subleading order through the one-loop effective action Γ_1. [2] Reference [P5] analysed quantum fluctuations around the deformation of the circular minimal surface by NSNS flux of chapter 4. Gaussian integration in the path integral of the partition function eventually reduces quantum fluctuations to a set of functional determinants of differential operators that provide Γ_1. In the mixed-flux regime, the computation of the functional determinants of [P5] involves the following steps. First, the conformal transformations that permits to define differential operators with respect to a flat inner product. The NSNS flux entirely factorises in the remnant and cancels due to Weyl invariance [136]. [3] Then, the computation of functional determinants through the Gel'fand-Yaglom method [167], the Abel-Plana formula [198], and

[2] The systematic analysis of quantum corrections to minimal surfaces in the $\mathrm{AdS}_5/\mathrm{CFT}_4$ correspondence was initiated in [136]. We refer to [196] for a review of the topic and a complete set of references.

[3] Reference [197] argues that the NSNS flux does not factorises, and, thus, the NSNS flux affects Γ_1. However, [197] seems to disregard the conformal anomaly.

the regularisation of [199]. The result, which coincides in the limit of pure RR flux and in the mixed-flux regime, is $\Gamma_1 = -\log\sqrt{2\pi}$. The heat kernel bears this result out [200]. In the limit of pure NSNS flux limit, [P5] argued that Γ_1 trivialises due to the adhesion to the boundary of Euclidean AdS_3. It would be interesting to extend the computation of Γ_1 in [P5] to the annular minimal surfaces of chapter 4. (The computation of Γ_1 for annular minimal surfaces in $\mathrm{AdS}_5 \times \mathrm{S}^5$ was performed in [138].) Since the NSNS flux does not factorise any more, it must explicitly affect functional determinants. Moreover, [P5] assumed Dirichlet boundary conditions for massless fermionic fluctuations. Another research line that is worth considering is the computation of functional determinants with other boundary conditions for massless fermionic fluctuations. Alternative boundary conditions have proved to be adequate in the $\mathrm{AdS}_4/\mathrm{CFT}_3$ correspondence [201, 202]. In addition, a stability analysis that parallels, for instance, [203] would be worth pursuing.

Moreover, we have proved that connected minimal surfaces on Euclidean AdS_3 fall into two classes separated by a threshold in the limit of pure NSNS flux. The organisation is analogous to that of pulsating strings in short-string and long-string representations. The parallelism is supported by the local spectral curves of minimal surfaces and pulsating strings, which can be mapped between them. This fact illustrates that classical solutions and elliptic curves offer complementary approaches, each of which sheds light on properties that would remain obscured in the other. A question raised by the organisation of pulsating strings and minimal surfaces concerns the local spectral curve of other classical solutions in AdS_3 with NSNS flux. The analysis should determinate whether the local spectral curve of other classical solutions singularises in the limit of pure NSNS flux, and whether two classes separated by a threshold appear. Our analysis of local spectral curves, which are elliptic, is furthermore based on modular functions. It would be interesting to explore the extent to which these modular functions could provide information about other classical solutions. In particular, it is an open question whether modular functions could discriminate special classical solution, in parallel with our analysis of minimal surfaces with $j = 0$ and $j = \infty$ of chapter 4.

In chapter 5, we have constructed the $\mathrm{SL}(2,\mathrm{R})$ and $\mathrm{SU}(2)$ spin-chain σ-models in the semi-classical limit of every spectrally flowed sector of the $\mathrm{PSU}(1,1|2)$ WZNW model. We have computed the associated effective action from both the classical action and the world-sheet spin chain of [109, 110], obtained the same result. Therefore, the quantum world-sheet spin chain directly produces the classical $\mathrm{SL}(2,\mathrm{R})$ WZNW model in the semi-classical limit. The recovery of the WZNW model fact suggests that the spin chain goes beyond the spectral problem analysed in [109, 110]. It may then possible to use the spin chain to compute other quantities of the WZNW model. For instance, [110] noted that the spin chain may permit the computation of the correlation functions of [204]. To clarify the scope of coherent states in the spin chain of [109, 110], some question must be answered.

The construction of the effective action from the spin chain is based on the ansatz for coherent states. We have postulated coherent states (5.25), which belong to the $j = 1/2$ unitary irreducible representation of the principal discrete series of $\mathrm{SL}(2,\mathrm{R})$, and (5.61), which belong to the $s = 1/2$ fundamental representation of $\mathrm{SU}(2)$. We have assumed the existence of the mapping between coherent states in the spin chain and states in the world-sheet CFT_2.

In order for the derivation of chapter 5 to be complete, the explicit mapping between the two sets of states is needed. The answer may rely on coherent states in the world-sheet CFT_2. Coherent states were defined in [205] as eigenstates of the lowering operator at the level $N = 1$ of the current algebra of the $\mathrm{SL}(2, \mathrm{R})$ WZNW model. These coherent states consist of an infinite linear superposition of states. Each state belongs to a different negative level of the current algebra. More precisely, the state at level $-N'$, where $N' \in \mathbb{N}$, follows from the application the rising operator at the level $N = -1$ to the BMN vacuum N' times. Coherent states thus defined minimise the Heisenberg uncertainty relation of a pair of 'position' and 'momentum' operators [205]. (Inequivalent coherent states were constructed in [206], but they do not minimise this relation in general.) To construct the coherent states (5.25), one should endeavour to assemble the coherent states of [205] in states that transform in the aforementioned $j = 1/2$ representation of $\mathrm{SL}(2, \mathrm{R})$. An extension of the coherent states [205] would in fact be necessary to embrace all the spectrally flowed sectors. The relationship between the sets of coherent states of [205] and (5.25) would clarify the completeness of the latter. Analogous considerations hold with respect to coherent states (5.61).

Subleading corrections to the $\mathrm{SL}(2, \mathrm{R})$ and $\mathrm{SU}(2)$ spin-chain σ-models are also important. Even though the lack of a proper characterisation of coherent states forbids computations from the spin chain, it should be still possible to proceed starting from the classical action. To compute subleading corrections, one may follow [44,52]. Canonical perturbation theory in particular would supply a systematic framework to address the task [44]. For the computation to be meaningful, the $\mathrm{SL}(2, \mathrm{R})$ and $\mathrm{SU}(2)$ sectors must be closed at the order being considered.

One may also attempt to construct a fermionic spin-chain σ-model. In the $\mathrm{AdS}_5/\mathrm{CFT}_4$ correspondence, fermionic spin-chain σ-model was constructed in [53, 54, 207–209]. The simplest fermionic sectors of the $\mathrm{PSU}(1, 1|2)$ WZNW model are the four $\mathrm{SU}(1|1)$ sectors [105, 110]. The computation from the classical action bring new challenges [54]. For instance, the imposition of an appropriate gauge-fixing condition for the κ-gauge symmetry of the action, the computation of consistent truncations, and the introduction of field redefinitions to identify slow Grassmann-odd target-space coordinates. In the spin chain, the steps could parallel those of chapter 5. The steps would be the postulation of coherent states in a representation of $\mathrm{SU}(1|1)$, and the subsequent derivation of a semi-classical path integral in the LL limit. Being nilpotent, Grassmann-odd variables may further clarify the LL limit. Again, the complete derivation would require the explicit connection between coherent states and states in the world-sheet CFT_2.

Appendix A

World-sheet conventions

Classical type II superstring theory on a semi-symmetric spaces is realised by a classical non-linear σ-model. Fields in the classical non-linear σ-model are defined over the world-sheet, a two-dimensional manifold embedded in the permutation supercoset. In this appendix, we settle our conventions for the elements of the word-sheet that we use throughout the body of the text. First, we write our conventions for the world-sheet coordinates, the world-sheet metric, and related objects. We then write our conventions for world-sheet differential forms and operations among them- This appendix is especially relevant to chapter 2.

We begin with the world-sheet coordinates. First, we consider a Lorentzian world-sheet. The world-sheet coordinates are:

- The coordinate $\tau = \sigma^0$ along the time-like world-sheet direction.
- The coordinate $\sigma = \sigma^1$ along the space-like world-sheet direction.

We consider an Euclidean world-sheet now. We obtain the world-sheet coordinates by Wick-rotating the coordinates of the Lorentzian world-sheet as $\tau \mapsto -\mathrm{i}\,\tau$ and $\sigma \mapsto \sigma$. We adapt a new nomenclature for the world-sheet coordinates to make the distinction between Lorentzian and Euclidean world-sheets explicit. The Wick-rotated world-sheet coordinates are:

- The coordinate $\tau = \sigma^0$ along the temporal world-sheet direction.
- The coordinate $\sigma = \sigma^1$ along the spatial world-sheet direction.

We can define tensor indices. We introduce lower-case Greek indices, which either run over 0 and 1, or τ and σ. We assume the Einstein summation convention over them.

We list the objects with tensor indices in the world-sheet that we need hereunder. First, we consider a Lorentzian world-sheet with the signature $(-,+)$. We need the following elements:

- The world-sheet metric $h_{\alpha\beta}$.
- The inverse world-sheet metric $h^{\alpha\beta}$.
- The determinant of the world-sheet metric h.
- The unimodular world-sheet metric $\gamma_{\alpha\beta} = h_{\alpha\beta}/\sqrt{-h}$.

- The inverse unimodular world-sheet metric $\gamma^{\alpha\beta} = \sqrt{-h}h^{\alpha\beta}$.
- The skew-symmetric symbol $\epsilon^{\alpha\beta}$ with $\epsilon^{\tau\sigma} = -\epsilon^{\sigma\tau} = 1$.
- The inverse skew-symmetric symbol $\epsilon_{\alpha\beta}$ with $\epsilon_{\tau\sigma} = -\epsilon_{\sigma\tau} = -1$. [1]

We consider an Euclidean world-sheet with the signature $(+,+)$ now. We obtain objects with tensor indices in the world-sheet through the Wick rotation $\tau \mapsto -\mathrm{i}\,\tau$ of the previous objects. The Wick rotation $\tau \mapsto -\mathrm{i}\,\tau$ amounts to the following replacements:

- The replacements $h_{\tau\tau} \mapsto -h_{\tau\tau}$, $h_{\tau\sigma} \mapsto \mathrm{i}\,h_{\tau\sigma}$, and $h_{\sigma\sigma} \mapsto h_{\sigma\sigma}$ in the world-sheet metric.
- The replacements $h^{\tau\tau} \mapsto -h^{\tau\tau}$, $h^{\tau\sigma} \mapsto -\mathrm{i}\,h^{\tau\sigma}$, and $h^{\sigma\sigma} \mapsto h^{\sigma\sigma}$ in the inverse world-sheet metric.
- The replacement $h \mapsto -h$ in the determinant of the world-sheet metric.
- The replacement $\epsilon^{\alpha\beta} \mapsto -\mathrm{i}\,\epsilon^{\alpha\beta}$ in the skew-symmetric symbol.
- The replacement $\epsilon_{\alpha\beta} \mapsto \mathrm{i}\,\epsilon_{\alpha\beta}$ in the inverse skew-symmetric symbol.

The Wick rotation of both $\gamma_{\alpha\beta}$ and $\gamma^{\alpha\beta}$ follows from that of $h_{\alpha\beta}$, $h^{\alpha\beta}$ and h, but we do not need them.

Given σ^α, $\epsilon^{\alpha\beta}$, and $h^{\alpha\beta}$, we can introduce world-sheet differential forms and their operations. First, we consider a Loretzian world-sheet. The elements that we need are:

- The holonomic basis of world-sheet one-forms $\mathrm{d}\sigma^\alpha$.
- The exterior product $\mathrm{d}\sigma^\alpha \wedge \mathrm{d}\sigma^\beta = (\mathrm{d}\sigma^\alpha \otimes \mathrm{d}\sigma^\beta - \mathrm{d}\sigma^\beta \otimes \mathrm{d}\sigma^\alpha)/2$.
- World-sheet zero-forms $A_0 = A$.
- World-sheet one-forms $A_1 = A_\alpha \mathrm{d}\sigma^\alpha = A_\tau \mathrm{d}\tau + A_\sigma \mathrm{d}\sigma$.
- World-sheet two-forms $A_2 = (A_{\alpha\beta}/2)\mathrm{d}\sigma^\alpha \wedge \mathrm{d}\sigma^\beta = A_{\tau\sigma}\mathrm{d}\tau \wedge \mathrm{d}\sigma$
- The exterior product of world-sheet one-forms $A_1 \wedge B_1 = A_\alpha B_\beta \mathrm{d}\sigma^\alpha \wedge \mathrm{d}\sigma^\beta$
- The exterior derivative of world-sheet zero-forms $\mathrm{d}A_0 = \partial_\alpha A \mathrm{d}\sigma^\alpha$.
- The exterior derivative of world-sheet one-forms $\mathrm{d}A_1 = \partial_\alpha A_\beta \mathrm{d}\sigma^\alpha \wedge \mathrm{d}\sigma^\beta$.
- The Hodge dual of world-sheet one-forms $*A_1 = \sqrt{-h}\epsilon_{\alpha\beta}h^{\beta\gamma}A_\gamma \mathrm{d}\sigma^\alpha$, where $*$ is the Hodge-duality operator.

We have omitted trivial items in the list, for instance $A_0 \wedge A_1 = A_0 A_1$ or $\mathrm{d}A_2 = 0$.

We consider a Euclidean world-sheet now. Differential forms are formally invariant under the Wick rotation $\tau \mapsto -\mathrm{i}\,\tau$. The components of differential forms in the holonomic basis transform under the Wick rotation. The Wick rotation $\tau \mapsto -\mathrm{i}\,\tau$ amounts to the following replacements:

[1] Equivalently, we could have introduced the tensor density $\epsilon'^{\alpha\beta} \equiv \epsilon^{\alpha\beta}/\sqrt{-h}$ and its inverse $\epsilon'_{\alpha\beta} \equiv \sqrt{-h}\epsilon_{\alpha\beta}$.

- The replacements $\mathrm{d}\tau \mapsto -\mathrm{i}\,\mathrm{d}\tau$ and $\mathrm{d}\sigma \mapsto \mathrm{d}\sigma$ in the holonomic basis of world-sheet one-forms.
- The replacements $A_\tau \mapsto \mathrm{i}\,A_\tau$ and $A_\sigma \mapsto A_\sigma$ in world-sheet one-forms A_1.
- The replacement $A_{\tau\sigma} \mapsto \mathrm{i}\,A_{\tau\sigma}$ in world-sheet two-forms A_2.
- The replacement $*A_1 \mapsto \mathrm{i}\,{*A_1}$ in the Hodge dual of a world-sheet one-form, that is the Wick rotation of the Hodge duality operator $* \mapsto \mathrm{i}\,*$.

Our conventions imply that the action S transforms as $\mathrm{i}\,S \mapsto -S$ under $\tau \mapsto -\mathrm{i}\,\tau$; see (2.9), (2.35), (2.46), and (2.47).

We close the appendix by commenting on the extension of one-forms on the world-sheet Σ into a three-dimensional manifold B such that $\mathrm{B} = \partial\Sigma$. The extension is necessary to supply the action with three-dimensional WZ terms; see (2.10), (2.35), and (2.46). We consider a Lorentzian Σ first. We introduce the coordinate $\rho \equiv \sigma^2$ on top of $\sigma^0 = \tau$ and $\sigma^1 = \sigma$ to parameterise the additional direction of B. We introduce $\mathrm{d}\rho$ in the holonomic basis of one-forms in B. One-forms in B read $A_1 = A_\tau \mathrm{d}\tau + A_\sigma \mathrm{d}\sigma + A_\rho \mathrm{d}\rho$. The WZ term is built on a three-form alike $A \wedge B \wedge C = A_\alpha B_\beta C_\gamma \mathrm{d}\sigma^\alpha \wedge \mathrm{d}\sigma^\beta \wedge \mathrm{d}\sigma^\gamma$, where $\mathrm{d}\sigma^\alpha \wedge \mathrm{d}\sigma^\beta \wedge \mathrm{d}\sigma^\gamma$ is the totally antisymmetric combination of $\mathrm{d}\sigma^\alpha \otimes \mathrm{d}\sigma^\beta \otimes \mathrm{d}\sigma^\gamma$ (times the combinatorial factor 1/6). If Σ were Euclidean, we would Wick-rotate the Lorentzian WZ term through $\tau \mapsto -\mathrm{i}\,\tau$ to obtain an Euclidean WZ term.

Appendix B

The defining representation of $\mathfrak{su}(1,1|2)$

The $\mathrm{PSU}(1,1|2)_L \times \mathrm{PSU}(1,1|2)_R/\mathrm{SL}(2,\mathrm{R}) \times \mathrm{SU}(2)$ permutation supercoset is the target space of the non-linear σ-model on $\mathrm{AdS}_3 \times \mathrm{S}^3$ with mixed flux. The action of the model can be made explicit in the defining representation of $\mathfrak{su}(1,1|2)_L \oplus \mathfrak{su}(1,1|2)_R$, wherein the supermatrices of $\mathfrak{psu}(1,1|2)_L \oplus \mathfrak{psu}(1,1|2)_R$ are defined. In this appendix, we write the conventions for $\mathfrak{su}(1,1|2)$ and $\mathfrak{psu}(1,1|2)$ that we use in subsection 2.1.2. The appendix is based on section 9 of [125] for the most part.

We start from $\mathfrak{sl}(2|2)$. The superalgebra $\mathfrak{sl}(2|2)$ consists of supertraceless (4×4)-supermatrices of the form

$$M = \begin{bmatrix} A & \Theta_1 \\ \Theta_2 & B \end{bmatrix} , \tag{B.1}$$

where A and B are (2×2)-matrices with complex bosonic (commuting) entries and Θ_1 and Θ_2 are (2×2)-matrices with complex fermionic (anti-commuting) entries. The supertrace is defined by

$$\operatorname{str} M = \operatorname{tr} A - \operatorname{tr} B , \tag{B.2}$$

and, thus, we have $\operatorname{tr} A = \operatorname{tr} B$ for $\mathfrak{sl}(2|2)$.

The defining representation of $\mathfrak{su}(1,1|2)$ is the invariant locus of $\mathfrak{sl}(2|2)$ under the Cartan involution

$$C(M) = -HM^\dagger H , \tag{B.3}$$

where $H = \operatorname{diag}(1,-1,1,1)$ and † denotes the adjoint operation, namely transposition and complex conjugation. The most general Θ_1 and Θ_2 that are invariant under the Cartan involution read

$$\Theta_1 = \begin{bmatrix} \theta_{11} & \theta_{12} \\ \theta_{21} & \theta_{22} \end{bmatrix} , \quad \Theta_2 = \begin{bmatrix} -\theta^*_{11} & \theta^*_{21} \\ -\theta^*_{12} & \theta^*_{22} \end{bmatrix} , \tag{B.4}$$

where * denotes the complex conjugation of fermionic numbers. The most general form of A and B that are invariant under the Cartan involution is

$$A = \begin{bmatrix} A_{11} & A_{12} \\ \overline{A_{12}} & A_{22} \end{bmatrix} , \quad \overline{A_{11}} = -A_{11} , \quad \overline{A_{22}} = -A_{22} , \tag{B.5}$$

$$B = \begin{bmatrix} B_{11} & B_{12} \\ -\overline{B_{12}} & B_{22} \end{bmatrix} , \quad \overline{B_{11}} = -B_{11} , \quad \overline{B_{22}} = -B_{22} , \tag{B.6}$$

where $\bar{\ }$ denotes the complex conjugation of bosonic numbers.

The bosonic truncation of $\mathfrak{su}(1,1|2)$ is obtained by setting to zero the entries of (B.4), which leaves A and B in (B.1). The bosonic truncation of $\mathfrak{su}(1,1|2)$ forms a bosonic subalgebra. Matrices A span $\mathfrak{u}(1,1)$, whereas matrices B span $\mathfrak{u}(2)$. The constraint (B.2) implies $A_{11}+A_{22}=B_{11}+B_{22}$. Therefore, we deduce that the bosonic truncation of $\mathfrak{su}(1,1|2)$ is $\mathfrak{sl}(2,\mathrm{R})\oplus\mathfrak{su}(2)\oplus\mathfrak{u}(1)$. (Note that $\mathfrak{sl}(2,\mathrm{R})\cong\mathfrak{su}(1,1)$.) The $\mathfrak{u}(1)$-subalgebra of $\mathfrak{su}(1,1|2)$ is generated by the identity supermatrix. The Lie superalgebra $\mathfrak{psu}(1,1|2)$ is defined as the quotient of $\mathfrak{su}(1,1|2)$ over this $\mathfrak{u}(1)$-subalgebra. We drop the $\mathfrak{u}(1)$-subalgebra from (B.5) and (B.6) by requiring

$$A_{11}=-A_{22}\ ,\quad B_{11}=-B_{22}\ . \tag{B.7}$$

Matrices A and B then span the defining representations of $\mathfrak{sl}(2,\mathrm{R})$ and $\mathfrak{su}(2)$, respectively. Finally, the Lie superalgebra of the permutation supercoset $\mathfrak{psu}(1,1|2)_L\oplus\mathfrak{psu}(1,1|2)_R$ is built on two copies of $\mathfrak{psu}(1,1|2)$ defined in this way.

Appendix C

Coordinate systems

Our analyses in the body of the text are always performed in specific coordinate systems of $\mathrm{AdS}_3 \times \mathrm{S}^3$ with NSNS flux. In this appendix, we present the coordinate systems that we need chapters 3–5. We first present the embedding coordinates, and write the target-space metric and the RR and NSNS three-form fluxes. Embedding coordinates allow us to relate the different coordinate systems which we eventually use. In the global coordinate system and the Poincaré patch, we write the embedding map g, the left current j, and the metric. We end the appendix by arguing and writting the appropriate B-field in the global coordinate system and the Poincaré patch.

We start from embedding coordinates in $\mathrm{AdS}_3 \times \mathrm{S}^3$. Embedding coordinates are defined through the quadratic form that embeds both AdS_3 and S^3 into their respective flat higher-dimensional space. AdS_3 is the locus of $\mathrm{R}^{2,2}$ defined by

$$-(Y^0)^2 + (Y^1)^1 + (Y^2)^2 - (Y^3)^2 = -1 \ , \tag{C.1}$$

where $Y^A \in (-\infty, \infty)$. S^3 is the locus of R^4 defined by

$$(X^1)^2 + (X^2)^1 + (X^3)^2 + (X^4)^2 = 1 \ , \tag{C.2}$$

where $X^A \in [-1, 1]$. We have set the radii of both AdS_3 and S^3 to one since we have isolated them in front of the Polyakov action via λ (see footnote 4 of chapter 2). If we arrange Y^A and X^A in entries of (2×2)-matrices, it follows from (C.1) and (C.2) that $\mathrm{AdS}_3 \cong \mathrm{SL}(2,\mathrm{R})$ and $\mathrm{S}^3 \cong \mathrm{SU}(2)$. The isomorphism can be alternatively deduced by considering the associated permutation cosets (see subsection 2.1.3).

The metric of AdS_3 is the pull-back by Y^A of (C.1):

$$\mathrm{d}s^2_{\mathrm{AdS}_3} = -(\mathrm{d}Y^0)^2 + (\mathrm{d}Y^1)^1 + (\mathrm{d}Y^2)^2 - (\mathrm{d}Y^3)^2 \ . \tag{C.3}$$

The metric of S^3 is the pull-back by X^A of (C.2):

$$\mathrm{d}s^2_{\mathrm{S}^3} = (\mathrm{d}X^1)^2 + (\mathrm{d}X^2)^2 + (\mathrm{d}X^3)^2 + (\mathrm{d}X^4)^2 \ . \tag{C.4}$$

The RR and NSNS three-form fluxes are the proportional to the sum of the volume forms of AdS_3 and S^3:

$$F = -2\bar{q}\left(\mathrm{vol}_{\mathrm{AdS}_3} + \mathrm{vol}_{\mathrm{S}^3}\right) \ , \quad H = -2q\left(\mathrm{vol}_{\mathrm{AdS}_3} + \mathrm{vol}_{\mathrm{S}^3}\right) \ . \tag{C.5}$$

The orientation of the volume forms does imply any ambiguity because the constraint (2.40) implies $-1 \leq \bar{q}, q \leq 1$. Recall nonetheless that we assume $0 \leq q \leq 1$ and $\bar{q} = \sqrt{1-q^2}$ for conciseness.

We consider the global coordinate system of $\mathrm{AdS}_3 \times \mathrm{S}^3$ now. The global coordinate system is suited to analyse closed-string configurations. The coordinates the maximal Abelian subgroup of both $\mathrm{SL}(2,\mathrm{R})$ and $\mathrm{SU}(2)$ are cyclic in the Polyakov action. Thus, the associated Noether charges have manageable expressions.

The relationship between embedding and global coordinates of AdS_3 is

$$Y^0 = \cosh\rho \sin t \ , \quad Y^1 = \sinh\rho\cos\psi \ , \quad Y^2 = \sinh\rho\sin\psi \ , \quad Y^3 = \cosh\rho\cos t \ , \tag{C.6}$$

where $\rho \in [0,\infty)$, $t \in (-\infty,\infty)$. and $\psi \in [0,2\pi)$. We have decompactified t on account of the definition of AdS_3 as the universal cover of $\mathrm{SL}(2,\mathrm{R})$. The decompactification forbids closed time-like curves: world-sheets cannot wind along the direction of t. The coordinate system (C.6) corresponds to

$$g = \begin{bmatrix} \mathrm{e}^{\mathrm{i}\,t}\cosh\rho & \mathrm{e}^{\mathrm{i}\,\psi}\sinh\rho \\ \mathrm{e}^{-\mathrm{i}\,\psi}\sinh\rho & \mathrm{e}^{-\mathrm{i}\,t}\cosh\rho \end{bmatrix} \ , \tag{C.7}$$

and

$$j = \begin{bmatrix} \mathrm{i}(\cosh^2\rho\mathrm{d}t + \sinh^2\rho\mathrm{d}\psi) & \mathrm{e}^{-\mathrm{i}(t-\psi)}\left[\frac{\mathrm{i}}{2}\sinh(2\rho)\,(\mathrm{d}t+\mathrm{d}\psi) + \mathrm{d}\rho\right] \\ \mathrm{e}^{\mathrm{i}(t-\psi)}\left[-\frac{\mathrm{i}}{2}\sinh(2\rho)\,(\mathrm{d}t+\mathrm{d}\psi) + \mathrm{d}\rho\right] & -\mathrm{i}(\cosh^2\rho\mathrm{d}t + \sinh^2\rho\mathrm{d}\psi) \end{bmatrix} \ . \tag{C.8}$$

Note that (C.8) is a $\mathfrak{sl}(2,\mathrm{R})$-valued one-form because it has the form (B.5) and satisfies (B.7). The metric of AdS_3 reads

$$\mathrm{d}s^2_{\mathrm{AdS}_3} = -\cosh^2\rho\mathrm{d}t^2 + \mathrm{d}\rho^2 + \sinh^2\rho\mathrm{d}\psi^2 \ . \tag{C.9}$$

The conformal boundary of AdS_3 is placed at $\rho = \infty$. We use (C.6) in chapter 3 and section 5.1.1.

The relationship between embedding and global coordinates of S^3 is

$$X^1 = \cos\theta\cos\varphi_1 \, , \quad X^2 = \cos\theta\sin\varphi_1 \, , \quad X^3 = \sin\theta\cos\varphi_2 \, , \quad X^4 = \sin\theta\sin\varphi_2 \, , \tag{C.10}$$

where $\theta \in [0,\pi/2]$ and $\varphi_1, \varphi_2 \in [0,2\pi)$. The coordinate system (C.10) corresponds to

$$g = \begin{bmatrix} \mathrm{e}^{\mathrm{i}\,\varphi_1}\cos\theta & \mathrm{e}^{\mathrm{i}\,\varphi_2}\sin\theta \\ -\mathrm{e}^{-\mathrm{i}\,\varphi_2}\sin\theta & \mathrm{e}^{-\mathrm{i}\,\varphi_1}\cos\theta \end{bmatrix} \ , \tag{C.11}$$

and

$$j = \begin{bmatrix} \mathrm{i}\,(\cos^2\theta\mathrm{d}\varphi_1 - \sin^2\theta\mathrm{d}\varphi_2) & \mathrm{e}^{-\mathrm{i}(\varphi_1-\varphi_2)}\left[\frac{\mathrm{i}}{2}\sin(2\theta)\,(\mathrm{d}\varphi_1+\mathrm{d}\varphi_2)+\mathrm{d}\theta\right] \\ \mathrm{e}^{\mathrm{i}(\varphi_1-\varphi_2)}\left[\frac{\mathrm{i}}{2}\sin(2\theta)\,(\mathrm{d}\varphi_1+\mathrm{d}\varphi_2)-\mathrm{d}\theta\right] & -\mathrm{i}\,(\cos^2\theta\mathrm{d}\varphi_1 - \sin^2\theta\mathrm{d}\varphi_2) \end{bmatrix} \ . \tag{C.12}$$

Note that (C.12) is a $\mathfrak{su}(2)$-valued world-sheet one-form because it has the form (B.6) and satisfies (B.7). The expression metric of S^3 in (C.4) is

$$\mathrm{d}s^2_{\mathrm{S}^3} = \mathrm{d}\theta^2 + \cos^2\theta\mathrm{d}\varphi_1^2 + \sin^2\theta\mathrm{d}\varphi_2^2 \ . \tag{C.13}$$

We use (C.10) in section 3.1 and subsection 5.2.1.

We consider the Poincaré patch now. We do not need the Poincaré patch of AdS_3 but of Euclidean AdS_3. In terms of Y^A, we obtain Euclidean AdS_3 by means of the Wick rotation $Y^0 \mapsto -\mathrm{i}\, Y^0$. The Wick rotation turns (C.1) into the quadratic form embedding the Euclidean AdS_3 in $\mathrm{R}^{3,1}$. As opposed to AdS_3, Euclidean AdS_3 is not a group manifold. [1] The Poincaré patch is suited to analyse open-string configurations. Open-string configurations are endowed with Dirichlet boundary conditions at the conformal boundary of Euclidean AdS_3. Unlike (the Euclidean counterpart of) the global coordinate system (C.6), the Poincaré patch locates the conformal boundary of Euclidean AdS_3 at finite values of their coordinates.

The relationship between embedding coordinates and the Poincaré patch of Euclidean AdS_3 is

$$\begin{aligned} Y^0 &= \frac{x^0}{z} \ , \quad Y^2 = \frac{\left(x^0\right)^2 + \left(x^1\right)^2 + z^2 - 1}{2z} \ , \\ Y^1 &= \frac{x^1}{z} \ , \quad Y^3 = \frac{\left(x^0\right)^2 + \left(x^1\right)^2 + z^2 + 1}{2z} \ , \end{aligned} \tag{C.14}$$

where $x^0, x^1 \in (-\infty, \infty)$, and $z \in (0, \infty)$. The coordinate system does not cover but half the whole space; the complementary Poincaré patch corresponds to (C.14) with $z \in (-\infty, 0)$. The coordinate system (C.14) corresponds to

$$g = \frac{1}{z} \begin{bmatrix} z^2 + \left(x^0\right)^2 + \left(x^1\right)^2 & x^1 + \mathrm{i}\, x^0 \\ x^1 - \mathrm{i}\, x^0 & 1 \end{bmatrix} \ , \tag{C.15}$$

and

$$j = \frac{1}{z^2} \begin{bmatrix} z\mathrm{d}z + \left(x^1 - \mathrm{i}\, x^0\right)\left(\mathrm{d}x^1 + \mathrm{i}\,\mathrm{d}x^0\right) & \mathrm{d}x^1 + \mathrm{i}\,\mathrm{d}x^0 \\ z^2\left(\mathrm{d}x^1 - \mathrm{i}\,\mathrm{d}x^0\right) - \left(x^1 - \mathrm{i}\, x^0\right)^2\left(\mathrm{d}x^1 + \mathrm{i}\,\mathrm{d}x^0\right) & -\left[z\mathrm{d}z + \left(x^1 - \mathrm{i}\, x^0\right)\left(\mathrm{d}x^1 + \mathrm{i}\,\mathrm{d}x^0\right)\right] \end{bmatrix} \ . \tag{C.16}$$

We emphasise that (C.16) is not $\mathfrak{sl}(2,\mathrm{R})$-valued, that is neither has the form (B.6) nor satisfies (B.7). This fact is not contradictory with our construction of subsection 2.1.3 because Euclidean AdS_3 is not a group manifold (see footnote 1 of this appendix). The metric of Euclidean AdS_3 reads

$$\mathrm{d}s^2_{\mathrm{AdS}_3} = \frac{\mathrm{d}z^2 + \left(\mathrm{d}x^0\right)^2 + \left(\mathrm{d}x^1\right)^2}{z^2} \ . \tag{C.17}$$

The global coordinate system (C.6) and the Poincaré patch are related. If we Wick-rotate (C.14) back to the Lorentzian signature , which corresponds to $x^0 \mapsto \mathrm{i}\, x^0$, we obtain

$$\begin{aligned} x^0 &= \frac{\cosh\rho \sin t}{\cosh\rho\cos t - \sinh\rho\sin\psi} \ , \quad x^1 = \frac{\sinh\rho\cos\psi}{\cosh\rho\cos t - \sinh\rho\sin\psi} \ , \\ z &= \frac{1}{\cosh\rho\cos t - \sinh\rho\sin\psi} \ . \end{aligned} \tag{C.18}$$

[1] Euclidean AdS_3 is not a group manifold. The action of the supercoset model cannot be supported with a topologically non-trivial WZ term (see subsection 2.1.2). To overcome the obstruction, we considering that the supercoset model on Euclidean AdS_3 is the analytic continuation of its Lorentzian counterpart. The analytic continuation is introduced at the expense of complex-valued fields. We refer to subsection 7.3 of [92] for a discussion.

The conformal boundary of Euclidean AdS_3 is located at $z = 0$. We use (C.10) in chapter 4.

We turn our attention to the B-field now. The B-field in a given coordinate system is not unambiguously determined. Any B-field whose exterior derivative equals H in (C.5) is, in principle, admissible. The B-field is defined modulo a gauge ambiguity, that is the addition of an exact two-form. The redundancy is ignorable in the action of closed-string configurations: periodic boundary conditions erases the contribution of the exact two-form. However, the ambiguity in the definition of the B-field matters in the action of open-string configurations. The definition also matters for dyonic giant magnons, introduced in [191–193], which are aperiodic limits of periodic classical solutions. The exact two-form contributes in the action through boundary terms, and, thus, it contributes to the Noether charges. In section 4.2, we exclude boundary terms by demanding that they vanish at the boundary of the open-string world-sheet. The condition imposes gauge invariance to the action with respect to the B-field on the open-string world-sheet. We single the proper B-field out in the global coordinate system and the Poincaré patch by three conditions.

First, invariance of the B-field under shifts along the directions on which the target-space metric does not depend. We can impose the condition to (C.6), since (C.9) does not depend on either t or ψ, to (C.10), since (C.13) does not depend on either φ_1 or φ_2, and to (C.14), since (C.17) does not depend on neither x^0 or x^1. Second, the AdS_3-component of the B-field in a given coordinate system must share the behaviour of the metric in the vicinity of the conformal boundary of (Euclidean) AdS_3. This behaviour is controlled by the conformal factor. We can impose the condition since the AdS_3-component of H in (C.5) is proportional to the volume form of AdS_3. The contributions of both target-space metric and the B-field in the vicinity of the boundary of AdS_3 stand on an equal footing. Third, the S^3-component of the B-field in a given chart must yield a finite Noether charges for dyonic giant magnons. The condition accounts for the realisation of dyonic giant magnons as solitons over the BMN vacuum and was derived in [101].

If we choose an orientation for the volume forms of both AdS_3 and S^3, we have the following B-fields. The AdS_3-component of the B-field in the global coordinate system (C.6) is

$$B_{\mathrm{AdS}_3} = q \sinh^2 \rho \mathrm{d}t \wedge \mathrm{d}\psi \ . \tag{C.19}$$

The S^3-component in the global coordinate system (C.10) is

$$B_{\mathrm{S}^3} = -q \sin^2 \theta \mathrm{d}\varphi_1 \wedge \mathrm{d}\varphi_2 \ . \tag{C.20}$$

The Euclidean AdS_3-component of the B-field in the Poincaré patch (C.10) is [2]

$$B_{\mathrm{AdS}_3} = -\,\mathrm{i}\,\frac{q}{z^2} \mathrm{d}x^0 \wedge \mathrm{d}x^1 \ . \tag{C.21}$$

[2]The imaginary unit of (C.21) is cancelled against the imaginary unit of the Wick-rotated $\epsilon^{\alpha\beta}$ (see appendix A). Moreover, our assumptions $\bar{q} = \sqrt{1-q^2}$ and $0 \leq q \leq 1$ from (2.40) holds after the Wick rotation. Neither the proof of invariance under κ-symmetry transformations of the action (2.35) nor of the existence of the Lax connection in (2.57) and (2.58) explicitly involves the signature of the world-sheet metric [88, 102].

Appendix D

Finite-gap equations with mixed flux

The spectral problem of classical integrable non-linear σ-models is encoded in the quasi-momenta. The quasi-momenta are single-valued meromorphic functions of the spectral parameter over the spectral curve. The series of the quasi-momenta around points of the spectral curve generates the infinite hierarchy of (local, multi-local and non-local) conserved charges. The analytic structure of the quasi-momenta determines the closed-superstring moduli, for instance filling fractions and mode numbers. The quasi-momenta admit an integral representation over the density functions. These density functions satisfy a set of linear integral equations called *finite-gap equations*.

The application of spectral curves to the $\mathrm{AdS}_5/\mathrm{CFT}_4$ correspondence was proposed in [58]. Reference [58] constructed the spectral curve to the coset model on $\mathrm{R} \times \mathrm{S}^3$, which is a bosonic truncation of the supercoset model on $\mathrm{AdS}_5 \times \mathrm{S}^5$. The approach of [58] was shortly afterwards applied to other bosonic truncations of $\mathrm{AdS}_5 \times \mathrm{S}^5$: reference [59] constructed the spectral curve in the truncation to $\mathrm{AdS}_3 \times \mathrm{S}^1$, [210] in the truncation to $\mathrm{R} \times \mathrm{S}^5$, and [211] in the truncation to $\mathrm{AdS}_5 \times \mathrm{S}^1$. Reference [60] eventually constructed the spectral curve of the supercoset model on the fully supersymmetric $\mathrm{AdS}_5 \times \mathrm{S}^5$. Since [60] just relied on classical integrability of $\mathrm{AdS}_5 \times \mathrm{S}^5$ (in turn based on its structure of semi-symmetric space), the spectral curve exist in other supercoset models that are relevant to the $\mathrm{AdS}_{d+1}/\mathrm{CFT}_d$ correspondence. Reference [212] wrote the spectral curve of the supercoset model $\mathrm{AdS}_4 \times \mathrm{CP}^3$. Reference [95] constructed the spectral curves in the permutation-supercoset truncations of $\mathrm{AdS}_3 \times \mathrm{S}^3 \times \mathrm{T}^4$ and $\mathrm{AdS}_3 \times \mathrm{S}^3 \times \mathrm{S}^3 \times \mathrm{S}^1$ in the limit of pure RR flux. On the basis of [95], reference [137] presented a uniform framework wherein previous algebraic curves were included together with new ones. Reference [213] discussed the incorporation of an external CFT_2 to the spectral curve of a non-critical semi-symmetric space. We refer to [214] for a review of the spectral curve and the finite-gap equations in the context of the $\mathrm{AdS}_5/\mathrm{CFT}_4$ correspondence. In this appendix, we present the finite-gap equations of $\mathrm{AdS}_3 \times \mathrm{S}^3$ in the mixed-flux regime following the original construction of [102]. We also follow [95, 137, 213] and [126] regarding general considerations on finite-gap equations and Lie superalgebras, respectively.

We begin with a brief presentation of the quasi-momenta of a non-linear σ-model based on a general semi-symmetric space G/H. To obtain the quasi-momenta, we must diagonalise the monodromy matrix M in (2.69). We recall that M is a G_{C}-valued function of the spectral parameter x. We also recall that the conjugacy class of M is invariant under gauge transformations of H and independent of the non-contractible loop that enters in the definition of M. We finally recall that the action of Ω on M follows from (2.54). The set of conjugacy classes of $\mathrm{G}_{\mathbb{C}}$ is isomorphic to the maximal Abelian Lie subgroup of G modulo the action of the Weyl group [95]. If the rank of the Cartan subalgebra of $\mathfrak{g}$ is N and a basis of bosonic generators thereof is H_A, we can diagonalise (2.69) as

$$M = U \exp\left(\sum_{A=1}^{N} p_A H_A\right) U^{-1} \ , \tag{D.1}$$

where p_A are the quasi-momenta and U is $\mathrm{G}_{\mathbb{C}}$-valued function of x.

The quasi-momenta are single-valued meromorphic functions of x over the spectral curve, which is a Riemann surface, that is a compact analytic variety of complex-dimension one. The quasi-momenta have branch cuts over the spectral curve, which consists of various sheets. The branch cuts of p_A arise due to the diagonalisation of M through U, which depends non-trivially on x. The monodromy of p_A across branch cuts is encoded in the action of the Weyl group W and $2\pi\mathbb{Z}$-shifts. We make the customary assumption that the number of branch cuts is finite and assume that the case with an infinite number of branch cuts can be retrieved as a of limit [60]. (*Finite* in *finite-gap equations* stands for this assumption.) The $\mathbb{Z}_4$-automorphism Ω of $\mathfrak{g}$ relates the branch cuts of p_A in different regions of the spectral curve. The action of Ω on p_A follows from the action on Ω on H_A. Since H_A are bosonic, the action of Ω on p_A actually corresponds to a $\mathbb{Z}_2$-automorphism. In addition, p_A have simple poles. Simple poles correspond to essential singularities of M and are induced by the simple poles of the Lax connection L at $x = \infty$, $x = 0$, and $x = \pm 1$ (see (2.55) and (2.56), respectively).

We focus on the permutation-supercoset model on $\mathrm{AdS}_3 \times \mathrm{S}^3$ in the mixed-flux regime now. The target space is (2.20), whose whose Lie superalgebra is $\mathfrak{psu}(1,1|2)_L \oplus \mathfrak{psu}(1,1|2)_R$. This Lie superalgebra has rank six. Hence, we have $N = 6$ quasi-momenta p_A. Lie superalgebras in general possess multiple inequivalent systems of simple root. Therefore, they can be endowed with multiple inequivalent Dynkin diagrams and Cartan matrices. We abide by the conventions of [102] in this appendix. The conventions of [102] lead to finite-gap equations that match the thermodynamic limit of the associated Bethe equations [99]. Our conventions amount to the choice of the Cartan matrix $A' = \sigma^3 \otimes A$ of $\mathfrak{psu}(1,1|2)_L \oplus \mathfrak{psu}(1,1|2)_R$, where σ^3 denotes the third Pauli matrix and

$$A = \begin{bmatrix} 0 & 1 & 0 \\ 1 & -2 & 1 \\ 0 & 1 & 0 \end{bmatrix} \ , \tag{D.2}$$

is the Cartan matrix of $\mathfrak{psu}(1,1|2)$. We emphasise that (D.2) does not correspond to the representation of $\mathfrak{psu}(1,1|2)$ that we present appendix B and use in chapter 2.

We consider the analytic structure of p_A now. We begin with their branch cuts. The monodromy of p_A across the branch cut is encoded in the action of W and $2\pi\mathbb{Z}$-shifts as we have already mentioned. We restrict ourselves to the set of elementary Weyl reflections within W for simplicity. The action of a general element of W is represented by the composition of elementary Weyl reflections. Let $C_{A,n}$ be the set of branch cuts of p_A, with $n = 1, ..., N_A$.

By assumption, $C_{A,n}$ do not intersect for $n = 1, ..., N_A$ and A fixed. We can characterise the discontinuity of p_A across $C_{A,n}$ by a density function $\rho_{A,n}$ with support in $C_{A,n}$:

$$\rho_{A,n}(x) = p_A^{\downarrow}(x) - p_A^{\uparrow}(x) \ , \quad x \in C_{A,n} \ , \tag{D.3}$$

the superscripts $^{\downarrow}$ and $^{\uparrow}$ denote the limit from above and below in the normal direction of $C_{A,n}$, respectively. Moreover, if p_A subject to a monodromy around the end point of $C_{A,n}$, we have

$$p_A \mapsto p_A + \sum_{B=1}^{6} A_{AB} p_B + 2\pi m_{A,n} \ . \tag{D.4}$$

This formula implies that $C_{A,n}$ fall into two classes. If $A_{AA} = \pm 2$, that is the A-th root is bosonic, $C_{A,n}$ is a *square-root* branch cut. If $A_{AA} = 0$, that is the A-th root is fermionic, $C_{A,n}$ is a *simple-pole* branch cut. (See subsection 2.3 of [60] for a detailed discussion.) To write the finite-gap equations, it is convenient to rephrase (D.4) as

$$\frac{1}{2}\sum_{B=1}^{6} A_{AB}(p_B^{\downarrow}(x) + p_B^{\uparrow}(x)) = 2\pi m_{A,n} \ , \quad x \in C_{A,n} \ . \tag{D.5}$$

The Z_4-automorphism Ω relates different p_A at different points of the spectral curve and intertwines $C_{A,n}$ among them. The action of Ω on p_A is induced by the action (2.54) on L and reads

$$\Omega_4(p_A(x)) = p_A(1/x) = \sum_{B=1}^{6} S'_{AB} p_B(x) \ , \tag{D.6}$$

where S squares to the identity matrix. We abide by the conventions of [102] again and choose $S' = \sigma^1 \otimes S$, where σ^1 is the first Pauli matrix and

$$S = \begin{bmatrix} 1 & -1 & 0 \\ 0 & -1 & 0 \\ 0 & -1 & 1 \end{bmatrix} \ . \tag{D.7}$$

By using S', we can focus on p_A over $|x| \geq 1$ because (D.6) relates p_A over $|x| \geq 1$ and $|x| \leq 1$. We can divide $C_{A,n}$ into $C^+_{A,n}$ with $n = 1, ..., N^+_A$, which belong to $|x| \geq 1$, and $C^-_{A,n}$ with $n = 1, ..., N^-_A$, which belong to $|x| \leq 1$. If a given $C_{A,n}$ crosses the circumference at $|x| = 1$, we split it into $C^+_{A,n}$ and $C^-_{A,n}$. We denote the density function with support over $C^{\pm}_{A,n}$ by $\rho^{\pm}_{A,n}$.

In addition, p_A inherit the simple poles of L. The Lax connection has two types of simple poles: the simple pole at $x = \infty$ (and at $x = 0$ by (2.54)), whose residue is (2.60), and the simple poles at $x = s, -1/s$ and $x = -s, 1/s$, whose residues are (2.61) and (2.62), respectively. The residues of p_A at $x = \infty$ are proportional then to the Noether charges (integrals of the Noether current (2.39) along the non-contractible loop that enters in the definition of M). These Noether charges are linear combinations of the energy the angular momenta; see formula (4.11) of [102]. We do not need the Noether charges to write the finite-gap equations however.

We need the simple poles of p_A at $x = \pm s$ and $x = \pm 1/s$. The Lax connection decomposes into L_L and L_R by (2.21); $x = s, -1/s$ are simple poles of L_L and $x = -s, 1/s$ are simple poles of L_R. The residues of L_L and L_R appear in (2.61) and (2.62), respectively. To write the residues of p_A, we need to split the quasi-momenta into two sets. First, the left quasi-momenta $\hat{p}_A = p_A$, with $A = 1, 2, 3$, which have simple poles at $x = -s, 1/s$. Second, the right quasi-momenta $\check{p}_{A-3} = p_A$, with $A = 4, 5, 6$, which have simple poles at $x = -s, 1/s$. (We refer to the objects associated to $\hat{p}_A$ and $\check{p}_A$, for instance branch cuts and densities by using ˆ and ˇ.) To simplify the finite-gap equations, we parameterise the residues as [1]

$$\operatorname*{res}_{x=s}\hat{p}_A = \frac{s}{2}(\hat{a}_A + \hat{b}_A) \ , \quad \operatorname*{res}_{x=-1/s}\hat{p}_A = \frac{1}{2s}(\hat{a}_A - \hat{b}_A) \ , \tag{D.8}$$

$$\operatorname*{res}_{x=-s}\check{p}_A = -\frac{s}{2}(\check{a}_A - \check{b}_A) \ , \quad \operatorname*{res}_{x=-1/s}\check{p}_A = -\frac{1}{2s}(\check{a}_A + \check{b}_A) \ . \tag{D.9}$$

The simple poles do not overlap with the branch cuts by assumption. In addition, both $\hat{p}_A$ and $\check{p}_A$ are defined up to the action of Ω; finite-gap equations account for the ambiguity through a constraint.

The quasi-momenta are exhaustively characterised by the densities and the residues. The reasoning behind the claim is the following (see footnote 15 of [213]). We define the function $\hat{f}_A$ as $\hat{p}_A$ minus the simple-pole contribution from $x = s$ and $x = -1/s$ and the function $\check{f}_A$ as $\check{p}_A$ minus an analogous contribution from $x = -s$ and $x = 1/s$. For each function $\hat{f}_A$ (function $\check{f}_A$), we define a closed contour Γ_A in the complex plane whose interior encompasses all $\hat{C}^{\pm}_{A,n}$ (respectively $\check{C}^{\pm}_{A,n}$). This step is possible because the number of branch cuts is finite. The function $\hat{f}_A$ (respectively $\check{f}_A$) is analytic in the outer region. Therefore, it admits a Cauchy integral representation therein. Finally, we can deform Γ_A until it surrounds the associated set of branch cuts. The Cauchy integral is fragmented into a sum of integrals over $\hat{C}^{\pm}_{A,n}$ and $\check{C}^{\pm}_{A,n}$, which are determined by $\hat{\rho}^{+}_{A,n}$ and $\check{\rho}^{+}_{A,n}$. An integral representation for each $\hat{f}_A$ and $\check{f}_A$ in this way follows. An integral representation for each $\hat{p}_A$ and $\check{p}_A$ then also follows.

The upshot of the foregoing argument is that the quasi-momenta admit the following an integral representation, called *spectral decomposition* [102]:

$$\hat{p}_A(x) = \frac{x\hat{a}_A + (\bar{q} + qx)\hat{b}_A}{\bar{q}(x-s)(x+1/s)} + \frac{1}{2\pi\mathrm{i}}\int_{\hat{C}^{+}_{A}} \mathrm{d}x' \frac{\hat{\rho}^{+}_{A}(x')}{x-x'} + \frac{1}{2\pi\mathrm{i}}\int_{\hat{C}^{-}_{A}} \mathrm{d}x' \frac{\hat{\rho}^{-}_{A}(x')}{x-x'} \ , \tag{D.10}$$

$$\check{p}_A(x) = -\frac{x\check{a}_A + (\bar{q} - qx)\check{b}_A}{\bar{q}(x+s)(x-1/s)} + \frac{1}{2\pi\mathrm{i}}\int_{\check{C}^{+}_{A}} \mathrm{d}x' \frac{\check{\rho}^{+}_{A}(x')}{x-x'} + \frac{1}{2\pi\mathrm{i}}\int_{\check{C}^{-}_{A}} \mathrm{d}x' \frac{\check{\rho}^{-}_{A}(x')}{x-x'} \ , \tag{D.11}$$

where

$$\hat{C}^{\pm}_{A} = \bigcup_{n=1}^{\hat{N}^{\pm}_{A}} \hat{C}^{\pm}_{A,n} \ , \quad \hat{\rho}^{\pm}_{A} = \sum_{n=1}^{\hat{N}^{\pm}_{A}} \hat{\rho}^{\pm}_{A,n} \ , \tag{D.12}$$

$$\check{C}^{\pm}_{A} = \bigcup_{n=1}^{\check{N}^{\pm}_{A}} \check{C}^{\pm}_{A,n} \ , \quad \check{\rho}^{\pm}_{A} = \sum_{n=1}^{\check{N}^{\pm}_{A}} \check{\rho}^{\pm}_{A,n} \ . \tag{D.13}$$

[1] The residues (2.61) and (2.62) satisfy algebraic constraints to account for the Virasoro constraints; see formula (2.49) of [102]. Nonetheless, we do not need them to write the finite-gap equations. In the limit of pure RR flux, the algebraic constraints admit an extension to if the permutation-supercoset model on $\mathrm{AdS}_3 \times \mathrm{S}^3$ and the CFT_2 couples to the external T^4 [213]. A similar extension should be possible here.

As we have already mentioned, the action of Ω in (D.6) allows us to omit a redundant set of branch cuts, say $\hat{C}^-_{A,n}$ and $\check{C}^+_{A,n}$. We perform the step through some constraints. First, $\hat{a}_A$, $\hat{b}_A$, $\check{a}_A$, and $\check{b}_A$ in the residues (D.8) and (D.9) satisfy

$$\hat{a}_A = \sum_{B=1}^{3} S_{AB}\check{a}_B \ , \quad \hat{b}_A = \sum_{B=1}^{3} S_{AB}\check{b}_B \ . \tag{D.14}$$

Second, since (D.6) is satisfied irrespective of the value x, the integrals over $\hat{C}^-_A$ and $\check{C}^-_A$ are expressible in terms of the integrals over $\hat{C}^+_A$ and $\check{C}^+_A$:

$$\frac{1}{2\pi\mathrm{i}}\int_{\hat{C}^-_A} \mathrm{d}x' \frac{\hat{\rho}^-_A(x')}{x-x'} = -\sum_{B=1}^{3} S_{AB}\frac{1}{2\pi\mathrm{i}}\int_{\check{C}^+_B} \mathrm{d}x' \frac{\check{\rho}^+_B(x')}{x'^2(x-1/x')} \ , \tag{D.15}$$

$$\frac{1}{2\pi\mathrm{i}}\int_{\check{C}^-_A} \mathrm{d}x' \frac{\check{\rho}^-_A(x')}{x-x'} = -\sum_{B=1}^{3} S_{AB}\frac{1}{2\pi\mathrm{i}}\int_{\hat{C}^+_B} \mathrm{d}x' \frac{\hat{\rho}^+_B(x')}{x'^2(x-1/x')} \ . \tag{D.16}$$

Finally, the residues (D.8) and (D.9) require certain cancellations to occur. A necessary and sufficient condition is that

$$\hat{b}_A = \frac{1}{2\pi\mathrm{i}}\int_{\hat{C}^+_A} \mathrm{d}x' \frac{\hat{\rho}^+_A(x')}{x'} - \sum_{B=1}^{3} S_{AB}\frac{1}{2\pi\mathrm{i}}\int_{\check{C}^+_A} \mathrm{d}x' \frac{\check{\rho}^+_B(x')}{x'} \ . \tag{D.17}$$

If we take the previous considerations into account and use the Shokhotski-Plemelj formulae, we obtain the finite-gap equations of the non-linear σ-model on $\mathrm{AdS}_3 \times \mathrm{S}^3$ with mixed flux:

$$\begin{aligned}
&\sum_{B=1}^{3}\sum_{C=1}^{3} A_{AB}\left[\delta_{BC}\frac{1}{2\pi\mathrm{i}}\fint_{\hat{C}^+_C} \mathrm{d}x' \frac{\hat{\rho}^+_C(x')}{x-x'} - S_{BC}\frac{1}{2\pi\mathrm{i}}\int_{\check{C}^+_C} \mathrm{d}x' \frac{\check{\rho}^+_C(x')}{x'^2(x-1/x')}\right] \\
&= -\sum_{B=1}^{3} A_{AB}\frac{x\hat{a}_B + (\bar{q}+qx)\,\hat{b}_B}{\bar{q}\,(x-s)\,(x+1/s)} + 2\pi\hat{m}_{A,n} \ ,
\end{aligned} \tag{D.18}$$

$$\begin{aligned}
&\sum_{B=1}^{3}\sum_{C=1}^{3} A_{AB}\left[\delta_{BC}\frac{1}{2\pi\mathrm{i}}\fint_{\check{C}^+_C} \mathrm{d}x' \frac{\check{\rho}^+_C(x')}{x-x'} - S_{BC}\frac{1}{2\pi\mathrm{i}}\int_{\hat{C}^+_C} \mathrm{d}x' \frac{\hat{\rho}^+_C(x')}{x'^2(x-1/x')}\right] \\
&= \sum_{B=1}^{3} A_{AB}\frac{x\hat{a}_B + (\bar{q}-qx)\,\hat{b}_B}{\bar{q}\,(x+s)\,(x-1/s)} - 2\pi\check{m}_{A,n} \ ,
\end{aligned} \tag{D.19}$$

where dashed integrals denote the Cauchy principal value.

Appendix E

Elliptic curves

Factorisable classical solutions admit local spectral curves. We postulate the curve in subsection 2.2.2 and apply our proposal in sections 4.3 and 3.3. Our local spectral curve turns out to be elliptic. In this appendix, we present the background material on elliptic curves that we need in the body of the text. Since the content of the appendix is rather elementary, a comprehensive bibliography is beyond our scope. We just refer the reader to [215] for an accessible treatment of elliptic curves in the context of the Seiberg-Witten theory.

The elliptic curve is a compact algebraic variety of complex-dimension one whose genus is one. In subsection 2.2.2, the elliptic curve is defined by (2.75), which is the locus within C^2 defined by a quartic polynomial. To analyse the elliptic curve, it is convenient to rephrase (2.75) in the Weierstrass form, which involves a cubic polynomial. The Weierstrass form is obtained through a birational transformation. Birational transformation (performable in any computer-algebra software) preserve the analytic structure of an algebraic curve once it is desingularised. The Weierstrass form of the elliptic curve is

$$y^2 = 4x^3 - g_2 x - g_3 \ , \tag{E.1}$$

where g_2 and g_3 are called *modular forms*. The elliptic curve is in general endowed with a Z_2-automorphism, which acts on (E.1) as $y \mapsto -y$ and $x \mapsto x$.

Let e_a be the roots of the cubic polynomial of (E.1). We can then rewrite (E.1) as

$$y^2 = 4(x - e_1)(x - e_2)(x - e_3). \tag{E.2}$$

If we compare (E.1) and (E.2), we deduce that

$$e_1 + e_2 + e_3 = 0 \ , \tag{E.3}$$

and that g_2 and g_3 are symmetric polynomials of e_a, namely

$$g_2 = -4(e_1 e_2 + e_2 e_3 + e_3 e_1) \ , \quad g_2 = 4 e_1 e_2 e_3 \ . \tag{E.4}$$

The discriminant of the cubic polynomial Δ, which is called *modular discriminant*, is

$$\Delta = g_2^3 - 27 g_3^2 = 4(e_1 - e_2)^2 (e_2 - e_3)^2 (e_3 - e_1)^2 \ , \tag{E.5}$$

where the overall normalisation is conventional.

The discriminant encodes the regularity properties of the elliptic curve. If $\Delta \neq 0$, all e_a differ among themselves and the curve is non-singular. If $\Delta = 0$, two or three e_a are degenerate, and the curve is singular. The type of singularity depends on whether $g_2 \neq 0$ or $g_2 = 0$. If $g_2 \neq 0$, the elliptic curve has a node singularity. If $g_2 = 0$, it has a cusp singularity.

If $\Delta \neq 0$, the elliptic curve is isomorphic to a complex torus (via the Weierstrass function). We define a complex torus T^2 from a parallelogram within C under the identification of opposite edges. We assume without loss of generality that the vertices of the parallelogram are located at $\{0, 1, \tau, \tau + 1\}$, where τ is the modular parameter of the torus. We assume $\Im\tau > 0$, that is $\tau \in \mathrm{H}$. Complex tori are endowed with a complex structure, which characterises them. Two T^2 and T'^2 are isomorphic if their respective τ and τ' are related by a modular transformation:

$$\tau \mapsto \tau' = \frac{a\tau + b}{c\tau + d} \ , \qquad \begin{bmatrix} a & b \\ c & d \end{bmatrix} \in \mathrm{PSL}(2, \mathrm{Z}) \ . \tag{E.6}$$

If τ and τ' further belong to $\mathrm{H}/\mathrm{PSL}(2, \mathrm{Z}) = \{\tau \in \mathrm{H} : -1/2 \leq \Re\tau \leq 1/2 \ , |\tau| \geq 1\}$, the tori T^2 and T'^2 are isomorphic when $\tau = \tau'$.

The dependence of (2.75) on τ is encoded in g_2 and g_3. The modular forms g_2 and g_3 have respective weights four and six, that is $g_2 \mapsto (c\tau + d)^4 g_2$ and $g_3 \mapsto (c\tau + d)^6 g_3$ under (E.6). Therefore, Δ is also a modular form, whose weight is twelve; see (E.5). The modular parameter $\tau \in \mathrm{H}/\mathrm{PSL}(2, \mathrm{Z})$ characterises the elliptic curve unambiguously. However, τ cannot be computed directly. We can equivalently identify the elliptic curve by means of the j-invariant.

The j-invariant is a modular form of weight zero, that is $j \mapsto j$ under (E.6), which is both one-to-one and onto in $\mathrm{H}/\mathrm{PSL}(2, \mathrm{Z})$. The j-invariant is

$$j = 1728 \frac{g_2^3}{\Delta} \ . \tag{E.7}$$

Three values of the j-invariant stand out; they reflect special cases among elliptic curves. First, $j = 0$, which corresponds to $\tau = \exp(2\pi\mathrm{i}/3)$ and $g_2 = 0$. The torus is defined by a rhombus. The Z_2-automorphism of the elliptic curve is enhanced to a Z_6-automorphism; the latter acts on (2.75) as $y \mapsto \exp(n\pi\mathrm{i})y$ and $x \mapsto \exp(2\pi\mathrm{i}n/3)x$, where $n \in \mathrm{Z} \mod 6$. Second, $j = 1728$, which corresponds to $\tau = \mathrm{i}$ and $g_3 = 0$. The torus is defined by a square. The Z_2-automorphism of the elliptic curve is enhanced to a Z_4-automorphism; the latter acts on (2.75) as $y \mapsto \exp(3\pi\mathrm{i}n/2)y$ and $x \mapsto \exp(n\pi\mathrm{i}/2)x$, where $n \in \mathrm{Z} \mod 4$. Third, $j = \infty$, which corresponds to $\tau = \mathrm{i}\,\infty$ and $\Delta = 0$. The elliptic curve is not a torus, but a singular elliptic curve. We can consider the singular elliptic curve to be a degenerate torus defined by a semi-infinite rectangle. The singularity of the elliptic curve is either a node or a cusp depending on whether g_2 vanishes or not, as we have already commented.

In sections 3.3 and 4.3, we use the quantities defined in the appendix (the modular forms g_2 and g_3, the roots e_a, the modular discriminant Δ, and the j-invariant) to classify elliptic curves. This classification complements the direct analysis of classical solutions. In section 4.3, we also use these quantities to classify the elliptic curve of classical solutions explicit expressions are not available in the mixed-flux regime. This approach permits to argue the behaviour of these solutions under NSNS flux.

Appendix F

Elliptic integrals and Jacobian elliptic functions

Classical solutions in chapters 3 and 4.1 involves elliptic integrals and Jacobian elliptic function. In this appendix, we present the elliptic integrals and the Jacobian elliptic functions that we use in the main text. We enumerate definitions, properties, and formulae. Formulae can be found on [216], whose conventions we follow.

Elliptic integrals

Definition

- Incomplete elliptic integral of the first kind:

$$\mathrm{F}(\varphi, m) = \int_0^{\sin\varphi} \mathrm{d}x \frac{1}{\sqrt{(1-x^2)(1-m^2x^2)}} \ . \tag{F.1}$$

- Complete elliptic integral of the first kind:

$$\mathrm{K}(m) = \mathrm{F}(\pi/2, m) \ . \tag{F.2}$$

- Incomplete elliptic integral of the second kind:

$$\mathrm{E}(\varphi, m) = \int_0^{\sin\varphi} \mathrm{d}x \sqrt{1-m^2x^2} \ . \tag{F.3}$$

- Complete elliptic integral of the second kind:

$$\mathrm{E}(m) = \mathrm{E}(\pi/2, m) \tag{F.4}$$

- Incomplete elliptic integral of the third kind:

$$\Pi(\varphi, n, m) = \int_0^{\sin\varphi} \mathrm{d}x \frac{1}{(1-nx^2)\sqrt{(1-x^2)(1-m^2x^2)}} \ . \tag{F.5}$$

- Complete elliptic integral of the third kind:

$$\Pi(n, m) = \Pi(\pi/2, n, m) \ . \tag{F.6}$$

The argument φ is called the *Jacobian elliptic amplitude* and it is real: $\varphi \in (-\infty, \infty)$. The argument m is called the *elliptic modulus*. We assume that the elliptic modulus belongs to the fundamental domain: $m \in [0, 1]$. If $m = 1$, we assume that Jacobian elliptic amplitude is bounded to $\varphi \in [-\pi/2, \pi/2]$ because quasi-periodicity (F.10)–(F.12) does not hold any more, see (F.19)–(F.21). The argument n of both $\Pi(\varphi, n, m)$ and $\Pi(n, m)$ is called *elliptic characteristic* and is real: $n \in (-\infty, \infty)$.

Properties

- The functions (F.1), (F.3) and (F.5) are odd with respect to φ:

$$\mathrm{F}(-\varphi, m) = -\mathrm{F}(\varphi, m) \ , \tag{F.7}$$

$$\mathrm{E}(-\varphi, m) = -\mathrm{E}(\varphi, m) \ , \tag{F.8}$$

$$\Pi(-\varphi, n, m) = -\Pi(\varphi, n, m) \ . \tag{F.9}$$

- The functions (F.1), (F.3) and (F.5) are quasi-periodic with respect to φ:

$$\mathrm{F}(\varphi + k\pi, m) = \mathrm{F}(\varphi, m) + 2k\,\mathrm{K}(m) \ , \tag{F.10}$$

$$\mathrm{E}(\varphi + k\pi, m) = \mathrm{E}(\varphi, m) + 2k\,\mathrm{E}(m) \ , \tag{F.11}$$

$$\Pi(\varphi + k\pi, n, m) = \Pi(\varphi, n, m) + 2k\Pi(n, m) \ , \tag{F.12}$$

  where $k \in \mathrm{Z}$.

- Let $m = 0$. The functions (F.1), (F.3) and (F.5) read

$$\mathrm{F}(\varphi, 0) = \varphi \ , \tag{F.13}$$

$$\mathrm{E}(\varphi, 0) = \varphi \ , \tag{F.14}$$

$$\Pi(\varphi, n, 0) = \frac{\arctan\left(\sqrt{1-n}\tan\varphi\right)}{\sqrt{1-n}} \ . \tag{F.15}$$

  The functions (F.2), (F.4) and (F.6) then read

$$\mathrm{K}(0) = \frac{\pi}{2} \ , \tag{F.16}$$

$$\mathrm{E}(0) = \frac{\pi}{2} \ , \tag{F.17}$$

$$\Pi(n, 0) = \frac{\pi}{2\sqrt{1-n}} \quad \text{if} \quad n < 1 \quad \text{or} \quad \Pi(n, 0) = \frac{1}{\sqrt{n-1}} \quad \text{if} \quad n > 1 \ . \tag{F.18}$$

- Let $m = 1$. The functions (F.1), (F.3) and (F.5) read

$$\mathrm{F}(\varphi, 1) = \operatorname{arctanh}(\sin\varphi) \ , \tag{F.19}$$

$$\mathrm{E}(\varphi, 1) = \sin\varphi \ , \tag{F.20}$$

$$\Pi(\varphi, n, 1) = \frac{\sqrt{n}\operatorname{arctanh}(\sqrt{n}\sin\varphi) - \operatorname{arctanh}(\sin\varphi)}{n-1} \ . \tag{F.21}$$

The functions (F.2), (F.4) and (F.6) then read

$$\mathrm{K}(1) = \infty \ , \tag{F.22}$$

$$\mathrm{E}(1) = 1 \ , \tag{F.23}$$

$$\Pi(n, 1) = -\operatorname{sign}(n-1)\infty \ . \tag{F.24}$$

Formulae

- Let φ, m and n be

$$\varphi = \arcsin\sqrt{\frac{(a-c)(x-b)}{(a-b)(x-c)}} \ , \quad m = \sqrt{\frac{a-b}{a-c}} \ , \quad n = \frac{(a-b)c}{(a-c)b} \ . \tag{F.25}$$

such that $c < b \leq x \leq a$. The following formulae hold.

$$\int_b^x \frac{\mathrm{d}y}{\sqrt{(a-y)(y-b)(y-c)}} = \frac{2}{\sqrt{a-c}}\,\mathrm{F}(\varphi, m) \ , \tag{F.26}$$

$$\int_b^x \frac{\mathrm{d}x}{y\sqrt{(a-y)(y-b)(y-c)}} = \frac{2}{c\sqrt{a-c}}\left[\mathrm{F}(\varphi, m) - \left(1 - \frac{b}{c}\right)\Pi(\varphi, n, m)\right] \ . \tag{F.27}$$

- Let φ_1, φ_2, m and n be

$$\varphi_1 = \arcsin\left(\frac{x}{a}\sqrt{\frac{a^2+b^2}{x^2+b^2}}\right) \ , \quad \varphi_2 = \arccos\frac{x}{b} \ , \quad m = \frac{b}{\sqrt{a^2+b^2}} \ , \quad n = \frac{b^2}{b^2+1} \ , \tag{F.28}$$

such that $0 \leq x \leq b$. The following formulae hold.

$$\int_0^x \frac{\mathrm{d}y}{\sqrt{(y^2+a^2)(b^2-y^2)}} = \frac{1}{\sqrt{a^2+b^2}}\,\mathrm{F}(\varphi_1, m) \ , \tag{F.29}$$

$$\int_x^b \frac{\mathrm{d}y}{(1+y^2)\sqrt{(y^2+a^2)(b^2-y^2)}} = \frac{1}{(1+b^2)\sqrt{a^2+b^2}}\Pi(\varphi_2, m, n) \ . \tag{F.30}$$

$$\begin{aligned}\int_x^b \frac{\mathrm{d}y}{y^2\sqrt{(y^2+a^2)(b^2-y^2)}} &= \frac{\sqrt{(x^2+a^2)(b^2-x^2)}}{a^2b^2x} \\ &+ \frac{1}{b^2\sqrt{a^2+b^2}}\,\mathrm{F}(\varphi_2, m) - \frac{\sqrt{a^2+b^2}}{a^2b^2}\,\mathrm{E}(\varphi_2, m) \ .\end{aligned} \tag{F.31}$$

Jacobian elliptic functions

Definition

- Jacobian elliptic amplitude:

$$\operatorname{am}(x, m) = \varphi(x, m) = F^{-1}(x, m) \ . \tag{F.32}$$

The function $F^{-1}(x, m)$ is the inverse function of (F.1) with respect to φ.

- Jacobian elliptic sine:
$$\mathrm{sn}(x,m) = \sin\varphi(x,m)\ . \tag{F.33}$$

- Jacobian elliptic cosine:
$$\mathrm{cn}(x,m) = \cos\varphi(x,m)\ . \tag{F.34}$$

- Jacobian sd-function:
$$\mathrm{sd}(x,m) = \frac{\mathrm{sn}\,(x,m)}{\sqrt{1-m^2\,\mathrm{sn}^2\,(x,m)}}\ . \tag{F.35}$$

The argument x is called the *elliptic argument* and belongs to the real line: $x \in (-\infty,\infty)$.

Properties

- The functions (F.32), (F.33) and (F.35) are odd with respect x:
$$\mathrm{am}(-x,m) = -\,\mathrm{am}(x,m)\ , \tag{F.36}$$
$$\mathrm{sn}(-x,m) = -\,\mathrm{sn}(x,m)\ , \tag{F.37}$$
$$\mathrm{sd}(x,m) = -\,\mathrm{sd}(x,m)\ . \tag{F.38}$$

  The function (F.34) is even with respect to x:
$$\mathrm{cn}(-x,m) = \mathrm{cn}(x,m)\ . \tag{F.39}$$

- If $m<1$, (F.32) is quasi-periodic with respect to x:
$$\mathrm{am}(x+2n\,\mathrm{K}(m),m) = \mathrm{am}(x,m) + n\pi\ , \quad n \in \mathrm{Z}\ . \tag{F.40}$$

  If $m<1$, (F.33)–(F.35) are semi-periodic with respect to x:
$$\mathrm{sn}(x+2\,\mathrm{K}(m),m) = -\,\mathrm{sn}(x,m)\ , \tag{F.41}$$
$$\mathrm{cn}(x+2\,\mathrm{K}(m),m) = -\,\mathrm{cn}(x,m)\ , \tag{F.42}$$
$$\mathrm{sd}(x+2\,\mathrm{K}(m),m) = -\,\mathrm{sd}(x,m)\ . \tag{F.43}$$

  Therefore, the half-periodic and the period of (F.33)–(F.35) are $2\,\mathrm{K}(m)$ and $4\,\mathrm{K}(m)$, respectively.

- The function (F.32) vanishes at $x=0$:
$$\mathrm{am}(0,m) = 0\ . \tag{F.44}$$

  If $m<1$, (F.33)–(F.35) have infinitely many zeros in the real line:
$$\mathrm{sn}(2k\,\mathrm{K}(m),m) = 0\ , \tag{F.45}$$
$$\mathrm{cn}((2k+1)\,\mathrm{K}(m),m) = 0\ , \tag{F.46}$$
$$\mathrm{sd}(2k\,\mathrm{K}(m),m) = 0\ , \tag{F.47}$$
$$\tag{F.48}$$

  where $k \in \mathrm{Z}$.

- The functions (F.33) and (F.34) are bounded with respect to x and lie in the interval $[-1, 1]$. The extrema are reached at

$$\operatorname{sn}((2k+1)\,\mathrm{K}(m), m) = \operatorname{sign}(k)(-1)^k \ , \tag{F.49}$$

$$\operatorname{cn}(2k\,\mathrm{K}(m), m) = (-1)^k \ , \tag{F.50}$$

where $k \in \mathrm{Z}$. If $m < 1$, (F.35) is bounded with respect to x and lies in the interval $[-1/\sqrt{1-m^2}, 1/\sqrt{1-m^2}]$. The extrema are reached at

$$\operatorname{sn}((2k+1)\,\mathrm{K}(m), m) = \operatorname{sign}(k)(-1)^k \frac{1}{\sqrt{1-m^2}} \ , \tag{F.51}$$

where $k \in \mathrm{Z}$.

- Let $m = 0$. The functions (F.32)–(F.35) read

$$\operatorname{am}(x, 0) = x \ , \tag{F.52}$$

$$\operatorname{sn}(x, 0) = \sin x \ , \tag{F.53}$$

$$\operatorname{cn}(x, 0) = \cos x \ , \tag{F.54}$$

$$\operatorname{sd}(x, 0) = \sin x \ . \tag{F.55}$$

- Let $m = 1$. The functions (F.32)–(F.35) read

$$\operatorname{am}(x, 1) = \arcsin(\tanh x) \ , \tag{F.56}$$

$$\operatorname{sn}(x, 1) = \tanh x \ , \tag{F.57}$$

$$\operatorname{cn}(x, 1) = \operatorname{sech} x \ , \tag{F.58}$$

$$\operatorname{sd}(x, 1) = \sinh x \ . \tag{F.59}$$

- The functions (F.34) and (F.35) are related by the following transformation:

$$\operatorname{sd}(z \pm \mathrm{K}\,(m)\,, m) = \pm \frac{1}{\sqrt{1-m^2}} \operatorname{cn}(z, m) \ . \tag{F.60}$$

Bibliography

[1] G. 't Hooft, 'Dimensional reduction in quantum gravity', in *Salamfestschrift*, vol. 4 of World Scientific Series in 20th Century Physics, pp. 284–296, World Scientific, 1994. [arXiv:gr-qc/9310026]

[2] L. Susskind, 'The world as a hologram', *J. Math. Phys.*, vol. 36, pp. 6377–6396, 1995. [arXiv:hep-th/9409089]

[3] J. Maldacena, 'The Large-N Limit of Superconformal Field Theories and Supergravity', *Int. J. Theor. Phys.*, vol. 38, pp. 1113–1133, 1999. [arXiv:hep-th/9711200]

[4] S. S. Gubser, I. R. Klebanov, and A. M. Polyakov, 'Gauge theory correlators from non-critical string theory', *Phys. Lett. B*, vol. 428, pp. 105–114, 1998. [arXiv:hep-th/9802109]

[5] E. Witten, 'Anti de Sitter Space and Holography', *Adv. Theor. Math. Phys.*, vol. 2, pp. 253–291, 1998. [arXiv:hep-th/9802150]

[6] O. Aharony, S. S. Gubser, J. Maldacena, H. Ooguri, and Y. Oz, 'Large N field theories, string theory and gravity', *Phys. Rept.*, vol. 323, pp. 183–386, 2000. [arXiv:hep-th/9905111]

[7] G. Arutyunov and S. Frolov, 'Foundations of the $\mathrm{AdS}_5 \times \mathrm{S}^5$ superstring: I', *J. Phys. A*, vol. 42, p. 254003, 2009. [arXiv:0901.4937]

[8] N. Beisert et al., 'Review of AdS/CFT Integrability: An Overview', *Lett. Math. Phys.*, vol. 99, pp. 3–32, 2012. [arXiv:1012.3982]

[9] A. Sfondrini, 'Towards integrability for $\mathrm{AdS}_3/\mathrm{CFT}_2$', *J. Phys. A*, vol. 48, no. 2, p. 023001, 2015. [arXiv:1406.2971]

[10] A. A. Tseytlin, 'Spinning Strings and AdS/CFT Duality', in *From Fields to Strings: Circumnavigating Theoretical Physics*, vol. 2, pp. 1648–1707, World Scientific, 2003. [arXiv:hep-th/0311139]

[11] A. A. Tseytlin, 'Semiclassical strings and AdS/CFT', in *String Theory: From Gauge Interactions to Cosmology*, vol. 208 of NATO Science Series II: Mathematics, Physics and Chemistry, pp. 265–290, Springer Netherlands, 2004. [arXiv:hep-th/0409296]

[12] A. A. Tseytlin, 'Review of AdS/CFT Integrability, Chapter II.1: Classical $AdS_5 \times S^5$ String Solutions', *Lett. Math. Phys.*, vol. 99, pp. 103–125, 2012. [arXiv:1012.3986]

[13] A. A. Tseytlin, 'On semiclassical approximation and spinning string vertex operators in $AdS_5 \times S^5$', *Nucl. Phys. B*, vol. 664, pp. 247–275, 2003. [arXiv:hep-th/0304139]

[14] E. I. Buchbinder, 'Energy-spin trajectories in $AdS_5 \times S^5$ from semiclassical vertex operators', *JHEP*, vol. 04, p. 107, 2010. [arXiv:1002.1716]

[15] E. I. Buchbinder and A. A. Tseytlin, 'On semiclassical approximation for correlators of closed string vertex operators in AdS/CFT', *JHEP*, vol. 08, p. 057, 2010. [arXiv:1005.4516]

[16] J. A. Minahan, 'Review of AdS/CFT Integrability, Chapter I.1: Spin Chains in $\mathcal{N} = 4$ Super Yang-Mills', *Lett. Math. Phys.*, vol. 99, pp. 33–58, 2012. [arXiv:1012.3983]

[17] R. R. Metsaev and A. A. Tseytlin, 'Type IIB superstring action in $\mathrm{AdS}_5 \times S^5$ background', *Nucl. Phys. B*, vol. 533, pp. 109–126, 1998. [arXiv:hep-th/9805028]

[18] I. Bena, J. Polchinski, and R. Roiban, 'Hidden symmetries of the $\mathrm{AdS}_5 \times \mathrm{S}^5$ superstring', *Phys. Rev. D*, vol. 69, p. 046002, 2004. [arXiv:hep-th/0305116]

[19] G. Mandal, N. V. Suryanarayana, and S. R. Wadia, 'Aspects of semiclassical strings in AdS_5', *Phys. Lett. B*, vol. 543, pp. 81–88, 2002. [arXiv:hep-th/0206103]

[20] S. S. Gubser, I. R. Klebanov, and A. M. Polyakov, 'A semi-classical limit of the gauge/string correspondence', *Nucl. Phys. B*, vol. 636, pp. 99–114, 2002. [arXiv:hep-th/0204051]

[21] D. Berenstein, J. Maldacena, and H. S. Nastase, 'Strings in flat space and pp waves from $\mathcal{N} = 4$ Super Yang Mills', *JHEP*, vol. 04, p. 013, 2002. [arXiv:hep-th/0202021]

[22] S. Frolov and A. A. Tseytlin, 'Semiclassical quantization of rotating superstring in $AdS_5 \times S^5$', *JHEP*, vol. 06, p. 007, 2002. [arXiv:hep-th/0204226]

[23] A. A. Tseytlin, 'Semiclassical quantization of superstrings: $\mathrm{AdS}_5 \times \mathrm{S}^5$ and beyond', *Int. J. Mod. Phys. A*, vol. 18, pp. 981–1006, 2003. [arXiv:hep-th/0209116]

[24] M. Blau, J. Figueroa-O'Farrill, C. Hull, and G. Papadopoulos, 'Penrose limits and maximal supersymmetry', *Class. Quant. Grav.*, vol. 19, pp. L87–L95, 2002. [arXiv:hep-th/0201081]

[25] R. R. Metsaev, 'Type IIB Green-Schwarz superstring in plane wave Ramond-Ramond background', *Nucl. Phys. B*, vol. 625, pp. 70–96, 2002. [arXiv:hep-th/0112044]

[26] D. J. Gross, A. Mikhailov, and R. Roiban, 'Operators with Large R-charge in $N = 4$ Yang-Mills Theory', *Ann. Phys.*, vol. 301, pp. 31–52, 2002. [arXiv:hep-th/0205066]

[27] A. L. Larsen, N. Sánchez, and H. J. de Vega, 'Semiclassical quantization of circular strings in de Sitter and anti-de Sitter spacetimes', *Phys. Rev. D*, vol. 51, pp. 6917–6928, 1995. [arXiv:hep-th/9410219]

[28] H. J. de Vega and I. L. Egusquiza, 'Planetoid string solutions in 3+1 axisymmetric spacetimes', *Phys. Rev. D*, vol. 54, pp. 7513–7519, 1996. [arXiv:hep-th/9607056]

[29] L. Freyhult, 'Review of AdS/CFT Integrability, Chapter III.4: Twist States and the Cusp Anomalous Dimension', *Lett. Math. Phys.*, vol. 99, pp. 255–276, 2012. [arXiv:1012.3993]

[30] S. Frolov and A. A. Tseytlin, 'Multi-spin string solutions in $AdS_5 \times S^5$', *Nucl. Phys. B*, vol. 668, pp. 77–110, 2003. [arXiv:hep-th/0304255]

[31] J. A. Minahan and K. Zarembo, 'The Bethe-ansatz for $\mathcal{N} = 4$ super Yang-Mills', *JHEP*, vol. 03, p. 013, 2003. [arXiv:hep-th/0212208]

[32] N. Beisert, 'The complete one loop dilatation operator of N = 4 super-Yang-Mills theory', *Nucl. Phys. B*, vol. 676, pp. 3–42, 2004. [arXiv:hep-th/0307015]

[33] N. Beisert and M. Staudacher, 'The N = 4 SYM integrable super spin chain', *Nucl. Phys. B*, vol. 670, pp. 439–463, 2003. [arXiv:hep-th/0307042]

[34] N. Beisert, C. Kristjansen, and M. Staudacher, 'The dilatation operator of conformal N = 4 super-Yang-Mills theory', *Nucl. Phys. B*, vol. 664, pp. 131–184, 2003. [arXiv:hep-th/0303060]

[35] S. Frolov and A. A. Tseytlin, 'Quantizing three-spin string solution in $AdS_5 \times S^5$', *JHEP*, vol. 07, p. 016, 2003. [arXiv:hep-th/0306130]

[36] S. Frolov and A. A. Tseytlin, 'Rotating string solutions: AdS/CFT duality in non-supersymmetric sectors', *Phys. Lett. B*, vol. 570, pp. 96–104, 2003. [arXiv:hep-th/0306143]

[37] G. Arutyunov, S. Frolov, J. Russo, and A. A. Tseytlin, 'Spinning strings in $AdS_5 \times S^5$ and integrable systems', *Nucl. Phys. B*, vol. 671, pp. 3–50, 2003. [arXiv:hep-th/0307042]

[38] G. Arutyunov, J. Russo, and A. A. Tseytlin, 'Spinning strings in $\mathrm{AdS}_5 \times \mathrm{S}^5$: New integrable system relations', *Phys. Rev. D*, vol. 69, p. 086009, 2004. [arXiv:hep-th/0311004]

[39] A. Mikhailov, 'Speeding strings', *JHEP*, vol. 12, p. 058, 2003. [arXiv:hep-th/0311019]

[40] D. Mateos, T. Mateos, and P. K. Townsend, 'Supersymmetry of tensionless rotating strings in $AdS_5 \times S^5$, and nearly-BPS operators', *JHEP*, vol. 12, p. 017, 2003. [arXiv:hep-th/0309114]

[41] A. Mikhailov, 'Slow evolution of nearly-degenerate extremal surfaces', *J. Geom. Phys.*, vol. 54, pp. 228–250, 2005. [arXiv:hep-th/0402067]

[42] D. Mateos, T. Mateos, and P. K. Townsend, 'More on supersymmetric tensionless rotating strings in $\mathrm{AdS}_5 \times \mathrm{S}^5$', in *Quantum Theory and Symmetries*, pp. 570–575, World Scientific, 2004. [arXiv:hep-th/0401058]

[43] A. Mikhailov, 'Supersymmetric null-surfaces', *JHEP*, vol. 09, p. 068, 2004. [arXiv:hep-th/0404173]

[44] M. Kruczenski and A. A. Tseytlin, 'Semiclassical relativistic strings in S^5 and long coherent operators in $\mathcal{N} = 4$ SYM theory', *JHEP*, vol. 09, p. 038, 2004. [arXiv:hep-th/0406189]

[45] N. Beisert, J. A. Minahan, M. Staudacher, and K. Zarembo, 'Stringing spins and spinning strings', *JHEP*, vol. 09, p. 010, 2003. [arXiv:hep-th/0306139]

[46] N. Beisert, S. Frolov, M. Staudacher, and A. A. Tseytlin, 'Precision spectroscopy of AdS/CFT', *JHEP*, vol. 10, p. 037, 2003. [arXiv:hep-th/0308117]

[47] G. Arutyunov and M. Staudacher, 'Matching higher conserved charges for strings and spins', *JHEP*, vol. 03, p. 004, 2004. [arXiv:hep-th/0310182]

[48] G. Arutyunov and M. Staudacher, 'Two-Loop Commuting Charges and The String/Gauge Duality', in *Lie Theory and Its Applications in Physics V*, pp. 204–216, 2004. [arXiv:hep-th/0403077]

[49] J. A. Minahan, 'Circular semiclassical string solutions on $AdS_5 \times S_5$', *Nucl. Phys. B*, vol. 648, pp. 203–214, 2003. [arXiv:hep-th/0209047]

[50] J. Engquist, J. A. Minahan, and K. Zarembo, 'Yang-Mills duals for semiclassical strings on $AdS_5 \times S_5$', *JHEP*, vol. 11, p. 063, 2003. [arXiv:hep-th/0310188]

[51] M. Kruczenski, 'Spin Chains and String Theory', *Phys. Rev. Lett.*, vol. 93, p. 161602, 2004. [arXiv:hep-th/0311203]

[52] M. Kruczenski, A. V. Ryzhov, and A. A. Tseytlin, 'Large spin limit of $AdS_5 \times S^5$ string theory and low energy expansion of ferromagnetic spin chains', *Nucl. Phys. B*, vol. 692, pp. 3–49, 2004. [arXiv:hep-th/0403120]

[53] R. Hernández and E. López, 'Spin chain sigma models with fermions', *JHEP*, vol. 11, p. 079, 2004. [arXiv:hep-th/0410022]

[54] B. Stefański Jr and A. A. Tseytlin, 'Super spin chain coherent state actions and $AdS_5 \times S^5$ superstring', *Nucl. Phys. B*, vol. 718, pp. 83–112, 2005. [arXiv:hep-th/0503185]

[55] B. Stefański Jr and A. A. Tseytlin, 'Large spin limits of AdS/CFT and generalized Landau-Lifshitz equations', *JHEP*, vol. 05, p. 042, 2004. [arXiv:hep-th/0404133]

[56] S. Bellucci, P.-Y. Casteill, J. F. Morales, and C. Sochichiu, 'SL(2) spin chain and spinning strings on $AdS_5 \times S^5$', *Nucl. Phys. B*, vol. 707, pp. 303–320, 2005. [arXiv:hep-th/0409086]

[57] I. Y. Park, A. Tirziu, and A. A. Tseytlin, 'Spinning strings in $AdS_5 \times S^5$: one-loop correction to energy in SL(2) sector', *JHEP*, vol. 03, p. 013, 2005. [arXiv:hep-th/0501203]

[58] V. A. Kazakov, A. Marshakov, J. A. Minahan, and K. Zarembo, 'Classical/quantum integrability in AdS/CFT', *JHEP*, vol. 05, p. 024, 2004. [arXiv:hep-th/0402207]

[59] V. A. Kazakov and K. Zarembo, 'Classical/quantum integrability in non-compact sector of AdS/CFT', *JHEP*, vol. 10, p. 060, 2004. [arXiv:hep-th/0410022]

[60] N. Beisert, V. A. Kazakov, K. Sakai, and K. Zarembo, 'The Algebraic Curve of Classical Superstrings on $AdS_5 \times S^5$', *Commun. Math. Phys.*, vol. 263, pp. 659–710, 2006. [arXiv:hep-th/0502226]

[61] N. Beisert, V. A. Kazakov, K. Sakai, and K. Zarembo, 'Complete spectrum of long operators in $\mathcal{N} = 4$ SYM at one loop', *JHEP*, vol. 07, p. 030, 2005. [arXiv:hep-th/0503200]

[62] S.-J. Rey and J.-T. Yee, 'Macroscopic strings as heavy quarks: Large-N gauge theory and anti-de Sitter supergravity', *Eur. Phys. J. C*, vol. 22, pp. 379–394, 2001. [arXiv:hep-th/9803001]

[63] J. Maldacena, 'Wilson Loops in Large N Field Theories', *Phys. Rev. Lett.*, vol. 80, pp. 4859–4862, 1998. [arXiv:hep-th/9803002]

[64] N. Drukker and B. Fiol, 'On the integrability of Wilson loops in $AdS_5 \times S^5$: some periodic ansatze', *JHEP*, vol. 01, p. 056, 2006. [arXiv:hep-th/0506058]

[65] R. A. Janik and P. Laskoś-Grabowski, 'Surprises in the AdS algebraic curve constructions — Wilson loops and correlation functions', *Nucl. Phys. B*, vol. 861, pp. 361–386, 2012. [arXiv:1203.4383]

[66] A. Dekel, 'Algebraic curves for factorized string solutions', *JHEP*, vol. 04, p. 119, 2013. [arXiv:1302.0555]

[67] D. Serban and M. Staudacher, 'Planar $\mathcal{N} = 4$ gauge theory and the inozemtsev long range spin chain', *JHEP*, vol. 06, p. 001, 2004. [arXiv:hep-th/0401057]

[68] C. G. Callan, H. K. Lee, T. McLoughlin, J. H. Schwarz, I. Swanson, and X. Wu, 'Quantizing string theory in $AdS_5 \times S^5$: beyond the pp-wave', *Nucl. Phys. B*, vol. 673, pp. 3–40, 2003. [arXiv:hep-th/0307032]

[69] N. Beisert, V. Dippel, and M. Staudacher, 'A novel long-range spin chain and planar $\mathcal{N} = 4$ super Yang-Mills', *JHEP*, vol. 07, p. 075, 2004. [arXiv:hep-th/0405001]

[70] G. Arutyunov, S. Frolov, and M. Staudacher, 'Bethe ansatz for quantum strings', *JHEP*, vol. 10, p. 016, 2004. [arXiv:hep-th/0406256]

[71] M. Staudacher, 'The factorized S-matrix of CFT/AdS', *JHEP*, vol. 05, p. 054, 2005. [arXiv:hep-th/0412188]

[72] N. Beisert and M. Staudacher, 'Long-range $\mathfrak{psu}(2,2|4)$ Bethe ansätze for gauge theory and strings', *Nucl. Phys. B*, vol. 727, pp. 1–62, 2005. [arXiv:hep-th/0504190]

[73] N. Beisert, 'The su(2|2) dynamic S-matrix', *Adv. Theor. Math. Phys.*, vol. 12, pp. 945–979, 2008. [arXiv:hep-th/0511082]

[74] G. Arutyunov, S. Frolov, and M. Zamaklar, 'The Zamolodchikov-Faddeev Algebra for $\mathrm{AdS}_5 \times \mathrm{S}^5$ superstring', *JHEP*, vol. 04, p. 002, 2007. [arXiv:hep-th/0612229]

[75] S. Frolov, J. Plefka, and M. Zamaklar, 'The $\mathrm{AdS}_5 \times \mathrm{S}^5$ superstring in light-cone gauge and its Bethe equations', *J. Phys. A*, vol. 39, pp. 13037–13082, 2006. [arXiv:hep-th/0603008]

[76] G. Arutyunov, S. Frolov, J. Plefka, and M. Zamaklar, 'The Off-shell Symmetry Algebra of the Light-cone $\mathrm{AdS}_5 \times S^5$ Superstring', *J. Phys. A*, vol. 40, pp. 3583–3606, 2007. [arXiv:hep-th/0609157]

[77] R. Hernández and E. López, 'Quantum corrections to the string Bethe ansatz', *JHEP*, vol. 07, p. 004, 2006. [arXiv:hep-th/0603204]

[78] R. A. Janik, 'The $\mathrm{AdS}_5 \times S^5$ superstring worldsheet S matrix and crossing symmetry', *Phys. Rev. D*, vol. 73, p. 086006, 2006. [arXiv:hep-th/0603038]

[79] G. Arutyunov and S. Frolov, 'On $\mathrm{AdS}_5 \times \mathrm{S}^5$ String S-matrix', *Phys. Lett. B*, vol. 639, pp. 378–382, 2006. [arXiv:hep-th/0604043]

[80] N. Beisert, R. Hernández, and E. López, 'A crossing-symmetric phase for $AdS_5 \times S^5$ strings', *JHEP*, vol. 11, p. 070, 2006. [arXiv:hep-th/0609044]

[81] N. Beisert, B. Eden, and M. Staudacher, 'Transcendentality and Crossing', *J. Stat. Mech.*, vol. 0701, p. P01021, 2007. [arXiv:hep-th/0610251]

[82] P. Vieira and D. Volin, 'Review of AdS/CFT Integrability, Chapter III.3: The Dressing factor', *Lett. Math. Phys.*, vol. 99, pp. 231–253, 2012. [arXiv:1012.3992]

[83] Z. Bajnok, 'Review of AdS/CFT Integrability, Chapter III.6: Thermodynamic Bethe Ansatz', *Lett. Math. Phys.*, vol. 99, pp. 299–320, 2012. [arXiv:1012.3995]

[84] F. Levkovich-Maslyuk, 'A review of the AdS/CFT Quantum Spectral Curve', *J. Phys. A*, vol. 53, no. 28, p. 283004, 2020. [arXiv:1911.13065]

[85] N. Seiberg and E. Witten, 'The D1/D5 system and singular CFT', *JHEP*, vol. 04, p. 017, 1999. [arXiv:hep-th/9903224]

[86] L. Eberhardt, 'A perturbative CFT dual for pure NS-NS AdS_3 strings'. [arXiv:2110.07535]

[87] O. O. Sax and B. Stefański, ‘Closed strings and moduli in $\mathrm{AdS}_3/\mathrm{CFT}_2$’, *JHEP*, vol. 05, p. 101, 2018. [arXiv:1804.02023]

[88] A. Cagnazzo and K. Zarembo, ‘B-field in AdS_3/CFT_2 Correspondence and Integrability’, *JHEP*, vol. 11, p. 133, 2012 [Erratum: JHEP, vol. 04, p. 003, 2013]. [arXiv:1209.4049]

[89] A. Giveon, D. Kutasov, and N. Seiberg, ‘Comments on String Theory on AdS_3’, *Adv. Theor. Math. Phys.*, vol. 2, pp. 733–782, 1998. [arXiv:hep-th/9806194]

[90] I. Pesando, ‘The GS type IIB superstring action on $AdS_3 \times S_3 \times T^4$’, *JHEP*, vol. 02, p. 007, 1999. [arXiv:hep-th/9809145]

[91] J. Rahmfeld and A. Rajaraman, ‘Green-Schwarz string action on $\mathrm{AdS}_3\times\mathrm{S}^3$ with Ramond-Ramond charge’, *Phys. Rev. D*, vol. 60, p. 064014, 1999. [arXiv:hep-th/9809164]

[92] N. J. Berkovits, C. Vafa, and E. Witten, ‘Conformal field theory of AdS background with Ramond-Ramond flux’, *JHEP*, vol. 03, p. 018, 1999. [arXiv:hep-th/9902098]

[93] J. Maldacena and H. Ooguri, ‘Strings in AdS_3 and $\mathrm{SL}(2,\mathrm{R})$ WZW model. I: The spectrum’, *J. Math. Phys.*, vol. 42, pp. 2929–2960, 2001. [arXiv:hep-th/0001053]

[94] G. Götz, T. Quella, and V. Schomerus, ‘The WZNW model on $\mathrm{PSU}(1,1|2)$’, *JHEP*, vol. 03, p. 003, 2007. [arXiv:hep-th/0610070]

[95] A. Babichenko, B. Stefański Jr, and K. Zarembo, ‘Integrability and the AdS_3/CFT_2 correspondence’, *JHEP*, vol. 03, p. 058, 2010. [arXiv:0912.1723]

[96] B. Hoare and A. A. Tseytlin, ‘On string theory on $AdS_3\times S^3\times T^4$ with mixed 3-form flux: Tree-level S-matrix’, *Nucl. Phys. B*, vol. 873, pp. 682–727, 2013. [arXiv:1303.1037]

[97] O. O. Sax, B. Stefański Jr, and A. Torrielli, ‘On the massless modes of the $\mathrm{AdS}_3/\mathrm{CFT}_2$ integrable systems’, *JHEP*, vol. 03, p. 109, 2013. [arXiv:1211.1952]

[98] S. Majumder, O. O. Sax, B. Stefański, and A. Torrielli, ‘Protected states in AdS_3 backgrounds from integrability’. [arXiv:2103.16972]

[99] B. Hoare and A. A. Tseytlin, ‘Massive S-matrix of $AdS_3 \times S^3 \times T^4$ superstring theory with mixed 3-form flux’, *Nucl. Phys. B*, vol. 873, pp. 395–418, 2013. [arXiv:1304.4099]

[100] P. Sundin and L. Wulff, ‘One- and two-loop checks for the $\mathrm{AdS}_3 \times S^3 \times T^4$ superstring with mixed flux’, *J. Phys. A*, vol. 48, no. 10, p. 105402, 2015. [arXiv:1411.4662]

[101] B. Hoare, A. Stepanchuk, and A. A. Tseytlin, ‘Giant magnon solution and dispersion relation in string theory in $AdS_3 \times S^3 \times T^4$ with mixed flux’, *Nucl. Phys. B*, vol. 879, pp. 318–347, 2014. [arXiv:1311.1794]

[102] A. Babichenko, A. Dekel, and O. O. Sax, ‘Finite-gap equations for strings on $\mathrm{AdS}_3 \times \mathrm{S}^3 \times \mathrm{T}^4$ with mixed 3-form flux’, *JHEP*, vol. 11, p. 122, 2014. [arXiv:1405.6087]

[103] L. Bianchi and B. Hoare, '$AdS_3 \times S^3 \times M^4$ string S-matrices from unitarity cuts', *JHEP*, vol. 08, p. 097, 2014. [arXiv:1405.7947]

[104] A. Stepanchuk, 'String theory in $AdS_3 \times S^3 \times T^4$ with mixed flux: semiclassical and 1-loop phase in the S-matrix', *J. Phys. A*, vol. 48, no. 19, p. 195401, 2015. [arXiv:1412.4764]

[105] T. Lloyd, O. O. Sax, A. Sfondrini, and B. Stefański Jr, 'The complete worldsheet S matrix of superstrings on $\mathrm{AdS}_3 \times \mathrm{S}^3 \times \mathrm{T}^4$ with mixed three-form flux', *Nucl. Phys. B*, vol. 891, pp. 570–612, 2015. [arXiv:1410.0866]

[106] B. Eden, D. le Plat, and A. Sfondrini, 'Integrable bootstrap for AdS3/CFT2 correlation functions'. [arXiv:2102.08365]

[107] R. Borsato, O. O. Sax, A. Sfondrini, B. Stefański Jr, and A. Torrielli, 'Dressing phases of $\mathrm{AdS}_3/\mathrm{CFT}_2$', *Phys. Rev. D*, vol. 88, p. 066004, 2013. [arXiv:1306.2512]

[108] R. Borsato, O. O. Sax, A. Sfondrini, B. Stefański Jr, and A. Torrielli, 'On the dressing factors, Bethe equations and Yangian symmetry of strings on $\mathrm{AdS}_3 \times S^3 \times T^4$', *J. Phys. A*, vol. 50, no. 2, p. 024004, 2017. [arXiv:1607.00914]

[109] M. Baggio and A. Sfondrini, 'Strings on NS-NS backgrounds as integrable deformations', *Phys. Rev. D*, vol. 98, no. 2, p. 021902, 2018. [arXiv:1804.01998]

[110] A. Dei and A. Sfondrini, 'Integrable spin chain for stringy Wess-Zumino-Witten models', *JHEP*, vol. 07, p. 109, 2018. [arXiv:1806.00422]

[111] K. Ferreira, M. R. Gaberdiel, and J. I. Jottar, 'Higher spins on AdS_3 from the worldsheet', *JHEP*, vol. 07, p. 131, 2017. [arXiv:1704.08667]

[112] A. Sfondrini, 'Long Strings and Symmetric Product Orbifold from the AdS_3 Bethe Equations', *EPL*, vol. 133, no. 1, p. 10004, 2021. [arXiv:2010.02782]

[113] M. Henneaux and L. Mezincescu, 'A σ-model interpretation of Green-Schwarz covariant superstring action', *Phys. Lett. B*, vol. 152, pp. 340–342, 1985.

[114] M. B. Green and J. H. Schwarz, 'Covariant description of superstrings', *Phys. Lett. B*, vol. 136, pp. 367–370, 1984.

[115] N. Berkovits, M. Bershadsky, T. Hauer, S. Zhukov, and B. Zwiebach, 'Superstring theory on $\mathrm{AdS}_2 \times S^2$ as a coset supermanifold', *Nucl. Phys. B*, vol. 567, pp. 61–86, 2000. [arXiv:hep-th/9907200]

[116] R. Roiban and W. Siegel, 'Superstrings on $AdS_5 \times S^5$ supertwistor space', *JHEP*, vol. 11, p. 024, 2000. [arXiv:hep-th/0010104]

[117] M. Magro, 'Review of AdS/CFT Integrability, Chapter II.3: Sigma Model, Gauge Fixing', *Lett. Math. Phys.*, vol. 99, pp. 149–167, 2012. [arXiv:1012.3988]

[118] A. M. Polyakov, 'Conformal fixed points of unidentified gauge theories', *Mod. Phys. Lett. A*, vol. 19, pp. 1649–1660, 2004. [arXiv:hep-th/0405106]

[119] I. Adam, A. Dekel, L. Mazzucato, and Y. Oz, 'Integrability of type II superstrings on Ramond-Ramond backgrounds in various dimensions', *JHEP*, vol. 06, p. 085, 2007. [arXiv:hep-th/0702083]

[120] K. Zarembo, 'Strings on semisymmetric superspaces', *JHEP*, vol. 05, p. 002, 2010. [arXiv:1003.0465]

[121] S. P. Novikov, 'The Hamiltonian formalism and a many valued analog of Morse theory', *Usp. Mat. Nauk*, vol. 37N5, no. 5, pp. 3–49, 1982.

[122] E. Witten, 'Global aspects of current algebra', *Nucl. Phys. B*, vol. 223, pp. 422–432, 1983.

[123] E. Witten, 'Non-abelian bosonization in two dimensions', *Commun. Math. Phys.*, vol. 92, pp. 455–472, 1984.

[124] E. Witten, 'On holomorphic factorization of WZW and coset models', *Commun. Math. Phys.*, vol. 144, pp. 189–212, 1992.

[125] K. Zarembo, 'Integrability in sigma-models', in *Integrability: From Statistical Systems to Gauge Theory*, vol. 106, Oxford Scholarship Online, 2019. [arXiv:1712.07725]

[126] L. Frappat, P. Sorba, and A. Sciarrino, 'Dictionary on Lie Superalgebras'. [arXiv:hep-th/9607161]

[127] I. N. McArthur, 'Kappa-symmetry of Green-Schwarz actions in coset superspaces', *Nucl. Phys. B*, vol. 573, pp. 811–829, 2000. [arXiv:hep-th/9908045]

[128] D. Berenstein and D. Trancanelli, 'S-duality and the giant magnon dispersion relation', *Eur. Phys. J. C*, vol. 74, p. 2925, 2014. [arXiv:0904.0444]

[129] N. Drukker et al., 'Roadmap on Wilson loops in 3d Chern–Simons-matter theories', *J. Phys. A*, vol. 53, no. 17, p. 173001, 2020. [arXiv:1910.00588]

[130] G. Arutyunov and S. Frolov, 'Superstrings on $\mathrm{AdS}_4 \times \mathbb{CP}^3$ as a coset sigma-model', *JHEP*, vol. 09, p. 129, 2008. [arXiv:0806.4940]

[131] B. Stefański Jr, 'Green-Schwarz action for Type IIA strings on $AdS_4 \times CP^3$', *Nucl. Phys. B*, vol. 808, pp. 80–87, 2009. [arXiv:0806.4948]

[132] V. G. Knizhnik and A. B. Zamolodchikov, 'Current algebra and Wess-Zumino model in two dimensions', *Nucl. Phys. B*, vol. 247, pp. 83–103, 1984.

[133] M. Cvetič, H. Lu, C. N. Pope, and K. S. Stelle, 'T-duality in the Green-Schwarz formalism, and the massless/massive IIA duality map', *Nucl. Phys. B*, vol. 573, pp. 149–176, 2000. [arXiv:hep-th/9907202]

[134] L. Wulff, 'The type II superstring to order θ^4', *JHEP*, vol. 07, p. 123, 2013. [arXiv:1304.6422]

[135] E. S. Fradkin and A. A. Tseytlin, 'Quantized string models', *Annals Phys.*, vol. 143, p. 413, 1982.

[136] N. Drukker, D. J. Gross, and A. A. Tseytlin, 'Green-Schwarz string in $AdS_5 \times S^5$: semiclassical partition function', *JHEP*, vol. 04, p. 021, 2000. [arXiv:hep-th/0001204]

[137] K. Zarembo, 'Algebraic Curves for Integrable String Backgrounds'. [arXiv:1005.1342]

[138] A. Dekel and T. Klose, 'Correlation function of circular Wilson Loops at strong coupling', *JHEP*, vol. 11, p. 117, 2013. [arXiv:1309.3203]

[139] G. Arutyunov and D. Medina-Rincón, 'Deformed Neumann model from spinning strings on $(\mathrm{AdS}_5 \times \mathrm{S}^5)_\eta$', *JHEP*, vol. 10, p. 050, 2014. [arXiv:1406.2536]

[140] M. Grigoriev and A. A. Tseytlin, 'Pohlmeyer reduction of $\mathrm{AdS}_5 \times \mathrm{S}^5$ superstring sigma model', *Nucl. Phys. B*, vol. 800, pp. 450–501, 2008. [arXiv:0711.0155]

[141] L. F. Alday, G. Arutyunov, and S. Frolov, 'New integrable system of 2dim fermions from strings on $\mathrm{AdS}_5 \times \mathrm{S}^5$', *JHEP*, vol. 01, p. 078, 2006. [arXiv:hep-th/0508140]

[142] M. Grigoriev and A. A. Tseytlin, 'On reduced models for superstrings on $\mathrm{AdS}_n \times \mathrm{S}_n$', *Int. J. Mod. Phys. A*, vol. 23, pp. 2107–2117, 2008. [arXiv:0806.2623]

[143] R. Hernández and J. M. Nieto, 'Spinning strings in $AdS_3 \times S^3$ with NS–NS flux', *Nucl. Phys. B*, vol. 888, pp. 236–247, 2014. [Corrigendum: Nucl. Phys. B, vol. 895, pp. 303–304, 2015] [arXiv:1407.7475]

[144] R. Hernández and J. M. Nieto, 'Elliptic solutions in the Neumann–Rosochatius system with mixed flux', *Phys. Rev. D*, vol. 91, no. 12, p. 126006, 2015. [arXiv:1502.05203]

[145] J. M. Nieto, *Spinning strings and correlation functions in the AdS/CFT correspondence.* PhD thesis, Unversidad Complutense de Madrid, 2017. [arXiv:1711.09993]

[146] C.-M. Chen, Y. Tsai, and W.-Y. Wen, 'Giant Magnons and Spiky Strings on S^3 with B-field', *Prog. Theor. Phys.*, vol. 121, pp. 1189–1207, 2009. [arXiv:0809.3269]

[147] C. Ahn and P. Bozhilov, 'String solutions in $AdS_3 \times S^3 \times T^4$ with NS-NS B-field', *Phys. Rev. D*, vol. 90, no. 6, p. 066010, 2014. [arXiv:1404.7644]

[148] A. Banerjee, K. L. Panigrahi, and P. M. Pradhan, 'Spiky strings on $AdS_3 \times S^3$ with NS-NS flux', *Phys. Rev. D*, vol. 90, no. 10, p. 106006, 2014. [arXiv:1405.5497]

[149] A. Loewy and Y. Oz, 'Large spin strings in AdS_3', *Phys. Lett. B*, vol. 557, pp. 253–262, 2003. [arXiv:hep-th/0212147]

[150] J. R. David and A. Sadhukhan, 'Spinning strings and minimal surfaces in AdS_3 with mixed 3-form fluxes', *JHEP*, vol. 10, p. 049, 2014. [arXiv:1405.2687]

[151] A. Banerjee and A. Sadhukhan, 'Multi-spike strings in AdS_3 with mixed three-form fluxes', *JHEP*, vol. 05, p. 083, 2016. [arXiv:1512.01816]

[152] A. Banerjee, S. Biswas, and K. L. Panigrahi, 'On multi-spin classical strings with NS-NS flux', *JHEP*, vol. 08, p. 053, 2018. [arXiv:1806.10934]

[153] A. Banerjee, S. Biswas, P. Pandit, and K. L. Panigrahi, 'On N-spike strings in conformal gauge with NS-NS fluxes', *JHEP*, vol. 08, p. 124, 2019. [arXiv:1906.06879]

[154] C. Bachas and M. Petropoulos, 'Anti-de-Sitter D-branes', *JHEP*, vol. 02, p. 025, 2001. [arXiv:hep-th/0012234]

[155] J. Klusoň, 'Integrability of a D1-brane on a group manifold with mixed three-form flux', *Phys. Rev. D*, vol. 93, no. 4, p. 046003, 2016. [arXiv:1509.09061]

[156] A. Banerjee, S. Biswas, and R. R. Nayak, 'D1 string dynamics in curved backgrounds with fluxes', *JHEP*, vol. 04, p. 172, 2016. [arXiv:1601.06360]

[157] J. Klusoň, '(m, n)-String in (p,q)-string and (p, q)-five-brane background', *Eur. Phys. J. C*, vol. 76, no. 11, p. 582, 2016. [arXiv:1602.08275]

[158] S. P. Barik, M. Khouchen, J. Klusoň, and K. L. Panigrahi, 'SL$(2, Z)$ invariant rotating (m, n) strings in $AdS_3 \times S^3$ with mixed flux', *Eur. Phys. J. C*, vol. 77, no. 5, p. 298, 2017. [arXiv:1610.03402]

[159] S. Biswas, P. Pandit, and K. L. Panigrahi, 'N spike D-strings in AdS space with mixed flux', *Eur. Phys. J. C*, vol. 80, no. 8, p. 714, 2020. [arXiv:2003.08604]

[160] A. Chakraborty and K. L. Panigrahi, 'Neumann-Rosochatius system for (m,n) string in $AdS_3 \times S^3$ with mixed flux', *Eur. Phys. J. C*, vol. 81, no. 4, p. 281, 2021. [arXiv:2008.05139].

[161] R. Hernández and J. M. Nieto, 'Spinning strings in the η-deformed Neumann-Rosochatius system', *Phys. Rev. D*, vol. 96, no. 8, p. 086010, 2017. [arXiv:1707.08032]

[162] G. Arutyunov, M. Heinze, and D. Medina-Rincón, 'Integrability of the η-deformed Neumann–Rosochatius model', *J. Phys. A*, vol. 50, no. 3, p. 035401, 2017. [arXiv:1607.05190]

[163] A. Banerjee, K. L. Panigrahi, and M. Samal, 'A note on oscillating strings in $\mathrm{AdS}_3 \times S^3$ with mixed three-form fluxes', *JHEP*, vol. 11, p. 133, 2015. [arXiv:1508.03430]

[164] M. Cho, S. Collier, and X. Yin, 'Strings in Ramond-Ramond Backgrounds from the Neveu-Schwarz-Ramond Formalism', *JHEP*, vol. 12, p. 123, 2020. [arXiv:1811.00032]

[165] L. Eberhardt and K. Ferreira, 'Long strings and chiral primaries in the hybrid formalism', *JHEP*, vol. 02, p. 098, 2019. [arXiv:1810.08621]

[166] N. Drukker, D. J. Gross, and H. Ooguri, 'Wilson loops and minimal surfaces', *Phys. Rev. D*, vol. 60, p. 125006, 1999. [arXiv:hep-th/9904191]

[167] M. Kruczenski and A. Tirziu, 'Matching the circular Wilson loop with dual open string solution at 1-loop in strong coupling', *JHEP*, vol. 05, p. 064, 2008. [arXiv:0803.0315]

[168] D. Berenstein, R. Corrado, W. Fischler, and J. Maldacena, 'Operator product expansion for Wilson loops and surfaces in the large N limit', *Phys. Rev. D*, vol. 59, p. 105023, 1999. [arXiv:hep-th/9809188]

[169] D. J. Gross and H. Ooguri, 'Aspects of large N gauge theory dynamics as seen by string theory', *Phys. Rev. D*, vol. 58, p. 106002, 1998. [arXiv:hep-th/9805129]

[170] K. Zarembo, 'Wilson loop correlator in the AdS/CFT correspondence', *Phys. Lett. B*, vol. 459, pp. 527–534, 1999. [arXiv:hep-th/9904149]

[171] P. Olesen and K. Zarembo, 'Phase transition in Wilson loop correlator from AdS/CFT correspondence'. [arXiv:hep-th/0009210]

[172] K. Zarembo, 'Supersymmetric Wilson loops', *Nucl. Phys. B*, vol. 643, pp. 157–171, 2002. [arXiv:hep-th/0205160]

[173] A. A. Tseytlin and K. Zarembo, 'Wilson loops in $\mathcal{N} = 4$ super Yang-Mills theory: Rotation in S^5', *Phys. Rev. D*, vol. 66, p. 125010, 2002. [arXiv:hep-th/0207241]

[174] K. Zarembo, 'Open string fluctuations in $AdS_5 \times S^5$ and operators with large R-charge', *Phys. Rev. D*, vol. 66, p. 105021, 2002. [arXiv:hep-th/0209095]

[175] R. Ishizeki, M. Kruczenski, and S. Ziama, 'Notes on Euclidean Wilson loops and Riemann Theta functions', *Phys. Rev. D*, vol. 85, p. 106004, 2012. [arXiv:1012.3995]

[176] M. Kruczenski and S. Ziama, 'Wilson loops and Riemann theta functions II', *JHEP*, vol. 05, p. 037, 2014. [arXiv:1311.4950]

[177] M. Cooke and N. Drukker, 'From algebraic curve to minimal surface and back', *JHEP*, vol. 02, p. 090, 2015. [arXiv:1410.54361]

[178] G. W. Semenoff and K. Zarembo, 'Wilson loops in SYM theory: From weak to strong coupling', *Nucl. Phys. B - Proc. Suppl.*, vol. 108, pp. 106–112, 2002. [arXiv:hep-th/0202156]

[179] K. Zarembo, 'Localization and AdS/CFT Correspondence', *J. Phys. A*, vol. 50, no. 44, p. 443011, 2017. [arXiv:1608.02963]

[180] D. H. Correa, V. I. Giraldo-Rivera, and M. Lagares, 'On the abundance of supersymmetric strings in $AdS_3 \times S^3 \times S^3 \times S^1$ describing BPS line operators', *J. Phys. A*, vol. 54, no. 50, p. 505401, 2021. [arXiv:2108.09380]

[181] L. F. Alday and A. A. Tseytlin, 'On strong-coupling correlation functions of circular Wilson loops and local operators', *J. Phys. A*, vol. 44, p. 395401, 2011. [arXiv:1105.1537]

[182] R. Hernández, 'Semiclassical correlation functions of Wilson loops and local vertex operators', *Nucl. Phys. B*, vol. 862, pp. 751–763, 2012. [arXiv:1202.4383]

[183] E. I. Buchbinder and A. A. Tseytlin, '$1/N$ correction in the D3-brane description of a circular Wilson loop at strong coupling', *Phys. Rev. D*, vol. 89, no. 12, p. 126008, 2014. [arXiv:1404.4952]

[184] C. A. Bayona and N. R. F. Braga, 'Anti-de Sitter boundary in Poincaré coordinates', *Gen. Rel. Grav.*, vol. 39, pp. 1367–1379, 2007. [arXiv:hep-th/0512182]

[185] J. Sonnenschein, 'What does the string/gauge correspondence teach us about Wilson loops?', in *Supersymmetry in the theories of fields, strings and branes*, pp. 219–269, World Scientific, 2000. [arXiv:hep-th/0003032]

[186] E. Fradkin, *Field Theories of Condensed Matter Physics*, ch. 7, pp. 189–250. Cambridge University Press, 2^{nd} ed., 2013.

[187] R. Hernández and E. López, 'The SU(3) spin chain sigma model and string theory', *JHEP*, vol. 04, p. 052, 2004. [arXiv:hep-th/0403139]

[188] A. Perelomov, *Generalized Coherent States and Their Applications*, ch. 5, pp. 67–83. Texts and Monographs in Physics, Springer, Berlin, Heidelberg, 1^{st} ed., 1986.

[189] A. Perelomov, *Generalized Coherent States and Their Applications*, ch. 4, pp. 54–66. Texts and Monographs in Physics, Springer, Berlin, Heidelberg, 1^{st} ed., 1986.

[190] E. Álvarez, L. Álvarez-Gaumé, and Y. Lozano, 'An introduction to T-duality in string theory', *Nucl. Phys. B - Proc. Suppl.*, vol. 41, pp. 1–20, 1995. [arXiv:hep-th/9410237]

[191] D. M. Hofman and J. Maldacena, 'Giant Magnons', *J. Phys. A*, vol. 39, pp. 13095–13118, 2006. [arXiv:hep-th/0604135]

[192] N. Dorey, 'Magnon bound states and the AdS/CFT correspondence', *J. Phys. A*, vol. 39, pp. 13119–13128, 2006. [arXiv:hep-th/0604175]

[193] H.-Y. Chen, N. Dorey, and K. Okamura, 'Dyonic giant magnons', *JHEP*, vol. 09, p. 024, 2006. [arXiv:hep-th/0605155]

[194] T. McLoughlin, 'Review of AdS/CFT Integrability, Chapter II.2: Quantum Strings in $\mathrm{AdS}_5 \times \mathrm{S}^5$', *Lett. Math. Phys.*, vol. 99, pp. 127–148, 2012. [arXiv:1012.3987]

[195] M. Beccaria, G. V. Dunne, G. Macorini, A. Tirziu, and A. A. Tseytlin, 'Exact computation of one-loop correction to the energy of pulsating strings in $\mathrm{AdS}_5 \times S^5$', *J. Phys. A*, vol. 44, p. 015404, 2011. [arXiv:1009.2318]

[196] D. R. Medina Rincón, *Holographic Wilson Loops: Quantum String Corrections.* PhD thesis, Uppsala University, 2018.

[197] D. Pajer, 'On quantum corrections to BPS Wilson loops in superstring theory on $\mathrm{AdS}_3 \times \mathrm{S}^3 \times \mathrm{T}^4$ with mixed flux'. [arXiv:2109.11318], 9 2021.

[198] C. Kristjansen and Y. Makeenko, 'More about one-loop effective action of open superstring in $\mathrm{AdS}_5 \times \mathrm{S}^5$', *JHEP*, vol. 09, p. 053, 2012. [arXiv:1206.5660]

[199] S. A. Frolov, I. Y. Park, and A. A. Tseytlin, 'On one-loop correction to energy of spinning strings in S^5', *Phys. Rev. D*, vol. 71, p. 026006, 2005.

[200] S. Giombi and A. A. Tseytlin, 'Strong coupling expansion of circular Wilson loops and string theories in $\mathrm{AdS}_5 \times S^5$ and $\mathrm{AdS}_4 \times CP^3$', *JHEP*, vol. 10, p. 130, 2020. [arXiv:2007.08512]

[201] D. Medina-Rincon, 'Matching quantum string corrections and circular Wilson loops in $AdS_4 \times CP^3$', *JHEP*, vol. 08, p. 158, 2019. [arXiv:1907.02984]

[202] M. David, R. de León Ardón, A. Faraggi, L. A. Pando Zayas, and G. A. Silva, 'One-loop holography with strings in $\mathrm{AdS}_4 \times \mathbb{CP}^3$', *JHEP*, vol. 10, p. 070, 2019. [arXiv:1907.08590]

[203] S. D. Avramis, K. Sfetsos, and K. Siampos, 'Stability of strings dual to flux tubes between static quarks in $\mathcal{N} = 4$ SYM', *Nucl. Phys. B*, vol. 769, pp. 44–78, 2007. [arXiv:hep-th/0612229]

[204] J. M. Maldacena and H. Ooguri, 'Strings in AdS_3 and the $\mathrm{SL}(2, R)$ WZW model. III. Correlation functions', *Phys. Rev. D*, vol. 65, p. 106006, 2002. [arXiv:hep-th/0111180]

[205] A. L. Larsen and N. Sánchez, 'New coherent string states and minimal uncertainty in WZWN models', *Nucl. Phys. B*, vol. 618, pp. 301–311, 2001. [arXiv:hep-th/0103044]

[206] A. L. Larsen and N. Sánchez, 'Quantum Coherent String States in AdS_3 and $\mathrm{SL}(2, R)$ WZWN model', *Phys. Rev. D*, vol. 62, p. 046003, 2000. [arXiv:hep-th/0001180]

[207] S. Bellucci, P.-Y. Casteill, and J. F. Morales, 'Superstring sigma models from spin chains: the $\mathrm{SU}(1, 1|1)$ case', *Nucl. Phys. B*, vol. 729, pp. 163–178, 2005. [arXiv:hep-th/0503159]

[208] S. Bellucci and P.-Y. Casteill, 'Sigma model from $\mathrm{SU}(1, 1|2)$ spin chain', *Nucl. Phys. B*, vol. 741, pp. 297–312, 2006. [arXiv:hep-th/0602007]

[209] B. Stefański Jr, 'Landau-Lifshitz sigma-models, fermions and the AdS/CFT correspondence', *JHEP*, vol. 07, p. 009, 2007. [arXiv:0704.1460]

[210] N. Beisert, V. A. Kazakov, and K. Sakai, 'Algebraic Curve for the SO(6) Sector of AdS/CFT', *Commun. Math. Phys.*, vol. 263, pp. 611–657, 2006. [arXiv:hep-th/0410253]

[211] S. Schäfer-Nameki, 'The algebraic curve of 1-loop planar $\mathcal{N} = 4$ SYM', *Nucl. Phys. B*, vol. 714, pp. 3–29, 2005. [arXiv:hep-th/0412254]

[212] N. Gromov and P. Vieira, 'The AdS_4/CFT_3 algebraic curve', *JHEP*, vol. 02, p. 040, 2009. [arXiv:0807.0437]

[213] T. Lloyd and B. Stefański Jr, 'AdS_3/CFT_2, finite-gap equations and massless modes', *JHEP*, vol. 04, p. 179, 2014. [arXiv:1312.3268]

[214] S. Schäfer-Nameki, 'Review of AdS/CFT Integrability, Chapter II.4: The Spectral Curve', *Lett. Math. Phys.*, vol. 99, pp. 169–190, 2012. [arXiv:1012.3989]

[215] N. Seiberg and E. Witten, 'Monopoles, duality and chiral symmetry breaking in $N = 2$ supersymmetric QCD', *Nucl. Phys. B*, vol. 431, pp. 484–550, 1994. [arXiv:hep-th/9408099]

[216] I. S. Gradshteyn and I. M. Ryzhik, *Table of integrals, series, and products.* Elsevier, 7^{th} ed., 2007.